Investigating the role of Galectin-9 in monocytes associated with atherosclerosis

By Franziska Krautter

A thesis submitted to the University of Birmingham for the degree of

DOCTOR OF PHILOSOPHY

Institute of Cardiovascular Sciences
College of Medical and Dental Science
University of Birmingham

January 2022

Abstract

Cardiovascular disease is the number one cause of death worldwide. They are most often caused by atherosclerotic plaques, formed by lipid depositions in the vessel wall of major blood vessels which cause an inflammatory immune response. While it has been long accepted that the immune response is a driving factor in atherosclerotic plaque progression, no suitable therapeutics have been developed so far to successfully target inflammation and reduce the risk of cardiovascular events. Therefore the identification of new therapeutic targets involved in the progression of atherosclerosis and their mechanism of action is required in order to develop successful therapies.

Monocyte recruitment and migration into the vessel wall and their differentiation into macrophages, which release pro-inflammatory factors, and lipid-laden foam cells are driving forces of atherosclerosis. Many major proteins involved in the multistep adhesion cascade of leukocyte recruitment have been well characterised, however there are still gaps in knowledge.

Galectin-9 is a ß-galactoside binding protein and has been shown to have a wide range of functions. More recently, various studies have demonstrated its role in the modulation of leukocyte trafficking. However, its role in monocyte recruitment and migration remains elusive.

The aim of this study is to characterise the role of Galectin-9 in monocyte migration and atherosclerotic plaque progression.

The results show that Galectin-9 is expressed and released by human monocytes, macrophages and endothelial cells and its upregulation is induced by pro-inflammatory

environments. Soluble Galectin-9 was demonstrated to induce human monocyte activation and the release of pro-inflammatory cytokines and chemokines by human monocyte derived macrophages. Additionally, it was observed that Galectin-9 upregulation by the endothelium is required for monocyte adhesion in vitro while PBMCs of peripheral arterial patients adhere to immobilised Galectin-9 with higher frequency compared to healthy young and aged controls. These inflammation-specific modes of function of Galectin-9 were confirmed in vivo: Galectin-9 induced monocyte and neutrophil migration into tissue during inflammation but not during homeostasis. Finally, the role of Galectin-9 in atherosclerotic plaque progression was demonstrated, since it was shown that ApoE-/- Gal-9-/- mice had a reduced plaque burden as well as a reduced macrophage and collagen content in aortic root plaques in a model of diet-induced atherosclerosis compared to ApoE-/- mice.

In conclusion this study demonstrates that inflammation-induced expression of Galectin-9 modulates atherosclerotic plaque progression in two ways: i) by facilitating monocyte recruitment and ii) through inducing a pro-inflammatory macrophage phenotype. These findings suggest that Galectin-9 is a novel therapeutic target in the prevention of atherosclerotic plaque progression.

Acknowledgements

First and foremost, I would like to thank my supervisor Dr. Asif Iqbal. You have made the past 3 and a half years a truly enjoyable experience. I could not have done this without your trust in my abilities, patience and your continuous interest in my growth as a scientist. I could not have asked for a better supervisor and I will be forever grateful for the opportunities you have given me to pursue a career in research!

I would also like to thank my two secondary supervisors Dr Myriam Chimen and Prof Ed Rainger: Thank you for your support, guidance and your excitement about my project, which always kept me going.

To the whole Leukocyte Trafficking Group, particularly Dr Helen McGettrick: Thank you for your feedback and shared knowledge. I have learnt everything I know about leukocyte trafficking from all of you! Helen, thank you for taking time to give me feedback on every annual report and during lab meetings.

To the office crew: I will never forget all the chats, the crazy times and the Pizza nights, barbeques and Friday Dinner Clubs. You all have kept me sane and were the necessary distraction when the science wasn't working!

Thank you to Dr Dianne Cooper, without whom I would have never found this PhD position and also thank you for the truly enjoyable time in your lab and throughout this collaboration.

To Mr Alok Tiwari and every single blood donor: Thank you! Without your donations, the realisation of this project would not have been possible.

Thank you to Drs Ed Fisher and Emily Brown for the great collaboration and access to their data which contributed to this project.

I would also like to acknowledge the Academy of Medical Sciences and the University of Birmingham for funding this research.

Lastly, I would like to thank my family and Ben.

An meine Familie: ohne eure nicht endende Unterstützung wäre ich nicht da wo ich heute bin und dafür bin ich euch für sehr dankbar.

Ben, I will never be able to thank you enough for your love, support and patience. You have been my rock. Thank you for believing in me even when I didn’t, for moving to Birmingham, for cooking all the delicious meals, for putting up with all my late nights of counting cells or writing manuscripts but also distracting me from work when I needed it most! You made Birmingham my home. X

Table of Contents

List of Figures

List of Tables

Abbreviations

ABI	Ankle-Brachial Index
ADAM17	A disintegrin and metalloprotease 17
ANOVA	Analysis of variance
APC	Allophycocyanin
ApoB	Apolipoprotein B
ApoE	Apolipoprotein E
APR	Acute phase response
Arg1	Arginase 1
ASO	Anti-sense oligonucleotide
Bax	B-cell lymphoma-2 associated X protein
Bcl-2	B-cell lymphoma-2
BMDM	Bone marrow derived macrophages
BSA	Bovine serum albumin
BV	Brilliant Violet
CANTOS	Canakinumab Anti-Inflammatory Thrombosis Outcome Study
CCL	C-C chemokine ligand
CCR	C-C chemokine receptor
CD	Cluster of differentiation
cDNA	Circular DNA
CIRT	Cardiovascular Inflammation Reduction Trial
CL	Classical monocyte subset
CRD	Carbohydrate recognition domain
CRP	C-reactive protein
CSF1R	Colony stimulating factor 1 receptor
Ctrl	control
CXCL	C-X-C chemokine ligand
CXCR	C-X-C chemokine receptor
Cy	Cyanine
DAMP	Damage-associated molecular pattern
DC	Dendritic cell

DNase	Deoxyrubonuclease
ECM	Extracellular matrix
ECGM	Endothelial cell growth medium
EDTA	Ethylenediaminetetraacetic acid
EGF	Epidermal Growth Factor
ELISA	Enzyme-linked immunosorbent assay
ERK1/2	Extracellular-signal regulated kinase 1/2
EtOH	Ethanol
F4/80	EGF-like module-containing mucin-like hormone receptor-like 1
FCS	Fetal calf serum
FcγR	Fc γ receptor
FITC	Fluorescein isothiocyanate
fMLP	N-formyl-methionyl-leucyl-phenylalanine
FSC	Forward Scatter
Fuc	fucose
GAG	Glycosaminoglycan
Gal	Galectin
GalNAc	N-Acetylgalactosamine
GCNT2	Glucosaminyl (N-Acetyl) Transferase 2
GlcNAc	N-Acetylglucosamine
GM-CSF	Granulocyte-macrophage colony stimulating factor
GPCR	G-Protein coupled receptor
Gr-1	Ly6C/Ly6G
HA	Healthy aged
HDAC	Histone deacetylase
HFD	High fat diet
hMDM	Human monocyte derived macrophages
HRP	Horse Radish Peroxidase
HUSMC	Human Umbilical Smooth Muscle cells
HUVEC	Human Umbilical Vein Endothelial Cells
HY	Healthy young

ICAM-1	Intercellular adhesion molecule 1
IDL	Intermediate density lipoprotein
lFNγ	Interferon γ
IL	Interleukin
IL-1RA	Interleukin-1 receptor antagonist
IRF	Interferon response element
ITM	Intermediate monocyte subset
i.p.	Intraperitoneal
i.v.	Intravenous
JAM	Junctional adhesion molecule
LDL	Low Density lipoprotein
LDLR	Low density lipoprotein receptor
Ldlr	Murine low density lipoprotein receptor (Gene)
LFA-1	Lymphocyte function-associated antigen 1
Lgals9	Murine Gal-9 (Gene)
LGALS9	Human Gal-9 (Gene)
LoDoCo	Low Dose Colchicine
LOX1	Lectin type Oxidised low density lipoprotein receptor
LPS	Lipopolysaccharide
Ly6C	Lymphocyte antigen 6C
Ly6G	Lymphocyte antigen 6G
M1	M1 macrophage
M2	M2 macrophage
Mac-1	Macrophage receptor 1
MAPK	Mitogen-activated protein kinase
M-CSF	Macrophage-colony stimulating factor
MFI	Median fluorescence intensity
MHC	Major histocompatibility complex
MMP	Matrix metalloprotease
mRNA	Messenger ribonucleic acid
Mttp	Microsomal triglyceride transfer protein large subunit (Gene)
NC	Non-classical monocyte subset

NF-IL6	Nuclear factor Interleukin 6
NF_KB	Nuclear factor ‘kappa-light-chain-enhance’ of activated B-cells
NK1.1	Killer cell lectin-like receptor subfamily B
NLRP3	NOD-, LRR- and pyrin domain-containing protein 3
oxLDL	Oxidised Low density lipoprotein
Pa	Pascal
PAD	Peripheral arterial disease
PAMP	Pathogen associated molecular pattern
PBMC	Peripheral Blood mononuclear cells
PBS	Phosphate buffered saline
PCSK9	Proprotein converstase subtilisin/kexin type 9
PCR	Polymerase chain reaction
PDGF	Platelet-derived growth factor
PE	Phycoerythrin
PECAM	Platelet endothelial cell adhesion molecule
PI3K	Phosphatidylinositol-3-kinase
PLC	Phospholipase C
PMA	Phorbol myristate acetate
PMN	Polymorphonuclear cells
Poly I:C	Poly inosinic:cytidylic acid
PPR	Patter recognition receptors
PSGL-1	P-selectin Glycoprotein ligand-1
qPCR	Quantitative polymerase chain reaction
RA	Rheumatoid Arthritis
ROS	Reactive oxygen species
RNA	Ribonucleic acid
RNASeq	RNA sequencing
RT	Room temperature
SDS	Sodium dodecyl sulfate
SELE	E-selectin (Gene)
SLE	Systemic lupus erythematosus

sLe^x	Sialyl $Lewis^x$
Siglec F	Sialic acid-binding Ig-like lectin F
siRNA	Silencing ribonucleic acid
SMC	Smooth muscle cell
SYK	Spleen tyrosine kinase
TBS	Tris Buffered Saline
TGFβ	Transforming growth factor β
THP-1	Tohoku Hospital Pediatrics 1
TIM-3	T-cell immunoglobulin and mucin-domain containing-3
TIMP	Tissue inhibitors of matrix metalloproteases
TLR	Toll-like receptor
TNFα	Tumour necrosis factor α
T_{reg}	Regulatory T-cell
VCAM-1	Vascular cell adhesion molecule
VEGF	Vascular endothelial growth factor
VLA-1/4	Very late antigen 1/4
VLDL	Very low density lipoprotein
VSCM	Vascular smooth muscle cells
Wnt	Wingless and Int-1
WT	Wild type

Forwards

Chapter 1: The material in Chapters 1.1.1 and 1.3 draws heavily on my previously published literature review “Glycans and Glycan-Binding Proteins as Regulators and Potential Targets in Leukocyte Recruitment” (Krautter, F**.**; Iqbal, A.J (2021)) and has been adapted for this thesis.

Chapter 3: The data relating Chapter 3.2 and 3.3 was published as “Characterisation of endogenous Galectin-1 and -9 expression in monocyte and macrophage subsets under resting and inflammatory conditions” (Krautter,F. and Recio C. *et al*. (2020)), previously to writing this thesis.

Chapter 6: Data in Chapter 6.3. was acquired in collaboration with Drs. E.A. Fisher and E. Brown from the Cardiovascular Research Center at New York University.

Some of the currently unpublished data in this thesis are currently prepared for submission at the time of writing this thesis.

Published papers mentioned above are attached in Chapter 9 – Appendix.

CHAPTER 1:

INTRODUCTION

1. Chapter 1: Introduction

1.1. Inflammation

Inflammation is the tightly controlled defence mechanism of the body against physical, environmental or pathogenic stress[1]. The physiological response is fast acting and occurs within seconds or minutes after the trauma[1], and is mediated through changes to the local vasculature such as vasodilation, activation of the endothelial cells lining the blood vessel, increased vascular permeability and platelet-mediated clotting in the microvasculature to prevent pathogens from spreading via circulation. These changes also facilitate leukocyte migration into the region of tissue damage to fight pathogens, repair damaged tissue and return to physiological tissue homeostasis[2]. While these processes are beneficial and necessary, tissue malfunction (impaired inflammation resolution) can cause homeostatic imbalance and result in chronic inflammation, independent of tissue trauma[3].

Upon tissue damage, danger- or pathogen associated molecular patterns (DAMPs or PAMPs, respectively) are released from damaged cells and initiate the innate immune response through the interaction with pattern recognition receptors (PRRs), for example Toll-like receptors (TLRs)[4,5] by tissue resident macrophages, dendritic cells and mast cells. They produce a variety of inflammatory mediators such as chemokines, cytokines and lipid mediators, vasoactive amines or proteolytic enzymes which lead to oedema which in turn enables leukocyte extravasation through endothelial activation[6].

In addition to the local inflammatory changes, systemic changes can occur as a result of the acute-phase response (APR). The release of pro-inflammatory cytokines locally

results in generation of acute phase reactants by the liver such as C-reactive protein (CRP) and serum amyloid A which in turn cause fever, leukocytosis, thrombocytosis, somnolence, and reduction in glyconeogenesis[7].

APR is followed by resolution during which tissue repair and remodelling take over to return to tissue homeostasis. This is generally facilitated by tissue resident and pro-resolution macrophages[8-11]. Particularly, lipid mediators play an important role in the switch between APR and resolution[10,12]. The release of anti-inflammatory lipoxins as well as resolvins and protectins instead of pro-inflammatory prostaglandins facilitates resolution by inhibiting neutrophil recruitment and promoting monocyte recruitment which play a role in removal of dead cells, a process referred to as efferocytosis, and tissue repair[12-14].

If APR is not sufficiently resolved, local inflammation can result in systemic events, such as septic shock, or chronic inflammation. However, unresolved APR is not the only cause of chronic inflammation: T-cell mediated immune response to “self-antigens” can also lead to chronic autoimmune conditions such as rheumatoid arthritis (RA)[15].

1.1.1. Leukocyte Trafficking

The phenomenon of leukocyte extravasation was first described in the nineteenth century by Dutrochet *et al*. who published his observations and drawings of leukocyte migration in 1824[16,17]. Since then, this fine-tuned cascade has been intensely investigated and distinct steps have been described: rolling, slow rolling, activation, firm adhesion, intraluminal crawling and transmigration[6]. These steps are mediated by selective activation and upregulation of a range of proteins.

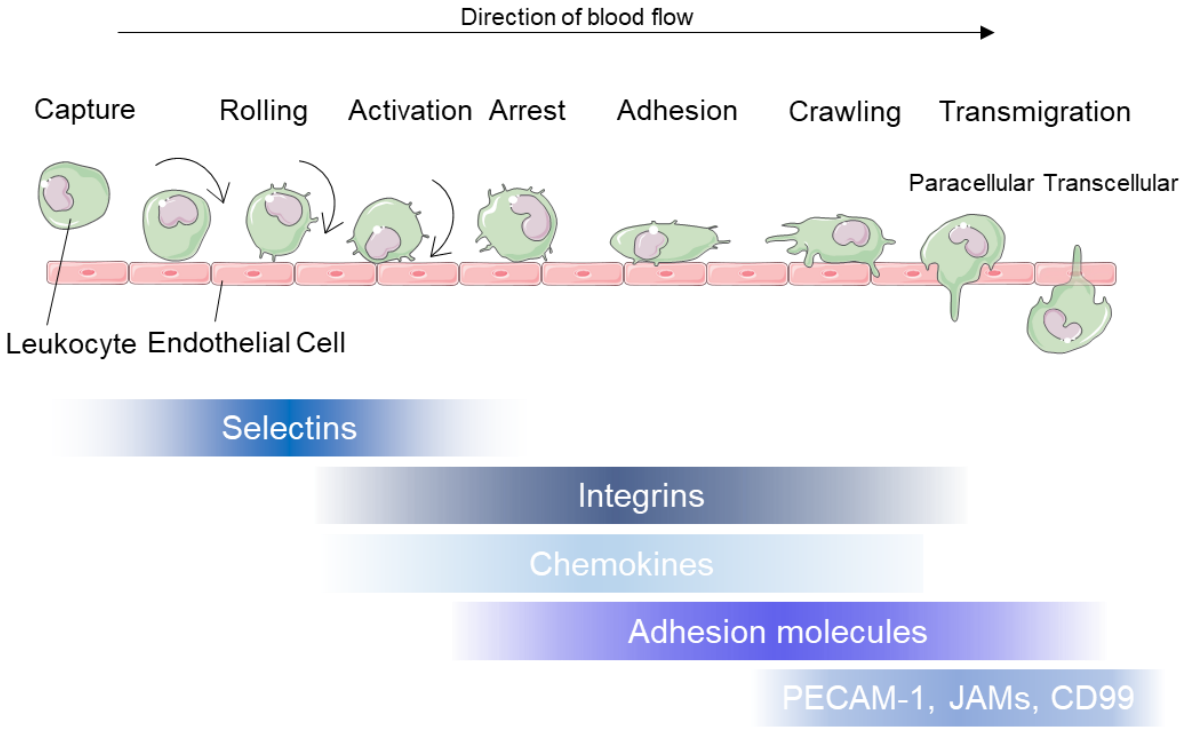

Figure 1: Leukocyte migration cascade across endothelium. The leukocyte migration cascade comprises of a sequence of steps which are mediated by a range of proteins. The initial steps of capture and rolling are dominated by the interaction of selectins with proteins such as P-selectin glycoprotein ligand (PSGL)-1, E-selectin ligand (ESL)-1 and Cluster of differentiation (CD) 44. Activation leads to a conformational change in integrins such as lymphocyte function-associated antigen (LFA)-1, Macrophage (Mac)-1 antigen and Very Late Antigen (VLA)-4 which then interact with adhesion molecules such as Intercellular Cell Adhesion Molecule (ICAM-1) and Vascular Cell Adhesion Molecule (VCAM)-1. Together with chemokines presented on the endothelial surface, arrest and adhesion are triggered. The final step, transmigration through the endothelial cell layer is mediated by proteins such as platelet endothelial cell adhesion molecule (PECAM)−1, CD99 and junctional adhesion molecule (JAM) -A.

A protein family of C-type lectins called selectins mediate the first steps in this cascade: capture, rolling and tethering (Figure 1). Three types of selectins have been identified to date in mammals: (I) E-selectin (Cluster of differentiation (CD) 62E) messenger RNA (mRNA) and subsequently the protein are generated by endothelium upon activation through inflammatory mediators such as tumour necrosis factor (TNF) α[18,19], interleukin (IL)-1β[19] or IL-6[20] released by tissue resident immune cells, and presented on the endothelial cell surface. (II) P-selectin is formed prior to cellular activation and stored in platelet granules and Weibel Palade bodies in endothelial cells[21,22]. Upon cellular activation, P-selectin is transported to the external plasma membrane[21,22]. (III) L-selectin is constitutively expressed by leukocytes before it is shed upon leukocyte activation[23,24]. These selectins all bind to O-glycans such as sialyl Lewis^x (sLe^x) on glycosylated proteins like P-selectin glycoprotein ligand (PSGL) 1 and CD44[25-27]. E- and P-selectins bind to glycans on leukocytes whereas L-selectin can bind O-glycans on endothelium and leukocytes. Interestingly, the glycosylation of cells has been demonstrated to depend on the activation state. Lymphocytes and monocytes upregulate sLe^x upon activation and therefore increase their susceptibility towards selectin interaction[26,28-30]. For example, while naïve T-cells do not express enzymes involved in glycosylation such as Glucosaminyl (N-Acetyl) Transferase (GCNT) 1 and Fucosyltransferase (Fut) 7, activated T-cells synthesise Core 2 O-glycans through the upregulation of these enzymes[31]. Proteins such as PSGL-1 and CD43, ligands of selectins are then glycosylated which in turn enables the binding of T-cells to selectins, while naïve T-cell selectin ligands remain un-glycosylated and therefore are unable to bind which prevents them from migrating into tissue[30]. Furthermore, PSGL-1 is upregulated in IL-1ß activated monocytes[26] and *in vivo* studies in mice have shown

that Lymphocyte antigen (Ly) 6C^{hi} monocytes express higher levels of PSGL-1 than Ly6C^{lo} monocytes and exhibit increased binding to P-, E- and L-selectin. Additionally, PSGL-1 was shown to mediate selective homing of Ly6C^{hi} monocytes to the arterial wall during atherosclerosis[32]. The interaction between selectins and glycosylated ligands initiate the first steps of the migration cascade: capture, rolling and tethering[24,33-35]. This interaction leads to further activation of both cell types through spleen tyrosine kinase (SYK) mediated- signalling pathways downstream of PSGL-1[36]. However, not only selectin-glycan interactions mediate leukocyte capture and rolling: the interaction between CD44 and the glycosaminoglycan (GAG) hyaluronic acid (HA) has previously been described to contribute to lymphocyte rolling *in vitro*[37] and calcein-AM labelled leukocyte rolling *in vivo*[38].

Eventually, rolling leukocytes slow down which enables contact with chemokines (Figure 1), presented by GAGs on the endothelial surface[39,40]. Chemokines are expressed by cells such as endothelial cells and macrophages during inflammation and act as chemoattractants for leukocytes. The interaction of chemokines with chemokine receptors on leukocytes leads to their activation which in turn causes G-protein coupled receptor (GPCR)- mediated conformational changes in integrins[41,42].

Integrins are proteins expressed on the cell surface consisting of two subunits: α and β. Depending on the leukocyte, the CD18/ß2 subunit and different α subunits determine the prevalent integrin: CD11a and CD18 make up lymphocyte function associated antigen 1 (LFA-1), CD49a and CD29 make up Very late antigen 1 (VLA-1). These two integrins are mostly found on lymphocytes, while Macrophage receptor-1 (Mac-1), made up of CD11b and CD18 is found on monocytes and macrophages. Upon activation, the conformational changes of the integrins enable their interaction with

several members of the Ig superfamily, including intercellular adhesion molecule-1 (ICAM-1) or vascular cell adhesion molecule-1 (VCAM-1) expressed by activated endothelium[43-45]. The interaction between these two protein types results in firm adhesion and cell arrest of leukocytes. This is regulated through Phospholipase C (PLC)-mediated calcium signalling, required for high-affinity binding of VLA-4 on monocytes[6]. Other proteins such as C-C and C-X-C chemokines (e.g. C-C chemokine ligand (CCL) 2) and IL-8 also mediate firm adhesion[46,47] and more recently studies have shown that at least some of these chemokines depend on glycosaminoglycans (GAG) for their presentation[40,48-52]. These studies suggest that the immobilisation of chemokines through GAGs on the cell surface contribute to a high local concentration of chemokines, concentration gradients and chemokine-receptor binding, all potentially modulating leukocyte migration. However, more studies are required to understand the regulatory mechanisms involved in GAG-chemokine interactions and their effect on leukocyte migration. Gangavarapu *et al*. and others have suggested that these GAG-chemokine interactions might be a key in better understanding tissue specific differences in leukocyte trafficking[53,54].

To transmigrate through the endothelium (Figure 1), leukocytes crawl on the endothelial surface to find a suitable site for transmigration. Mac-1, LFA-1 and ICAM-1 as well as chemokines such as C-X-C chemokine ligand (CXCL) 12 or lipid chemoattractants (e.g. leukotriene B4) mediate crawling[55]. The final step, transmigration, can occur in a trans- or paracellular manner. Transcellular migration occurs when leukocytes move through endothelial cells which has been shown to require membrane fusion[56]. The more common route is paracellular, where leukocytes travel through cellular junctions. Adherent leukocytes release signals to dissociate

adherens junctions, disrupting the endothelial layer[57,58]. VE-cadherin plays a crucial role as junction protein and is disrupted when monocyte adhesion changes the phosphorylation state of the VE-cadherin, breaking its bond to α-catenin[59]. Furthermore, the junctional adhesion molecule (JAM) family proteins such as JAM-A, which is located within tight junctions, participate in transmigration by interacting with Mac-1[60] and LFA-1[61]. Additionally, Platelet endothelial cell adhesion molecule (PECAM) 1 and CD99 also play a role in this step of the leukocyte recruitment cascade. PEACAM-1 forms homophilic interactions which play a key role in vascular permeability[62,63], detecting flow[64,65] and leukocyte transmigration[66,67].

1.1.2. Monocytes

Monocytes are a heterogeneous group of circulating myeloid leukocytes which act during inflammation and resolution. Upon migration into tissue, monocytes differentiate into dendritic cells, macrophages or foam cells and exert their specific functions.

1.1.2.1. Monocyte subsets

Human monocytes are divided into subsets based on the surface expression of CD14 and CD16: classical monocytes (CL) are $CD14^{++}$ and $CD16^{-}$, intermediate monocytes (ITM) are $CD14^{+}$ and $CD16^{+}$ and non-classical monocytes (NC) are $CD14^{-}$ and $CD16^{+}$ [68]. C-C chemokine receptor (CCR) 2, CX_3CR1 and Major Histocompatibility complex (MHC) Class II are additional markers used to characterise human monocyte subsets: CCR2 is highly expressed on classical monocytes while expression levels of CX_3CR1 and MHC Class II are high in non-classical and intermediate monocytes respectively[68]. Classical monocytes are the most abundant subset and generally considered to be pro-inflammatory with antimicrobial functions, while non-classical monocytes act as

patrolling monocytes[69] and are thought to act during early stages of inflammation as well as in tissue repair[2,10,68,70-72]. The intermediate subset is the smallest subset and considered to be monocytes transitioning from classical to non-classical monocyte. They have been shown to act in a pro-inflammatory manner[73,74] and also express higher levels of IL-1β and TNFα[74,75].

In mice, subsets are identified and distinguished by the expression of lymphocyte antigen 6C (Ly6C) expression. Other markers used for further characterisation of the two populations are Gr-1 (Ly6C and Ly6G combined), CCR2 and CX_3CR1[68,76]. $Ly6C^{hi}$ ($Gr\text{-}1^{hi}$, $CCR2^{hi}$, and $CX3_3CR1^{low}$) monocytes, also referred to as inflammatory monocytes, correspond functionally to human classical monocytes. $Ly6C^{low}$ ($Gr\text{-}1^{low}$, $CCR2^{low}$, and CX_3CR1^{hi}) monocyte subset, also referred to as patrolling monocytes, is functionally similar to human non-classical monocytes.

1.1.2.2. Monocyte differentiation

Monocytes differentiate from hematopoietic progenitor cells in the bone marrow. The growth factor macrophage-colony stimulating factor (M-CSF) within the bone marrow environment is critical for the process of differentiation[77]. Various studies investigating the origins of the monocyte subsets have found that intermediate and non-classical monocytes stem from classical monocytes. This has been shown in studies applying lineage-tracing in mice[78] and by deuterium-labelling of monocytes in humans[79]. Interestingly, disease-dependent changes in the proportions of respective monocyte subsets have been reported in rheumatoid arthritis[80], inflammatory bowel disease[9], cardiovascular disease[81] and sepsis[82] and changes in monocyte subset levels correlate with poor clinical outcomes in for example stroke[83,84] and RA[85].

Differentiated monocytes migrate from the bone marrow into circulation which requires CCL2 and CCL7, for example expressed by B-cells[86], and the receptor CCR2, expressed by monocytes. This has been demonstrated *in vivo* using CCR2 deficient mice which have lower circulating monocyte numbers but increased numbers in the bone marrow[87]. However, there is also evidence that Ly6C^{low} cells have a different CCR2-independent precursor since the number of patrolling Ly6C^{low} monocytes was not reduced in CCR2 deficient mice while Ly6C^{hi} cells were reduced in circulation[88].

1.1.2.3. Monocyte function

The three circulating human monocyte subsets have different functions. Classical monocytes are phagocytic cells and migrate towards CCL2 and CCL3 gradients. This suggests that this monocyte subset responds to tissue injury. Further evidence of their pro-inflammatory role is their ability to release IL-6, -8, CCL2 and CCL3 upon Lipopolysaccharide (LPS) stimulation[69,75] and differentiation into monocyte- derived macrophages and dendritic cells (DC)[89]. Like classical monocytes, intermediate monocytes secret IL-6 and CCL3 upon LPS stimulation, but express higher levels of MHC Class II than the other two monocyte subsets, which suggests a role in defence against pathogens. They also express high levels of IL-1ß and TNFα [75,90] at steady state. Furthermore, this subset is expanded in circulation in patients with systemic infections[91,92]. However, their precise role remains elusive. Non-classical monocytes are CX_3CR1^{hi} cells, enabling them to migrate on endothelium which expresses the CX_3CR1 ligand fractalkine[93,94]. Migration and patrolling of the blood vessel wall is a major part of the non-classical monocyte function. They respond in TLR7-mediated inflammation and migrate into tissue after sterile infection[88]. Furthermore, non-classical monocytes are found in the peritoneal cavity 1 to 2 h post infection of the peritoneal

cavity with *Listeria monocytogenes.* This makes them the first subset to migrate in response to the infectious stimulant, even before polymorphonuclear cells (PMN)[94]. Once they have migrated into tissue these cells start producing cytokines such as TNFα and IL-1[94] which exacerbates the inflammatory response. On the other hand, it has been suggested that non-classical monocytes can also give rise to anti-inflammatory macrophages which act in wound healing and have anti-inflammatory properties[95].

1.1.3. Macrophages

Macrophages are a diverse type of phagocytic cell which can be found in virtually all tissues. Their diversity is reflected in their functions which range from efferocytosis to contributing to antigen presentation, angiogenesis, protection against pathogens and fibrosis[9,71,96-99].

1.1.3.1. Macrophage phenotypes

The microenvironment of the tissue determines the phenotype of macrophages, which can have pro- or anti-inflammatory properties[100]. However, macrophages are not only present in tissues during inflammation. Tissue-resident macrophages are found during homeostasis and are tissue specific: for example Langerhans cells in the skin and Kupffer cells in the liver[78,101].

The classification of macrophages is based on the expression of certain markers such as CD80 and CD86, which are highly expressed in pro-inflammatory (M1) macrophages, or CD206 which is highly expressed in anti-inflammatory (M2) macrophages[102].

Classically activated, M1 macrophages develop through activation with Toll-like receptor ligands such as LPS as well as Interferon (IFN) γ. These macrophages act in host defence against pathogens and secrete pro-inflammatory cytokines such as IL-1ß and TNFα[103,104]. Alternatively activated, M2 macrophages develop in the presence of IL-4 and IL-13[103]. They display high endocytic activity and release anti-inflammatory cytokines such as Interleukin-1 Receptor Antagonist (IL-1RA) and IL-10[99,105].

While in many studies this simplified idea of two separate macrophages subsets is often applied, numerous studies have highlighted the plasticity of macrophages. These studies showed that macrophages respond to signals from their environment by reprogramming their phenotype, creating a spectrum of phenotypes rather than two distinct subpopulations[99,106-110]. For example, studies have suggested a link between hypoxic conditions in wounds and tumours and pro-arteriogenic macrophages which was induced through the prolyl-hydroxylase oxygen sensor which initiated the Nuclear factor 'kappa-light-chain-enhance' of activated B-cells (NF_kB) pathway[111].

1.1.3.2. Macrophage differentiation

Most tissue resident macrophages arise from embryonic precursor cells and are maintained locally[78,112]. These progenitor cells first develop from the ectoderm of the yolk sac and have been detected as early as day 8 in mouse embryos[78,112]. However, some macrophages also derive from the foetal liver or bone marrow. The bone marrow lineage gives rise to circulating monocytes which can differentiate into macrophages or dendritic cells upon migration into tissue, often in response to inflammatory stimuli[68,77,78,113]. Interestingly, while macrophages can have this diverse range of origins, studies have indicated, that colony stimulating factor receptor 1 (CSF1R), the receptor of M-CSF (or CSF1) acts as a major regulator. *In vivo* studies with CSF1R

deficient mice and rats have shown that its absence it leads to the depletion of macrophages[114,115]. However, depending on the lineage and tissue, other regulators of macrophage development have been proposed. For example, IL-34 has been described as ligand for CSF1R which affects microglia and Langerhans cells, but not macrophages in bone marrow, liver or spleen[116]. Other regulators are Granulocyte-macrophage colony stimulating factor (GM-CSF) and IL-3[117,118] as well as vascular endothelial growth factor (VEGF)[119].

1.1.3.3. Macrophage function

All macrophage phenotypes have the ability to phagocytose and are widely known for their function in the immune system where they act either as pro-inflammatory or anti-inflammatory cells. Pro-inflammatory macrophages release a range of inflammatory modulators such as TNFα or IL-1β[90] to initiate defence mechanisms against pathogens, or IL-12 and IL-23 which are required for the expansion of T_H1 and T_H17 cells[120,121]. While these responses to tissue injury are important and necessary, lack of control of the pro-inflammatory response by macrophages can lead to chronic inflammation or autoimmune disease[122-124]. Anti-inflammatory macrophages on the other hand dampen pro-inflammatory responses by secreting factors such as IL-10[125] or Arginase 1 (Arg1)[126-129]. These immune modulatory proteins act by promoting the expansion of T_H2 cells and T_{regs} to reduce the pro-inflammatory response and return to homeostasis[130]. Furthermore, M2 macrophages facilitate wound healing. M2 macrophages are known to produce growth factors such as transforming growth factor-ß1 (TGFß1) and Platelet-derived growth factor (PDGF) which promote fibroblast differentiation into myofibroblasts and therefore contribute to tissue regeneration[131,132]. They additionally generate matrix metalloproteinases (MMPs) and tissue inhibitors of

matrix metalloproteases (TIMPs) which regulate Extracellular matrix (ECM) turnover[133] while phagocytising apoptotic cells and components of the ECM to prevent a M1 macrophage response.

Macrophages also play a critical role in development: mice lacking M-CSF, the ligand of CSF1R are depleted of many macrophage populations which results in developmental abnormalities such as increased bone density, also called osteopetrosis, caused by a loss of osteoclasts[134-136]. These abnormalities are caused by the missing signals macrophages normally provide during tissue development, such as Wnt ligands which act on hepatic progenitor cells[137]. Additionally, the phagocytic function of macrophages is important for their functions in development. For example, macrophages surround erythroblasts and ingest the extruded erythrocyte nuclei during erythropoiesis[138] or phagocytose apoptotic cells during limb formation[114].

Furthermore, macrophages act in angiogenesis. Wnt signals and VEGF, generated by macrophages, have been shown to be required in vascular development[139-141].

These functions clearly highlight, that apart from their phagocytic function, macrophages also have very important signalling functions through the release of mediators which act on a wide range of cell types.

1.2. Atherosclerosis

Atherosclerosis is an inflammatory disease[142] driven by two main factors: dyslipidemia and vascular inflammation[142]. Various risk factors such as smoking, hyperlipidemia, aging, diet, diabetes mellitus and hypertension are associated with it[143,144]. Atherosclerosis is characterised by a build-up of lipids in the arterial wall. This process occurs over decades, starting with fatty streak lesions which can be detected in

children and young adults[145]. Over time these fatty streaks form mature plaques which occlude the lumen of arteries and promote ischaemic events. People suffering from atherosclerosis may experience symptoms such as impaired wound healing, cold limbs and brittle nails due to poor circulation. If the peripheral arteries are affected, the clinical term is peripheral arterial disease (PAD). PAD is mostly diagnosed using the Ankle-Brachial Index (ABI) whereby the blood pressure in the ankle is compared to the blood pressure in the arm. A ratio of less than 0.9 indicates possible PAD because the measured blood pressure in the ankle is significantly lower than in the arm due to the reduced blood circulation as a result of plaque build-up in the arteries. Furthermore, blood tests detecting cholesterol, triglyceride or blood sugar levels are used for a diagnosis. Imaging techniques such as X-ray, computer tomography angiography or magnetic resonance angiography are also utilised to support diagnosis. If left untreated it can lead to lethal complications such as stroke and heart attacks[46,146] which are the leading causes of deaths worldwide[147]. Current therapies are a legacy of the original classification of atherosclerosis as metabolic disease and aim to reduce plasma cholesterol levels. However, these therapies do not reduce the risk of cardiovascular events efficiently[148,149]. In addition to medicinal intervention, patients are encouraged to change their lifestyle by losing weight and/or stopping smoking[144]. And finally, surgical intervention, for example stents, angioplasty or bypasses are used to treat patients with atherosclerosis. Neither of these therapies address inflammation, which is recognised as major driver of atherosclerosis[142]. However, in 2017, the Canakinumab Anti-inflammatory Thrombosis Outcome Study (CANTOS) trial showed that targeting inflammation is beneficial for patients with atherosclerosis[150]. While the treatment of patients with canakinumab, a blocking anti-IL-1ß receptor antibody, lead

to a reduction in recurring cardiovascular events, it increased patients risk to opportunistic infections. While canakinumab is not a suitable treatment, it is now seen as important proof-of-concept study which highlights the potential of anti-inflammatory drugs for the treatment of atherosclerosis. Since then, further clinical trials of anti-inflammatory drugs have been conducted. Some have shown positive results such as the Low Dose Colchicine (LoDoCo)[151] and LoDoCo2[152] trials, but other have reported no reduction in the risk of cardiovascular events such as the Cardiovascular Inflammation Reduction Trial (CIRT)[153], which used low doses of methotrexate, an immunosuppressant drug readily used in autoimmune disease such as rheumatoid arthritis.

Retrospectively, these trials and studies act as important proof-of-concept which highlight the significant role inflammation plays in driving atherosclerosis. Moreover, they also demonstrate that current drugs are lacking in terms of efficacy and have potential side-effects , highlighting the need for further research in the area to develop more targeted therapeutics in the future.

1.2.1. Atherogenesis

During the early stages of atherosclerotic plaque formation, endothelial cells of the vessel wall lining become activated upon lipid accumulation and disturbed blood flow (Figure 2). Plaques do not form in random places but in areas of non-laminar flow such as in inner curvatures or branch points (bifurcations) of arteries[154]. This disruption of laminar flow is known to alter the endothelial layer, thereby enabling particularly modified low density lipoproteins (LDL) such as oxidised (ox) LDL and LDL bound to proteoglycans to accumulate on the extracellular matrix in the intima of major blood

vessels. The accumulation of LDLs leads to endothelial dysfunction via the interaction of oxLDL with two scavenger receptors: CD36[155] and lectin-type oxidized low density lipoprotein receptor (LOX) 1[156]. Studies have revealed that this leads to the upregulation of adhesion molecule expression by the endothelium[157,158]. Circulating monocytes interact with these adhesion molecules to transmigrate across activated vascular endothelium to the intima layer (Figure 2). The deposited lipids act as damage signals, leading to differentiation of monocytes into macrophages and foam cells. These cells release a range of pro-inflammatory stimuli such as TNFα, Il-1ß, IL-6 and IL-10[96] and contribute to a TLR-induced inflammation[159,160] thereby attracting more leukocytes and initiating smooth muscle cell (SMC) proliferation[161,162]. SMCs migrate from the media to intima layer releasing components such as collagen and elastin, forming a fibrous cap[163]. SMCs are also very plastic cells and are able to take up lipids which promotes the generation of a foam cell-like phenotype[161,164]. Over time, within the plaque microenvironment, dying macrophages release their lipid contents, and calcification leads to formation of a necrotic core[161] (Figure 2). The continuous influx of leukocytes results in an expansion of the necrotic core, restricting blood flow and leading to ischemic events downstream of the plaque. Eventually, thinning of the fibrous cap is caused by a decrease in SMC deposits due to their cell death[165] and degradation of ECM by proteinases such as metalloproteinases produced by macrophages and SMCs[166,167]. These now termed unstable plaques can rupture in some cases and release their contents (Figure 2). Plaque rupture is most likely caused by mechanical stress[154], further proteolytic degradation[168] or microcalcification[161,169,170]. The release of these thrombogenic components from the

necrotic core can lead to thrombus formation, potentially resulting in stroke or myocardial infarction.

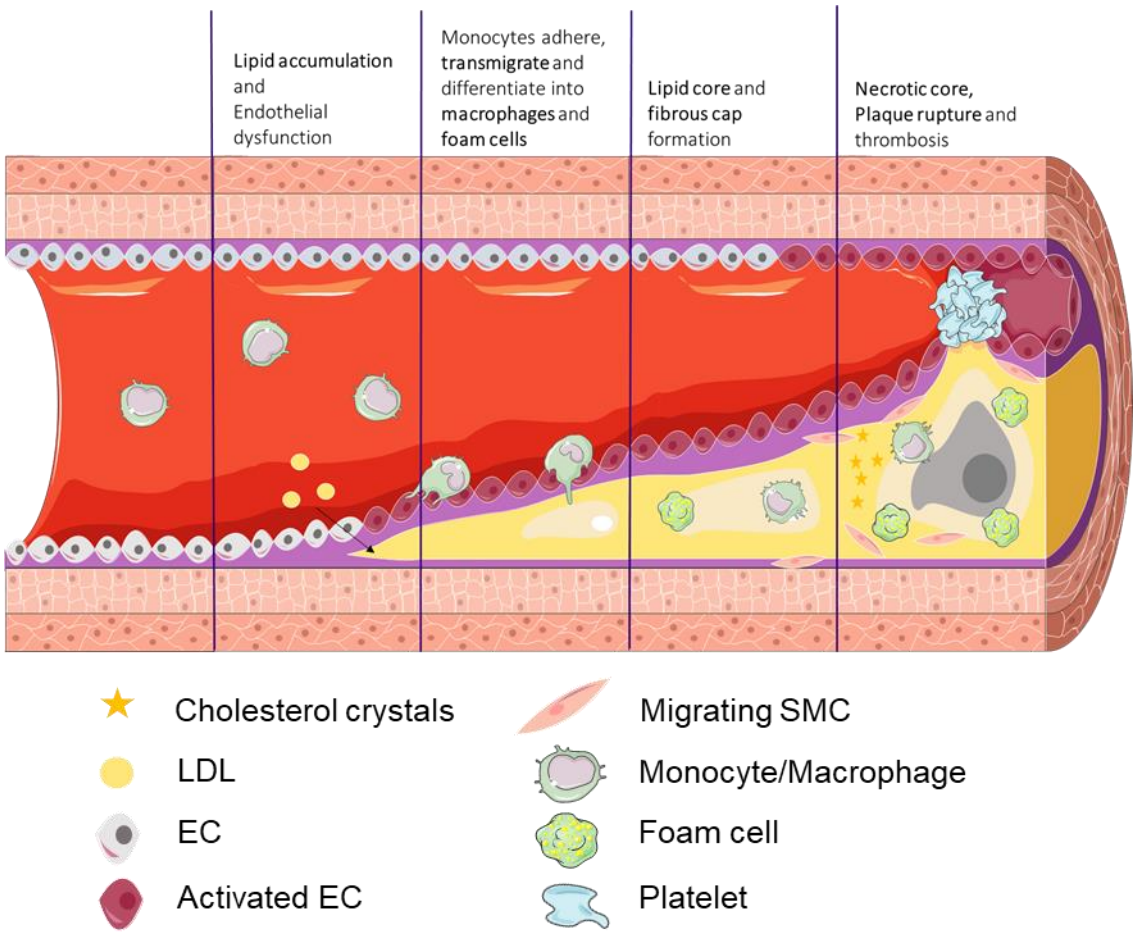

Figure 2: Atherogenesis and plaque formation. High levels of cholesterol in circulation can lead to the deposition of lipids in the vessel wall which causes the activation of the endothelial cell (EC) lining of the blood vessel. Monocytes are able to adhere to the endothelium and transmigrate into the intimal space where they differentiate into macrophages or foam cells by accumulating low density lipoproteins (LDL). These cells release pro-inflammatory stimuli which also promote migration of smooth muscle cells (SMC) and the release of collagen from these cells which forms the fibrous cap. In the later stages of atherosclerotic disease, excessive apoptosis leads to necrotic core formation. The fibrous cap can be degraded which can lead to plaque rupture. Thrombotic events such as stroke and myocardial infarction are a result of ruptured plaques which can have lethal consequences.

1.2.2. Role of monocytes and monocyte derived cells in atherosclerosis

Monocytes are involved in all stages of atherogenesis. Their migration into the vessel wall drives inflammation during the progression phase, but also can contribute to decreasing inflammation during resolution/regression.

Initially the activated endothelium at sites of lipid deposition facilitates monocyte transmigration into the intima. Monocytes and endothelial cells interact via selectins, such as P-selectin, in the capture phase of their recruitment and roll along the vessel wall[6,32]. This enables monocytes to come into contact with chemokines, presented by GAGs on the luminal side of the endothelium, which activates them[40]. Activation of monocytes leads to L-selectin (CD62L) shedding and conformational changes in monocytic integrins such as VLA-4 and Mac-1, enabling their interaction with adhesion molecules ICAM-1 and VCAM-1 on the endothelial surface. These interactions are followed by monocyte arrest. For example, the interaction of CCL5 on murine Ly6C^{hi} monocytes with CC-chemokine receptor (CCR) 5 and CCR1 is required for their arrest[171], while the interaction between ICAM-1 and Mac-1 leads to firm adhesion[6]. Before monocyte migrate into the intima, they follow chemokines secreted by endothelial cells, macrophages and smooth muscle cells, particularly CCL2, fractalkine (CX_3CL1) and CCL5[172,173]. For example, studies using Apolipoprotein E deficient ($ApoE^{-/-}$)CC-chemokine receptor deficient 2 ($CCR2^{-/-}$) mice on high fat diet showed decreased atherosclerotic lesions area and macrophages in the aortic sinus compared to $ApoE^{-/-}$, highlighting the role of CCL2/CCR2 interaction in atherogenesis[173]. Upon migration into the intima, monocytes differentiate into macrophages and foam cells by taking up LDL through the LDL receptor. The activity of this receptor is downregulated by increased cellular cholesterol levels, particularly during the early stages of foam cell

formation[174]. However, scavenger receptors such as CD36 and LOX1 recognize modified LDL which also promotes foam cell formation[175]. Modified LDLs are taken up by these cells and then metabolically transformed in the endolysosomal system to fatty acid esters[176]. The accumulation of these esters as well as free cholesterol in cells and cell membranes results in enhanced pro-inflammatory signalling through TLRs[160,177] and cell stress which leads to apoptosis[178,179]. Surrounding macrophages help clear these dead cells through efferocytosis. However, an intact lipid metabolism is required for efficient efferocytosis. During atherosclerosis, the lipid metabolism is disrupted which impedes efferocytosis. A combination of insufficient efferocytosis and increased cell death leads to the formation of a necrotic core within the plaque[97,179].

The excessive lipid accumulation also triggers more inflammatory responses: studies have shown that the phagocytosis of cholesterol crystals induces the NOD-, LRR- and pyrin domain-containing protein (NLRP) 3 inflammasome[180-182]. Furthermore, TLR also appear to contribute by the recognition of oxLDL by macrophages via CD14-TLR4-MD2 which results in the release of TNFα, IL-6 and IL-10[96].

These studies highlight the crucial role of monocyte-derived cells in the progression of atherosclerosis, but monocyte-derived cells also play a significant part in the resolution of atherosclerosis[105,183-186]. A decrease of pro-inflammatory macrophages is a hallmark of atherosclerotic resolution and is mediated through different ways: I) suppressed recruitment of monocytes from circulation into plaque[186]; II) apoptosis of plaque macrophages[179] and III) emigration of macrophages from the plaque[185,187]. Studies have shown that during regression, the number of monocytes recruited to plaques is reduced significantly and in combination with macrophage apoptosis, leads to a reduction of macrophage numbers within the plaques, independent of macrophage

egress[186]. Nevertheless, studies have also demonstrated the importance of macrophage egress for regression[185] . It appears that chemokines CCL19 and CCL21 and their respective receptor CCR7 are required for this process[188], while mediators such as netrin-1 have been shown to prevent the emigration of macrophages from plaques and therefore inhibiting regression[187]. These studies highlight the importance of clearance of pro-inflammatory macrophages from plaques to promote plaque regression. However, regression also requires an enrichment of anti-inflammatory macrophages[184,189,190]. Studies have shown that monocytes are still recruited to the plaque during regression[191], but it appears, that Ly6C^{hi} monocytes are recruited and differentiate into M2-like macrophages[192]. While it is long known that IL-4 is required for the differentiation into M2 macrophages, a recent study by Weinstock *et al*., has shown, that the differentiation also depends on Wnt signalling[183]. IL-13 has been suggested as mediator of M2 polarisation in plaques as well[193]. The recruitment and differentiation of circulating monocytes into M2 macrophages is clearly important, however, further studies have revealed that already present macrophages can alter their phenotype to an anti-inflammatory phenotype during regression[189,191,194].

Overall, monocytes and monocyte-derived cells drive atherosclerotic progression as well as regression. Monocyte migration into plaques is crucial for these processes and further understanding how it is regulated will help to develop more targeted therapeutics.

1.2.3. Experimental models of atherosclerosis

Many of the findings in atherosclerotic studies are based on murine models of atherosclerosis. While wild type mice do not develop atherosclerosis unless fed a

Western type/high fat diet for extended period of time of several months[195], various knock out models have been developed to accelerate the investigation of atherogenesis *in vivo*. The first knock out model with accelerated atherosclerotic plaque formation was reported in 1992[196-198]. Plump *et al*., as well as Piedrahita and Zhang *et al*., generated (apolipoprotein E deficient) ApoE$^{-/-}$ mice and reported five times higher plasma cholesterol levels and foam-cell rich plaques in the aortas of these mice after three months. After eight months, these mice showed progressed lesions and severe occlusion of the coronary arteries[196]. The mouse model was designed based on ApoE being a part of the very low-density lipoprotein and being involved in cholesterol transport in cells[197]. Shortly after the publication of the ApoE$^{-/-}$ model, a second knock down mouse model for atherosclerosis was published: the ApoE receptor knock out Ldlr$^{-/-}$ mouse[199]. Ishibashi *et al*., reported a two-fold increase in plasma cholesterol levels compared to wild type mice. This mouse model was based on the role of the LDL receptor (LDLr) in the removal of LDL from plasma by binding to ApoE in intermediate density lipoproteins (IDLs) which have been cleaved from very low density lipoproteins (VLDL) by protein lipases. These IDLs are cleared in to the liver[199]. Interestingly, Ishibashi *et al*., also reported that they were able to rescue the model by the intravenous injection of a recombinant replication deficient adenovirus encoding the human LDL receptor[199]. Both of these knock out mouse models show even more accelerated atherosclerotic plaque formation when these mice were placed on a high fat (Western) diet which increases total cholesterol plasma levels even more compared to a standard chow diet[198,199]. Another approach is with the proprotein convertase subtilisin/kexin type 9 (PCSK9) gain-of function model. PCSK9 is a protein expressed by most cells and binds to the LDL receptor, preventing the uptake and

recycling of LDL. By injection of a recombinant adeno-associated viral vector encoding PCSK9 into mice, followed by a high fat diet (HFD) hypercholesteremia is induced which results in atherosclerotic plaque formation[200]. This is a useful model since it can be induced via a single injection of virus particles and does not require crossing of mice strains with ApoE$^{-/-}$ or Ldlr$^{-/-}$ mice to establish the role of a certain protein in atherosclerosis.

While these mouse models are widely applied in atherosclerosis research, more recently, atherosclerotic regression came into focus and various mouse models have been developed to investigate this process. For example, aortic transplants of mice with atherosclerotic plaques are transplanted into mice on a chow diet[201]. Here, different mouse strains can also be combined to investigate the effects of certain proteins in atherosclerotic plaque regression. This model enables the investigation of migration of certain leukocyte subsets during regression if the respective leukocyte subset of the receiving mouse is expressing fluorescent proteins or is labelled. Another model of inducing atherosclerotic regression is the use of REVERSA mice. These mice are Ldlr$^{-/-}$ mice with a conditional inactivation of the microsomal triglyceride transfer protein large subunit (*Mttp*) gene[189]. The inactivation of *Mttp* results in the reversal of hyperlipidemia and regression of atherosclerosis. Other approaches of inducing regression are injection of mice with progressing atherosclerosis with either anti-sense oligonucleotide (ASO) to Apolipoprotein B (ApoB)[183,202] or injection with recombinant replication deficient adenovirus encoding the gene that was originally knocked out of the respective mouse strain, for example human LDL receptor into Ldlr$^{-/-}$ mice[199] or ApoE into ApoE$^{-/-}$[186]. The ASO approach is very useful as it can be used in combination with the PCSK9 gain-of-function model to first induce progression and later regression,

making it possible to use any kind of wild type or knock out model for atherosclerotic *in vivo* studies.

1.3. Galectins

Galectins (Gal) are a family of ß-galactoside binding lectins. They are found in almost all species from sponges[203] to mammals and to date 16 human galectins (Gal-1 to -16) have been identified. These highly evolutionarily conserved proteins bind ß-galactoside residues on glycoproteins or -lipids on cell surfaces or in the extracellular matrix[204] via carbohydrate recognition domains (CRD)[205]. Most galectin CRDs recognise highly specific ß-galactoside regions, however studies have shown that the binding affinities to these structures are relatively low[206]. These interactions enable galectins to carry out a wide range of functions, from cell adhesion to cell differentiation and inflammation regulation.

1.3.1. Galectin structure and binding specificity

Galectins can be divided into three groups based on their structure: I) prototype, II) chimeric type and III) tandem-repeat galectins (Figure 3). All galectins consist of at least one CRD of about 130 amino acids which are formed of two antiparallel β-sheets composed of five and six β-strands each[204]. The first type of galectins are prototype galectins and include Gal-1, -2, -5, -7, -10, -11, -13, -14, -15, and -16. They are made up of a single CRD but can form homo- or heterodimers[204]. Gal-3 is the only known chimeric type and consists of one CRD with a long N-terminal tail. Gal-4, -6, -8, -9 and -12 make up the tandem-repeat type galectins which are made up of two distinct CRDs which are connected by a linker domain. The length of the linker region can be between around 5 and 50 amino acids and determines the galectin isoform. Studies have shown

that different isoforms can have different functions[207]. While the CRDs define the structure and the ß-galactoside specificity, it is only certain residues within the CRD which directly interact with these glycans[208]. With the exception of Gal-10 which appears to have a preference to ß-mannosides, each CRD has a preference for a specific ß-galactoside containing glycan structure. For example, Gal-1 is known to bind poly-N-acetyllactosamine chains while the Gal-3 CRD preferentially binds repeating [-3Galβ1-4GlcNAcβ1-]n structures[204,209]. The two CRDs of tandem-repeat galectins have distinct binding preferences. For example, the C-terminal CRD of Gal-8 binds to GalNAcα1-3(Fucα1-2)Gal residues while the N-terminal CRD binds to α2-3-sialylated glycans[210].

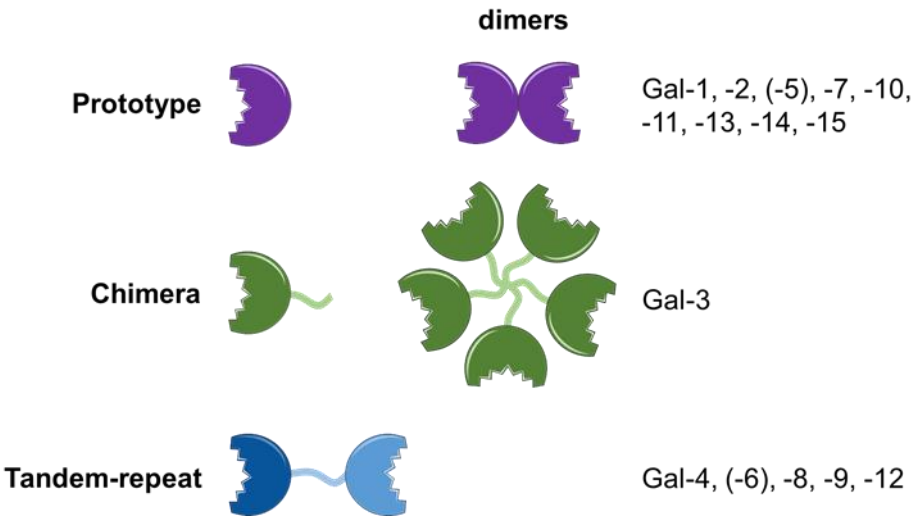

Figure 3: Structure of Galectins. Galectins are divided into three groups based on their structure: Prototype, Tandem-repeat and Chimera. Prototype are formed of one Carbohydrate Recognition Domain (CRD) but can form homo- and heterotypic dimers or multimers. Tandem-repeat galectins consist of two distinct CRDs which are connected by a linker region. The two CRDs can have different functions and different isoforms can occur depending on the length of the linker region. Only a single chimeric galectin has been identified to date: Gal-3. It is made up of a C-terminal CRD and a longer N-terminal tail.

More complexity to the structure of galectins is added by the formation of bivalent or multivalent oligomers[211]. These oligomers can be homo-oligomers or hetero-oligomers formed with other galectins[211] and can result in clustering of binding partners. Homodimers of prototype galectins are held together by noncovalent electrostatic forces which are concentration dependent[206,212]. Gal-3, the only chimera type galectin also forms oligomers and it has been proposed that its proline, glycine and tyrosine rich residues in the N-terminus contribute to this activity[204,206,212].

1.3.2. Export from the cell

Galectins are expressed by a range of different cell types, including endothelial cells and leukocytes, localised throughout several cellular compartments[213-215]. Their expression and release can be altered in various pathological settings[216-220].

Galectins lack a classical signal peptide and are therefore thought to be released from cells via a non-classical secretory pathway. However, it is postulated that the secretion or release of galectins is a tightly controlled mechanism since galectins have different, and sometimes even opposing functions intra- and extracellularly[221]. For example, extracellular Gal-3 can induce apoptosis in T-cells whereas it inhibits cell death intracellularly[222].

Various possible secretory and extracellular transport pathways for galectins have been proposed to date (Figure 4). The vast majority of studies have focused on mechanisms involved in the release of Gal-1 and Gal-3. Several groups have proposed roles for Gal-3 in the formation of lipid rafts and trafficking of intracellular organelles, however, the exact mechanism of transport remains unclear[223]. Multiple studies have demonstrated the release of Gal-1-rich extracellular vesicles via ectocytosis[224,225].

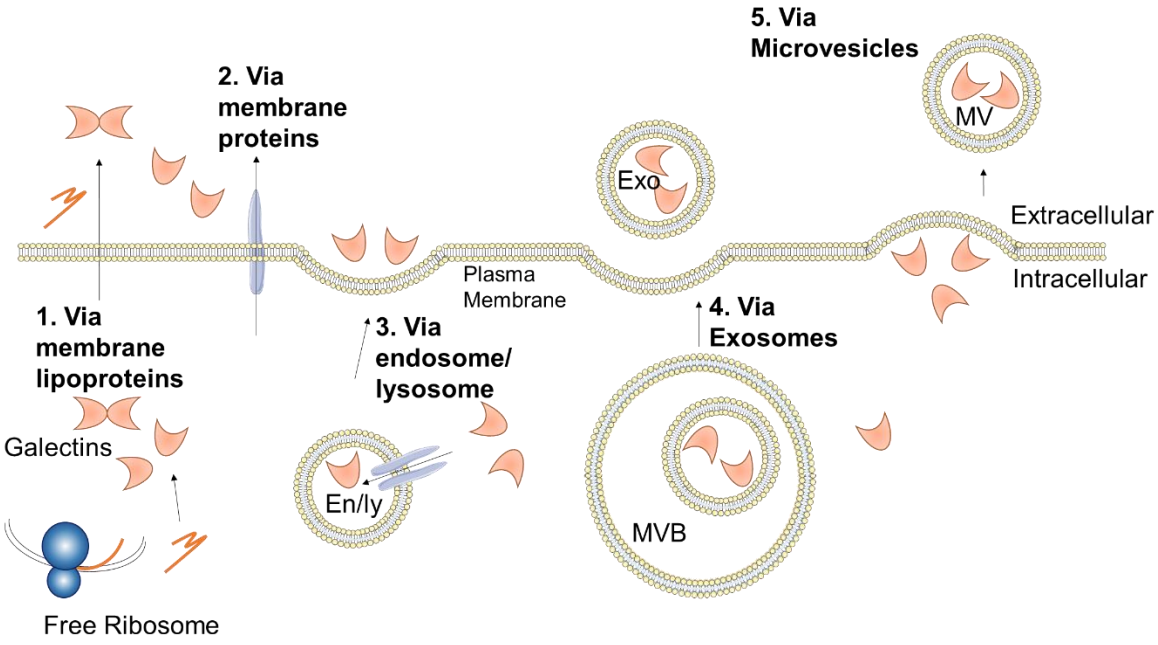

Figure 4: Release of Galectins. Galectins do not have a classical signal peptide and are therefore released via a non-classical pathway from the cell. Different studies have suggest a variety of pathways which are summarised in this figure. Galectins have been found to directly interact with membrane proteins or lipoproteins to directly cross the cell membrane. Other studies have shown that galectins are found in endosomes and suggested that galectins are released via the endosomal pathway (En/ly). Furthermore, exosomes (Exo), enriched with galectins have been identified suggesting a tightly regulated export via exosomes. Another vesicle based export pathway which has been suggested is via microvesicles bodies (MVB). Galectins have been found at areas of microvesicular budding on the cell membrane and in microvesicles (MV) released by cells

A further mechanism for the release of galectins from cells via vesicles has been described for Gal-9. A study by Keryer-Bibens *et al*. demonstrated the presence of Gal-9 in exosomes released from EBV- infected nasopharyngeal carcinoma cells[226] (Figure 4). Other mechanisms involving a direct translocation across the cell membrane have also been proposed. It has been reported that Gal-3 can cross the lipid bilayer by a

direct interaction with membrane lipids[227] (Figure 4). A study on Gal-1 demonstrated the requirement of molecular interactions of integral and peripheral membrane proteins for the transport across membranes[228].

However, more evidence is required to determine whether these proposed mechanisms of release apply to other galectins.

1.3.3. Galectin functions

To date, galectins are known to have great diversity of intra- and extracellular functions. Various studies have demonstrated that galectins can modulate the cell cycle/apoptosis, RNA processing and cellular differentiation but also in pathological processes such as tumorigenesis and immune responses[223].

Intracellularly, galectins have been shown to interact with proteins such as B-cell lymphoma-2 (Bcl-2), Bcl-2 associated X (Bax), CD95 or synexin, which are all involved in apoptosis[204,222]. For example, a study by Harazono *et al*. demonstrated the ability of Gal-3 to heterodimerise with Bax and prevent apoptosis in thyroid carcinoma cells[222]. In contrast, the interaction between Bcl-2 and Gal-7 has been shown to trigger the intrinsic apoptotic pathway by releasing apoptogenic factors from the mitochondrial membrane, such as cytochrome c or Smac/DIABLO[229]. Furthermore, Gal-1 and Gal-3 have been proposed to play roles in pre-mRNA splicing which is critical for mRNA stability of glycoprotein Mucin-4, a main component of mucus[230-232].

Once released from cells, galectins can act in a wide range of functions. They have been shown to bind to cell membrane proteins modulating cell activity or forming cell-cell and/or cell-matrix interactions. Extracellular Gal-9 for example supports monocyte-derived dendritic cell maturation by inducing phosphorylation of Mitogen-activated

protein kinase (MAPK) p38 and ERK1/2[233]. Gal-1 has been shown to cause the co-clustering of CD43 and CD45 on DCs and in turn activating DCs by mediating Syk and protein kinase C tyrosine kinases[233]. However, on T-cells, Gal-1 binds CD43 and CD45 but separates them into different clusters with CD7 and CD3 respectively[234]. Differential clustering has been suggested to be necessary for the induction of apoptosis[234]. Other galectins, such as Gal-3, have also been found to cause co-clustering or form lattices with cell-surface proteins [204]. Gal-1 and -3 also form interactions between cells and the ECM[235,236]. Gal-3 was proposed to mediate the interaction between integrins and the ECM which regulated cell migration and promoted wound healing in monkey corneal epithelium[236]. Furthermore interactions between pathogens and cells can also be mediated by galectins. Kleshchenko *et al*. found Gal-3 promoted the adhesion of Trypanosoma cruzi to human coronary artery smooth muscle cells[237].

1.3.3.1. Galectins in Inflammation

Galectins have been identified as modulators of immune regulation. They are expressed endogenously in a range of immune cells but can also act as exogenous soluble proteins.

Gal-1 drives naïve T-cells towards a Th2 phenotype by inducing apoptosis in Th1 and Th17 cells. This specificity in regulation of cell polarisation or death results from differential sialylation of glycoproteins in different T-cell subsets which in turn alters the binding affinity of the galectin. Other galectins have also been shown to induce apoptosis in different subsets of T-cells such as Gal-2, Gal-3, Gal-4 and Gal-9 (reviewed in[211]). Galectins have been shown to affect other immune cells including B-

cells, neutrophils and monocytes. Gal-1 activates and polarizes macrophages towards an M2 phenotype[211]. Gal-9 on the other hand was observed to promote an anti-inflammatory programme by inhibiting the production of IL-1β and TNFα but upregulating IL-10 in immune complex-stimulated macrophages[211]. A preclinical model of pristane-induced lupus also indicated a pro-inflammatory function for Gal-9 since Gal-9 deficient mice exhibited less severe nephritis and arthritis[238]. Various galectins modulate neutrophil function. Gal-1 for example disrupts the interaction between neutrophils and endothelial cells while Gal-4 induces phosphatidylserine exposure selectively on activated neutrophils[211].

Interestingly, various studies have demonstrated increased levels of soluble galectins in serum or plasma of patients with inflammatory diseases such systemic sclerosis, atherosclerotic stroke and systemic lupus erythematosus (SLE)[239-241].

1.3.3.2. Galectins in leukocyte trafficking

Galectins are also implicated in leukocyte recruitment (Figure 5). Even though from the same protein family, different galectins have been shown to affect leukocyte migration in opposing manner. Exogenous Gal-1, for example inhibits rolling of polymorphonuclear cells (PMN) *in vitro* as well as *in vivo* during acute inflammation[242,243] (Figure 5). Conversely, endogenous chimera-type Gal-3 has been reported to promote recruitment of PMN and lymphocytes *in vivo*[244,245]. Impaired slow rolling and emigration was observed in Gal3$^{-/-}$ mice during acute inflammation, while the administration of recombinant Gal-3 reduced rolling velocity and increased the number of adherent neutrophils and monocytes *in vivo*[245] (Figure 5). The *in vitro* models support direct effects of Gal-1 and−3 on leukocyte migration. However, *in vivo*

studies using endothelial-specific knock out mice or bone marrow chimera models could help to distinguish between the role of endogenous galectins in hematopoietic and non-hematopoietic cells in context of recruitment[246,247].

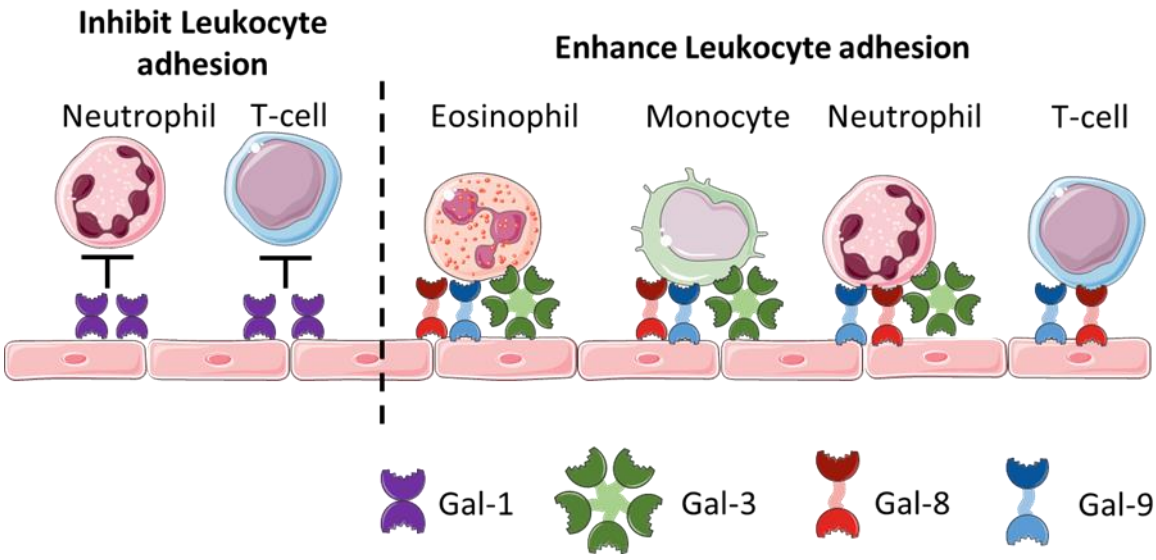

Adapted from Cooper et al. 2012

Figure 5: Galectins can modulate leukocyte trafficking. Galectins have a wide variety of functions in the immune system. The leukocyte trafficking cascade has been shown to be modulated by galectins. Galectin-1 has been shown to inhibit the recruitment of T-cells and neutrophils. On the other hand, Gal- 2, -3, -8 and -9 have been shown to increase leukocyte recruitment.

Various studies have also investigated the role of galectins in the next step of the migration cascade: adhesion. For example, a study revealed Gal-3 can mediate chemokine function. The study revealed Gal-3 forms heterodimers with CXCL12[248] a chemokine known to interact with C-X-C chemokine receptor (CXCR) 4. This interaction between CXCL12 and CXCR4 is known to modulate tissue infiltration of neutrophils and monocytes in myocardial infarction and atherosclerosis[249-251]. Eckardt *et al*. showed that Gal-3 inhibited CXCL12 mediated migration of neutrophils and

monocytes *in vitro* as well as the infiltration of the peritoneum *in vivo*. The study also showed that the recruitment of classical monocytes *in vivo* was significantly increased to the peritoneum of Gal-3$^{-/-}$ mice after thioglycollate treatment compared to wild type mice, further indicating a role for Gal-3 in CXCL12 mediated recruitment of classical monocytes. Whether circulating Gal-3, which is upregulated in various inflammatory pathologies[239,252,253] is also able to interfere with CXCL12 mediated leukocyte recruitment in situ remains unknown. The authors of the study nevertheless suggest that, based on their data, the CRD of Gal-3 may be a promising anti-inflammatory target. Other galectins have also been shown to modulate leukocyte adhesion[242,245,254,255]; multiple studies have found that Gal-1 inhibits leukocyte extravasation[242,254,256]. Conversely, several other galectins have been shown to promote leukocyte adhesion to the endothelium[255]. Yamamoto *et al*. treated peripheral blood leukocytes with Gal-8 (Figure 5), and found increased adhesion to human umbilical vein endothelial cells (HUVECs) which they believed was α4-integrin-dependent. An important caveat of this study was that these assays were performed under static conditions. Due to the lack of physiological flow, the leukocytes automatically come into contact with the endothelium and the effect of these galectins on the capture of leukocytes by the endothelium cannot be assessed. The use of physiological flow would help to uncover whether galectins also affect the capture, and therefore adhesion and transmigration.

1.3.3.3. Galectins in atherosclerosis

Galectins are involved in many inflammatory diseases and some studies have highlighted their role atherosclerosis. He *et al*. tested Gal-1 serum levels in patients with larger artery atherosclerotic strokes at day 1 and 6 as well as 4 weeks post stroke

as well as in age and sex-matched controls. In their study, He *et al*. found that Gal-1 levels were upregulated 4 weeks after the stroke occurred, compared to the healthy controls, suggesting that Gal-1 serum levels may be associated with large artery atherosclerotic stroke[239]. Gal-1 levels in plaques however do not change with increasing inflammation as shown by Lee *et al.*, when they compared Gal-1 levels using immunohistochemistry in plaques of ApoE$^{-/-}$ mice on high fat diet for either 16 or 26 weeks[257]. They also showed that statin treatment did not alter Gal-1 mRNA and protein levels either[257]. Furthermore, a study investigating VSMCs showed that Gal-1 increased VSMC binding to extracellular matrix (ECM) components by strengthening the integrin-ECM interaction and thereby decreasing vascular smooth muscle cell (VSCM) motility[258]. Since VSMC motility is an important part of atherogenesis, Gal-1 may play a role in this pathological process. However this needs further investigation.

Numerous studies have also shown that Gal-3 levels in serum or plasma are increased as a result of peripheral[259-263] or coronary artery disease[264-266], large artery atherosclerotic stroke[239] in humans and diet-induced atherosclerosis in ApoE$^{-/-}$ mice[257]. Many of these studies also show a positive correlation between the Gal-3 levels in serum or plasma and the severity of the disease[262,266,267] or inflammation markers such as CCL2 or CRP. Other studies looked at Gal-3 binding protein which was also increased in plasma levels of coronary artery disease patients and was associated with long-term mortality[268]. Investigations of Gal-3 binding protein levels as part of a 4-biomarker signature in vascular extracellular matrix of atherosclerosis patients showed a positive correlation of ECM levels with atherosclerosis progression and incidences of cardiovascular diseases[269]. These studies all highlight the use of Gal-3 and Gal-3 binding protein as biomarkers for (the severity of) arterial disease. Especially since

Gal-3 also can be used to differentiate inflammatory cardiovascular disease from other inflammatory diseases such as diabetes mellitus[265] or rheumatoid arthritis[263]. However, it has to be used in combination with other biomarkers to make reliable predictions and a standardised ELISA test has to be established since the detected levels vary greatly (between average values of 4.5[261] - 17.6 ng/ml[259] in arterial disease patients and 2.8[261] -14.4[259] ng/ml in healthy controls).

In vivo studies using ApoE$^{-/-}$ Gal-3$^{-/-}$ mice showed that these mice had significantly lower numbers of atherosclerotic lesions and atheromatous plaques as well as smaller plaques with a smaller lipid core and less collagen compared to ApoE$^{-/-}$ mice[270 271], highlighting the role Gal-3 in atherogenesis, not just as biomarker. Additional studies have demonstrated two separate pathways in which Gal-3 enhances the activation of endothelial cells by oxidised low density lipoprotein (oxLDL). Chen *et al.* demonstrated that Gal-3 increases oxLDL-mediated upregulation of inflammatory markers Il-1ß, IL-6, IL-8, CXCL-1, CCL2, ICAM-1 and VCAM-1 on HUVECs through a ß1-integrin-RhoA-JNK mediated pathway[272]. On the other hand, Ou *et al.* highlighted a different pathway leading to increased inflammation of HUVECs after oxLDL-mediated inflammation. They found that Gal-3 promoted inflammation by upregulating LOX-1, a oxLDL receptor, which mediates a Reactive oxygen species (ROS)/p38/NF$_K$B-mediated signalling pathway, leading to increased adhesion molecule expression and resulting in increased adhesion of monocytic cells as well as IL-8 secretion[273]. Whether the different pathways leading to enhanced activation of oxLDL-stimulated HUVECs occur due to the different amounts of Gal-3 (250 ng/ml [272] and 2.5-20 µg/ml[273] or different sources of the oxLDL used needs to be established. Increasing adhesion of monocytic cells by activating the endothelium[273] is not the only way in which Gal-3 contributes to

monocyte-mediated atherogenesis. An earlier study has shown that Gal-3 induces monocyte and macrophage migration in a concentration dependent manner[274]. Lee *et al.* initially showed a positive correlation between macrophage content and Gal-3 content of plaques in ApoE$^{-/-}$ mice on high fat diet[257]. Madrigal-Matute *et al*. furthered this and identified Phorbol myristate acetate (PMA)-activated monocytes and macrophages as source of Gal-3 which was released through a pathway involving exosomes[267]. Furthermore, Di Gregorli *et al.* have recently shown that Gal-3 marks a macrophage subset in atherosclerotic plaques with potentially beneficial characteristics by regulating macrophage polarisation as well as invasiveness which leads to a slower plaque progression[253]. Further investigations need to be done to show how Gal-3 can act as pro- and anti-atherogenic factor.

The phenotypic change of vascular smooth muscle cells as well as their migration marks atherosclerotic progression. Fort-Gallifa *et al*. showed that the Gal-3 expression patterns in the arterial wall differed between PAD patients and healthy controls: in healthy controls, Gal-3 was mainly in the adventitia whereas in PAD patients, Gal-3 was mainly found in the media, adjacent to SMCs[260]. Another study by Tian *et al.* further highlights the role of Gal-3 on VSMCs in atheroprogression. Using Gal-3 knockdown in SMCs, they showed that endogenous Gal-3 expression in VSMCs upon oxLDL stimulation is essential for the phenotypic change marked by increased osteoponin, calponin and alpha-actin expression leading to increased migration, proliferation as well as phagocytosis[275]. They suggested that a canonical Wnt/ß-catenin signalling pathway is responsible for this Gal-3 mediated phenotypic shift. The same group further expanded the understanding of how Gal-3 is involved in SMC regulation in a follow up study. They showed that exogenous Gal-3 also promoted

human umbilical vascular smooth muscle cell (HUSMC) proliferation and migration as well as the proteins marking the phenotypic changes in their previous study. These changes are triggered through a Wnt/ß-catenin signalling pathway[276]. Menini *et al.* showed that the same pathway is involved in Gal-3/RAGE mediated calcification patterns of VSMCs[277]. These findings were further expanded by a study in the commonly applied atherosclerotic *in vivo* model using ApoE$^{-/-}$ mice. Sun *et al.* showed that Gal-3 and RAGE regulate sortilin in opposite ways, resulting in up- and downregulation respectively. This consequently lead to different calcification patterns where RAGE caused microcalcification and Gal-3 caused macrocalcification of atherosclerotic plaques in the ApoE$^{-/-}$ mice[278].

These studies show that Gal-3 is contributing in various ways to atheroprogression but also its ability to act as beneficial regulator in macrophages, highlighting the complex activity of Gal-3. To investigate its potential as therapeutic target, several studies used modified citrus pectin (MCP), a carbohydrate known to bind Gal-3. They treated ApoE$^{-/-}$ mice on high fat diet with MCP *i.v.* and found that the treatment decreased plaque volume[271], atherosclerotic lesion numbers as well as decreased macrophage and smooth muscle cell numbers[279]. Lu *et al*. also showed that MCP treatment has an direct effect on monocyte adhesion to oxLDL stimulated endothelium by decreasing adhesion[279]. The short-term treatment of ApoE$^{-/-}$ mice on high fat diet with atorvastatin, a statin, decreased Gal-3 mRNA and protein levels in aortic plaques[257]. Another study in patients with carotid artery atherosclerosis however showed that long term treatment with statins increased Gal-3 intraplaque levels but decreasing macrophage numbers inside of plaques[280]. They concluded that this might mediate plaque stabilisation[280]. These studies clearly highlight the therapeutic potential of Gal-3, either as therapeutic

or as target. However, further studies are needed to understand the complex mechanisms in which in acts in atherogenesis to be able to use it as successful therapeutic target.

To date, only a limited number of studies have analysed Gal-9 in context of atherosclerosis. A study reported increased serum levels of Gal-9 in patients suffering from large artery atherosclerotic stroke and reported[239]. Interestingly, a study which measured Gal-9 serum levels in coronary artery disease patients found decreased levels compared to healthy controls[218]. The study also evaluated the effects of Gal-9 on T-cells. They reported that Gal-9 shifted T-cell phenotypes towards T_{regs}, while suppressing T-helper 17 cells, therefore decreasing IL-17 production[218] which are both crucial for the resolution of atherosclerosis[105]. Furthermore, Gal-9 treated peritoneal macrophages release less pro-inflammatory cytokines than Phosphate buffered saline (PBS) treated peritoneal macrophages when stimulated with heat-aggregated IgGs[281]. These findings suggest that Gal-9 could have an atheroprotective role, as was suggested in a recent review[282]. Furthermore, a study investigating the effects of galectins on leukocyte adhesion found that the incubation of monocytes with Gal-9 increased their adhesion to HUVECs[255]. However, the transmigration of monocytes was not quantified and whether the increased adhesion might contribute to increased plaque formation needs to be further established. However the role of Gal-9 in the development of atheroma, particularly in context of monocytes has not yet been investigated and requires further research.

1.3.4. Galectin-9

Gal-9 is 36 kDa-large protein, encoded in humans by the *LGALS9* gene and located on Chromosome 17, long arm at locus 11.2 (17q11.2). It belongs to the tandem-repeat subset of the ß-galactoside binding galectin family. Gal-9 is made up of two distinct CRDs at the C- and N-termini which are connected by a flexible linker region. The N-terminal CRD consists of 148 amino acids and is connected to the 149 amino acid long C-terminal CRD via a 14-56 amino acid long linker. The length of the linker region determines the isoforms of Gal-9 which are generated through post-transcriptional splicing. So far five variants have been found: full length Gal-9 and Gal-9 with deletions of exons 5, 6 or 10 in various combinations[283]. Studies have shown that three different isoforms of Gal-9 have different functional characteristics. Zhang *et al*. demonstrated that the expression of the longest isoform decreased the expression of E-selectin in LoVo cells whereas the other two isoforms increased E-selectin expression[207].

Gal-9 is expressed in a wide range of tissues at different levels of expression[213,214,284-289]. Studies in endothelial cells for example have shown that Gal-9 is upregulated when these cells are treated with pro-inflammatory stimuli such as IFNγ[214,288] or double stranded RNA (Poly I:C)[289,290]. A series of studies have reported increased serum or plasma levels of Gal-9 in patients with various inflammatory diseases such as SLE[241], autoimmune hepatitis[291], systemic sclerosis[240], rheumatoid arthritis[292] and large artery atherosclerotic stroke[239] while a recent review suggested that circulating Gal-9 levels correlate with diseases severity[293]. These studies indicate a disease/ inflammation specific regulation of Gal-9 expression, which suggests that its function is associated with inflammatory processes.

Previous studies have identified various functions of Gal-9 intra- and extracellularly. The variety in functions has been attributed to the differences in binding affinities of the two CRDs. The C-terminal CRD primarily recognises receptors and induces downstream signalling whereas the N-terminal CRD and linker region contribute to the potency of the signalling process[294].

Many functions of Gal-9 are in immune regulation. Gal-9 induces apoptosis in T_H1 and T_H17 cells via TIM3 binding, but not in T_H2 cells [295]. More recent studies on Gal-9 binding to T-cells identified Protein disulphide isomerase (PDI) as a binding partner of Gal-9 and thereby increasing T-cell migration through ECM via β3-integrins[296]. In macrophages, Gal-9 has been shown to modulate the expression of FcγR[211]. Other studies concerning the extracellular function of Gal-9 on macrophages have demonstrated its ability to suppress the production of TNFα and IL-1β and enhance the release of IL-10 production following stimulation with immune complexes[211]. Interestingly, Matuusra *et al*. showed that the overexpression of Gal-9 in THP-1 cells resulted in an increase in the mRNA expression of inflammatory cytokines IL-1α and IL-1β through interactions with nuclear factor (NF)-IL6[297]. Studies have also shown that Gal-9 induces pro-inflammatory cytokine production in T helper cells, dendritic cells and myeloid derived suppressor cells[298,299]. Gal-9 was first described as eosinophil chemoattract[300] and has since also been reported to promote monocyte chemotaxis[301]. To date, only a single study has investigated the role of Gal-9 on monocyte recruitment *in vitro*. Treatment of primary monocytes with soluble Gal-9 was shown to increase their adhesion to HUVEC under static conditions[255]. Additionally, it has been proposed that by forming lattices, Gal-9 can cluster several receptors and trigger interactions between cells[302]. Interestingly, various *in vivo* studies have reported seemingly

contradicting effects for Gal-9 in various models of inflammatory diseases: O'Brien *et al*. showed that direct injection of Gal-9 into knees of mice caused an increase in the knee circumference as well as an increase in F4/80^{+} macrophage infiltration[301]. On the other hand other studies also using exogenous Gal-9 have shown that it improved clinical symptoms such as arthritis in a murine model of SLE[303] and Arikawa *et al*. showed that injecting Gal-9 subcutaneously into mice with collagen induced arthritis resulted in an improvement of their clinical scores significantly[281]. These varying results of the effect of Gal-9 in inflammatory models highlight the necessity of a better understanding of Gal-9 modulated inflammation, particularly in leukocyte recruitment.

1.4. Aim and hypothesis

Based on previous research highlighting the immunomodulatory effects of Gal-9 in several models of inflammation the following hypothesis was formulated: "Gal-9 contributes to atherosclerosis in a pro-inflammatory manner by modulating monocyte recruitment". To challenge this hypothesis, several of the following aims were addressed:

a. Characterisation of Gal-9 expression in cells involved in atherogenesis: monocytes, macrophages and endothelial cells
b. Characterisation of effect of Gal-9 on monocytes and macrophages and their recruitment
c. Assessing atherosclerotic plaque progression in ApoE$^{-/-}$ Gal-9$^{-/-}$ mice on high fat diet

The results of this study might provide insight into a potential role of Gal-9 in atherogenesis which could hold potential as novel therapeutic target in the prevention of cardiovascular events by reducing atherosclerotic plaque progression.

1.5. Publications

1.5.1. Related to this thesis

a. **Krautter, F.**; Hussain, M.T.; Lezama, D.R., Brown, E.; Raucci, F.; Recio, C., Chimen, M., Maione, F.; Tiwari, A.; Cooper, D.; Fisher, E.A.; Iqbal, A.J. (2022), Galectin-9: a novel promoter of monocyte recruitment and atherosclerosis progression. (*In preparation)*

b. **Krautter, F.**; Iqbal, A.J (2021) Glycans and Glycan-Binding Proteins as Regulators and Potential Targets in Leukocyte Recruitment. *Front Cell Dev Biol*, 9, 624082.

c. **Krautter, F.**; Recio, C.; Hussain, M.T.; Lezama, D.R.; Maione, F.; Chimen, M.; Iqbal, A.J. (2020) Characterisation of endogenous Galectin-1 and -9 expression in monocyte and macrophage subsets under resting and inflammatory conditions. *Biomed Pharmacother*, 130, 110595.

1.5.2. Contributions to other publications during this PhD

a. Iqbal, A.J.; **Krautter, F.;** Blacksell, I.A.; Wright, R.D.; Austin-Williams, S.N.; Voisin, M.B.; Hussain, M.T.; Law, H.L.; Niki, T.; Hirashima, M.; Bombardieri, M.; Pitzalis, C.; Tiwari, A.; Nash, G.B.; Norling, L.V.; Cooper, D. (2022) Galectin-9 mediates neutrophil capture and adhesion in a CD44 and β2 integrin-dependent manner., *FASEB J.,* 36, e22065.

b. Gilbert, S.G.; **Krautter, F.;** Cooper, D.; Chimen, M.; Iqbal, A.J.; Spill, F. (2020) CASTLE: cell adhesion with supervised training and learning environment. *J. Phys. D: Appl. Phys.*, 53, 424002.

c. **Krautter, F.;** Hopkin, S.J.; Lewis, J.W.; Chimen, M.; McGettrick, H.M. (2019) Triggering the Resolution of Immune Mediated Inflammatory Diseases: Can Targeting Leukocyte Migration Be the Answer?. *Front Pharmacol*, 10, 184.

CHAPTER 2:

MATERIALS

AND

METHODS

2. Chapter 2: Materials and Methods

2.1. Ethical approval

All participants provided informed written consent before samples were collected. The use of biological samples for this study was approved by the local ethics committee. This study was conducted following Good Clinical Laboratory Practise and in accordance with the Declaration of Helsinki.

2.2. Stable form of recombinant Gal-9

The recombinant Gal-9 protein used in this study is a stable, linkerless form purchased from GalPharma. In order to reduce the susceptibility of Gal-9 to proteolysis, the linker region is removed, which increases its stability. Studies have revealed that the linkerless version of Gal-9 does not affect eosinophil chemoattraction[304]. However, differences between native forms and this recombinant form of Gal-9 in their functions due to the variable flexibility of the linker cannot fully be excluded.

2.3. Human blood leukocyte isolation

All healthy donors were required to be over 18 years old with no previous diagnosis of cardiovascular disease. Donors between 24 and 34 years were considered healthy young donors (HY, average age 28.00, SD 3.55). Healthy aged donors (HA) were between 56 and 82 years old (average age 68.16 SD 6.76) and matched the age of the peripheral arterial disease patients (PAD, average age 70.71 SD 9.85). The PAD patients were selected by a clinical assessment at Queen Elisabeth II Hospital, Birmingham.

Blood samples were collected via venepuncture in ethylenediaminetetraacetic acid (EDTA) coated Vacuette® tubes (Greiner Bio-One). Peripheral Blood Mononuclear

Cells (PBMCs) were isolated as previously described. Briefly, 5 mL whole blood was layered on top of 5 mL of Histopaque 1077 (Sigma Aldrich) in a round bottom tube and centrifuged at 800 g for 30 min (Figure 6). The resulting top layer of plasma was collected and stored at -80 °C. The PBMC layer was aspirated using Pasteur pipettes and diluted in 11 ml PBS without Ca^{2+} and Mg^{2+} (PBS(-/-),) before centrifugation at 300 g for 5 min. This step was repeated once before the cell pellet was diluted in 1 mL PBS(-/-) and cells were counted using the Cellometer Auto T4 (Nexcelcom Bioscience, USA).

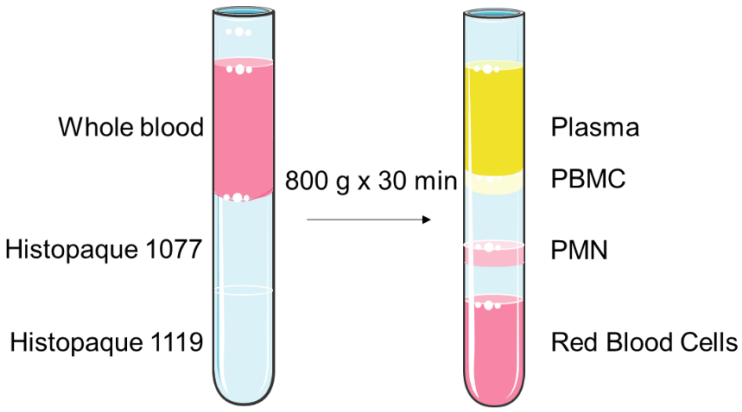

Figure 6: Separation of whole blood. In order to separate Peripheral blood mononuclear (PBMC) or Polymorpho nuclear cells (PMN) from other cell components, a sugar density gradient is used. Whole blood is layer on top of Histopaque with two different densities (1.077 g/ml and 1.119 g/ml) and centrifuged at 800 g for 30 min at room temperature. The various components of blood such as blood plasma, PBMC or PMN can then be collected and processed further.

2.3.1. Gal-9 treatment of PBMC

In order to stimulate PBMC with Gal-9 in the presence or absence of lactose or sucrose, 1 x 10^6 cells per condition were incubated with 100 nM Gal-9 in PBS (+/+) for 20 min at room temperature. If lactose or sucrose were used to block Gal-9, a 25 mM

solution of each sugar was prepared in PBS (+/+) and 100 nM Gal-9 were added for 20 min at room temperature before the addition of the PBMC. N-formyl-methionyl-leucyl-phenylalanine (fMLP) treatment was used as positive control for monocyte activation. The PBMC were incubated with 1 µM fMLP in PBS (+/+) also for 20 min at room temperature. The PBMC were then stained with antibodies for flow cytometry analysis as described below in Chapter 2.5.

2.3.2. CD14+ Monocyte isolation

$CD14^+$ monocytes were isolated by washing PBMC in ice cold MACS buffer (PBS(-/-) supplemented with 0.5 % Bovine serum albumin (BSA) and 2 mM EDTA). After determining the cell number, per 1 x 10^6 cells, 80 µL of MACS buffer and 20 µL of magnetic anti-CD14 MicroBeads (Miltenyi) were incubated on ice for 20 min before separating $CD14^+$ monocytes from the other $CD14^-$ cell fraction using magnetic columns. The $CD14^+$ monocytes were eluted from the magnetic column using 5 mL MACS buffer. Cell numbers were determined by centrifugation of the eluate and resuspending the pellet in 1 mL MACS buffer before analysis on the Cellometer Auto T4 cell counter (Nexcelom). Purity of the cell isolation was determined using flow cytometric analysis of CD14 and CD16.

2.3.3. Macrophage culture

Macrophages were cultured by plating 3 x 10^5 $CD14^+$ monocytes per well of 24-well culture dish. The cells were initially cultured in Medium 199 (Gibco) + 0.1 % BSA for 45 min until the cells have adhered to the culture dish. The media was then replaced by Medium 199 containing 10ng/ml EGF (Sigma Aldrich) and 10 % autologous serum and the cells were cultured for 6 days. On day 6 the macrophages were treated with

Medium 199 containing 10 ng/ml EGF and 1 % autologous serum with either 100 ng/ml LPS (Sigma Aldrich) and 20 µg/ml IFNγ (Peprotech), to generate M1 phenotype macrophages, or with 20 ng/ml IL-4 (Peprotech) to generate M2 phenotype macrophages in the presence or absence of 100 nM Gal-9 for 24 h.

2.4. Human Umbilical Vein Endothelial Cell isolation and culture

Umbilical cords were collected from donors who gave their informed consent and underwent elective C-sections at City Hospital Birmingham.

2.4.1. HUVEC isolation from umbilical cords

A previously published protocol was followed to isolated HUVECs[305]. Briefly, umbilical cords were stored at 4 °C for up to 24 h until isolation of vein endothelial cells. PBS (-/-) was used to clean the intubated vein from any remaining blood, before the PBS (-/-) was removed. 1 mg/ml collagenase Type Ia (Sigma Aldrich) in PBS (-/-) was passed into the umbilical cord vein and incubated for 15 min at 37 °C. Following the incubation period, the umbilical cord was carefully massaged and the collagenase solution containing the endothelial cells was flushed out of the umbilical vein with PBS (-/-). The cell suspension was centrifuged at 800 g for 5 min and the cell pellet was resuspended in M199 medium supplemented with 10 ng/ml human epidermal growth factor, 1 µg/ml hydrocortisone (Sigma Aldrich) , 2.5 µg/ml amphotericin B (Sigma Aldrich), 1 % penicillin and streptomycin (Sigma Aldrich) and 20 % fetal calf serum (Merck) and transferred to tissue culture treated cell culture flasks. HUVECs were cultured in standard culture conditions (37 °C, 5 % CO_2). Once cells reached 80-90 % confluency, cells were lifted by washing them with 0.02 % EDTA and then treating them with 2.5 mg/ml trypsin until the cells dissociated from the surface. Trypsin was inactivated by

the addition of culture media. The cell suspension was centrifuged at 800 g for 5 min and the pellet was resuspended in the culture media and seeded into respective culture dishes. HUVECs were used in assays between passages 1-3.

2.4.2. Culture of commercially available HUVEC

Commercially available, single-donor cells (Promocell) were cultured in Endothelial Cell Growth Medium (ECGM, Promocell) in standard culture conditions and used at passage 6.

2.4.3. HUVEC stimulation

In order to activate HUVECs, the cells were treated with 20 ng/ml TNFα, 20 ng/ml IFNγ, a combination of the two or with 20 µg/ml Poly I:C (Tocris) in M199 containing 2 % Fetal Calf Serum (Merck). The cells were stimulated for 4-48 h and their mRNA and protein levels were analysed using quantitative polymerase chain reaction (qPCR) and flow cytometry respectively. The supernatant of the various culture conditions were also collected for subsequent analysis for Gal-9 levels with Enzyme-linked Immunosorbent assay.

2.4.4. Knock down of Galectin-9 in HUVEC

3.33×10^5 commercially available HUVEC at passage 5 were seeded into each well of a 6-well culture dish and grown for 24 h to reach confluency. The endothelial monolayers were treated with either 25 nM Gal-9 siRNA (Qiagen; FlexiTube GeneSolution GS3965 for LGALS9, Cat# 1027416) or 25 nM control siRNA (Negative control siRNA, Qiagen, Cat# 1027310) in OptiMEM reduced serum medium (Gibco) containing Lipofectamin RNAiMax (Invitrogen) for 4 h at standard culture conditions. The treatment was removed and replaced with ECGM and cultured for another 20 h.

Then, endothelial cells were detached using Accutase™ Cell Dissociation Reagent (Accutase, Gibco) and seeded into µ-Slide IV 0.4 channel slides (ibidi). 4 h after seeding, the endothelial cells were treated with ECGM with or without 20 µg/ml Poly I:C and incubated for 24 h. Knock down of Gal-9 and activation of cells was confirmed by flow cytometric analysis of Gal-9 and ICAM-1 levels.

2.5. Quantitative polymerase chain reaction

qPCR was applied to quantify mRNA levels.

2.5.1. Total RNA extraction

RNA was extracted using RNEasy Mini Kit (Qiagen) according to the manufacturer's instructions. Briefly, the respective cells were lysed in 350 µl RLT buffer and stored at -80 °C. After defrosting, samples were added to Qiashredder spin columns (Qiagen) and centrifuged at 8000 g for 8000 g for 30 sec at 4 °C. 350 µl ice cold 70 % EtOH in H_2O were added per samples and transferred to a RNeasy spin column for centrifugation at 8000 g for 30 sec at 4 °C. The spin column was washed twice by adding 700 µl RW1 buffer and centrifuging at 8000 g for 15 s at 4 °C. Detergents were cleared from the column by washing it with 500 µl RPE buffer and centrifuging at 8000 g for 2 min at 4 °C. To clear the column of remaining EtOH contained in the RPE buffer, the columns are centrifuged empty at 8000 g for 1 min at 4 °C before eluting the RNA from the spin column in 15 µl of RNase free H_2O. The RNA samples were stored at -80 °C until circular DNA (cDNA) conversion was performed. RNA concentrations were determined using NanoDrop and adjusted to 40- 300 ng/µl RNA per sample using RNase free water.

2.5.2. cDNA synthesis

In order to convert RNA to cDNA, the Applied Biosystems High Capacity cDNA Reverse Transcription Kit (Thermo Fisher) was used. Per 10 µl of RNA sample, 2 µl of 10 x RT buffer, 0.8 µl 25 x dNTP Mix, 2 µl 10 x Random primers, 3.2 µl RNase free H_2O, 1 µl Applied Biosystems RNaseOUT inhibitor (Thermo Fisher) and 1 µl MultiScribe™ Reverse Transciptase (Applied Biosystems) was used. The reverse transcription was performed in a thermal cycler set to 10 min at 25 °C followed by 120 min at 37 °C and 5 min at 85 °C. cDNA samples were then stored at -20 °C.

2.5.3. qPCR measurement

mRNA quantification was performed using respective 0.5 µl Applied Biosystems TaqMan™ Gene Expression Assay (FAM) primers (see Table 1 for details) and the Applied Biosystems TaqMan™ Universal PCR Master Mix and 1 µl respective cDNA. The quantification was performed in MicroAmp® Optical 384-Well Reaction plate (ThermoFisher) for 2 min at 50 °C followed by 10 min at 95 °C followed by 40 cycles of 95 °C for 15 sec and 1 min at 60 °C in a Applied Biosystems ABI 7900HT Fast Real-Time PCR Thermal Cycler. The data was expressed as fold change of ΔΔCT. *18S* mRNA was used as housekeeping gene.

Table 1: Applied Biosystems TaqMan™ Gene Expression Assay (FAM) primers used in this study

Target gene	Code	Manufacturer
18S	Hs03003631_g1	Thermo Fisher
CD80	Hs00175478_m1	
CD86	Hs01567026_m1	
CD206	Hs00267207_m1	
SELE	Hs00174057_m1	
ICAM1	Hs00164932_m1	
LGALS9	Hs04190742_mH	
VCAM1	Hs01003372_m1	

2.6. Flow Cytometry

Flow cytometry was used to analyse total or extracellular protein in single cell suspensions.

2.6.1. Extracellular staining

Single cell suspensions containing PBMCs or PMN (Figure 7A) were incubated with a species-specific Fc-receptor blocking agent (Miltenyi) for 20 min on ice to prevent non-specific antibody binding to Fc receptors. Endothelial cells were directly stained with antibodies. Each sample was stained with 100 µl of the corresponding antibody mix in PBS(-/-) (see Table 2 and Table 3) which also Zombie Aqua Fixable Viability Kit (Biolegend) to exclude dead cells from analysis (Figure 7B). The samples were incubated on ice for 20 min. If a secondary antibody was required, the cells were incubated with the primary antibody first, washed in PBS (-/-) and then incubated for 20 min on ice with the corresponding secondary antibody and the other, fluorescent-conjugated antibodies of interest. The samples were incubated on ice for 20 min in the dark, washed at 800 g for 5 min and resuspended in 300 µl PBS containing 1 % PFA. The samples were stored at 4 °C until analysis on CyAn ADP Analyser (Beckman Coulter).

2.6.2. Intracellular staining

In order to detect total protein levels, cells were stained with extracellular markers as described above and then fixed for 20 min in 4 % PFA in PBS (-/-). The cells were permeabilised by washing three times in 1x eBioscience™ Permeabilisation buffer (Thermo Fisher, UK) at 800 g for 5 min and incubated with the respective antibody mix in 1 x eBioscience™ Permeabilisation buffer for 20 min at room temperature. In case

of intracellular staining, the cells were washed three times with 1x eBioscience™ Permeabilisation buffer before incubation with the corresponding secondary antibody in 1x eBioscience™ Permeabilisation buffer for 20 min at room temperature. The cells were washed three times in 1x eBioscience™ Permeabilisation buffer and resuspended in 300 µl PBS (-/-) and stored at 4 °C until analysis on CyAn ADP Analyser.

Table 2: Antibodies used for the staining of human cells

Target	Fluorophore	Clone	Dilution	Manufacturer
CCR2	APC Cy7	K036C2	1:50	Biolegend
CD11b	BV421	ICRF44	1:50	Biolegend
CD11c	BV510	S-HCL-3	1:50	Biolegend
CD14	PE Texas Red	TuK4	1:100	ThermoFisher
CD16	BV421/FITC	3G8	1:100	Biolegend
CD18 (active)	APC	MEM-148	1:50	invitrogen
CD44	APC	IM7	1:100	ThermoFisher
CD45	FITC	2D1	1:50	Biolegend
CD62L	APC Cy7	DREG-56	1:50	Biolegend
CX_3CR1	PerCP-eFluor™ 710	2A9-1	1:50	Biolegend
Gal-9	unconjugated	polyclonal	1:50	R&D
Anti-goat IgG (H+L)	Alexa Fluor 488	polyclonal	1:100	Invitrogen
ICAM-1	APC	HA58	1:200	BD Pharmingen
MHC Class II	FITC	L243	1:50	Biolegend
TIM-3 (CD366)	PE	F38-2E2	1:50	Biolegend
VCAM-1	FITC	51-10C9	1:50	BD Pharmingen

Table 3: Antibodies used for the staining of murine cells

Target	Fluorophore	Clone	Dilution	Manufacturer
CD4	APC	GK1.5	1:50	Biolegend
CD8	PE-Texas Red	5H10	1:50	ThermoFisher
CD3	eFluor 450	145-2C11	1:50	ThermoFisher
CD25	PerCP Cy5.5	PC61.5	1:50	Biolegend
CD45.2	PE	104	1:50	BD Bioscience
CD45 (I.V.)	APC Cy7	30-F11	10 mg/ml	Biolegend
F4/80	FITC	Cl:A3-1	1:50	ThermoFisher
Ly6C	BV421	AL-21	1:50	BD Bioscience
Ly6G	APC	1A8	1:50	BD Bioscience
NK1.1	FITC	PK136	1:50	Biolegend
Siglec F	PE-Texas Red	E50-2440	1:50	BD Bioscience

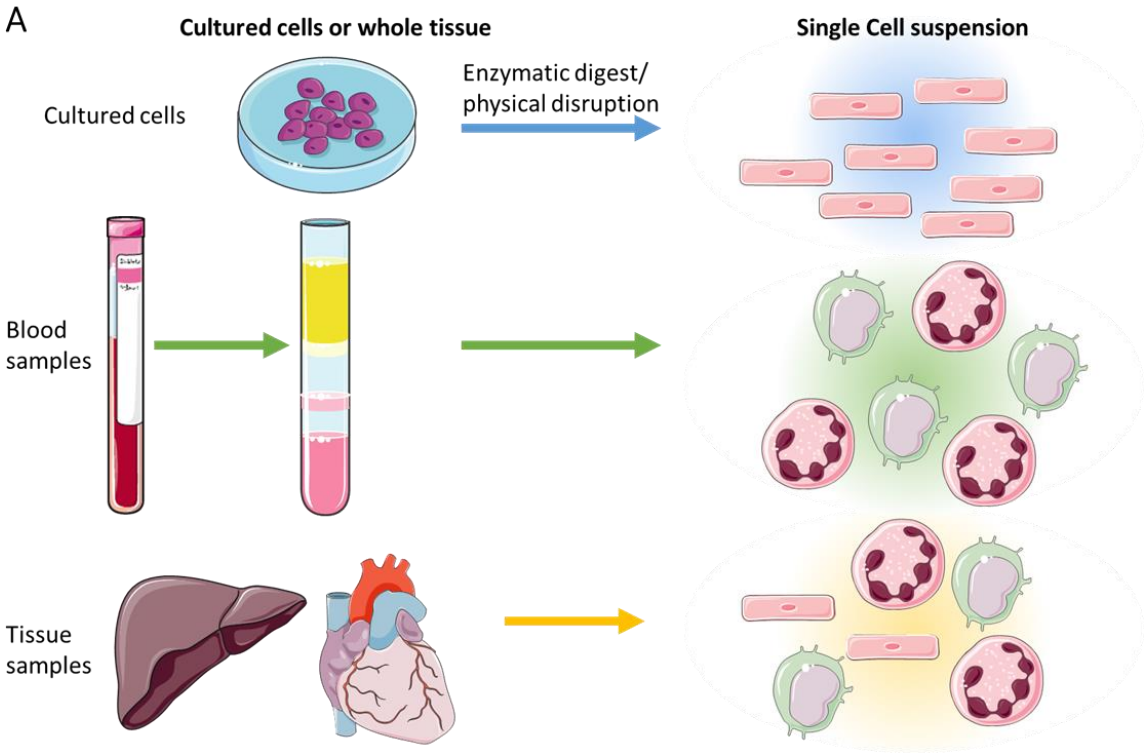
A
Cultured cells or whole tissue
Single Cell suspension
Cultured cells
Enzymatic digest/
physical disruption
Blood
samples
Tissue
samples

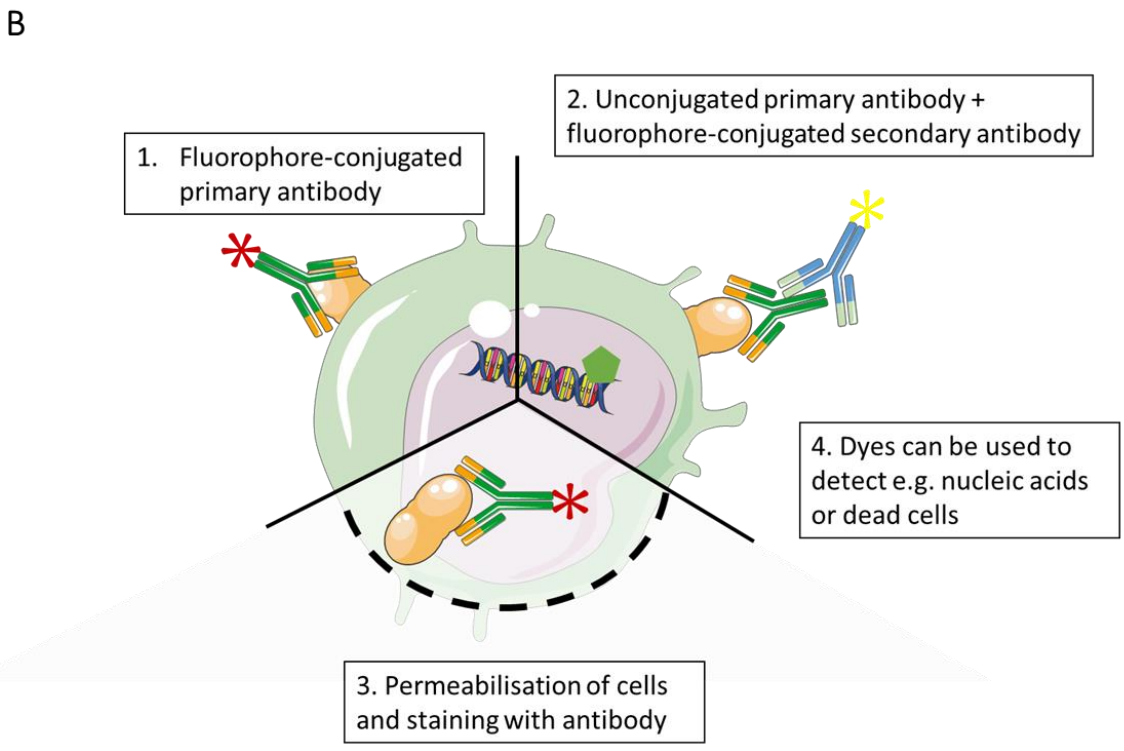
B
1. Fluorophore-conjugated primary antibody
2. Unconjugated primary antibody + fluorophore-conjugated secondary antibody
4. Dyes can be used to detect e.g. nucleic acids or dead cells
3. Permeabilisation of cells and staining with antibody

Figure 7: Flow cytometric analysis. Flow cytometry enables analysis of protein and nucleic acids in single cells suspensions. These can be generated from cultured cell lines, blood samples or tissue samples which can be digested enzymatically or disrupted physically resulting in single cell suspensions made up of one cell type or a mix of cells. These single cell suspensions can either express fluorescent proteins or antibodies can be used for protein analysis. These antibodies can be either directly conjugated to fluorophores or a fluorophore-conjugated secondary antibody can be used. Fluorescent dies are used to stain the nucleic acid content of cells or to distinguish live from dead cells. Permeabilisation enables detection of surface and intracellular proteins.

2.7. Western blot

2.7.1. Sample preparation

In order to determine total protein levels in differentiated macrophages, these macrophages were lysed in RIPA buffer (Table 4) containing the protease inhibitor (Roche) for 30 min on ice. The protein concentration in each sample was determined using the Pierce™ BCA Protein Assay Kit (Thermo FIsher). The protein concentration was adjusted using RIPA buffer and samples were denatured by adding the appropriate amount of 4 x SDS sample buffer (Table 5) containing 10 % ß-mercaptoethanol and heating for 10 min at 95 °C.

Table 4: RIPA buffer

Material	Amount	Manufacturer
Sodium chloride	150 mM	Sigma Aldrich
Triton X-100	1.0 %	Sigma Aldrich
Sodium deoxycholate	0.5 %	Sigma Aldrich
Sodium dodecyl sulfate	0.1 %	Sigma Aldrich
Tris, pH 8.0	50 mM	Sigma Aldrich

Table 5: SDS sample buffer, pH 6.8

Sodium dodecyl sulfate	8 %	Sigma Aldrich
Glycerol	40 %	Sigma Aldrich
Bromophenol Blue	0.008 %	Sigma Aldrich
Tris HCl	0.125 M	Sigma Alrich

2.7.2. Protein electrophoresis

25 µl of sample were loaded onto a 10-well 4-12 % NuPAGE™ 4-12 % Bis-Tris mini protein gel (Thermo Fisher). 5 µl of PageRuler™ Prestained Protein Ladder was also loaded. The protein electrophoresis was performed by at 120 V in a tank containing 1 x NuPage™ Running Buffer (Thermo Fisher) which was supplemented in the upper chamber with NuPAGE™ Antioxidant (1:500, Thermo Fisher).

2.7.3. Protein transfer

After protein electrophoresis, proteins inside the gel were transferred onto a PVDF membrane using a 1 x NuPAGE® Transfer Buffer (Novex by life technologies) with 10 % methanol and 1 % Antioxidant. The transfer was performed at 40 A for 2 h. Successful protein transfer was assessed by staining the PVDF membrane with Ponceau S solution followed by washing in ddH_2O.

2.7.4. Processing and imaging of membrane

Membranes were blocked with Tris buffered saline (TBS) supplemented with 1 % Tween 20 (TBST) containing 10 % milk powder for 1-1.5 h at room temperature on a shaker. After blocking, the membrane was washed three times for 10 min in TBST at RT on an orbital shaker. If required, the membrane was then cut into respective sections and incubated over night at 4 °C on a shaker with respective primary antibodies in TBST containing 5 % BSA (polyclonal anti-alpha Tubulin antibody, #2144,

Cell Signalling Technology, 1:1000 and polyclonal anti-Gal-9 antibody, AF2045, R&D Systems, 1:500).

Following incubation with the primary antibodies, the membrane was washed three times for 10 min at RT on a shaker with TBST followed by incubation with the secondary antibody. The secondary Horse Radish Peroxidase (HRP)-conjugated antibodies (polyclonal rabbit anti-goat IgG (H+L) secondary antibody, Invitrogen, UK, 1:5000 and polyclonal anti-rabbit IgG secondary antibody, #7074, Cell Signaling Technology, 1:1000) were prepared in TBST containing 10 % milk powder and incubated with the membrane for 1 h at RT on a shaker. The membrane was then washed three times 10 min with TBST at room temperature on a shaker.

To detect the proteins by visualising the antibodies, the membrane was incubated for 1 min at RT with Amersham^{TM} ECL Prime Western Blotting Detection Reagent (GE Healthcare). An Amersham^{TM} Hyperfilm ECL film (GE Healthcare) was then exposed to the membrane for 1-5 min and subsequently developed.

The developed film was scanned and densiometric analysis of the detected protein bands was performed using ImageJ software.

2.8. Immunofluorescent staining

$CD14^+$ monocytes were isolated from PBMCs as described above. 3×10^5 cells were cultured per well in an ibidi µ-slide 8 well dish (ibidi) for 16 h as described above. For extracellular staining the cells were fixed in 2 % PFA, followed by repeated washing in PBS or PBS containing 25 mM lactose (Sigma Aldrich). Cells for intracellular staining were fixed with ice cold methanol and washed three times in PBS afterwards. The cells were blocked with 1 % BSA and 10 % donkey serum in PBS before incubating the cells

with the primary antibody for 1 h at room temperature. Antibodies used were polyclonal Gal-9 antibody (AF2045, R&D Systems, 1:50). Cells were washed repeatedly in PBS before the Alexa Fluor 488 donkey anti-Goat IgG (H + L) antibody (Invitrogen, 1:200) was applied for 1 h at room temperature in the dark. The cells were washed repeatedly after the incubation. Vectashield anti-fade mounting media containing DAPI (Vectorlabs) was applied just before imaging the cells using the Zeiss LSM780 confocal microscope (Zeiss). All buffers for the intracellular staining contained 1 % Tween-20 (Sigma-Aldrich). Monocytes, both permeabilized and non-permeabilized, were also stained with the secondary antibody in the absence of the primary to measure the extent of non-specific binding.

2.9. Enzyme-linked immunosorbent assay

For the detection of Gal-9 in human plasma samples as well as culture media of Macrophage and endothelial cell cultures, the Human Galectin-9 Quantikine ELISA Kit (Biotechne) was used according to manufacturer's instructions. Briefly, plasma samples were diluted 4-fold with the Calibrator Diluent, whereas cell culture supernatants were used without diluting. A 1:1 mix of sample or standard with Assay Diluent was prepared and added to each well of the microplate. The plate was incubated on a shaker for 2 h at room temperature before each well was washed with Wash Buffer. The human Galectin-9 Conjugate was added to each well and incubated for a further 2 h at room temperature on a shaker. This was followed by thorough washing with Wash Buffer before Substrate Solution was added. The plate was incubated for around 20 min at room temperature protected from light before Stop Solution was added and the plate was analysed on a plate reader at 540 nm.

The optical density measurements of Gal-9 in each sample were normalised to the optical density measurements of the standard curve to calculate the amount of Gal-9 in each sample.

2.10. Flow based adhesion assay

2.10.1. Preparation of channel slides

For coating the µ-Slide VI 0.4 Channel Slides (Ibidi) with recombinant Gal-9 protein, solutions of 5- 100 µg/ml recombinant Gal-9 in PBS (-/-) were prepared and 30 µl of the respective solution was used to fill each channel. The slides were incubated for 1 h at standard culture conditions before replacing the Gal-9 solution, washing with each channel three times with 200 µl of 1.5 % BSA in PBS (-/-) and blocking the channel with 200 µl 1.5 % BSA in PBS (-/-) for 1 h in standard culture conditions. In case Gal-9 was blocked with lactose or sucrose, 25 mM lactose or sucrose in 1.5 % BSA in PBS (-/-) was incubated for 20 min at 37 °C prior to the use of the channel in the flow based assay.

When an monolayer of activated, Gal-9 siRNA treated endothelial cells were cultured in the µ-Slide VI 0.4 Channel Slides, the cells were prepared and seeded in the channel slides as described above (Chapter 2.3.4.).

2.10.2. Preparation of PBMC or monocyte suspension

PBMC or $CD14^+$ monocytes were isolated from whole blood of HY, HA and PAD as described above (Chapter 2.2.). Cell suspensions of 1×10^7 cells/ml in PBS(-/-) were prepared. If $CD14^+$ cells were treated with antibodies against CD18, 5×10^6 cells were incubated in 500 µl PBS (-/-) containing CD18 antibody (10 µg/ml, Clone IB4,

Calbiochem) or a IgG_{2a} isotype control for 20 min on ice immediately before being added to the flow assay.

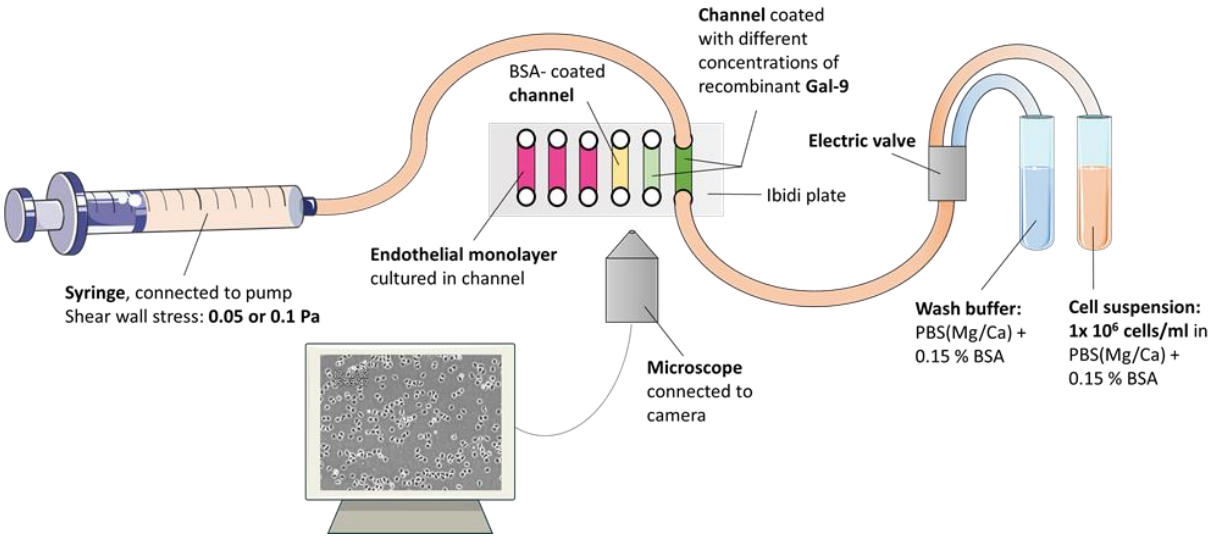

Figure 8: Schematic set up of flow based adhesion assay. In order to assess capture and adhesion properties of recombinant proteins or observe transmigration through endothelial monolayers in physiological flow conditions, a flow based assay is used. The set up enables to perfuse cell suspensions over channels coated with either recombinant protein or endothelial cell monolayers. The wall shear stress and time of perfusion and wash out can be controlled via the pump and the capture, adhesion and transmigration can be observed live through a microscope connected to a camera.

2.10.3. Set up of flow based adhesion assay and cell perfusion

The flow assay box was preheated to 37 °C and the tubing was attached (Figure 8). PBS (+/+) containing 0.15 % BSA (Flow buffer) was prepared and warmed to 37 °C and perfused through the flow assay tubing prior to the perfusion of cells to ensure the absence of bubbles. The channel slide was attached with Luer adapters and flow buffer was added to the wash reservoir.

The pump was set to flow rates of either 0.4 or 0.8 ml/min to generate a wall shear stress in the channel slides of 0.05 or 0.1 Pa respectively. Following formula was used to calculate the flow rate:

$$Q = \frac{(\tau * w * h^2)}{6n}$$

Q: flow rate
τ: wall shear stress (0.1 or 0.05 Pa)
w: width of the channel; 3.8 mm in µ-Slide VI 0.4 Channel Slides
h: height of the channel; 0.4 mm in µ-Slide VI 0.4 Channel Slides
n: viscosity of flow buffer; 0.7 mPa*s in this case

Once a stable flow was established, the respective number of cells was diluted in flow buffer to a concentration of 1 x 10^6 cells/ml and added to the sample reservoir. PBMC or $CD14^+$ monocytes were perfused over the recombinant protein or endothelial cell monolayer for 4 min, followed by a 1 min wash out period with flow buffer. This was followed by imaging seven random fields along the middle of the channel.

For each repeat of experiments, the order in which the various channels were perfused was changed to ensure that the length of time at which the PBMC or $CD14^+$ were not used did not affect the number of adherent cells observed.

In order to quantify the adhered or transmigrated cells (Figure 9A, B), the mean number of adhered or transmigrated cells per image were counted. From this, the average of adherent/transmigrated cells of all seven images was then normalised to the number of adhered cells per 1 mm^2 per 1 x10^6 perfused cells[305]. Adhered cells were classified as the total number of static cells (Phase bright and phase dark), while spread cells (in

case of recombinant protein) and transmigrated cells (in case of endothelial monolayers) were classified as Phase dark cells (Figure 9B).

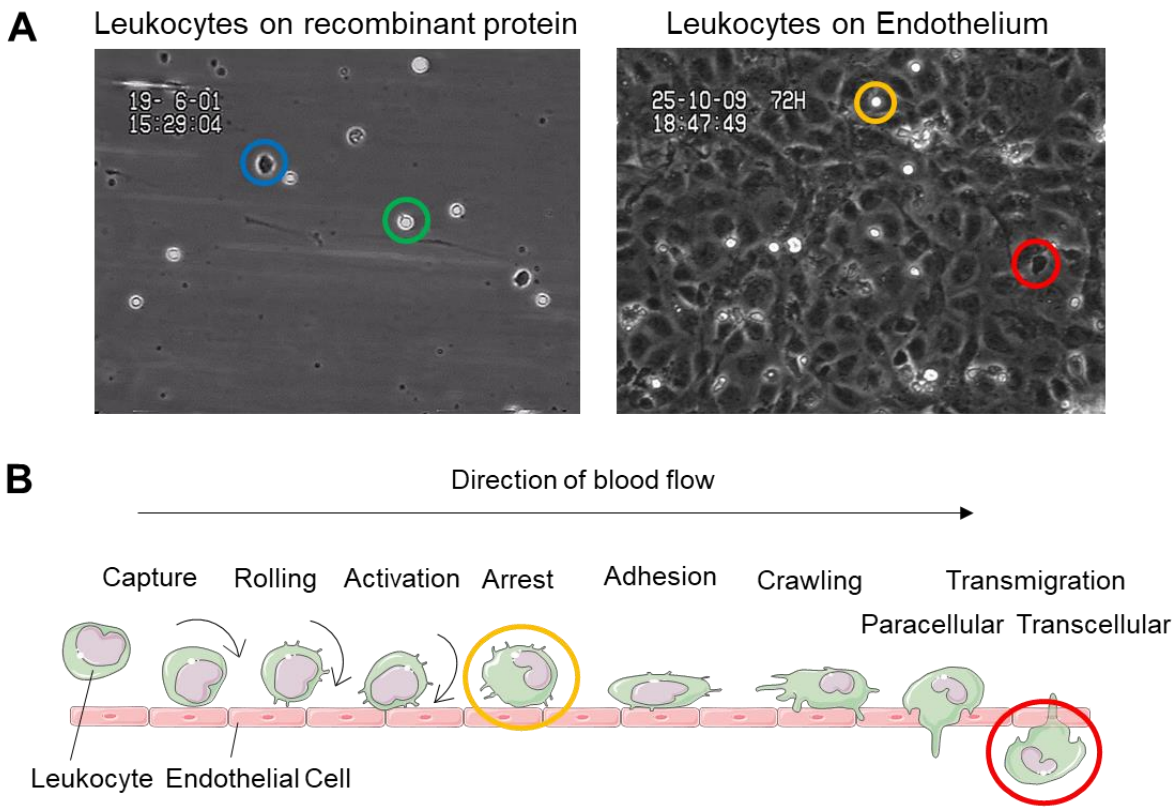

Figure 9: Adhesion and transmigration observed in the flow based adhesion assay. Adhered, spread and transmigrated cells were quantified based on their appearance in the images captured through a phase contrast microscope. On recombinant protein, adhered, non-activated cells appear phase bright (green circle) while spread cells appear phase dark (blue circle). Leukocytes adherent to an endothelial monolayer appear phase bright (orange circle) while transmigrated cells appear phase dark (red circles).

2.10.4. Bisbenzamide staining

In order to visualise the shape of the nuclei of adhered cells post perfusion, the channels were perfused with 1 µg/ml bisbenzamide in PBS (+/+) and incubated in the

dark for 15 min at room temperature. The channels were imaged using a fluorescent microscopy.

2.11. Animal models

All animal studies were performed in accordance with UK laws [Animal (Scientific Procedures) Act 1986] with approval of the local ethical committee and UK Home Office approval. All mice were kept in a 12 h light 12 h dark cycle and food and water were supplied *ad libitum*.

2.11.1. Tracking of $CD45^+$ cells *in vivo*

Six week old male C57BL/6J (WT) mice and Galectin-9 knockout mice (B6(FVB)-*Lgals9*$^{tm1.1Cfg}$/Mmucd, RRID:MMRRC_031952-UCD were obtained from Charles River, UK and the Mutant Mouse Resource and Research Center (MMRRC) at University of California at Davis, an NIH-funded strain repository, and was donated to the MMRRC by Jim Paulson, Ph.D., The Scripps Research Institute. Mice were injected with 200µl of anti-CD45 APC-Cy7 antibody (10 µg/ml, Clone 30.F11, Biolegend, UK) one hour prior to their sacrifice. Blood samples were collected by cardiac puncture in EDTA coated tubes and the body was perfused with PBS (-/-). Spleen, liver, lungs as well as femur and tibia were collected for isolation of leukocytes.

Femur and tibia were flushed with PBS (-/-) to collect the bone marrow and spleens were crushed before they were passed through 70 µm strainer to collect a single cell suspension which was stored on ice.

Each lung was crushed and incubated at 37 °C for 1 h in 1 ml digestion buffer containing 500 ng/ml Liberase TL (Roche) and 100 ng/ml DNase (Roche) in PBS (-/-)

on a shaker. Post incubation, the digested tissue was passed through a 70 µm strainer and stored on ice.

In order to isolate leukocytes from liver tissue, livers were crushed and passed through a 70 µm strainer. The cells were pelleted at 900 g for 5 min at 4 °C and resuspededd in 10 ml PBS (-/-). 5 ml of the cell suspension were layered on top of 7 ml of Optiprep dilution (4.69 ml Optiprep and 11.62 ml PBS (-/-), Stemcell Technologies). The samples were centrifuged at 1000 g for 25 min and the cell at the interface between Optiprep and PBS were collected. The samples were washed in ice cold PBS (-/-) at 900 g for 5 min at 4 °C.

Once all single cell suspensions were prepared, the cells were pelleted at 800 g for 5 min at 4 °C and then resuspended in 1 ml Red Blood Cell lysis buffer for 10 min at room temperature. The red blood cell lysis buffer was also added to 200 µl of whole blood. 9 ml PBS (-/-) were added after the incubation period and the samples were centrifuged at 800 g for 5 min.

The cell pellets were stained with antibodies (Table 3) as described above. The appropriate single stain and isotype controls were also prepared. The samples were analysed on the CyAn ADP^{TM} Analyser.

2.11.2. Zymosan induced peritonitis in the presence of soluble Gal-9 *in vivo*

Zymosan (0.2 mg, Sigma-Aldrich) was injected *i.p.* 1 hour after injection with PBS(-/-) with or without 10 mg Gal-9 *i.p.* to WT C57BL/6J mice. Mice were sacrificed at either 2, 4 or 16 h and the peritoneal cavities were lavaged with ice-cold PBS containing 2 mM EDTA. Samples from the peritoneal lavage were prepared for flow cytometric

analysis as described in Chapter 2.6. Cell free lavage fluid was retained for analysis of inflammatory mediator levels by Luminex (Labospace Milan).

2.11.3. Murine model of atherosclerosis

Apolipoprotein E deficient ($ApoE^{-/-}$) mice on a C57BL/6J background were obtained from Charles River. $ApoE^{-/-}$ and $Gal\text{-}9^{-/-}$ mice were crossed in house to generate double deficient offspring ($ApoE^{-/-}$ $Gal\text{-}9^{-/-}$). 9 week male mice were placed on high fat diet (HFD) (21.4% cocoa butter [w/w] and 0.2% cholesterol [w/w]; Special Diet Services) for 12 weeks before they were sacrificed. Blood was collected for serum analysis and whole aorta and heart were excised for histological analysis. Hearts and aortas were incubated in 4 % PFA in PBS (-/-) over night at 4 °C. The PFA solution was replaced with 30 % sucrose in PBS (-/-) and incubated over night at 4 °C. The samples were incubated in PBS (-/-) for a further 24 h before the top half of the heart was mounted in OCT, frozen and stored at -80 °C. 8 µm thick sections of the aortic root were prepared and stored at -20 °C until staining. Aortas were cleared off visceral adipose tissue and cut open longitudinally for *en face* staining.

2.11.3.1. Hematoxylin and Eosin staining

The tissue sections were brought to room temperature and incubated in tap water for 2 min. The sections were transferred to Harris Hematoxylin solution (Pioneer Research Chemicals Ltd.) for 6 min before rinsing in tap water for 2 min followed by 30 sec incubation in 1 % acetic alcohol (Pioneer Research Chemicals) and washing in tap water for 2 min. The samples were incubated in Scott's tap water substitute (Pioneer Research Chemicals Ltd.) for 30 seconds followed by rinsing in tap water for 2 min. The sections were dunked into Eosin solution (1 % Aqueous, Pioneer Research

Chemicals Ltd.) followed by immediate rinsing in tap water for 2 min. The sections were dapped dry, mounted with DPX mounting medium (Sigma Aldrich) and covered with a coverslip (Figure 10A).

2.11.3.2. Oil Red O staining

The Oil Red O solution was freshly prepared before each staining. 3 % (w/v) Oil Red O powder (Sigma Aldrich, UK) was incubated in 100 % isopropanol overnight. The solution was filtered through Whatman paper and diluted 2:5 in ddH_2O. Finally, the resulting solution was filtered through 0.22 µm filters.

For *en face* staining, each aorta was incubated in ddH_2O for 1 min, followed by incubation in 60 % isopropanol in ddH_2O for 1 min before being transferred to the Oil Red O solution for 5 min. The aortas are then washed in 60 % isopropanol in ddH_2O for 1 min before being transferred to ddH_2O for 1 min. The aortas were then mounted onto double sided sticky tape and fixed onto sample slides. The aortas were imaged using a Nikon D10 Camera and quantified using Photoshop and ImageJ software. The plaque burden was quantified as percentage of Oil Red O positive areas of the total area of the aorta.

The aortic root sections were brought to room temperature and incubated in ddH_2O for 2 min followed by one minute in 70 % isopropanol. The samples were then transferred into the freshly prepared Oil Red O solution for 15 min before rinsing in ddH_2O. The slides were mounted in PBS (-/-) and covered with a cover slip (Figure 10B).

2.11.3.3. Van Gieson staining

Aortic root sections were brought to room temperature and incubated in ddH_2O for 2 min followed by incubation in van Gieson Extra solution (Atomic) for 1 min. The slides

were rinsed for 2 min in 100 % EtOH, followed by 2 min incubation in 100 % EtOH. The slides were mounted in DPX mounting medium and covered with a cover slip (Figure 10C).

2.11.3.4. Immunohistochemical staining of CD68

Aortic root sections were first blocked with PBS containing 10 % FCS (Merck) and 10 % goat serum (Sigma) at room temperature for 30 min. Following incubation with rat anti-CD68 antibody (10 µg/ml, clone FA11, Novus Biologicals) at room temperature for 1.5 h, sections were washed in PBS followed by incubation with secondary AlexaFluor 546 conjugated goat anti-rat IgG antibody (10 µg/ml, Invitrogen) for 1.5 h at room temperature. After washing, sections were mounted with Vectashield® Antifade mounting medium with DAPI (Vector Laboratories) (Figure 10D).

2.11.3.5. Imaging and analysis

All sections were scanned using the AxioScan Z4 (Zeiss, Germany) at 20x magnification. The plaque area, collagen content and macrophage content were quantified using ImageJ software. Collagen content and macrophage content are plotted as the average collagen content of each individual plaque within the aortic root. The collagen and macrophage content was calculated as percentage of the total area of the plaque.

2.12. Statistics

For all statistical analysis, GraphPad Prism software (GraphPad Software) was used. Normal distribution was tested using Shaprio-Wilks test. Differences were analysed using t- test to analyse differences between two groups. One and two way Analysis of variance (ANOVA) with appropriate post hoc testing were applied to compare data

comprising of more than two groups. For data which was not normally distributed, a Kruskal-Wallis test was performed. A p value ≤ 0.05 was considered significant.

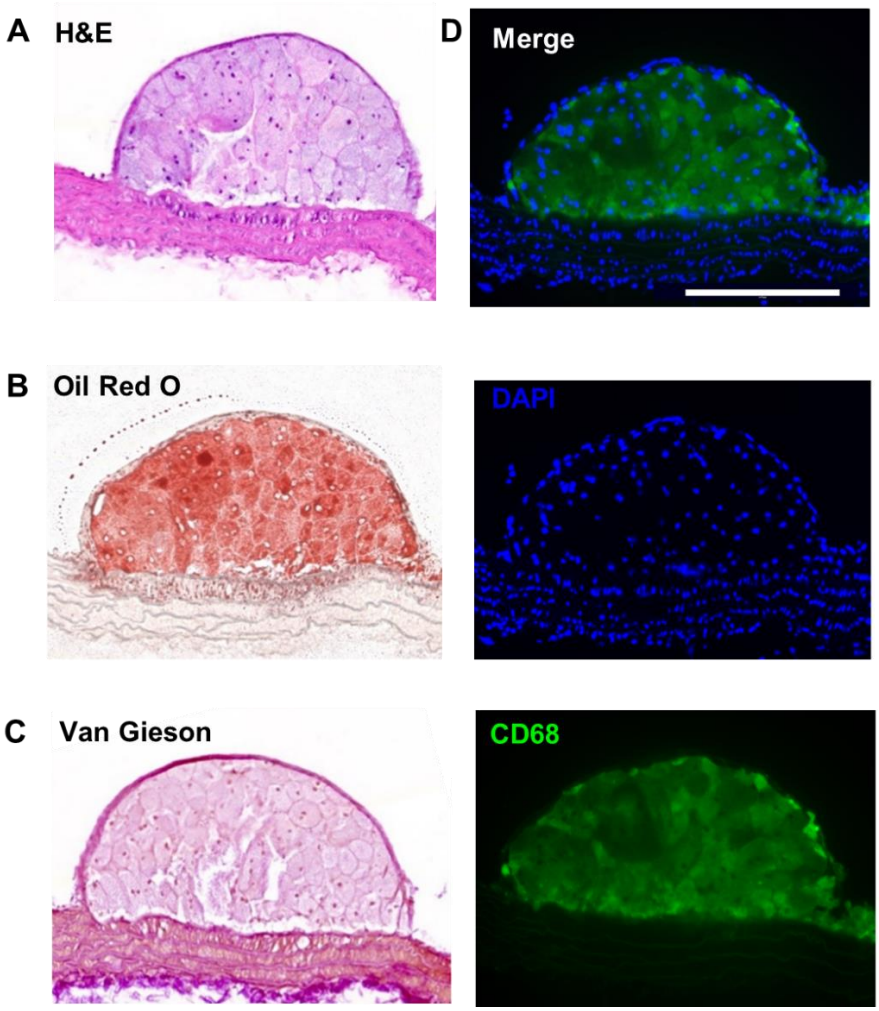

Figure 10: Histological and immunofluorescent staining of murine atherosclerotic plaque sections. Sections of cryopreserved atherosclerotic plaques were prepared and then stained with various staining methods to visualise and quantify different parts and cell types in the tissue. Hematoxilin and eosin staining (A) was used to visualise the general tissue structure. Nuclei appear dark blue while the cytoplasm and extracellular matrix appear pink. In order to visualise lipids, Oil Red O (B) was used. This stains lipids in red while leaving the rest of the tissue unstained. Van Gieson staining (C) was used to quantify collagen content of plaques. Collagen fibers appear in pink while other cell organelles appear yellow and red. Immunofluorescent staining using anti-CD68 antibodies (D) were used to quantify the macrophage content while DAPI was used to stain nuclei. The sections were imaged using the Zeiss AxioScan.

CHAPTER 3:

ENDOGENOUS GAL-9 EXPRESSION IN MONOCYTES MACROPHAGES AND ENDOTHELIAL CELLS

3. Chapter 3: Endogenous Gal-9 expression in monocytes macrophages and endothelial cells

3.1. Rationale

Gal-9 has previously been shown to be upregulated in range of cell types including macrophages[306], myeloid derived suppressor cells[299] and endothelial cells in response to inflammatory stimuli, e.g. IFNγ[213,214,288]. Furthermore, increased circulating levels of Gal-9 have been detected in plasma and serum of patients with various inflammatory diseases such as rheumatoid arthritis, type 1 diabetes, SLE and large artery atherosclerotic stroke, however the source of circulating Gal-9 remains unknown.

This chapter characterises endogenous Gal-9 expression in monocytes, macrophages and endothelial cells in basal and various inflammatory conditions.

3.2. Characterisation of Gal-9 expression in monocytes

Monocytes are broadly classified into three subsets based on their differential expression of CD14 and CD16: $CD14^{+}CD16^{-}$ cells are considered classical monocytes (CL), $CD14^{+}$ $CD16^{+}$ cells as intermediate monocytes (ITM) and $CD14^{-}$ $CD16^{+}$ cells as non-classical monocytes (NC). Further markers such as CCR2, CX_3CR1 and MHC Class II have also been assigned to these subsets[68]. Here we have characterised the basal expression of Gal-9 in these subsets. Gal-9 lacks a traditional signal peptide, which regulates protein translocation to the cell surface, we therefore investigated whether it is presented in a glycan-dependent manner. Furthermore, we compared the levels of Gal-9 in monocytes of healthy donors to those of PAD patients to investigate whether Gal-9 expression in monocyte subsets is disease dependent. Since the average age of the PAD patients was 70.71 (SD 9.85) years, we used healthy young

and healthy aged controls (average age 28.00 (SD 3.55) and 68.16 (SD 6.76), respectively) to establish whether potential differences are disease and/or age dependent.

3.2.1. *LGALS9* mRNA is expressed in human monocytes

To determine *LGALS9* mRNA levels in primary monocytes from healthy young, aged and PAD patients, qPCR was employed. $CD14^+$ monocytes were isolated from whole blood using CD14 magnetic microbeads. RNA was isolated from these cells and converted to cDNA. Commercial primers against *LGALS9*, as well as *IL6* and *CD36*, *TNF* which have been shown to be elevated in monocytes of PAD patients were used[307,308]. The expression levels were normalised to the 18S housekeeping gene which is constitutively expressed.

As expected *CD36* and *TNF* mRNA levels were increased in PAD patients compared to the two healthy controls (Figure 11 A and B, respectively), however no significant differences were found in *IL6* mRNA levels between the cohorts (Figure 11 C). While *LGALS9* mRNA is present in $CD14^+$ monocytes, no significant differences in *LGALS9* mRNA between the three different cohorts were detected (Figure 11D).

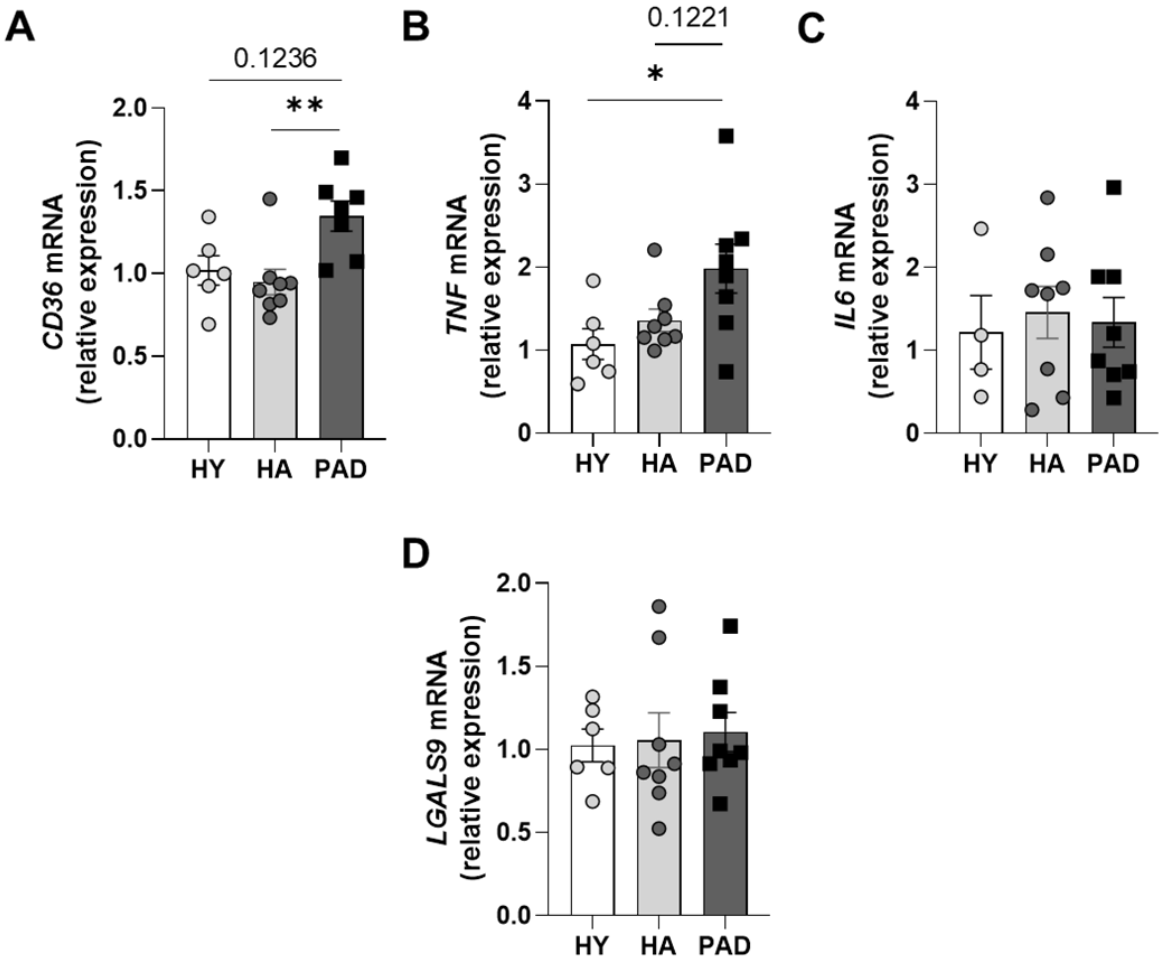

Figure 11: mRNA levels of CD36, TNFα, IL6 and LGALS9 in CD14⁺ monocytes. CD14⁺ monocytes were isolated from whole blood of healthy young (HY), healthy aged (HA) and peripheral arterial patients (PAD). RNA was isolated and converted to cDNA before quantitative polymerase chain reaction analysis was performed using specific primers against *18S*, *CD36* (A), *TNF* (B), *IL6* (C) and *LGALS9* (D). *18S* were used as housekeeping gene and the fold change of the ΔΔCT values of each individual were plotted.N=6-8. Statistical significance was determined by performing a One Way ANOVA test and Tukey‘s post hoc test or Kruskal-Wallis test if the data was not normally distributed. * $p < 0.05$; ** $p < 0.01$

3.2.2. Human monocytes express surface and intracellular Gal-9 protein

Gal-9 protein expression on monocyte subsets were determined using flow cytometry. A viability dye was used to exclude dead cells from the analysis (Figure 12A). CD14 and CD16 were used as monocyte subset markers: $CD14^{+}CD16^{-}$ cells were considered classical monocytes (CL), $CD14^{+}$ $CD16^{+}$ cells as intermediate monocytes (ITM) and $CD14^{-}$ $CD16^{+}$ cells as non-classical monocytes (NC) (Figure 12A). CCR2 (Figure 12B), CX_3CR1 (Figure 12C) and MHC Class II (Figure 12D) were initially used as additional monocyte subset markers to confirm the gating strategy and subsets.

The highest levels of CCR2 expression were detected in classical monocytes, and the lowest in non-classical monocytes. CX_3CR1 levels showed the reverse pattern of expression with lowest levels observed in CL and highest in NC. MHC Class II expression were elevated in ITM pool compared to other subsets. Taken together, the expression pattern of these additional markers confirmed that the gating strategy using CD14 and CD16 did indeed validate the three monocyte subsets.

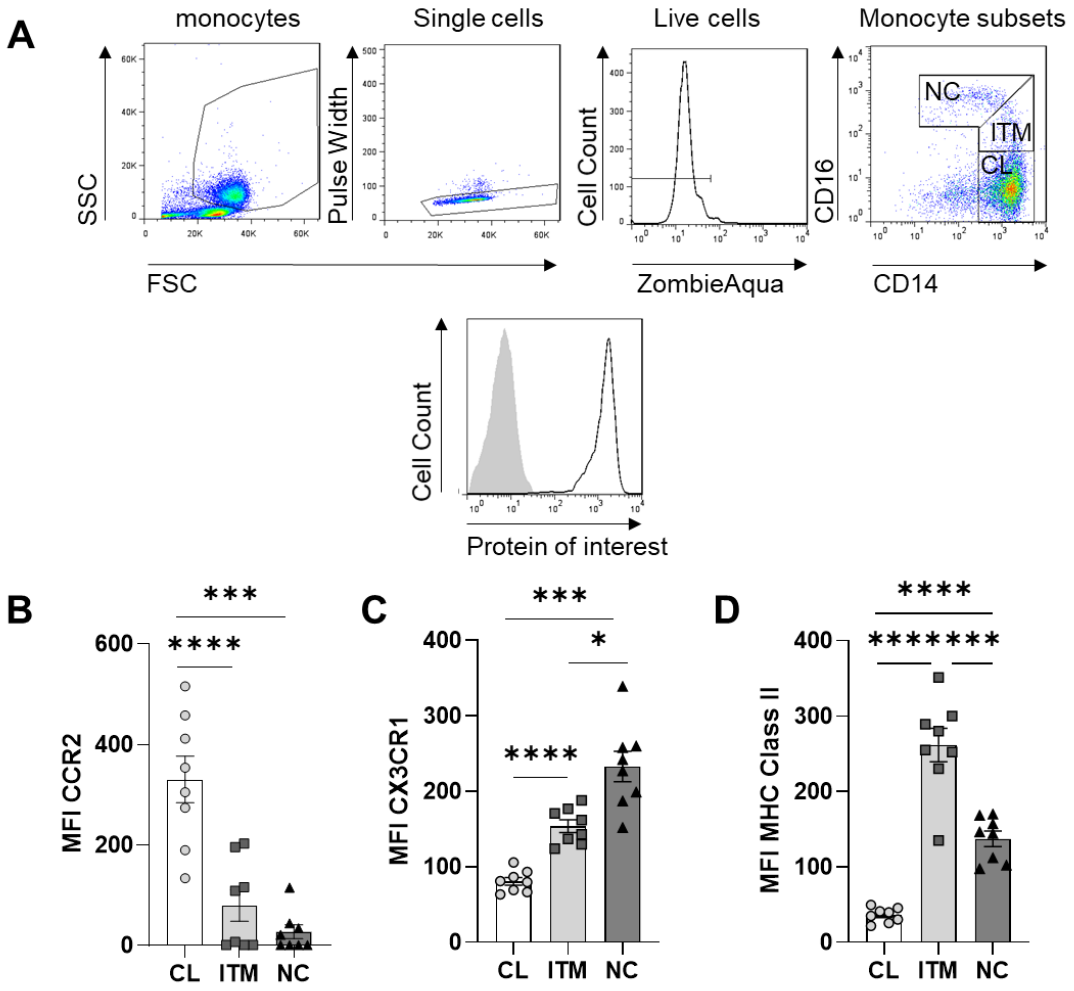

Figure 12: Characterisation of monocyte subsets. Flow cytometric analysis was used to characterise monocyte subsets in the PBMC fraction of whole blood from healthy young donors. PBMCs were stained using antibodies against CD14 and CD16. Antibodies against CCR2, CX3CR1 and MHC Class II were used to confirm the applied gating strategies. Only single, live cells were considered in the analysis. Classical monocytes (CL) were considered to be $CD14^{++}$ $CD16^{-}$ $CCR2^{++}$ $CX3CR1^{-}$ MHC Class II^{-}. Intermediate monocytes (ITM) are classified as $CD14^{+}$ $CD16^{+}$ $CCR2^{-}$ $CX3CR1^{++}$ MHC Class II^{++} cells. Non-classical monocytes (NC) are characterised as $CD14^{-}$ $CD16^{++}$ $CCR2^{-}$ $CX3CR1^{++}$ MHC Class II^{+} cells. The median fluorescent intensity (MFI) value of each sample was blotted. N=7-8. Statistical significance was determined by performing a One Way ANOVA test and Tukey's post hoc test or Kruskal-Wallis test with Dunn's post hoc test if the data was not normally distributed. *=$p < 0.05$; **=$p < 0.01$, ***=$p<0.005$; ****= $p<0.001$

To investigate if glycans are involved in the presentation of Gal-9 on the surface of monocytes, cells were incubated with the ß-galactose containing sugar lactose before staining and analysis (Figure 13). Sucrose, a sugar of the same molecular weight as lactose which does not contain galactose, was used as control for osmolality.

Here, it is shown that Gal-9 was present in all three monocyte subsets of healthy young and that there are were no significant differences in surface or total Gal-9 levels between the three monocyte subsets. Washing the cells in lactose or sucrose containing solution also did not affect surface (Figure 13A) or total Gal-9 levels (Figure 13B) in all monocyte subsets. These observations were also confirmed by anti-Gal-9 labelled monocytes that were imaged using confocal microscopy: monocytes treated with or without lactose both revealed the presence of Gal-9 protein (Figure 13C).

The surface (Figure 14 A) Gal-9 and total levels of Gal-9 (Figure 14B) also revealed no significant differences in Gal-9 between monocyte subset or between HY, HA and PAD patients. However, Gal-9 levels appear to be slightly decreased in NC monocytes.

In summary we have shown that *LGALS9* mRNA as well as Gal-9 protein is present in all monocyte subsets of HY, HA and PAD patients. However no significant differences in mRNA or protein expression were found between cohorts, indicating a disease independent regulation of Gal-9 expression in monocytes. Interestingly, we also showed that, while lacking a traditional signalling peptide, the ß-galactoside binding protein Gal-9 is presented in a glycan-independent manner on the monocyte surface. This suggests that Gal-9 is bound to a novel binding partner on the monocyte surface since the binding interactions between Gal-9 and its known binding partners such as

CD44, CD45 and T-cell immunoglobulin and mucin-domain containing (TIM) 3 are glycan dependent[309-311].

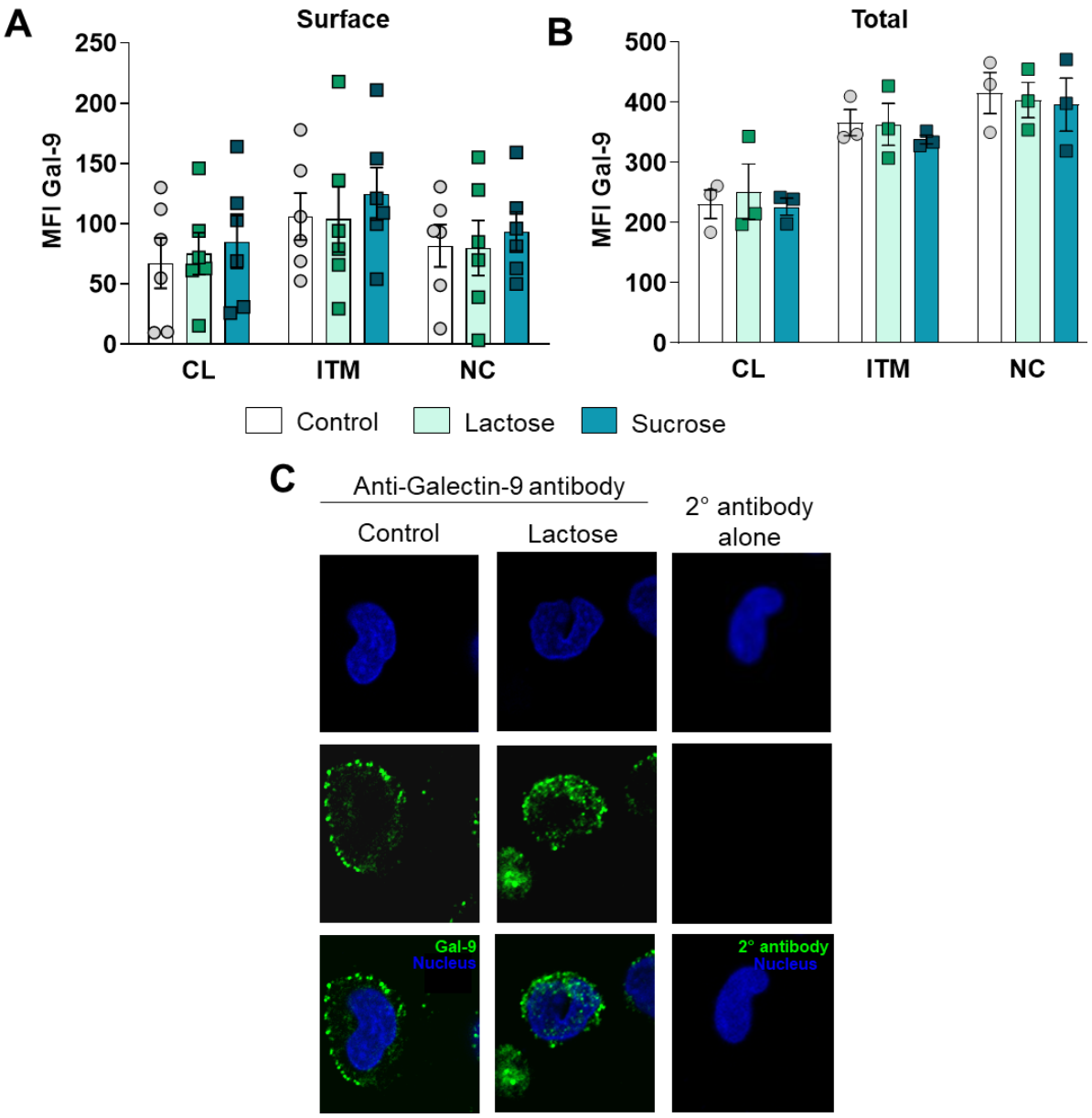

Figure 13: Endogenous, cell surface expression of Gal-9 on monocyte subsets. Flow cytometric and immunofluorescent staining analysis were performed to determine the endogenous surface levels of Gal-9 in monocyte subsets. PBMCs were isolated from whole blood of young healthy donors, washed in PBS(-/-) containing 25 mM lactose or sucrose and stained with antibodies for CD14 and CD16, to determine classical (CL), intermediate (ITM) and non-classical (NC) monocytes, as well as Gal-9 (A). In order to determine total protein levels, the cells were permeabilised in the presence of 25 nM lactose and sucrose before staining for Gal-9 (B). The median fluorescent intensity (MFI) was determined and blotted for each donor. For immunostaining, $CD14^+$ monocytes were isolated from PBMCs and cultured for 16 h

before staining with anti-Gal-9 antibodies (C). Mounting medium containing DAPI was used to visualise the nuclei before imaging via confocal microscopy. N=3-6. Statistical significance was determined by performing a Two Way ANOVA test with a Tukey's post hoc test.

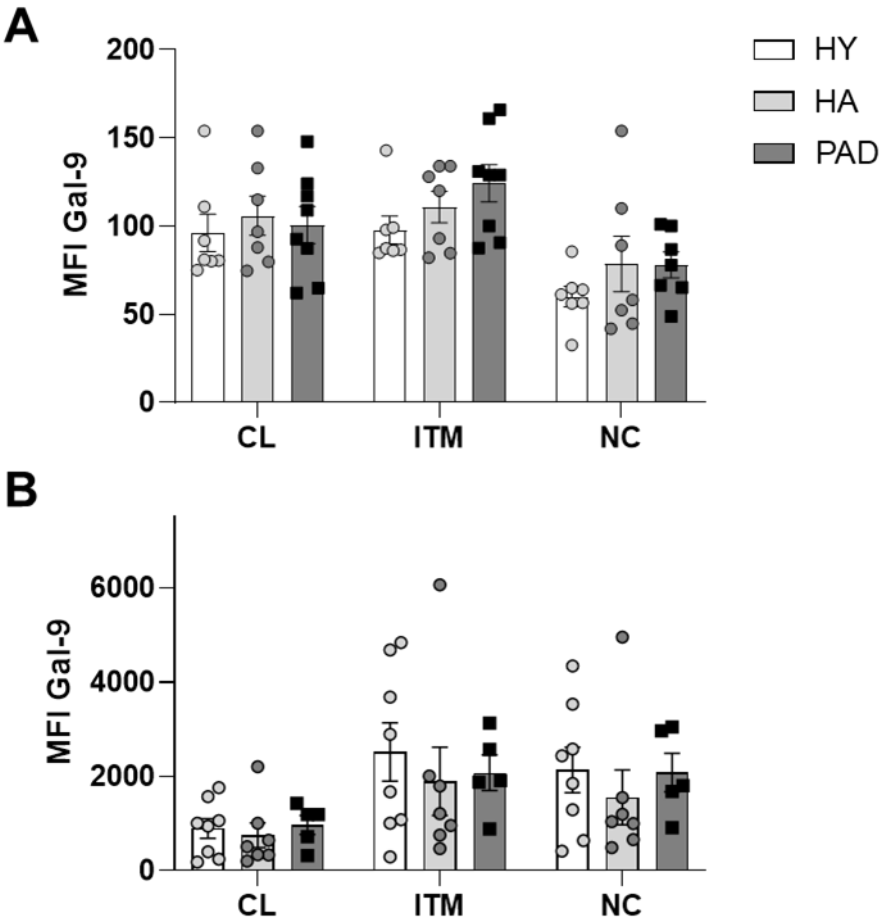

Figure 14: Endogenous expression of Gal-9 on monocyte subsets from healthy young, healthy aged and peripheral arterial disease patients. Flow cytometric analysis was performed to determine the endogenous surface (A) and total levels (B) of Gal-9 in monocyte subsets of from healthy young (HY), healthy aged (HA) and peripheral arterial disease patients (PAD). PBMCs were isolated from whole blood of HY, HA and PAD and stained with antibodies against CD14 and CD16, to determine classical (CL), intermediate (ITM) and non-classical (NC) monocytes. Antibodies against Gal-9 were used as well. In order to determine total Gal-9 levels, cells were permeabilised before staining with antibodies against Gal-9. The median fluorescent intensity (MFI) value of each sample was blotted. N=5-8. Statistical significance was determined by performing a Two Way ANOVA test with a Tukey's post hoc test.

3.3. Characterisation of Gal-9 expression in macrophages

Macrophages can differentiate into different phenotypes depending on the tissue environment[312-314]. *In vitro*, most commonly, pro-inflammatory or M1 macrophages are generated by treating macrophages with a mix of LPS and IFNγ, while the anti-inflammatory or M2 macrophage phenotype is generated by treating macrophages with IL-4[100]. Considering previous reports of upregulation of Gal-9 in cells treated with pro-inflammatory stimuli, potential differences in *LGALS9* mRNA and protein expression in response to pro- and anti-inflammatory polarisation were investigated. Therefore, we generated macrophages from $CD14^+$ selected primary monocytes and treated them with either LPS and IFNγ or IL-4 for 24 h before gene and protein expression analysis using qPCR and Western blot, respectively. The cell culture supernatants was also collected to quantify released Gal-9 via ELISA.

3.3.1. *LGALS9* mRNA is expressed in M1 and M2 macrophages

Transcript levels of *CD80* (Figure 15A), *CD86* (Figure 15B) and *CD206* (Figure 15C) were quantified via qPCR to confirm macrophage phenotypes and *18S* was used as housekeeping gene.

As expected, *CD80* and *CD86* mRNA were significantly increased in M1 macrophages, while *CD206* mRNA was significantly increased in M2 macrophages compared to basal, M0 macrophages. While the data is not statistically significant, *LGALS9* levels in M1 macrophages were increased compared to M0 macrophages (Figure 15D). M2 macrophages showed similar *LGALS9* levels to M0 macrophages. However, the data also showed a high degree of variation in Gal-9 levels between donors in response to the various stimulants.

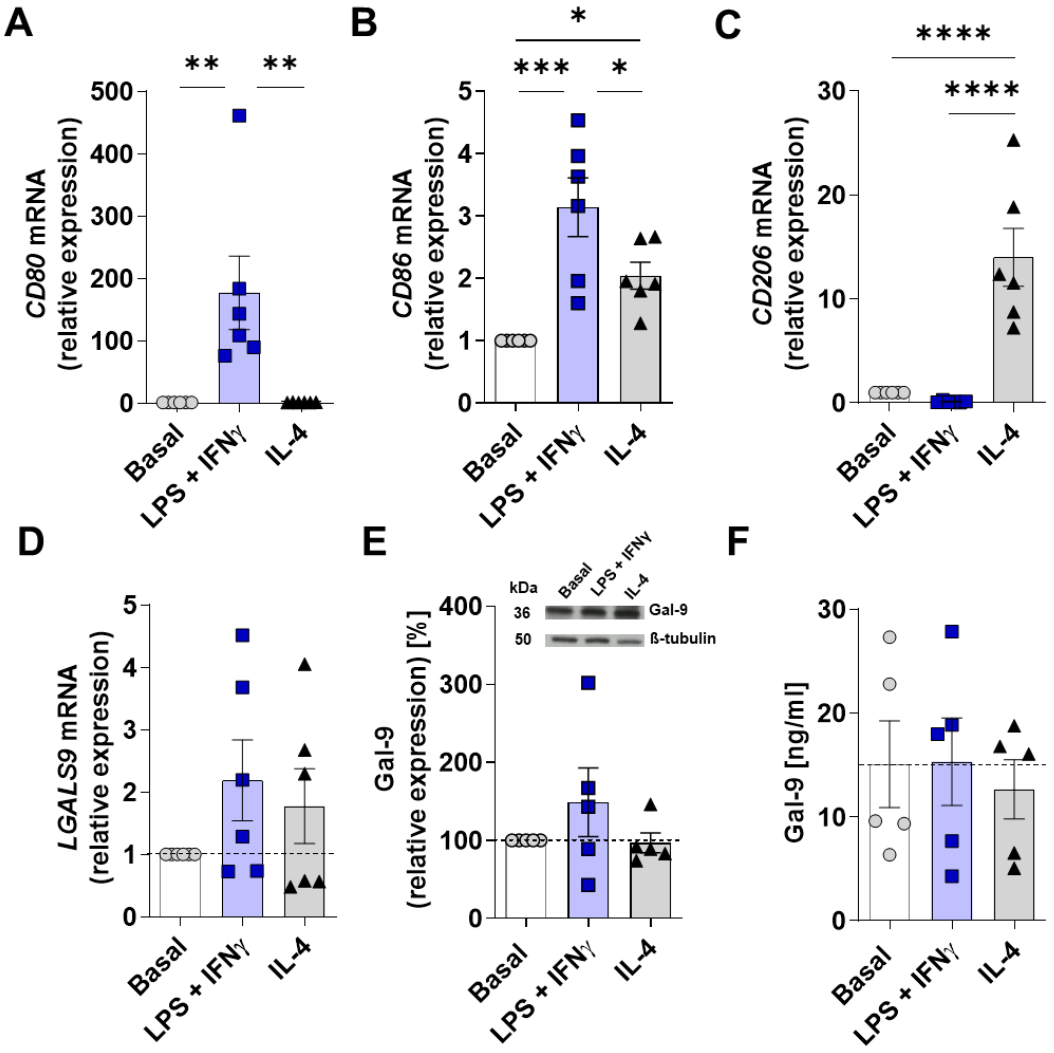

Figure 15: Gal-9 expression in human monocyte derived macrophages. Macrophages were cultured by incubating CD14⁺ monocytes in autologous serum for 6 days before treating them with either LPS and IFNγ or IL-4 for 24 h to generate pro-inflammatory M1 or anti-inflammatory M2 macrophages respectively. Successful phenotype generation was confirmed by determining levels of *CD80* (A), *CD86* (B) and *CD206* (C) mRNA via qPCR. *LGALS9* mRNA levels were also determined by qPCR (D). 18S was used as housekeeping gene and the fold change of the ΔΔCT values were plotted. Total protein levels of Gal-9 were quantified by using western blotting(E). Gal-9 expression was normalized to ß-tubulin levels and then normalized to levels of untreated macrophages. Gal-9 released into the supernatant of the three macrophage phenotypes were detected using ELISA (F). N=5-6. Statistical significance was determined by performing a One Way ANOVA test and Tukey's post hoc test.

3.3.2. Gal-9 protein is expressed by M1 and M2 macrophages

Gal-9 protein levels were assessed by Western blot and normalised to tubulin levels. While Gal-9 protein was detected in all three macrophage phenotypes, no significant differences between them were observed (Figure 15E). Consistent with the mRNA data, macrophages treated with LPS and IFNγ had slightly elevated Gal-9 protein levels compared to untreated macrophages and those treated with IL-4. Again donor variation in Gal-9 levels was observed in all treatment conditions.

3.3.3. Gal-9 protein is secreted from M1 and M2 macrophages

Secreted Gal-9 was detected in the supernatant of the cultured macrophage phenotypes using ELISA. While Gal-9 was detected in supernatant of macrophages in all three conditions, no significant differences between the treatments were detected (Figure 15F). However, IL-4 treated macrophages released slightly less Gal-9 compared to the other two phenotypes and similar to mRNA and total protein expression, we also observed a great range in the amount of released Gal-9 between donors.

In summary, we show here that macrophages express Gal-9 on mRNA and protein level, particularly in pro-inflammatory environments. For the first time, we also show that macrophages are a source of soluble Gal-9. These findings suggest that Gal-9 plays a role in modulation of inflammation induced by macrophages.

3.4. Characterisation of Gal-9 expression in endothelial cells

Several studies have reported an upregulation of Gal-9 transcript and protein expression in endothelial cells cultured in pro-inflammatory conditions. For example,

IFNγ upregulates Gal-9 in a Histone deacetylase (HDAC) dependent manner in HUVEC[213], while LPS treatment only upregulates *LGALS9* mRNA without affecting protein levels[289]. Furthermore, Poly I:C has also been demonstrated to increase Gal-9 expression in endothelium[289,290]. However, neither of these studies revealed the changes in expression over time. Here, the mRNA and protein levels of Gal-9 were characterise in a time course study in HUVEC. HUVEC, isolated from umbilical cords were treated with TNFα, IFNγ in combination and alone or with TLR3 ligand Poly I:C for 4, 8, 16, 24 or 48 h. Gal-9 mRNA was quantified with qPCR. Protein levels were detected using flow cytometry and ELISA.

3.4.1. *LGALS9* mRNA is upregulated by endothelial cells in inflammatory environments

Primers for *LGALS9*, *SELE*, *VCAM1* and *ICAM1* were used. The latter three were used to confirm the response to the various treatments of the endothelial cells as they are known to be upregulated at different time points of the time course in response the various stimulants.

The levels of *SELE* (Figure 16A)*, VCAM1* (Figure 16B) and *ICAM1* (Figure 16C) were all upregulated in response to inflammatory stimulation with peak expression observed between 8 and 16 h while basal media and IFNγ treatment did not upregulate *SELE*, *VCAM1* or *ICAM1* mRNA. Furthermore, the qPCR analysis revealed increased *LGALS9* levels in HUVEC treated with IFNγ, TNFα and IFNγ and Poly I:C (Figure 16D), with highest levels at 24 h and were significantly higher in TNFα and IFNγ and Poly I:C treated cells compared to untreated cells. The levels at 48 h have decreased back to levels similar to levels around 4 h. HUVEC only treated

with medium and HUVEC treated with TNFα only did not reveal any changes in *LGALS9* levels compared to untreated cells.

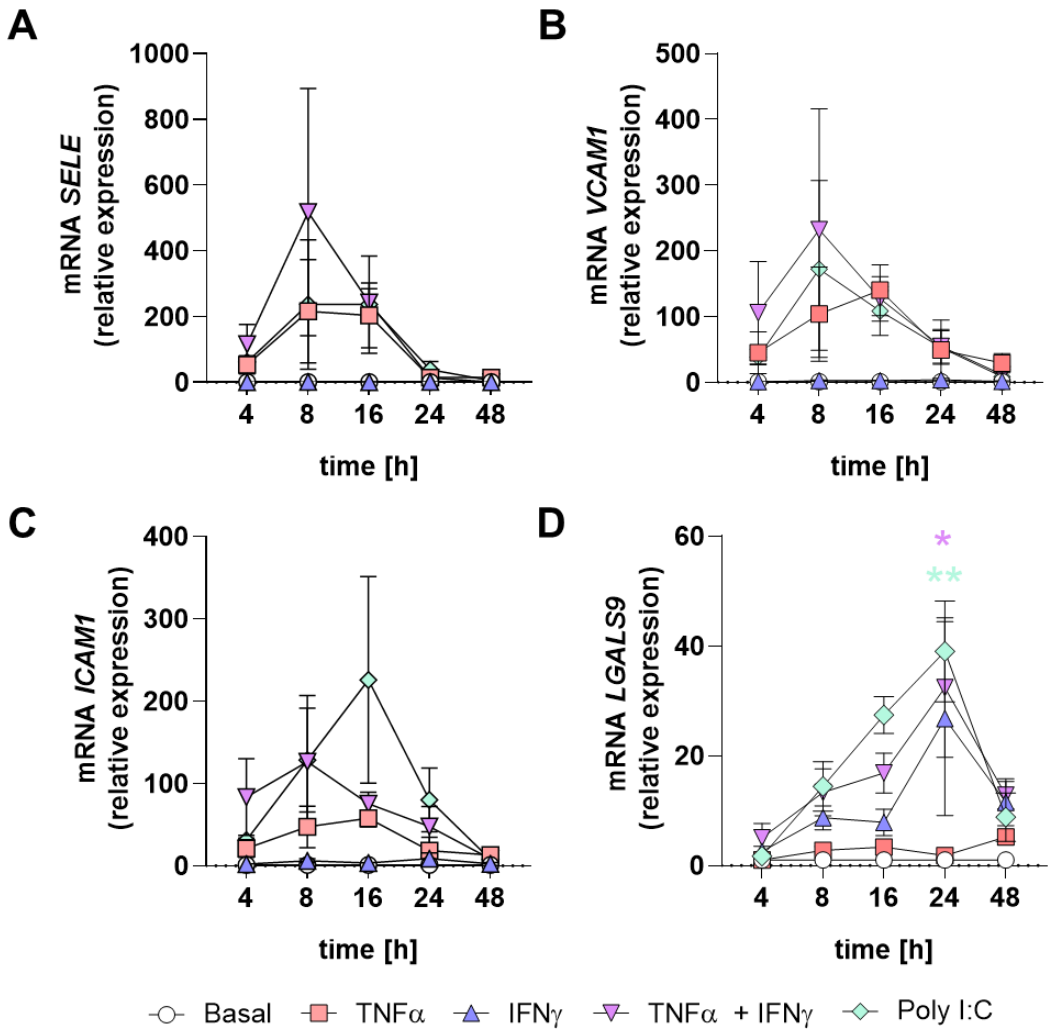

Figure 16: *LGALS9* mRNA expression in Human Umbilical Vein Endothelilal Cells. Human Umbilical Vein Endothelial Cells (HUVEC) were isolated from umbilical cords, cultured and treated with pro-inflammatory stimulants TNFα, IFNγ, TNFα and IFNγ or Poly I:C for 4-48 h. Successful activation of the endothelial cells was confirmed by determining levels of *SELE* (A), *VCAM1* (B) and *ICAM1* (C) mRNA via qPCR. *LGALS9* mRNA levels were also determined by qPCR (D). 18S was used as housekeeping gene and the fold change of the ΔΔCT values were plotted. N=3. Statistical significance was determined by performing a Two Way ANOVA test and Tukey's post hoc test *= $p<0.05$, **= $p<0.01$, colour of * indicates significance of treatment to basal level at same time point.

3.4.2. Gal-9 protein is upregulated by endothelial cells in inflammatory environments

To confirm increases in Gal-9 protein expression in HUVEC following pro-inflammatory stimulation, treated HUVEC at 4, 8, 16, 24 and 48 h post treatment were analysed using flow cytometry (Figure 17). Antibodies against Gal-9 were used as well as against VCAM-1 and ICAM-1 to confirm activation of HUVEC.

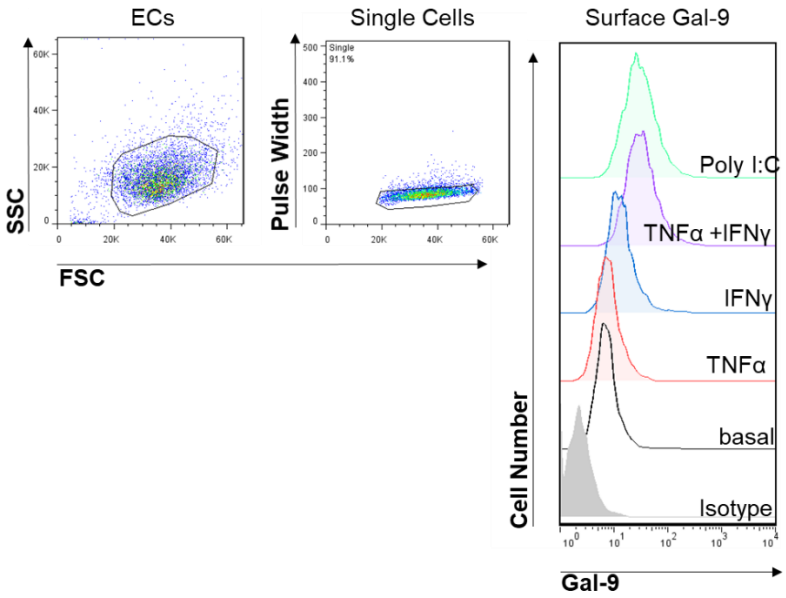

Figure 17: Gating strategy and representative histogram of flow cytometric analysis of Gal-9 expression in endothelial cells. HUVECs treated with various inflammatory stimuli were stained with anti-Gal-9, -ICAM-1 and -VCAM-1 antibodies and analysed via flow cytometry. Single endothelial cells (ECs) were determined using Forward and side scatter (FSC and SSC) as well as pulse width. The Median fluorescent intensity (MFI) for the fluorescence of the respective antibodies was plotted.

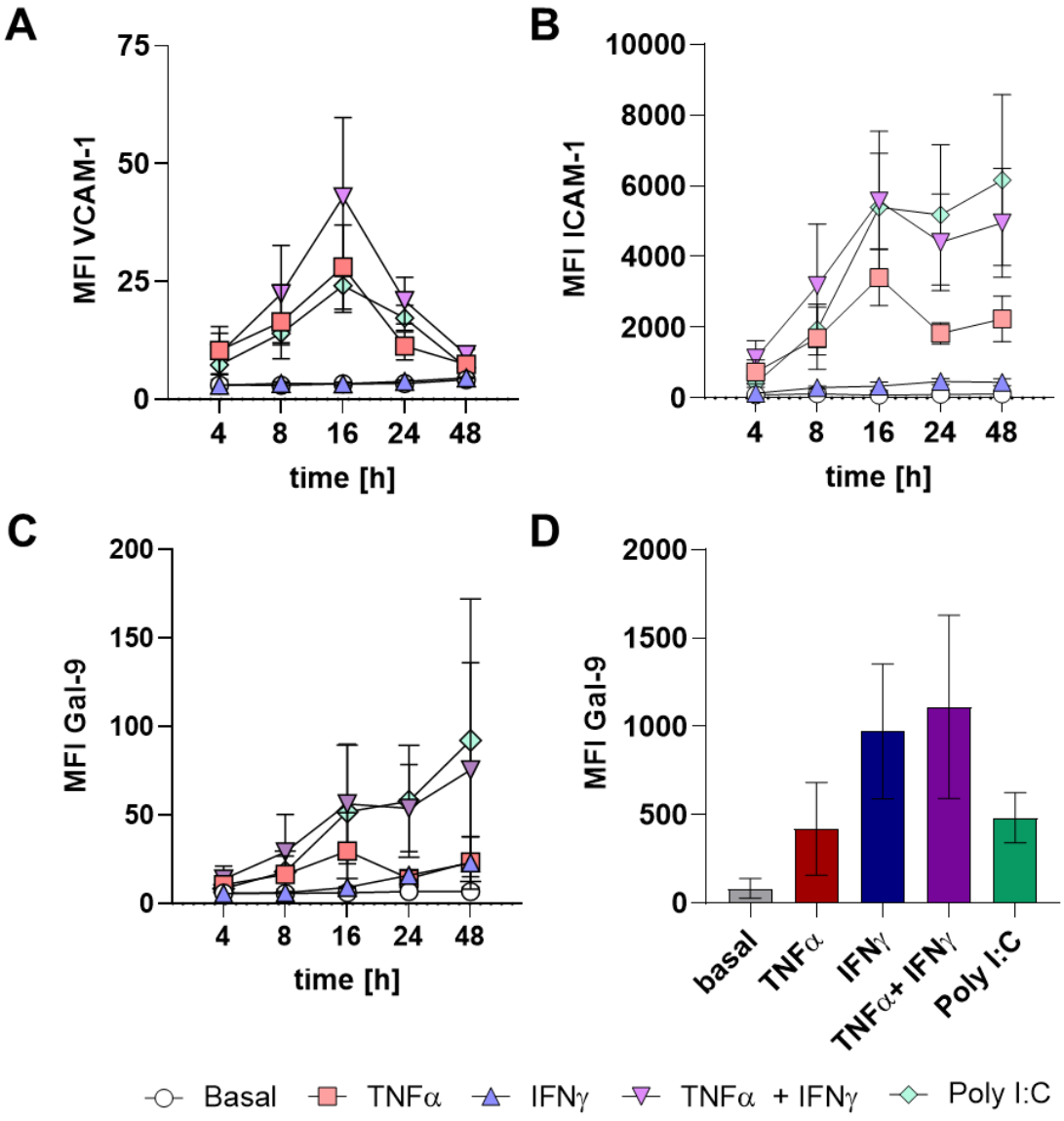

Figure 18: Protein expression of HUVEC at different time points. HUVEC were stimulated with pro-inflammatory stimuli for 4-48 h. Surface protein expression of ICAM-1 (A) and VCAM-1 (B) were used to confirm activation of the endothelial cells. Gal-9 expression was determined extracellularly after 4-48 h of treatment (C) and intracellularly after 24 h of treatment (D). The median fluorescent intensity (MFI) value of each sample was plotted. N=3. Two Way ANOVA was used to investigate significance differences between treatments and time points while One Way ANOVA was used to determine significance in intracellular Gal-9 levels between different treatments. Tukey's post hoc test was used for all.

Consistent with the mRNA data, VCAM-1 (Figure 18 A) and ICAM-1 (Figure 18B) were upregulated on the surface on HUVECs in response to treatment and confirmed activation. VCAM-1 levels peaked at 16 h of TNFα, TNFα + IFNγ or Poly I:C treatment. ICAM-1 was consistently upregulated 16 h post TNFα, TNFα + IFNγ or Poly I:C treatment. While TNFα + IFNγ or Poly I:C treatment further increased levels of ICAM-1 at 24 and 48 h, TNFα treatment alone resulted in a decrease after 16 h. Both, VCAM-1 and ICAM-1 protein expression was not induced in basal media or IFNγ treatment alone. The lack of significant differences is most likely due to the high variability between donors and low n numbers.

Surface Gal-9 levels were upregulated in response to TNFα + IFNγ or Poly I:C treatment (Figure 18C). This increase continued up to 48 h post treatment. The treatment of the endothelial cells with TNFα or IFNγ alone did not upregulate surface Gal-9 levels. Interestingly, both, TNFα or IFNγ treatments did upregulated the intracellular pool of Gal-9 levels after 24 h, while the combined treatment increased this even further (Figure 18D). Poly I:C treatment also increased total Gal-9 levels 24 h post treatment both intra- and extracellularly (Figure 18C, D).

3.4.3. Activated endothelial cells secret Gal-9

Gal-9 is increased in serum or plasma of patients with various inflammatory diseases such as RA and SLE, however the source of circulating Gal-9 remains unknown. Since it was shown here that Gal-9 is released by pro-inflammatory macrophages and that Gal-9 is increased in activated ECs, it was investigated whether endothelial cells are a source of circulating Gal-9.

The supernatant of HUVEC 4 and 24 h post treatment was analysed using ELISA. The analysis shows that Gal-9 is released by HUVEC 24 h after treatment with IFNγ , TNFα + IFNγ and Poly I:C (Figure 19A). The treatment of HUVEC with basal media or TNFα alone had no effect on the release of Gal-9 from these cells, which reflects the surface expression patterns of Gal-9. This data suggests that the endothelium is a source of circulating Gal-9 during inflammation.

In summary, here previous findings of endothelial Gal-9 expression on transcriptional and translational level in inflammatory environments were confirmed. These findings also showed that activated endothelial cells release soluble Gal-9 which suggests that endothelial cells are a source of elevated circulating Gal-9 levels in patients with inflammatory diseases.

3.5. Circulating Gal-9 levels are increased in patients with peripheral arterial disease

Since various studies have shown increased circulating levels of Gal-9 in various inflammatory diseases, Gal-9 levels in plasma from PAD patients were analysed and compared to levels in healthy young and healthy aged controls using ELISA.

While Gal-9 was detected in plasma of all three cohorts (Figure 19B), no age-dependent increase in circulating Gal-9 were detected. However, the levels were significantly increased in PAD patients (Figure 19B), indicating a disease specific increase in Gal-9 in circulation.

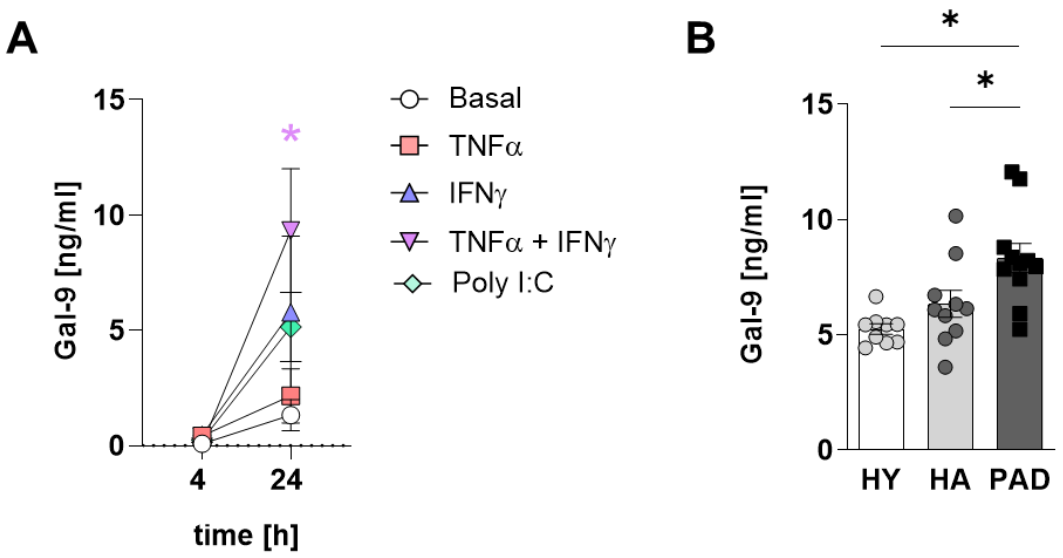

Figure 19: Soluble Gal-9 is released from endothelial cells and found in human plasma. HUVEC were stimulated with pro-inflammatory stimuli for 4 and 24 h (n=3). The culture media was analysed for Gal-9 using ELISA (A). The Gal-9 content of plasma from healthy young (HY), healthy aged (HA) and peripheral arterial disease patients (PAD) was also detected using ELISA (n=9-12). Statistical analysis was performed using Two Way ANOVA for (A) and One Way ANOVA for (B). Tukey's post hoc tests were performed; *=$p<0.05$. The colour of * in (A) represents the significant difference in Gal-9 levels after TNFα +IFNγ treatment.

3.6. Discussion

Gal-9 is a member of the galectin family which has been previously reported to be expressed by immune cells[233,311,315-317] and endothelial cells[214,283,288-290]. However, the role of Gal-9 in modulating the inflammatory response has not been fully explored and the source of soluble Gal-9 in circulation has not been established. In this chapter, we have characterised Gal-9 expression in monocytes subsets, macrophages and HUVEC and investigated Gal-9 levels in HY, HA and PAD patients.

It was demonstrated that unstimulated human monocytes, isolated from healthy whole blood, express Gal-9. Despite surface expression of both proteins on all three major monocyte subsets, CL, ITM and NC, each subset also had a intracellular pool of Gal-9. Similar patterns of expression have been previously reported in other cell types, such as endothelial cells and T-cells[214,215,294,297]. The importance of surface versus intracellular expression has been well documented as the different cellular localizations of galectins can have different, and sometimes opposing, functions[318]. For example, extracellular Gal-3 promotes cell death while intracellular Gal-3 inhibits apoptosis[318]. In the context of human monocytes specifically, Matsuura *et al*. showed that intracellular Gal-9 regulates genes of inflammatory cytokines such as IL-1α and -1β via direct interaction with NF-IL6 in THP-1 cells, a monocyte cell line, while exogenous Gal-9 had no impact on pro-inflammatory genes[297]. Similarly, Ma *et al*. showed that the association of intracellular Gal-9 with TIM-3 induced a pro-inflammatory phenotype in the presence of toll-like receptor (TLR) stimulation in THP-1 monocytes. It was observed that intracellular ligation of Gal-9 with TIM-3 prompted the secretion of IL-12/ IL-23 in a STAT-3 dependent manner[215]. Interestingly, while these studies suggest a

pro-inflammatory role of Gal-9 and studies have reported increases of Gal-9 expression in macrophages and endothelial cells in inflammatory conditions, no increased mRNA or protein Gal-9 levels in monocyte subsets from PAD patients compared to healthy young or healthy aged individuals were detected. This indicates that the expression of Gal-9 in monocytes is independent of disease or age. Furthermore, NC and ITM monocytes trend towards a greater enrichment of surface Gal-9 compared to CL monocytes. Additional studies are needed in order to determine whether the differential expression of galectins amongst monocyte subsets impacts their function. Further characterisation of the role of intracellular versus surface Gal-9 in monocytes is also required, particularly in the context of inflammatory diseases.

The data revealed that Gal-9 is also expressed and released by macrophages and is upregulated in pro-inflammatory environments. These findings confirm previous studies which demonstrated an upregulation of Gal-9 in LPS-treated murine Bone marrow derived macrophages (BMDM)[306]. These findings further corroborate reports of the pro-inflammatory role of Gal-9. For example, the injection of exogenous Gal-9 into mouse knee joint has been reported to drive arthritogenicity by the increased infiltration of monocytes into the joint[301]. Gal-9 deficient mice have also been shown to have attenuated pathology in models of lung inflammation and addition of exogenous Gal-9 to wildtype mice with endotoxic shock has been reported to increase the incidence of mortality[319]. Furthermore, previously, decreased neutrophil and monocyte numbers in Gal-9 deficient mice compared to wild type mice after *i.p.* injections of zymosan have been reported[315]. However, the exact pathway mechanisms which are responsible for the upregulation in Gal-9 still need to be investigated. Particularly

whether intracellular Gal-9 expressed by pro-inflammatory macrophages is involved in cytokine expression in a similar manner as it is in monocytes.

We also observed high variations in Gal-9 expression in monocytes and macrophages between donors which did not coincide with gender or age. Further studies are required to determine the possible causes for these variations, such as lifestyle. However, culturing human monocyte derived macrophages (hMDMs) in autologous serum may also give rise to variations due to differences in M-CSF levels in serum amongst donors[320].

Endothelial cells have also been described as a major source of galectins[214,288-290,321]. Studies have previously demonstrated an upregulation of Gal-9 expression in endothelial cells in response to pro-inflammatory stimuli. Here these findings were confirmed and furthered by showing that Gal-9 mRNA and protein levels increase upon stimulation and peak at 24 h post stimulation. These findings are in line with a study by Imaizumi *et al*. which demonstrated a peak in endothelial Gal-9 mRNA expression 24 h after INFγ treatment. However, while they also reported a peak in protein expression, increased Gal-9 expression was only observed here when cells were treated with a combination of TNFα and IFNγ, rather than IFNγ alone. Studies have revealed that IFNγ treatment increases Gal-9 expression in a HDAC 3-dependent manner[213]. HDAC3 enables phosphoinositol 3-kinase (PI3K) interaction with IFN response factor (IRF) 3 leading IRF3 phosphorylation, its nuclear translocation and Gal-9 expression. Interestingly, a similar mechanism has been described for Poly I:C induced Gal-9 expression. Poly I:C-dependent Gal-9 expression is mediated through TLR3, PI3K and IRF3[289] while NF_KB and p38 MAPK are not involved in Gal-9

expression[290]. All of these results indicate that endothelial Gal-9 expression is induced as antiviral, anti-proliferative, anti-tumour and immunomodulatory activity since IFNγ, TNFα and Poly I:C are immunomodulatory molecules involved in these functions[214]. IFNγ is produced by T_H1 cells which also upregulate the expression of proteins involved in leukocyte adhesion such as IP-10 and fractalkine. TNFα is generated by monocytes and macrophages during acute inflammation while Poly I:C is a double stranded RNA molecule which is used to model RNA virus infections. Both upregulate adhesion molecules such as ICAM-1 and VCAM-1 on endothelial cells. Since all of these stimulants induce expression of proteins involved in leukocyte migration, a role of Gal-9 in leukocyte migration may be postulated.

Increased levels of Gal-9 have been found in serum and plasma of patients with inflammatory diseases such as SLE, large artery atherosclerotic stroke and rheumatoid arthritis and increased levels have also been suggest as marker for disease severity[239,292,293], but the source of circulating Gal-9 remains unknown. Here it was demonstrated that also peripheral arterial disease patients have increased circulating Gal-9 levels. Furthermore, the data suggests that circulating Gal-9 stems from activated vascular endothelial cells and potentially macrophages. Whether increased levels of IFNγ and TNFα in atherosclerotic plaques[322] and in circulation[323,324] contribute to increased Gal-9 expression and a subsequent increase in circulating Gal-9 levels of PAD patients is subject to further investigation. Gal-9 lacks a traditional signal peptide and its release and presentation on the surface of cells are mostly unknown. Chabot *et al*. have shown that Gal-9 released Jurkat T-cells was partly dependent on the activity of matrix metalloproteinases and protein kinase C activity[317]. It can therefore be hypothesized that the release of Gal-9 is through association with a carrier protein.

The inability to elute surface Gal-9 from monocytes using lactose under basal conditions further suggests that Gal-9 is associated with a protein on the cell surface via protein-protein interactions. Whether this mechanism is also involved in the release of Gal-9 from macrophages or endothelial cells requires further investigation. Interestingly, so far the interactions between Gal-9 and its known binding partners such as CD44, CD45 and TIM-3 have all been described as glycan dependent [311,325] [309,310]. Therefore we suggest that further binding partners of Gal-9 exist and are required for the surface presentation and release of Gal-9.

In summary, in this chapter we have shown that Gal-9 is expressed by monocytes, macrophages and endothelial cells, particularly during inflammatory conditions. It is also released by macrophages and activated endothelium, which suggests that these cells are sources of increased Gal-9 levels in inflammatory diseases. However the function of Gal-9 in inflammation requires further investigation.

CHAPTER 4:

BINDING OF EXOGENOUS GAL-9 TO MONOCYTE SUBSETS

4. Chapter 4: Binding of exogenous Gal-9 to monocyte subsets

4.1. Rational

In the previous chapter the expression of Gal-9 by monocytes, macrophages and endothelial cells was shown. Furthermore, it was demonstrated that circulating Gal-9 is present in plasma of healthy young and aged and is increased in patients with PAD. In various studies, it has been shown that soluble Gal-9 can bind to and induce activation of human primary neutrophils[315] as well as maturation of monocyte-derived dendritic cells[233]. Glycoproteins such as TIM-3, CD44 and CD45 have been characterised as binding partners of Gal-9 on various cell types such as T-cells and B-cells[298,311,315,326], while integrins are also known to interact with other members of the galectin family[327-331]. However, the effect of Gal-9 binding to monocyte and macrophages has not yet been fully characterised.

This chapter characterises the binding of Gal-9 to monocyte subsets of healthy young and aged as well as PAD patients and investigates the effect of Gal-9 binding to monocytes on selectins and integrins. Furthermore, known binding partners of Gal-9, CD44, CD45 and TIM-3 as well as Glucosaminyl (N-Acetyl) Transferase 2 (GCNT2), an glycosylation enzyme known to modulate glycans involved in Gal-9 binding in all three donor cohorts were quantified. Additionally, the effect of exogenous Gal-9 on the release of cytokines and chemokines from macrophages was investigated.

4.2. Monocytes bind exogenous Gal-9

Exogenous Gal-9 has been shown to induce activation or differentiation of various cell types such as neutrophils and dendritic cells, but its role on monocytes remains unknown. Here, binding of exogenous Gal-9 to monocyte subsets in HY, HA and PAD

patients was characterised to establish whether there are age and disease specific differences in Gal-9 binding. Furthermore, it was investigated whether Gal-9 binding to monocytes is glycan dependent and the levels of known Gal-9 binding partners on monocyte subsets of HY, HA and PAD patients were characterised.

4.2.1. Gal-9 binding to monocytes is glycan dependent

Gal-9 binding to monocytes was investigated by incubating PBMC isolated from whole blood with 100 nM Gal-9 before analysing monocytes by flow cytometry using antibodies against CD14, CD16 and Gal-9. Since Gal-9 is a glycan binding protein, glycan dependent Gal-9 binding to monocytes was observed. Therefore, incubated Gal-9 was incubated with lactose prior to the addition to PBMCs. Sucrose was used as unspecific carbohydrate control.

We show here that soluble, exogenous Gal-9 binds to mixed monocytes since the MFI of Gal-9 treated monocyte is significantly increased by approximately 17 fold compared to basal, untreated monocytes (Figure 20A, B). Additionally, it was shown that the binding of exogenous Gal-9 to mixed monocytes is glycan dependent since the combined treatment of lactose and Gal-9 of monocytes significantly decreased the MFI of Gal-9, while the combined treatment of sucrose and Gal-9 did not significantly decrease the MFI compared to Gal-9 treated monocytes (Figure 20B). The same trends were observed in all three monocyte subsets and no differences were observed between them.

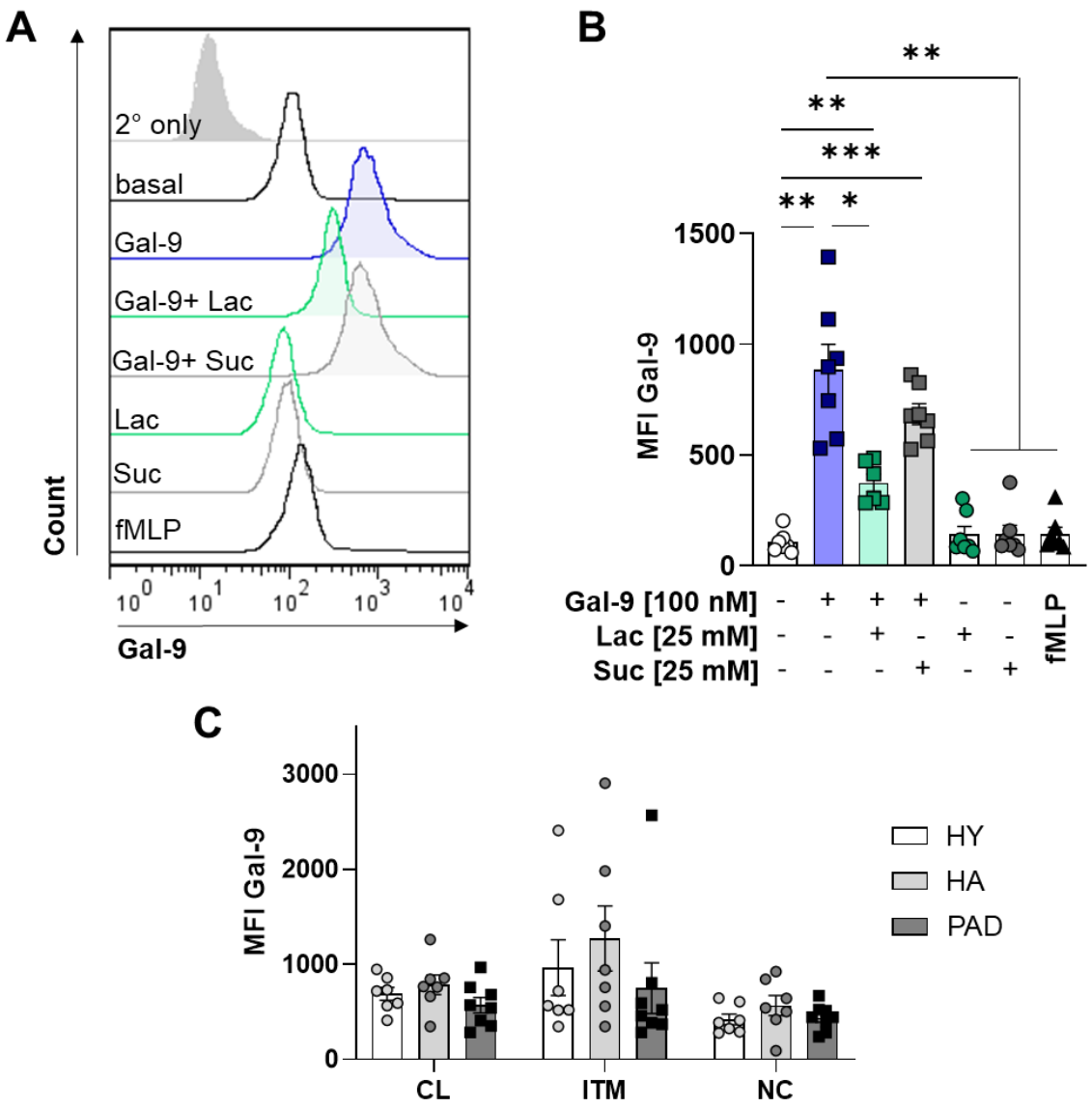

Figure 20: Gal-9 is binding to monocytes in glycan dependent manner. Gal-9 binding to monocytes was investigated by incubating PBMC with Gal-9 in the presence of lactose (Lac) or sucrose (Suc). Gal-9 levels on mixed monocytes after the incubation period were analysed using flow cytometry (A, B; n=7). CD14 and CD16 were used to determine classical (CL), intermediate (ITM) and non-classical (NC) monocyte subsets. Gal-9 binding to monocytes of healthy young (HY), healthy aged (HA) and peripheral arterial disease patients (PAD) was also determined (C, n=7). The median fluorescent intensity (MFI) value of each sample was blotted. Statistical analysis was performed using One Way ANOVA for (B) and Two Way ANOVA for (C) with the respective post hoc tests. *= p<0.05; **= p<0.01; ***= p<0.005.

4.2.2. PAD does not affect binding of Gal-9 to monocytes

Since it was previously shown that circulating Gal-9 levels are increased in the plasma of PAD patients, Gal-9 binding to PBMC from PAD patients was compared to Gal-9 binding to PBMC from HY and HA. To address this, PBMCs were isolated from whole blood of HY, HA and PAD patients and incubated with 100 nM Gal-9 before staining with antibodies against monocyte subset markers CD14 and CD16 as well as Gal-9.

It was shown here that all monocyte subsets bind exogenous Gal-9. The MFI was increased significantly compared to basal Gal-9 surface levels reported in Chapter 3 (Figure 20C). However, no significant differences in Gal-9 binding between monocyte subsets or between the cohorts were detected (Figure 20C).

In summary, Gal-9 binds to all monocyte subsets in a glycan dependent manner. However no differences in binding capacity were detected between healthy individuals and PAD patients. This indicates that soluble Gal-9 binding is not disease dependent, and therefore, the levels of Gal-9 binding partners are disease independent.

4.2.3. Gal-9 binding to monocytes induces changes in CD62L, CD11b and CD18 levels

To investigate whether Gal-9 binding does induce monocyte activation, antibodies against CD62L, CD11b, CD11c and the active conformation of CD18 were used to analyse the respective protein levels on monocytes after incubation with soluble, exogenous Gal-9 in the presence of Ca^{2+} and Mg^{2+}, which are required for integrin activation[332]. fMLP was used as positive control for monocyte activation to induce CD62L shedding and an increase in integrin levels CD11b. Furthermore, lactose was used to determine any glycan dependent changes.

Gal-9 binding did not induce CD62L shedding to the same extent as fMLP treatment. However, Gal-9 binding to monocytes caused a decrease in CD62L surface levels (Figure 21A), which is considered an indicator of cellular activation. This Gal-9-induced decrease in CD62L levels was also found to be glycan dependent since the effect was blocked in the presence of lactose. Interestingly, levels of total CD11b and the active conformation of CD11b, also indicators of monocyte activation, behaved in opposite manners (Figure 21B and C). While total CD11b levels trended towards an increase upon treatment with Gal-9 (Figure 21B), active CD11b decreased (Figure 21C). Both of these observations were rescued in the presence of lactose. As expected, both, total and active CD11b levels were increased when the cells were treated with fMLP. No differences in CD11c levels were detected in Gal-9 or carbohydrate treated cells (Figure 21D). However, a significant increase in CD11c was observed in fMLP treated monocytes.

The active conformation of CD18, a further indicator of monocyte activation, was not significantly affected by any of the treatments (Figure 21E). However, in the presence of Gal-9 a trend towards decreasing CD18 levels were observed, which was rescued in the presence of lactose, while fMLP treatment caused a slight increase in the active conformation of CD18.

This Gal-9 induced trend towards a reduction in the MFI of active CD18 was apparent in all three cohorts (HY, HA and PAD) (Figure 22A), while fMLP increased levels in all three. CD62L was shed in all three cohorts in the presence of both, Gal-9 or fMLP, indicating activation of monocytes (Figure 22B). However, the basal levels of CD62L were lower in healthy aged and even lower in PAD patients compared to the healthy young controls, indicating a more activated monocyte phenotype in PAD patients.

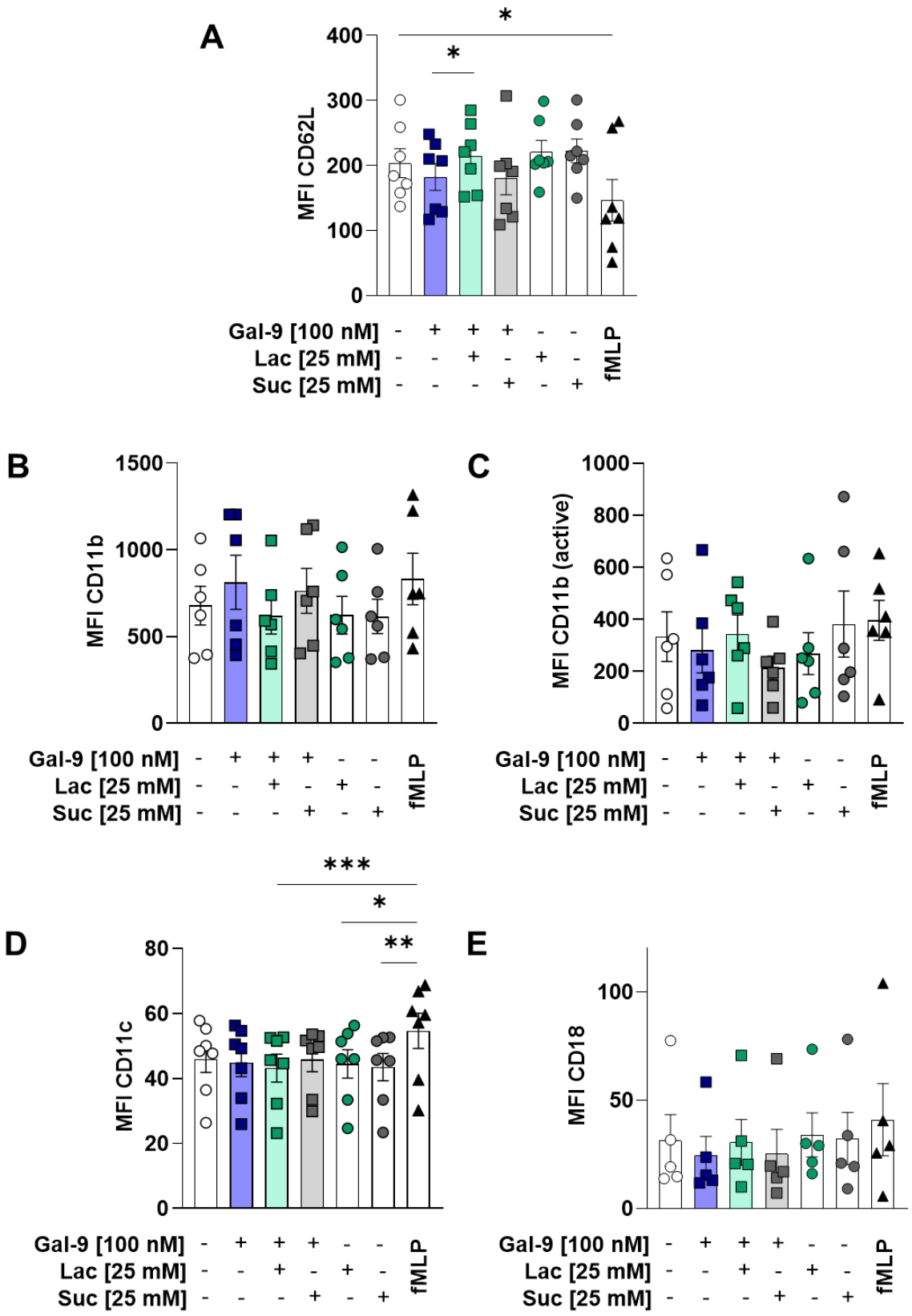
A
MFI CD62L
400
300
200
100
0
*
*
Gal-9 [100 nM] - + + + - - fMLP
Lac [25 mM] - - + - + -
Suc [25 mM] - - - + - +
B
MFI CD11b
1500
1000
500
0
Gal-9 [100 nM] - + + + - - fMLP
Lac [25 mM] - - + - + -
Suc [25 mM] - - - + - +
C
MFI CD11b (active)
1000
800
600
400
200
0
Gal-9 [100 nM] - + + + - - fMLP
Lac [25 mM] - - + - + -
Suc [25 mM] - - - + - +
D
MFI CD11c
80
60
40
20
0
***
*
**
Gal-9 [100 nM] - + + + - - fMLP
Lac [25 mM] - - + - + -
Suc [25 mM] - - - + - +
E
MFI CD18
100
50
0
Gal-9 [100 nM] - + + + - - fMLP
Lac [25 mM] - - + - + -
Suc [25 mM] - - - + - +

Figure 21: Effect of Gal-9 binding to monocytes on selectins and integrins. Levels of CD62L (A), CD11b (B), active CD11b (C), CD11c (D) and CD18 (E) on monocytes were analysed via flow cytometry after incubation of PBMCs were incubated with Gal-9 in the presence of PBS (+/+). Lactose was used to establish a glycan dependent effect of Gal-9 binding. Antibodies against CD14 and CD16 were used to determine classical (CL), intermediate (ITM) and non-classical (NC) monocyte subsets. fMLP treatment was used as positive control for monocyte activation. The median fluorescent intensity (MFI) value of each sample was blotted. N=5-7. Statistical analysis was performed using One Way ANOVA with Tukey's post hoc tests. *= $p<0.05$; **= $p<0.01$; ***= $p<0.005$.

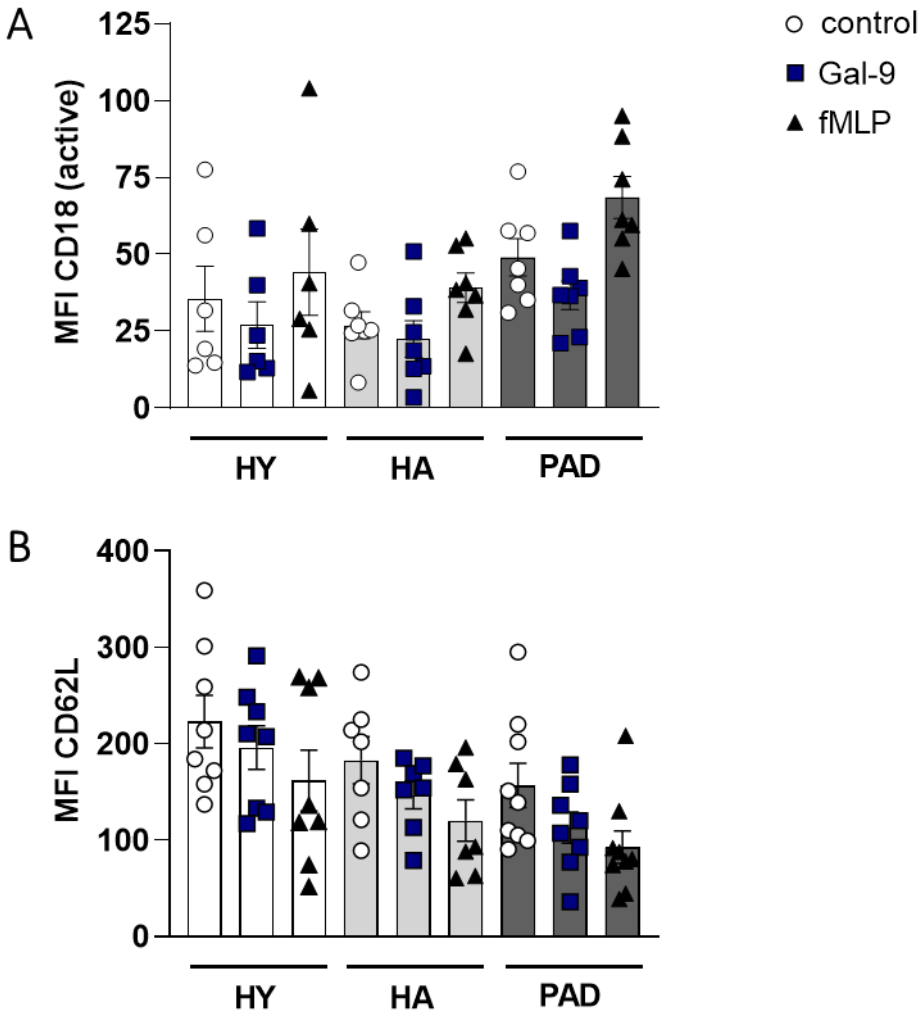

Figure 22: Active CD18 and CD62L levels on monocytes of healthy young, healthy aged and peripheral arterial disease patients. PBMC of healthy young (HY), healthy aged (HA) and peripheral arterial disease patients (PAD) were treated with Gal-9 and active CD18 and CD62L levels were detected using flow cytometry. CD14 and CD16 were used as monocyte markers. fMLP treatment was used as positive control of monocyte activation. The median fluorescent intensity (MFI) value of each sample was blotted. N=6-8. Statistical analysis was performed using Two Way ANOVA with Tukey's post hoc tests.

In summary, it appears that Gal-9 induces shedding of CD62L and modulates integrin levels in human primary monocytes of HY, HA and PAD patients. This suggests that Gal-9 plays a role in monocyte activation, however the precise mechanisms involved remain unknown.

4.2.4. Age and PAD do not affect CD44, CD45 and TIM-3 expression in monocytes

Various glycoproteins such as CD44, CD45 and TIM-3 are known to bind Gal-9[215,298,311,315,326,333]. Here their expression levels in monocytes subsets of HY, HA and PAD patients was characterised. mRNA levels of *Cd44* were determined using qPCR and flow cytometric analysis of surface levels of CD44, CD45 and TIM-3 was performed.

No significant differences were detected in *Cd44* mRNA levels of $CD14^+$ monocytes or CD44 protein levels in monocytes of donors from all three cohorts (Figure 23A). Also no differences were detected in surface CD44 protein levels of all three monocyte subsets (Figure 23B).

No differences in CD45 surface protein levels were found between monocyte subsets of all three cohorts, however non-classical monocytes of PAD patients had significantly higher CD45 levels compared to classical monocytes of PAD patients (Figure 23C). The non-classical monocytes of HY and HA also trended towards increased CD45 levels compared to classical monocytes, however these observations were not significant.

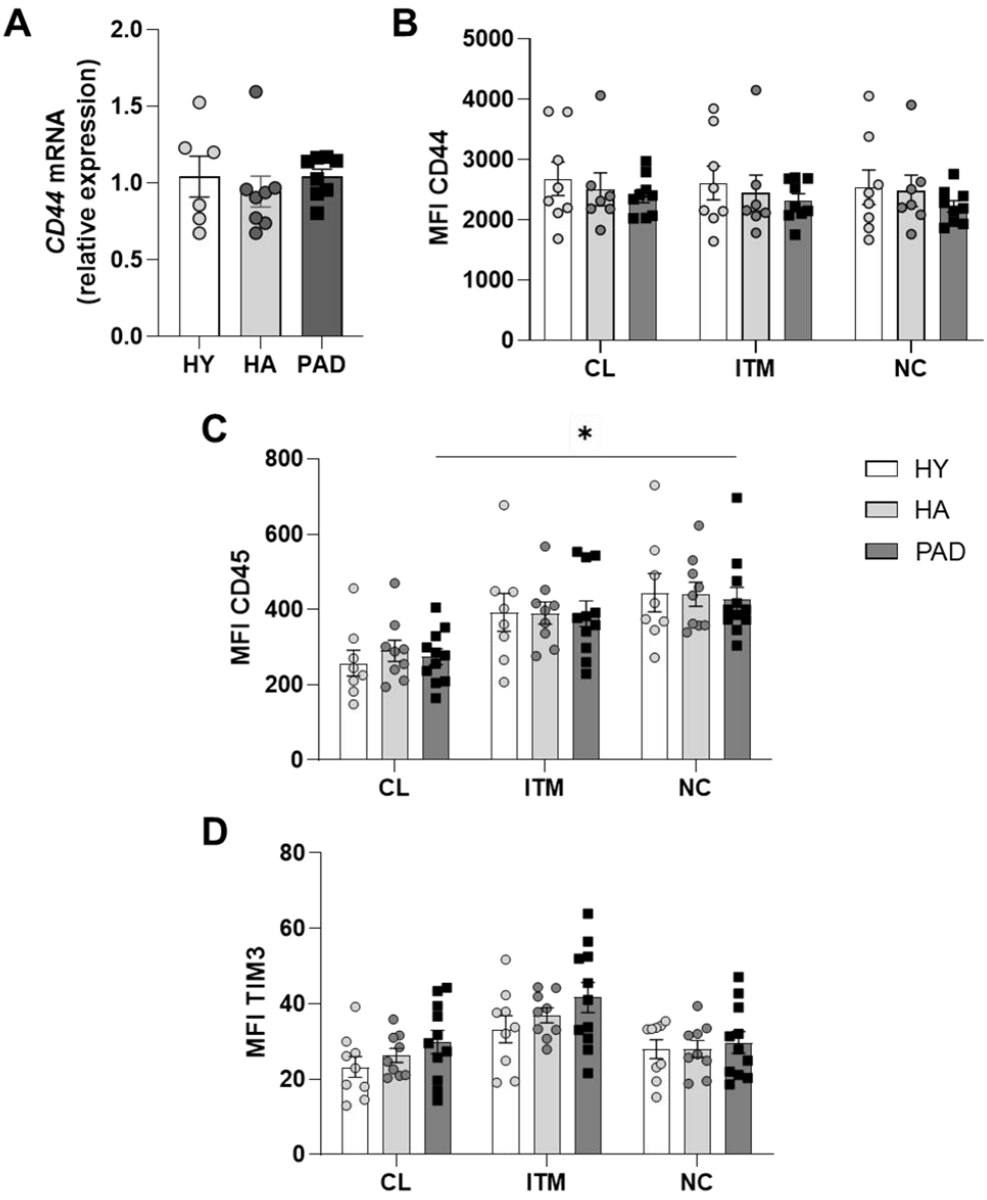

Figure 23: Expression of Gal-9 binding partners CD44, CD45 and TIM-3 on monocyte subsets of healthy young, healthy aged and peripheral arterial disease patients. *CD44* mRNA levels of $CD14^+$ monocytes from healthy young (HY), healthy aged (HA) and peripheral arterial disease patients (PAD) were quantified by qPCR. Protein levels of CD44, CD45 and TIM-3 on monocyte subsets were detected using flow cytometry. Classical (CL), intermediate (ITM) and non-classical (NC) monocytes were distinguished using CD14 and CD16 expression levels. The median fluorescent intensity (MFI) value of each sample was blotted. N=6-11. Statistical analysis was performed using One Way ANOVA for (A) and Two Way ANOVA for (B-D) with the respective post hoc tests. *= $p<0.05$

No significant differences were observed in TIM-3 surface levels either, neither between monocyte subsets nor between cohorts (Figure 23D). However, while not significant, all three cohorts appeared to have slightly increased TIM-3 levels in the intermediate monocyte subset.

4.2.5. Age and PAD do not affect *GCNT2* mRNA levels in monocytes

A previous study showed that GCNT2 regulates Gal-9 binding to B-cells by inducing changes in the glycosylation of B-cells. It catalyses the formation of I-branched N-glycans which inhibit Gal-9 binding[311]. We therefore investigated whether this enzyme is expressed in $CD14^+$ monocytes of all three cohorts, HY, HA and PAD.

qPCR measurements using *GCNT2* primers revealed *GCNT2* mRNA expression in monocytes. However, no significant differences in the *Gcnt2* mRNA levels of $CD14^+$ monocytes of all three cohorts were found (Figure 24).

The analysis of Gal-9 binding partners CD44, CD45 and TIM-3 as well as *GCNT2* mRNA in monocytes of HY, HA and PAD patients revealed no differences in expression between these cohorts. These findings corroborate findings earlier in this chapter which showed no differences in the binding capacity of monocytes from the three cohorts.

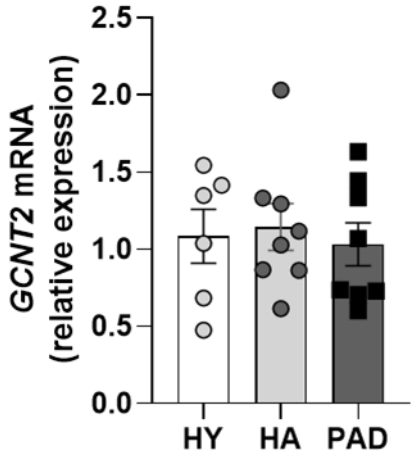

Figure 24: GCNT2 mRNA levels on monocyte healthy young, healthy aged and peripheral arterial disease patients. *GCNT2* mRNA levels of $CD14^{+}$ monocytes isolated from blood of healthy young (HY), healthy aged (HA) and peripheral arterial disease patients (PAD) were quantified by qPCR and normalised to *18S* mRNA levels. N= 6-8. Statistical analysis was performed using One Way ANOVA with Tukey's post hoc tests.

4.3. Exogenous Gal-9 induces release of chemokines from macrophages similar to M1 macrophages

Previous studies have shown a immunomodulatory effect on myeloid cells by Gal-9, therefore its effect on macrophages was investigated. In order to analyse the effect of Gal-9 on the cytokine and chemokine profile released by $CD14^+$ monocyte derived macrophages, macrophages were treated with LPS and IFNγ or IL-4 to generate M1 and M2 macrophages, respectively, in the presence of absence of Gal-9. After 24 h, the supernatant was harvested and analysed for cytokines and chemokines using a cytokine array.

The heat map shows the relative levels of cytokines and chemokines released by macrophages (Figure 25). Exogenous Gal-9 induced the release of chemokines and cytokines similar to M1 macrophages. Pro-inflammatory cytokines such as IL-6 and TNFα were upregulated as well as IL-8, MIP, CCL5, CXCL1, CXCL10 and 11. The combined treatment of LPS and IFNγ with Gal-9 did not increase the cytokine release. Interestingly, while M2 macrophages do not release these chemokines and cytokines, macrophages treated with a combination of IL-4 and Gal-9 also released these to a similar extend as Gal-9 or LPS and lFNγ treated macrophages.

These data indicate that Gal-9 has the capacity to promote local inflammation via the release of pro-inflammatory cytokines and chemokines.

A

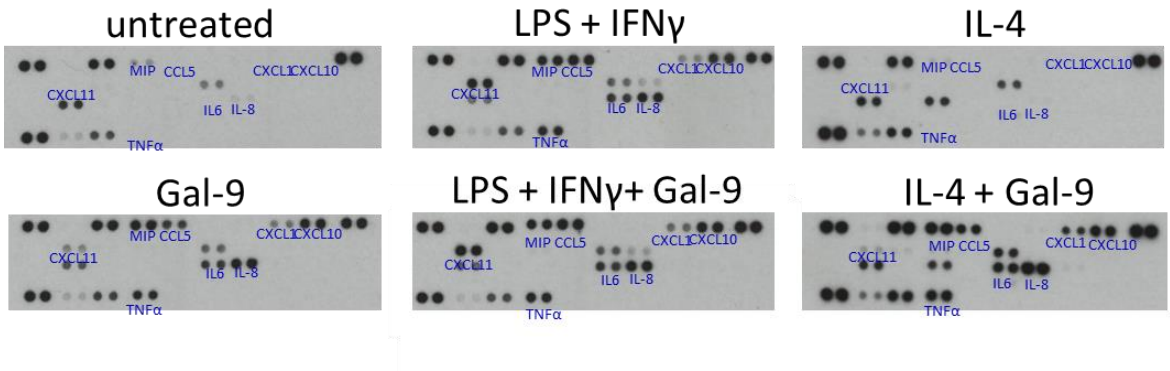

B

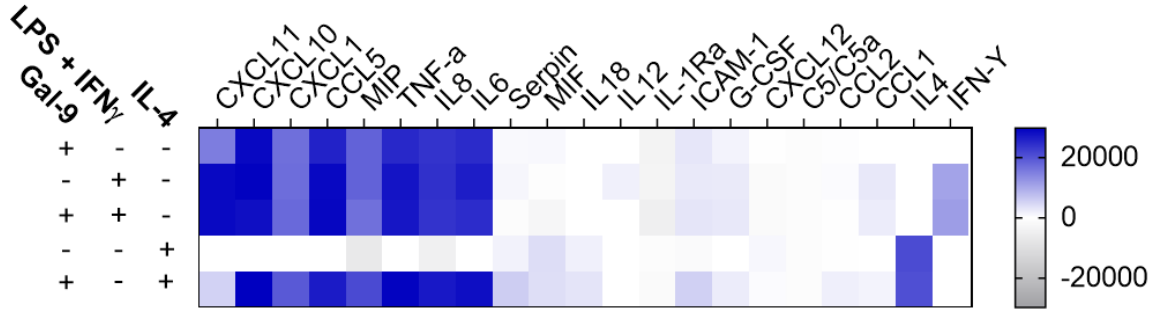

Figure 25: Gal-9 stimulation of macrophages. CD14^{+} monocyte derived macrophages were treated for 24 h with either LPS (100ng/ml) and IFNγ (20 ng/ml) or IL-4 (20 ng/ml) to generate M1 or M2 macrophage phenotypes respectively in the presence or absence of Gal-9 (100 nM). The supernatant of four separate cultures were then pooled and analysed for released cytokines and chemokines using a cytokine array (A). Their relative levels are represented as heat map (B).

4.4. Discussion

In this chapter it was shown that soluble, exogenous Gal-9 binds to all human monocyte subsets in a glycan-dependent manner and induces changes is CD62L, CD11b and CD18 levels.

Increased soluble Gal-9 in circulation has been suggested as an indicator of disease severity[293] and soluble Gal-9 has also been shown to mediate inflammation. For example, Gal-9 treatment of dendritic cells causes the release of TNFα[298] and IL-1β and IL-6 production in myeloid derived suppressor cells[299]. Here, the understanding of the role of soluble Gal-9 *in vitro* was expanded by showing that levels of CD62L trend towards a decrease and total CD11b levels trend towards an increase in monocytes while inducing the release of a pro-inflammatory cyto- and chemokine profile from macrophages.

CD62L shedding is induced in monocytes by a wide range of agents such as fMLP, PMA or LPS and it was shown here, that CD62L levels are decreased in monocytes of PAD patients compared to the healthy controls. This confirms previous studies in other pathologies such as cancer[334] , COPD[335], IBD[336] and hypertriglyceridemia[307,337] which have reported decreased CD62L levels in leukocytes. Sheddases such as A disintegrin and metalloprotease 17 (ADAM17) are known to cleave off the extracellular part of CD62L. While ADAM17 induced-CD62L shedding is required for transendothelial migration of neutrophils, studies in chimera models of *Adam17*$^{+/+}$ an *Adam17*$^{-/-}$ mice have suggested that ADAM17 is not required for monocyte transendothelial migration into the peritoneum[338]. However, other *in vitro* studies have shown that the use of broad range metalloproteinase inhibitors prevent the transendothelial migration of monocytes

under static and flow conditions, suggesting that not just ADAM17 plays a role in CD62L shedding, resulting in the transmigration of monocytes[339-341]. While it has been previously reported that Gal-9 induces CD62L shedding in primary human neutrophils[315], the exact mechanisms of Gal-9 mediated CD62L shedding are still unknown. No proteolytic properties have been described for Gal-9 or any other galectins, therefore it is unlikely that Gal-9 cleaves CD62L itself. Whether Gal-9 acts as inducer of one or multiple of these sheddases and therefore reduces CD62L levels or whether Gal-9 acts in a different way requires further investigation.

Increases in CD11b levels have also been reported during inflammation and as marker of cellular activation it was previously shown that Gal-9 increases CD11b levels in neutrophils[315]. Here these findings were expanded by demonstrating increases in total CD11b on monocytes treated with fMLP or Gal-9, further indication that Gal-9 induces monocyte activation.

Changes of extracellular conformation of integrins and their clustering have both been demonstrated to be modulators of integrin adhesion[342-344]. These conformational changes to active conformations induce high affinity to their ligands[345], enabling them to bind to adhesion molecules on the endothelium such as VCAM-1[24]. Cytoplasmic proteins kindlin and talin are recruited to the cytoplasmic tail of integrins during activation which leads to the opening of the extracellular integrin domains[346]. Several studies have reported the upregulation of total ß2 integrin[337] in monocytes of PAD patients and increased CD11b/CD18 in patients with unstable angina[347], as well as CD11c, Mac-1 and LFA-1 in patients with myocardial infarction[45,348]. Interestingly, no increased levels of the active conformation of CD18 the second integrin subunit of Mac-1, in PAD patients compared to the healthy control cohorts were detected. Also,

due to the previously observed signs of monocyte activation after Gal-9 treatment, increased levels of active conformations of CD11b and CD18 were expected. However, contrary to these expectations, the active conformations of CD11b and CD18 only increased with fMLP treatment but decreased in the presence of Gal-9. These data suggest that Gal-9 alone cannot induce complete monocyte activation, but initiates the process while another substrate is required for full activation. Whether this is another protein or whether this process is mechanosensitive and requires shear stress needs further investigation. Another possibility for the decreased MFI in active CD18 could be that Gal-9 directly interacts with Mac-1 integrins and therefore obstructs the access of the antibody to its epitope on CD18. While no studies have reported direct interactions of Gal-9 and integrins yet, other galectins are known to interact with various integrins[327,329-331]. For example Gal-8 has been identified as the ß2 integrin LFA-1 binding partner which inhibits the interaction of PBMC with immobilised ICAM-1 under static conditions[329]. Whether a similar interaction between Gal-9 and ß2 integrins is occurring and its effects on monocytes, particularly on monocyte migration, requires further investigation.

Interestingly, known binding partners of Gal-9 such as CD44, CD45 and TIM-3 were found on all monocyte subsets, but no differences in the surface protein levels of these Gal-9 binding partners in either of the cohorts were detected. This could also explain why no differences in the amount of bound Gal-9 between the cohorts or between the monocyte subsets were found. Gal-9 is also known to bind glycans on glycoproteins rather than interact with the protein itself. Additionally, inflammatory diseases can alter the glycan profile of cells[349,350]. Here it was shown that Gal-9 binds to monocytes in a glycan-dependent manner, but whether changes in the glycan profile of PBMCs of PAD

patients facilitates enhanced capture by Gal-9 remains unknown. Therefore, *GCNT2* mRNA levels, coding for an enzyme involved in the formation of elongated linear N-glycans, which are known to reduce Gal-9 binding[311] were measured. However, no differences in mRNA expression of this glycosidase have been detected. Further investigations on a translational level of this enzyme and also other enzymes involved in glycosylation of proteins may provide a better insight into potential PAD specific changes in enzyme protein levels which could impact the glycosylation of Gal-9 binding partners.

Further indication of a pro-inflammatory role of exogenous Gal-9 was the release of pro-inflammatory cytokines by Gal-9 treated macrophages. Previous studies have revealed similar effects in other myeloid cells: for example, Gal-9 treatment of dendritic cells causes the release of TNFα[298] and IL-1β and IL-6 production in myeloid derived suppressor cells[299]. Additionally, it was shown here that soluble Gal-9 has the potential to alter anti-inflammatory signals: Gal-9 treatment of macrophages overrode the IL-4 induced anti-inflammatory M2 phenotype and promotes the release of a pro-inflammatory cytokines and chemokines associated with M1 phenotype[351]. This suggests that not only intracellular Gal-9[297] but also exogenous, soluble Gal-9 can act in a pro-inflammatory manner on macrophages. Whether the presence of Gal-9 in plaques can prevent IL-4 signalling necessary for plaque regression[183] or whether its downregulation is required for resolution of inflammation and regression of plaques requires further validation.

In summary, in this chapter it was shown that glycan-dependent Gal-9 binding to monocytes potentially induces monocyte activation and induces a pro-inflammatory phenotype in macrophages. This may contribute to the pro-inflammatory milieu during

inflammation. It was hypothesised that ß2 integrins are a potential binding partner of Gal-9 on monocytes. Whether this interaction also modulates monocyte adhesion requires further investigation. Additionally, more experiments are also required to determine whether the increased circulating levels of Gal-9 found in PAD patients described in Chapter 3 contribute to the inflammatory milieu and increased activation of monocytes in circulation. The vascular endothelium holds potential as source given the endothelial dysfunction and increased levels of circulating cytokines (including IFN-γ) associated with PAD [323,352]. However, it remains to be determined whether also macrophage-derived Gal-9 can act in an autocrine and/or paracrine manner to induce the pro-inflammatory phenotype. Furthermore, it is also required to characterise the role of Gal-9 within the atherosclerotic plaques and whether it contributes to the pro-inflammatory milieu within progressing plaques.

CHAPTER 5:

EFFECTS OF GAL-9 ON MONOCYTE TRAFFICKING

5. Chapter 5: Effects of Gal-9 on monocyte trafficking

5.1. Rational

Leukocyte migration is regulated by many known proteins such as selectins, integrins and adhesion molecules[6]. Each protein has a very distinct function in the cascade of leukocyte migration. Selectins such as L- or E-selectin interact with glycans on proteins such as PSGL-1 resulting in transient binding which mediates capture and rolling[6]. Integrins such as LFA-1 or Mac-1 facilitate crawling and adhesion through their interaction with adhesion molecules such as ICAM-1 or VCAM-1[6]. However, not all molecules involved in this cascade and their precise roles are known.

Gal-9 has previously been shown to modulate leukocyte trafficking in a range of *in vitro* and *in vivo* studies[255,288,301,315,353]. For example, Gal-9 treatment of monocytes, lymphocytes and neutrophils increased their adhesion to HUVEC *in vitro*[255], while the injection of Gal-9 into mouse knees increased the number of monocytes recruited locally into the joint[301]. Additionally, it has previously been shown that Gal-9 acts as capture and adhesion molecule on neutrophils in a ß2-integrin dependent manner *in vitro* while neutrophil and monocyte recruitment into the peritoneum of Gal-9 deficient mice was reduced after zymosan injections [315]. Furthermore, the data from Chapter 3 and 4 shows that Gal-9 is upregulated on the surface of endothelial cells in inflammatory environments while exogenous Gal-9 induces activation of monocytes and macrophages. However, the precise role of Gal-9 in monocyte migration remains unknown.

This chapter describes the characterisation of the role of Gal-9 in monocyte capture, adhesion and migration *in vitro*. Furthermore, the basal (homeostatic) migration of leukocyte subsets into various tissues in C57BL6 wild type and Gal-9 deficient C57BL6 (Gal-$9^{-/-}$) mice is characterised and the role of exogenous Gal-9 in zymosan induced peritonitis in C57BL6 mice is analysed.

5.2. Recombinant Gal-9 facilitates capture and adhesion of PBMC under physiological flow

In order to assess the role of Gal-9 in leukocyte migration, flow based adhesion assays were performed. The flow based adhesion assay allowed direct measurement of recruitment of leukocyte subsets in a tightly controlled system by perfusing PBMC and $CD14^{+}$ monocytes over channels coated with recombinant Gal-9 using physiological levels of flow.

5.2.1. PBMC of healthy young, healthy aged and PAD patients adhere to Gal-9 under physiological flow

Here the actions of Gal-9 on capture and adhesion of leukocytes from HY, HA and PAD patients were observed to determine disease specific differences in leukocyte recruitment to Gal-9 under flow conditions.

PBMCs isolated from whole blood of HY, HA and PAD patients were perfused over immobilised recombinant Gal-9 and adhesion and spreading of monocytes were quantified. 0.1 Pa was used as wall shear stress as this resembles physiological flow conditions in post capillary venules. The number of adherent cells was calculated as the sum of stationary phase bright cells and phase dark cells. The percentage of phase dark cells represented the percentage of spread/activated cells.

For the first time, it is shown here that Gal-9 captures PBMC under flow conditions (Figure 26A). Interestingly, no rolling was observed. Cells adhered immediately after capture and began to spread as indicated by turning phase dark. No differences in the adhesion of PBMCs between HY and HA were observed. However, significantly more PBMCs of PAD patients adhered to immobilised Gal-9 compared to PBMCs from HY or HA donors (Figure 26B).

To quantify firm adhesion, spread cells were represented as percentage of the total number of adherent cells. PBMCs of each cohort started spreading during the recorded time period of the experiment (Figure 26A). There were no significant differences in percentage of spread cells between HY and HA donors while there was a significant disease-dependent increase in the percentage of spread cells (Figure 26C).

Bisbenzamide nuclear staining of the adherent cells showed that the majority of spread cells appeared to be monocytes (Figure 26D), based on the shape of the nuclei.

Diseases can affect the percentage of circulating leukocyte subsets[91,92]. To determine whether PAD patients had a higher percentage of monocytes in their PBMC which could explain the increased percentage of spread cells, the percentage of $CD14^+$ monocytes in PBMC were quantified (Figure 27A). No significant differences in percentage of $CD14^+$ monocytes were found between the three cohorts (Figure 27B).

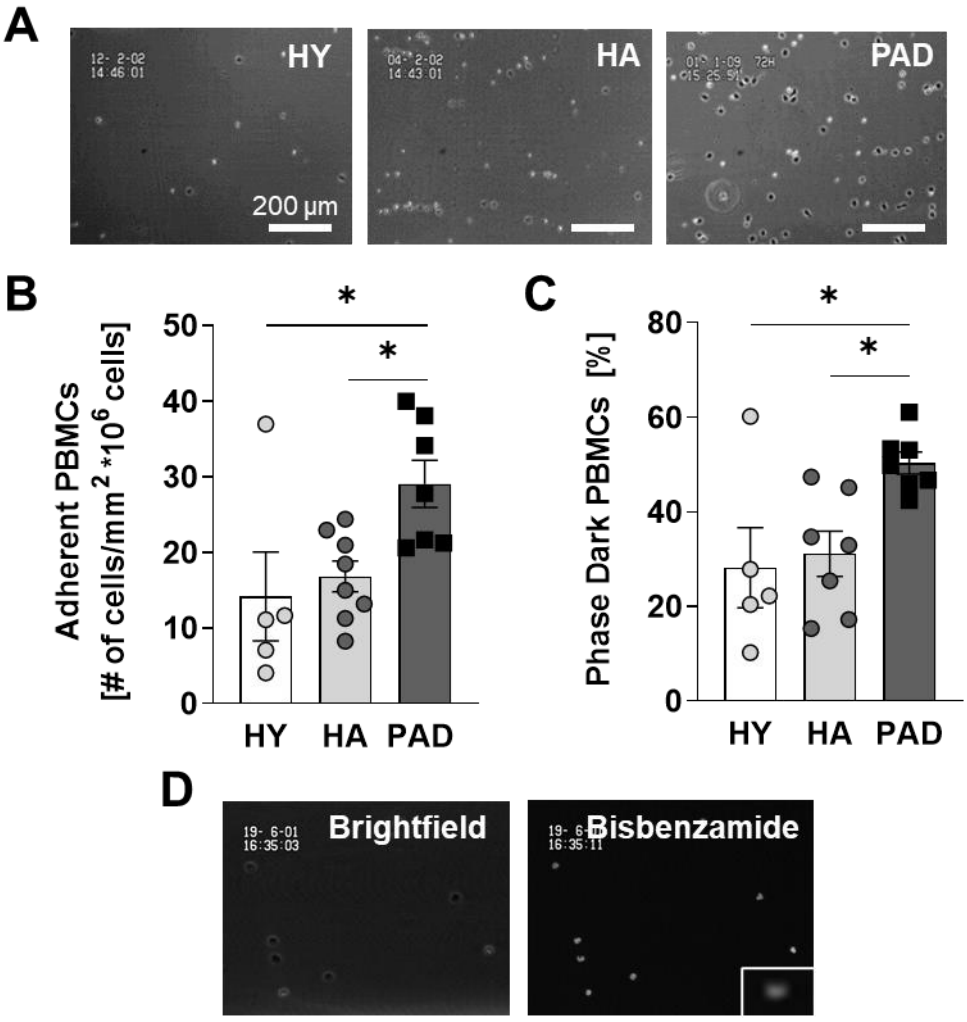

Figure 26: Gal-9 acts as capture and adhesion molecule for PBMC of healthy young, healthy aged and peripheral arterial disease patients. PBMC isolated from blood of healthy young (HY), healthy aged (HA) and peripheral arterial disease patients (PAD) were perfused over immobilised recombinant Gal-9 at a wall shear stress of 0.1 Pa (A-C). The number of adherent cells (A) and percentage of phase dark cells (B) were blotted. Bisbenzamide nuclear staining was used to determine the morphology of the nuclei of the adherent cells after perfusion (D). N=5-7. Statistical analysis was performed using One Way ANOVA with the Tukey's post hoc test. *= $p<0.05$.

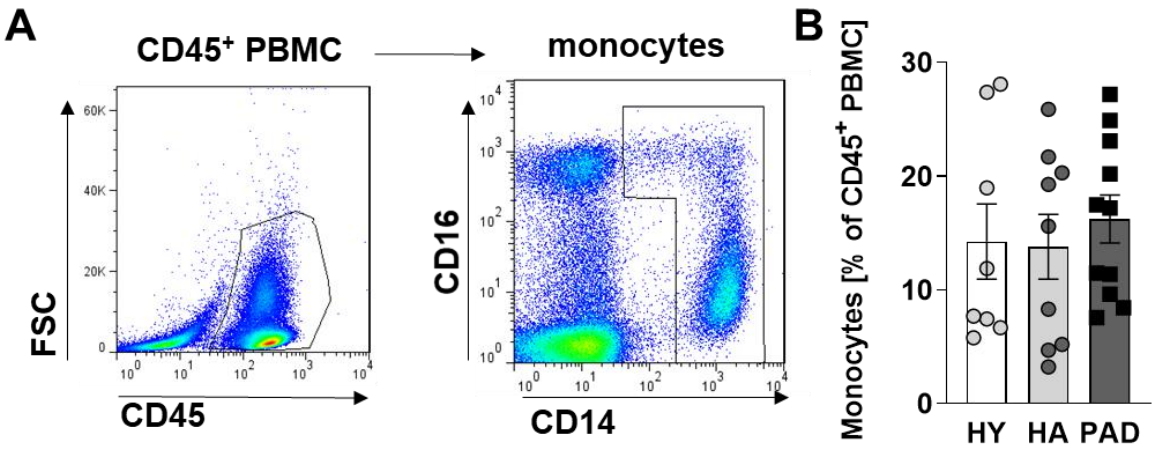

Figure 27: Quantification of CD14⁺ monocytes in PBMC samples from healthy young, healthy aged and peripheral arterial disease patients. PBMC isolated from blood of healthy young (HY), healthy aged (HA) and peripheral arterial disease patients (PAD) were analysed for their surface expression of these proteins was quantified using flow cytometry (A). CD14+ CD16+ cells were classed as monocytes and their percentage was blotted (B). N= 8-11. Statistical analysis was performed using One Way ANOVA with Tukey's post hoc test.

5.2.2. Gal-9 induces monocyte capture and adhesion

Monocyte migration is a key factor of atherogenesis[71,113,172,354] and since Gal-9 acts as capture molecule for PBMC in a peripheral arterial disease-dependent manner, Gal-9 mediated monocyte capture and adhesion was investigated. $CD14^+$ monocytes were isolated from blood of HY donors and perfused over various concentrations of immobilised Gal-9 at 0.1 Pa wall shear stress. Adhesion and spreading were quantified.

Like PBMCs, $CD14^+$ monocytes were captured and adhered immediately without rolling on all concentrations of immobilised Gal-9 (Figure 28A). The highest numbers of adherent cells were observed at 20 µg/ml and reduced with increasing concentration of Gal-9 (Figure 28B). Interestingly, over 90 % of $CD14^+$ monocytes spread and adhered firmly to Gal-9 throughout the duration of flow, independent of the concentration (Figure 28C).

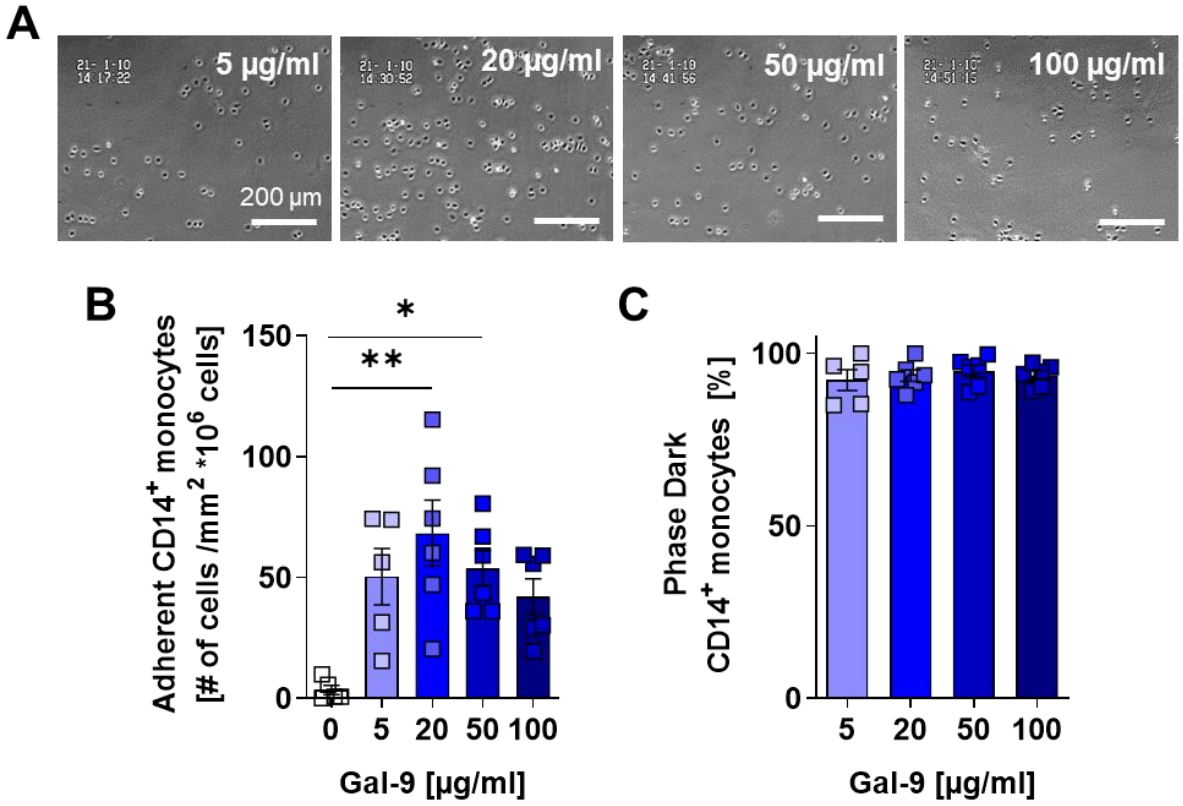

Figure 28: Quantification of CD14⁺ monocytes adhesion to immobilised Gal-9 under flow conditions. CD14⁺ monocytes isolated from blood of healthy young (HY), healthy aged (HA) and peripheral arterial disease patients (PAD) were perfused over different concentrations of immobilised Gal-9 at 0.1 Pa wall shear stress (A). Adhesion (B) was defined as the total number of adherent cells (Phase bright and phase dark) while spread cells (phase dark cells) were expressed as the percentage of adherent cells (C). N=5-6. Statistical analysis was performed using One Way ANOVA with Tukey's post hoc test; *=$p<0.05$, **=$p<0.01$.

5.2.2.1. Capture and adhesion of monocytes by Gal-9 is glycan dependent

Gal-9 is a ß-galactoside binding protein and having shown that its binding to monocytes in solution was glycan dependent, therefore the role of glycans in $CD14^+$ monocyte binding to Gal-9 under flow conditions was examined. 20 µg/ml immobilised Gal-9 were blocked with 25 mM lactose, a galactose containing sugar, prior to perfusion with $CD14^+$ monocytes. Incubation of 20 µg/ml Gal-9 with 25 mM sucrose, a non-galactose containing sugar with the same molecular weight as lactose, was used as non-specific glycan control.

Consistent with data presented in Chapter 4, Gal-9 capture of $CD14^+$ monocytes under flow conditions was also glycan dependent (Figure 29), evident through the significantly reduced number of adherent $CD14^+$ cells to lactose-blocked Gal-9 (Figure 29B). The number of adherent cells was reduced by 90% in the lactose treated sample compared to untreated or sucrose-treated Gal-9.

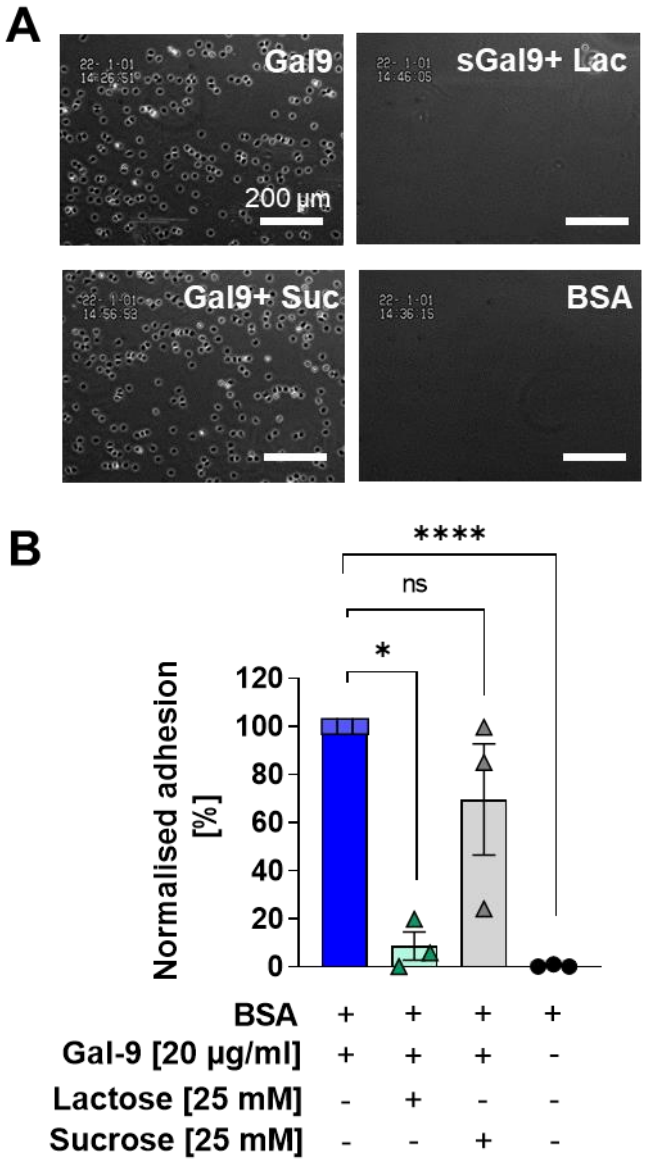

Figure 29: Quantification of glycan dependent adhesion of CD14⁺ monocyte to immobilised Gal-9 under flow conditions. CD14⁺ monocytes isolated from blood of healthy young were perfused at 0.1 Pa wall shear stress over immobilised Gal-9 which was blocked with lactose or sucrose (A) . Adhesion (B) was defined as the total number of adherent cells (Phase bright and phase dark) and normalised to the number of adherent cells to Gal-9. N=3. Statistical analysis was performed using One Way ANOVA with the Tukey's post hoc test; *=p<0.05, ****=p<0.001.

5.2.2.2. Capture and adhesion of monocytes by Gal-9 is ß2-integrin dependent

Integrins are an integral part of monocyte adhesion and are known to bind to members of the Ig superfamily[6] and we have also shown in Chapter 4, that Gal-9 affects ß2 integrins on monocytes. To investigate whether there is a direct interaction between Gal-9 and ß2 integrin and if this plays a role in Gal-9 mediated $CD14^+$ monocyte adhesion, $CD14^+$ monocytes were incubated with a blocking anti-CD18 antibody [355,356] prior to perfusion over Gal-9.

Incubation of $CD14^+$ monocytes with a blocking anti-CD18 antibody reduced capture and adhesion to immobilised Gal-9 by approximately 90% compared to untreated $CD14^+$ monocytes or $CD14^+$ monocytes treated with the isotype control, indicating a role of the ß2 integrin subunit in Gal-9 mediated adhesion (Figure 30A and B).

In summary, recombinant immobilised Gal-9 was shown to capture $CD14^+$ monocytes under flow conditions and induce cell spreading, a sign of cellular activation. Furthermore, Gal-9 mediated capture is glycan and ß2 integrin dependent and PBMC from PAD patients are captured in an increased manner. These data propose Gal-9 as novel monocyte capture and adhesion molecule which may play a role in monocyte migration contributing to atherogenesis.

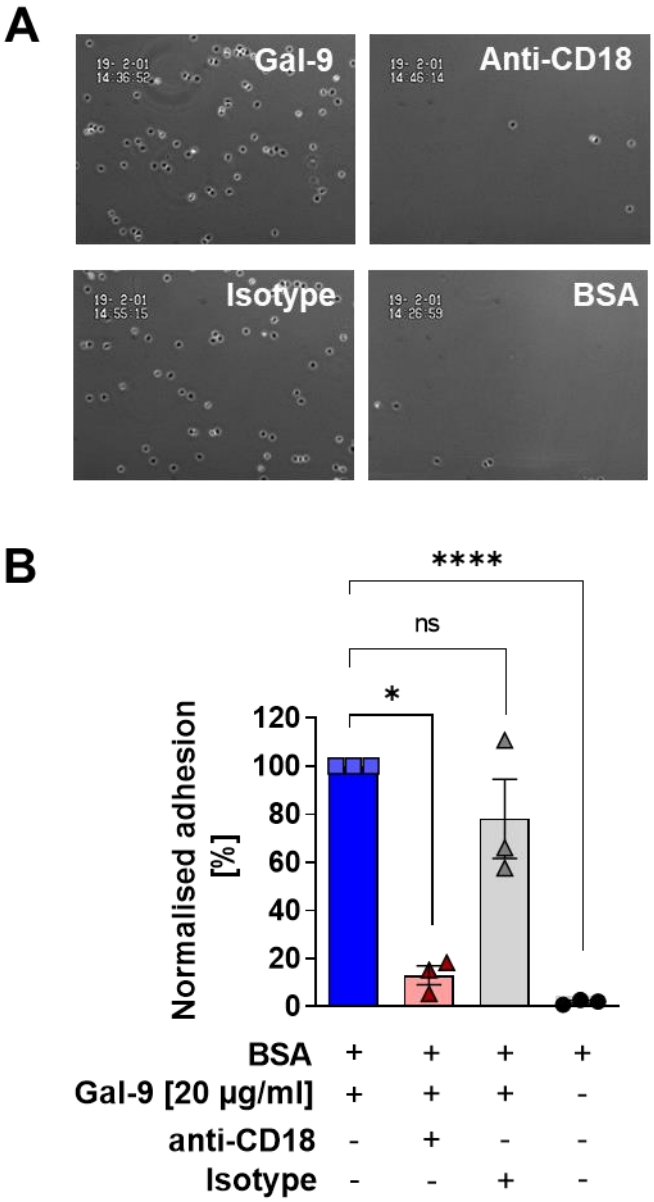

Figure 30: Quantification of CD18 dependent adhesion of CD14$^+$ monocyte to immobilised Gal-9 under flow conditions. CD14$^+$ monocytes isolated from blood of healthy young were incubated with anti-CD18 antibody or the appropriate isotype before they were perfused over immobilised Gal-9 at 0.1 Pa wall shear stress (A) . Adhesion (B) was defined as the total number of adhered cells (Phase bright and phase dark) and normalised to the number of untreated adherent cells to Gal-9. N=3. Statistical analysis was performed using One Way ANOVA with the Tukey's post hoc test; *=p<0.05, ****=p<0.001

5.3. Endothelial Gal-9 is required for monocyte adhesion

After establishing recombinant Gal-9 as capture and adhesion molecule, the role of endothelial Gal-9 in monocyte trafficking was explored. Gal-9 was knocked down in HUVECS using siRNA before treating them with Poly I:C, which is known to upregulate endogenous Gal-9[289,290,315].

Successful knock down of intracellular and surface Gal-9 in activated HUVECs was confirmed by flow cytometry. Expression of ICAM-1, as a marker of activation, was also measured.

Flow cytometric analysis of endothelial cells post transfection showed that ICAM-1 levels were significantly increased after 24 h of Poly I:C treatment (Figure 31A). No significant differences in ICAM-1 expression were found in endothelial cells treated with the different siRNA conditions, confirming endothelial activation and showing that the siRNA treatment had no effect on ICAM-1 expression. The flow cytometric measurements also showed that extracellular Gal-9 was upregulated in response to Poly I:C stimulation of HUVECs treated with no siRNA or control siRNA compared to the unstimulated controls (Figure 31B). There was a significant increase in extracellular Gal-9 in stimulated, compared to unstimulated, Gal-9 siRNA treated endothelium. However, there was significantly less Gal-9 surface expression in stimulated HUVECS transfected with Gal-9 siRNA compared to ctrl siRNA treated cells. Intracellular Gal-9 levels were also significantly reduced by about 75 % (Figure 31C) by Gal-9 siRNA treatment compared to control siRNA treatment 24 h after stimulation with Poly I:C, confirming successful Gal-9 knockdown.

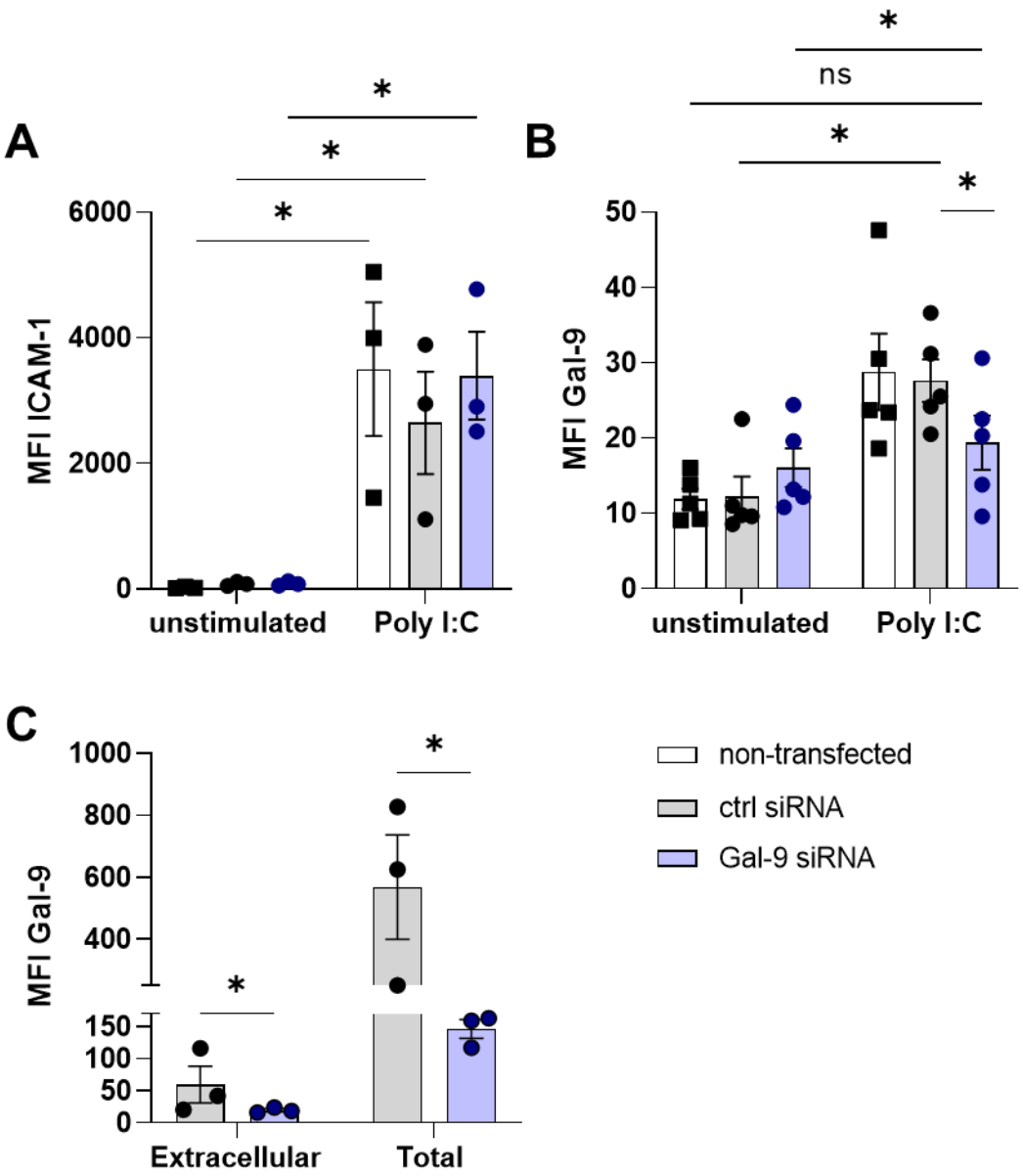

Figure 31: Quantification of ICAM-1 and Gal-9 expression of HUVEC after treatment with Gal-9 siRNA. HUVEC were treated with Gal-9 or control siRNA and then stimulated with 20 µg/ml Poly I:C. Extracellular ICAM-1 (A) and Gal-9 (B) expression were determined by flow cytometry. Extracellular and total Gal-9 levels were compared by also permeabilising Poly I:C treated cells before flow cytometric analysis (C). N=3-5. Statistical analysis was performed using Two Way ANOVA with the Tukey's post hoc test; *=$p<0.05$.

The effect of endothelial Gal-9 on monocyte recruitment was determined by perfusing $CD14^+$ monocytes over stimulated endothelial cells transfected with either control or Gal-9 siRNA at a wall shear stress of 0.05 Pa. The number of adherent $CD14^+$ monocytes in addition to the percentage transmigrated was quantified.

Perfused monocytes adhered to endothelial cells transfected with control siRNA as well as Gal-9 siRNA (Figure 32 A), however, there was a 25 % reduction in number of adherent $CD14^+$ monocytes to HUVEC transfected with Gal-9 siRNA compared to ctrl siRNA (Figure 32B). No difference in the percentage of transmigrated $CD14^+$ monocytes was observed throughout the time of the experiment (Figure 32C).

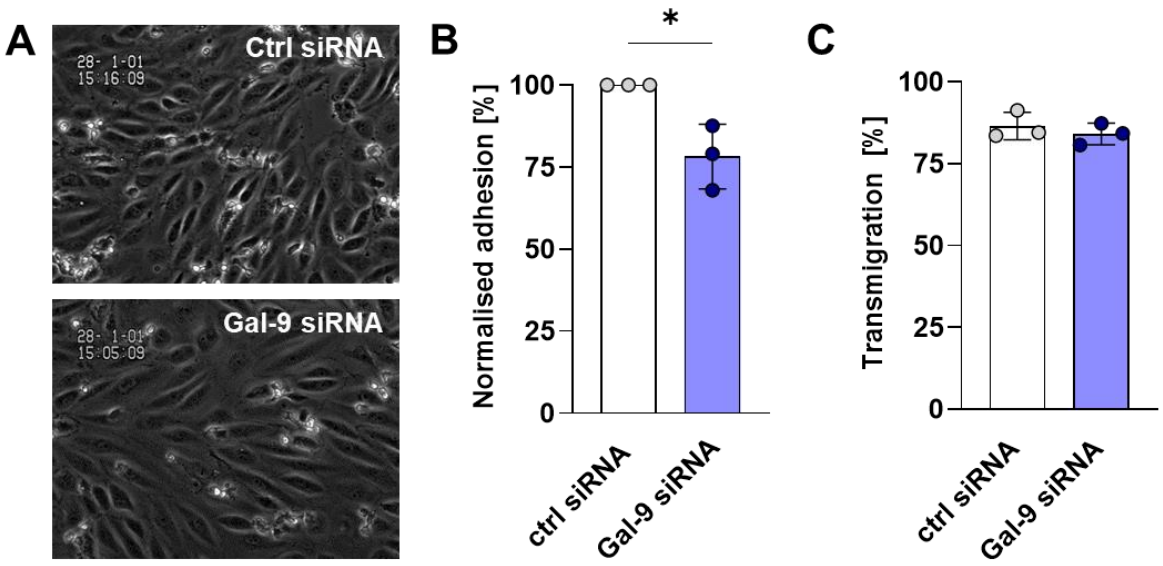

Figure 32: Quantification of CD14$^+$ monocyte adhesion and transmigration Gal-9 expression of HUVEC after treatment with Gal-9 siRNA. HUVEC were treated with Gal-9 or control siRNA and then stimulated with 20 µg/ml Poly I:C. CD14$^+$ monocytes of healthy young donors were perfused over the stimulated cells at 0.05 Pa wall shear stress (A). The number of total adherent monocyte to Gal-9 siRNA treated HUVEC was normalised to the number of adherent monocytes to ctrl siRNA treated HUVEC (B). The number of transmigrated cells was expressed as percentage of total adherent cells (C). N=3. Statistical analysis was performed using student's t-test; *=$p<0.05$.

5.3.1. Endogenous Gal-9 does not affect leukocyte migration under homeostatic conditions

Since it was established *in vitro* that exogenous Gal-9 modulates leukocyte migration and various models of inflammation have also demonstrated a role for Gal-9 in leukocyte migration, the impact of endogenous Gal-9 on leukocyte trafficking *in vivo* under homeostatic conditions was assessed. To address this, fluorescently conjugated anti-CD45 antibody was injected *i.v.* into C57BL6 (WT) mice or Gal-$9^{-/-}$ mice to label circulating $CD45^{+}$ cells and track their migration into tissue. After one hour post injection, mice were sacrificed and various tissues were collected to analyse leukocyte subsets in these tissues using flow cytometry (Figure 33 and 34).

Firstly, the total cell numbers of each leukocyte subset (CD45i.v.$^{+}$ and CD45i.v.$^{-}$ combined) between wild type (WT) and Gal-$9^{-/-}$ mice were determined, which show that there were significantly more neutrophils in circulation and in the bone marrow of Gal-$9^{-/-}$ mice compared to WT mice (Figure 35). No significant differences in cell numbers of any other leukocyte subsets in any tissue were found between WT and Gal-$9^{-/-}$ mice. However, significant differences in the number of cells in different leukocyte populations were found between different tissues. For example, as expected, $CD4^{+}$ and $CD8^{+}$ T cells were the predominant cell types in the spleen, whereas monocytes ($Ly6C^{hi}$ and $Ly6C^{low}$) and neutrophils were the most common cell types in whole blood and bone marrow and lung tissue (Fig. 35). No significant differences between WT and Gal-$9^{-/-}$ mice in CD45i.v.$^{+}$ cells in any of the tissues were detected (Table 6).

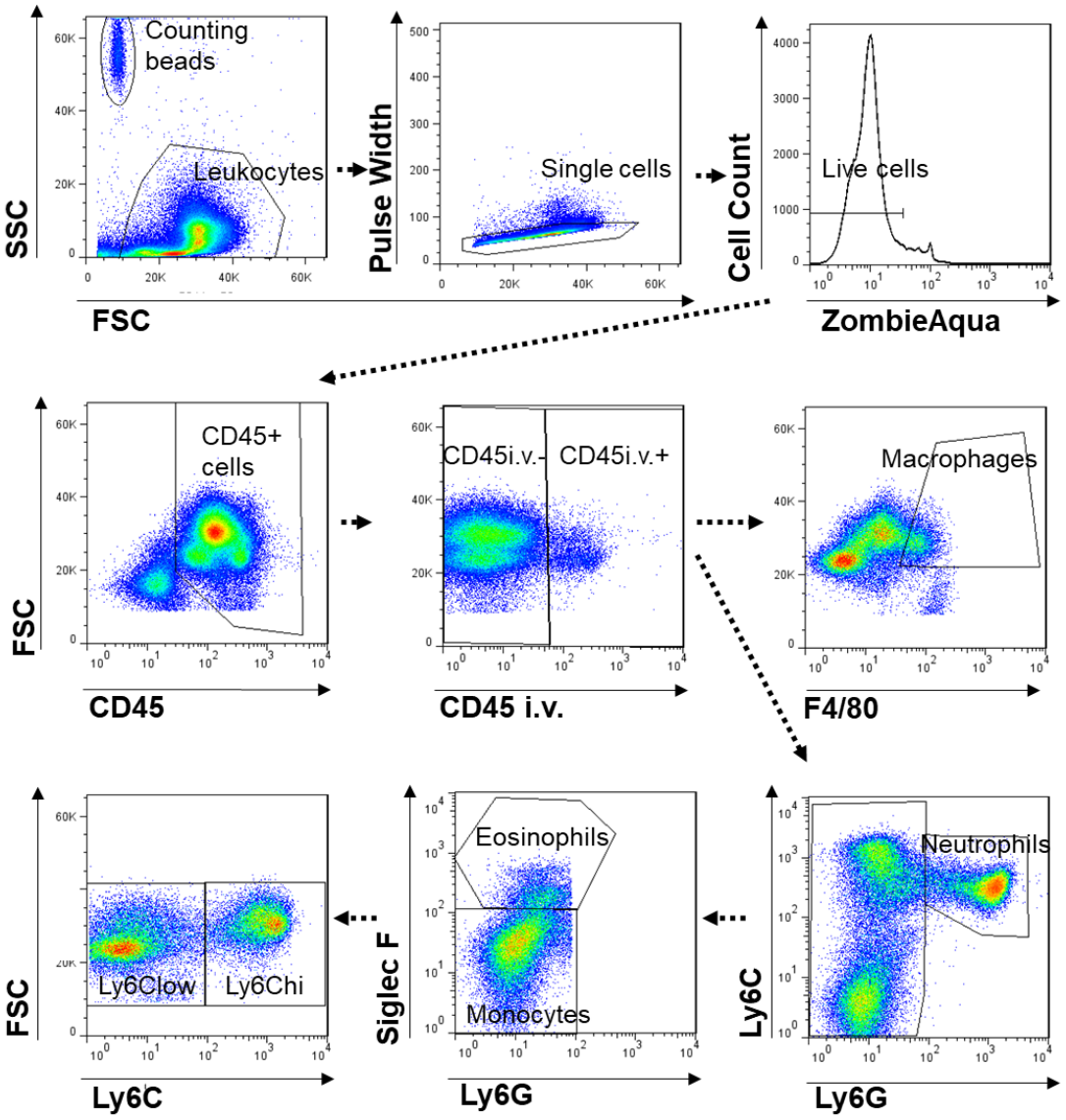

Figure 33: Gating strategy for myeloid cells in leukocytes isolated from tissues of C57BL6 and Gal-9$^{-/-}$ mice at homeostatic conditions. Leukocytes were selected using forward and side scatter (FSC and SSC). Single cells were identified by using FSC and pulse width before identifying living cells as ZombieAqua^{-} cells. CD45 was used as general leukocyte marker before these CD45^{+} cells were split up into *in vivo* stained CD45i.v.$^{+}$ and CD45i.v^{-} cells. These populations were then analysed for myeloid cell subsets. Macrophages and Neutrophils were classified as F4/80^{+} and Ly6G^{+} cells respectively, while Eosinophils and monocytes were classified as Ly6G^{-} cells. While eosinophils were defined as Siglec F^{+} cells, Monocytes were divided up into Ly6Clo and Ly6Chi subsets.

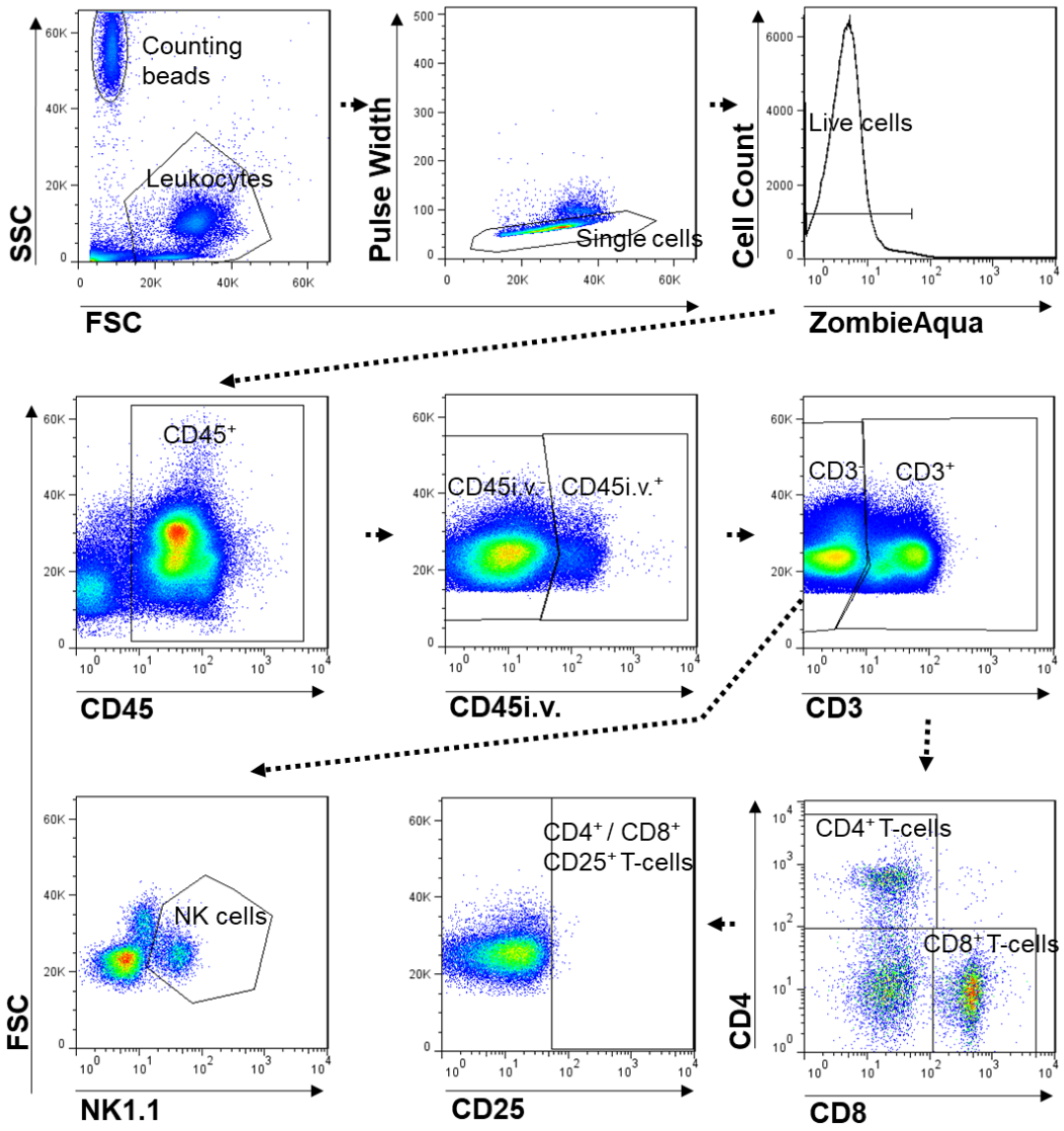

Figure 34: Gating strategy for lymphoid cells in leukocytes isolated from tissues of C57BL6 and Gal-9$^{-/-}$ mice at homeostatic conditions. Leukocytes were selected using forward and side scatter (FSC and SSC). Single cells were identified by using FSC and pulse width before identifying living cells as ZombieAqua^{-} cells. CD45 was used as general leukocyte marker before these CD45^{+} cells were split up into *in vivo* stained CD45^{+} and CD45^{-} cells. These populations were then analysed for lymphoid cell subsets. T-cells were defined as CD3^{+} CD4^{+} or CD3^{+} CD8^{+} cells and further analysed for activation by determining the expression of CD25^{+}. Natural Killer cells were defined as CD3^{-} NK1.1^{+} cells.

The data further reveals that only a very small percentage of leukocytes were labelled with CD45-antibody ($CD45iv^+$) one hour after injection (Table 7). No significant differences in percentages of $CD45i.v.^+$ cells between WT and $Gal\text{-}9^{-/-}$ mice were detected in any leukocyte subset in any of the tissues. However, there was a significant difference in the percentage of circulating $CD45i.v.^-$ neutrophils. $Gal\text{-}9^{-/-}$ mice had a significantly higher percentage of circulating neutrophils compared to WT mice. No significant differences were detected in any of the other circulating $CD45i.v.^-$ leukocytes subsets. Analysis of the percentage of the different $CD45i.v.^-$ leukocyte subsets in the bone marrow revealed no significant differences between WT and $Gal\text{-}9^{-/-}$ mice. Significant differences between WT and $Gal\text{-}9^{-/-}$ mice were found in the percentage of $CD45i.v^-$, $CD8^+$ cells in spleen, while $CD4^+$ and NK cells also trended towards a decreased percentage in $Gal\text{-}9^{-/-}$ mice. In lung tissue, no significant differences between WT and $Gal\text{-}9^{-/-}$ mice were found in any of the $CD45i.v.^-$ leukocyte subsets. However, the $Ly6C^{lo}$ monocyte population in the lungs of $Gal\text{-}9^{-/-}$ mice were trending towards a lower percentage than those in WT mice. In liver tissue, $CD4^+$ cells were the only $CD45i.v.^-$ subset which showed a significant difference between the two mouse strains: $Gal\text{-}9^{-/-}$ had a significantly smaller percentage of $CD4^+$ cells in the liver than WT mice. While the percentage $CD45i.v.^-$ $CD8^+$ cells also appeared to be lower in the lungs of $Gal\text{-}9^{-/-}$ mice, the difference is not quite significant.

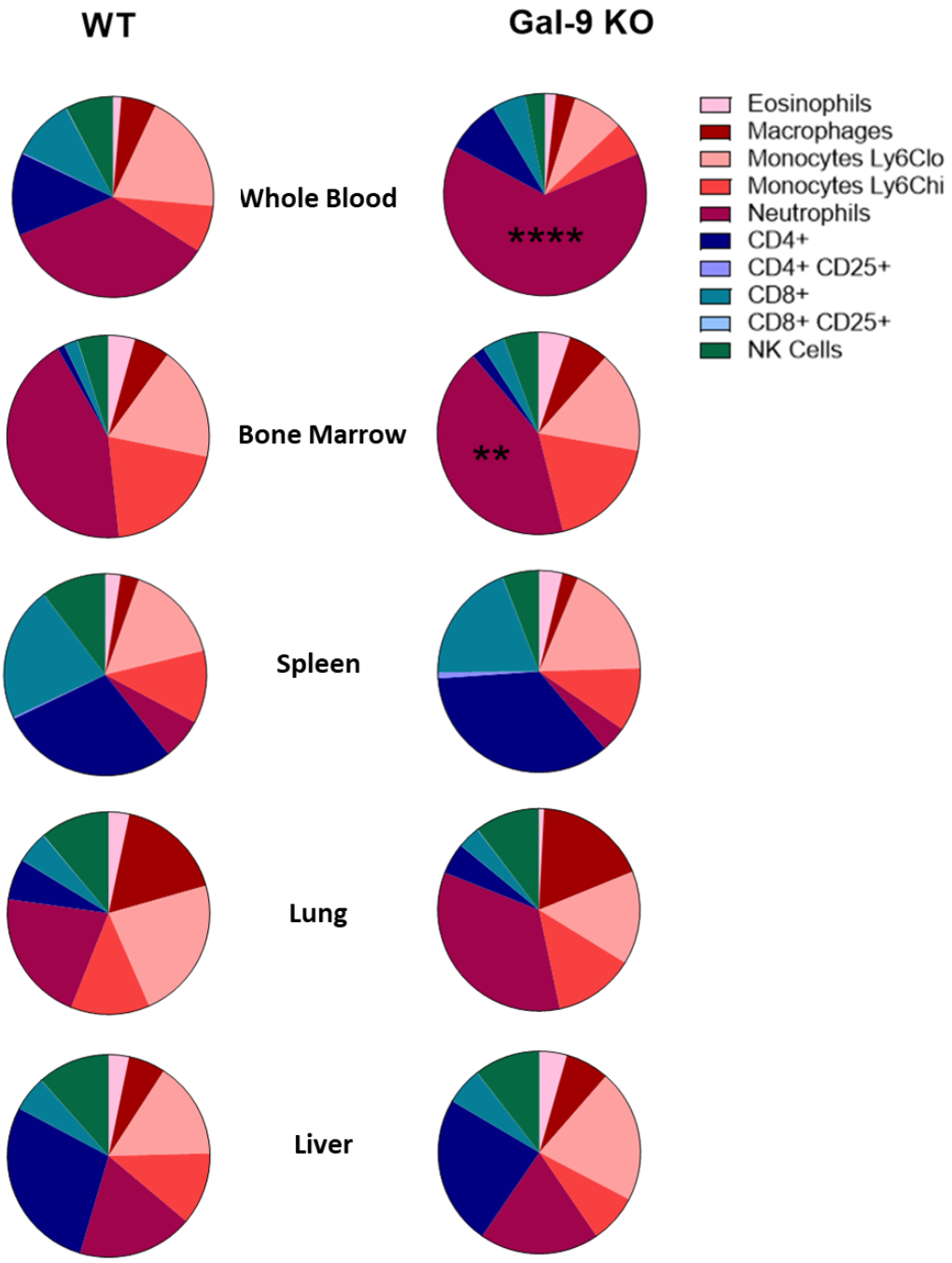

Figure 35: Leukocyte populations in tissues isolated from C57BL6 and $^{-/-}$ mice. Leukocytes were isolated from whole blood, bone marrow, spleen lung and liver of three C57BL6 (WT) and three Gal-9$^{-/-}$ (KO) mice. The distribution of leukocyte populations within these tissues was analysed using flow cytometry. N=3. Statistical significant differences in the distribution of leukocyte subsets between the two mouse strains were calculated using Two Way ANOVA with Tukey's post hoc test. **= $p<0.01$; ****= $p<0.001$.

Table 6: Total number of migrated leukocyte subsets in WT and Gal-9$^{-/-}$ mice under basal conditions. WT and Gal-9$^{-/-}$ mice were injected with fluorescent CD45^{+} antibodies *i.v.* (CD45i.v.). 1 h post injection, leukocytes from different tissues were isolated and stained with antibodies against various leukocyte subset markers for flow cytometric analysis. The number of cells per subset were acquired using counting beads. Each value is the average cell number from three mice. Statistical analysis was performed by using Two Way ANOVA with Tukey post hoc test.

	CD45i.v.$^{+}$				**CD45i.v.$^{-}$**			
	WT		**Gal-9$^{-/-}$**		**WT**		**Gal-9$^{-/-}$**	
Whole Blood	Mean	SD	Mean	SD	Mean	SD	Mean	SD
Eosinophils	233,6	125,1	1057,0	1131,9	654,7	294,2	2724,1	3352,8
Macrophages	1346,7	1205,4	2162,6	1377,8	2345,0	2186,9	4584,1	1417,2
Monocytes Ly6Clo	1833,0	1182,6	4503,6	3057,1	11032,5	7906,7	12916,0	4294,7
Monocytes Ly6Chi	1188,5	685,2	2835,1	3092,1	3789,9	2576,1	8892,7	6357,8
Neutrophils	307,2	162,0	3688,9	4353,9	22675,4	10333,2	135460,9	54409,0
CD4^{+}	692,3	428,6	1843,6	1606,1	8063,8	3662,9	16720,3	12959,9
CD4^{+} CD25^{+}	2,9	4,1	1,5	2,2	117,7	120,8	69,9	51,0
CD8^{+}	623,9	405,2	923,9	604,1	5956,0	2875,4	10653,0	9557,8
CD8^{+} CD25^{+}	13,1	18,5	6,1	4,3	48,6	29,1	30,7	11,2
NK Cells	2553,1	1465,7	3420,8	1086,4	2515,7	972,6	3378,7	1104,5
Bone Marrow								
Eosinophils	2282,3	312,7	6530,1	765,0	108401,9	78846,3	216183,1	46957,6
Macrophages	11500,3	4307,2	18698,7	7735,6	134265,2	52305,0	262402,4	125981,2
Monocytes Ly6Clo	34019,8	23700,1	91040,5	58786,0	433487,8	340761,7	621456,3	380466,0
Monocytes Ly6Chi	15891,9	2076,5	23075,6	2153,1	498909,6	173417,3	779193,5	113781,1
Neutrophils	5763,8	2436,0	12611,6	9759,7	1108227,5	547321,7	1857262,7	265735,5
CD4^{+}	2061,4	1152,8	11482,7	9350,7	27171,1	12846,4	78663,2	57669,3
CD4^{+} CD25^{+}	13,3	9,6	200,3	161,2	800,1	555,9	968,5	84,9
CD8^{+}	2131,5	321,7	15465,0	9006,3	52853,0	26491,1	138849,1	109148,7
CD8^{+} CD25^{+}	34,9	49,4	130,7	76,6	1342,9	1144,1	914,3	784,8
NK Cells	9708,4	3045,0	23446,9	18226,0	116406,6	62240,9	220934,0	224127,3

Spleen								
Eosinophils	98376,5	47028,6	262753,2	80006,6	835596,0	241374,7	1617312,2	887116,3
Macrophages	346935,1	131322,9	428058,0	118916,4	769548,3	45795,5	844505,3	492865,6
Monocytes Ly6Clo	668595,5	476026,3	824922,1	176947,4	5320957,4	2476111,1	8370645,7	1272595,7
Monocytes Ly6Chi	448685,4	364750,1	406820,8	158278,7	3967381,4	3001826,7	4720047,8	1286269,3
Neutrophils	127056,7	106787,1	120124,7	69783,7	2334328,0	988641,5	1924069,9	451481,8
$CD4^+$	502904,2	393991,2	1018684,7	76839,1	10332456,6	7362928,9	16681387,1	2352422,5
$CD4^+$ $CD25^+$	767,1	468,1	5550,4	3379,7	90802,4	34486,4	474641,8	319280,9
$CD8^+$	313434,5	197634,6	520242,6	155571,4	7855972,5	5026627,1	9173021,9	911248,7
$CD8^+$ $CD25^+$	915,3	1016,2	4138,1	3672,4	8744,5	2678,1	20058,0	12700,3
NK Cells	599012,3	269511,6	628994,0	180547,8	3344627,3	1767165,9	2320197,1	98433,9
Liver								
Eosinophils	1183,2	1173,0	1554,4	1902,6	1498,9	1139,2	1474,6	1779,4
Macrophages	2969,4	2247,8	2950,1	3324,5	1920,6	991,8	1883,4	1732,9
Monocytes Ly6Clo	6697,3	7014,0	8804,1	10720,8	6101,7	5695,1	5825,4	7293,4
Monocytes Ly6Chi	5807,4	6294,6	2837,1	3420,6	3742,3	2880,6	2520,6	2922,4
Neutrophils	5568,8	6608,4	1683,2	2289,9	9668,7	5398,6	11471,3	12094,9
$CD4^+$	4917,0	5881,5	10279,0	13766,8	18441,3	22799,6	6180,3	7983,9
$CD4^+$ $CD25^+$	7,2	5,3	3,1	4,4	9,3	7,6	15,8	9,4
$CD8^+$	371,2	203,7	517,7	424,3	4275,5	3522,3	3559,6	4651,4
$CD8^+$ $CD25^+$	4,1	3,9	11,6	5,8	22,1	7,6	13,1	18,5
NK Cells	5141,9	6313,1	3831,5	5124,5	4431,7	5469,4	3426,2	4662,3
Lung								
Eosinophils	1000,0	1065,5	203,2	244,3	18801,4	19946,0	219,1	235,8
Macrophages	25701,8	29438,8	10394,7	12206,4	54420,1	60074,4	43268,2	46164,4
Monocytes Ly6Clo	23596,7	25105,1	11372,6	12731,5	87424,0	94397,5	26328,4	28028,0
Monocytes Ly6Chi	21021,1	22925,5	8438,6	9859,5	17212,0	19603,8	30447,1	32318,7
Neutrophils	6017,9	6384,5	2560,1	2948,8	74346,9	82249,1	102072,6	118725,1
$CD4^+$	2036,2	2215,2	1175,1	1271,3	8120,5	9699,3	3199,5	3413,8
$CD4^+$ $CD25^+$	32,0	34,8	9,5	10,8	172,4	206,6	129,2	155,9
$CD8^+$	1942,3	2139,3	680,4	827,7	8198,5	9705,7	2858,4	3035,4
$CD8^+$ $CD25^+$	82,5	87,7	22,7	25,3	117,4	142,0	155,5	168,5
NK Cells	19493,8	21047,8	9107,2	9736,1	12548,1	14845,5	14724,9	15649,3

Table 7: Migration of leukocyte subsets in WT and Gal-9$^{-/-}$ mice under basal conditions. WT and Gal-9$^{-/-}$ mice were injected with fluorescent CD45^{+} antibodies *i.v.* (CD45i.v.). 1 h post injection, leukocytes from different tissues were isolated and stained with antibodies against various leukocyte subset markers for flow cytometric analysis. Each leukocyte subset was plotted as percentage of CD45^{+} cells . Each value is the average value of the percentage from three mice. Statistical analysis was performed by using Two Way ANOVA with Tukey post hoc test; P-values are indicated in superscript or as **=p<0.01; ****=p<0.00.

	CD45i.v.$^{+}$				**CD45i.v.$^{-}$**			
	WT		**Gal-9$^{-/-}$**		**WT**		**Gal-9$^{-/-}$**	
Whole Blood	Mean	SD	Mean	SD	Mean	SD	Mean	SD
Eosinophils	0.228	0.141	0.259	0.156	0.881	0.647	0.565	0.573
Macrophages	1.094	0.772	0.755	0.219	1.883	1.510	1.967	0.824
Monocytes Ly6Clo	1.631	0.374	1.528	0.462	9.662	3.665	5.516	2.482
Monocytes Ly6Chi	1.103	0.172	0.680	0.455	3.326	0.689	2.943	0.248
Neutrophils	0.290	0.023	0.809	0.702	22.136	1.400	54.813****	17.301
CD4^{+}	0.629	0.265	0.539	0.129	7.906	0.973	5.331	1.294
CD4^{+} CD25^{+}	0.002	0.003	0.001	0.002	0.089	0.081	0.047	0.044
CD8^{+}	0.564	0.325	0.318	0.044	5.737	0.268	3.066	0.849
CD8^{+} CD25^{+}	0.007	0.013	0.004	0.004	0.048	0.032	0.017	0.013
NK Cells	2.369	0.312	1.501	0.822	2.532	0.330	1.443	0.627
Bone Marrow								
Eosinophils	0.082	0.015	0.153	0.017	3.683	2.673	5.111	1.457
Macrophages	0.431	0.265	0.442	0.215	4.623	1.408	6.445	4.293
Monocytes Ly6Clo	1.190	0.892	2.222	1.761	14.655	11.607	15.191	11.629
Monocytes Ly6Chi	0.572	0.131	0.541	0.050	16.877	4.740	18.129	1.428
Neutrophils	0.206	0.100	0.280	0.246	35.755	16.458	43.140	1.969
CD4^{+}	0.071	0.045	0.255	0.236	0.886	0.300	1.761	1.441
CD4^{+} CD25^{+}	0.000	0.000	0.004	0.004	0.027	0.019	0.023	0.006
CD8^{+}	0.075	0.009	0.349	0.219	1.714	0.643	3.113	2.746
CD8^{+} CD25^{+}	0.001	0.002	0.003	0.002	0.043	0.035	0.021	0.020
NK Cells	0.350	0.135	0.521	0.459	4.075	2.461	4.867	5.753
Spleen								
Eosinophils	0.169	0.127	0.224	0.063	1.752	1.289	1.458	1.016
Macrophages	0.641	0.491	0.366	0.096	1.496	0.802	0.751	0.578
Monocytes Ly6Clo	0.944	0.431	0.727	0.234	8.225	0.693	7.233	1.061
Monocytes Ly6Chi	0.591	0.268	0.345	0.133	5.299	1.493	4.033	0.976
Neutrophils	0.285	0.384	0.100	0.063	4.064	2.805	1.648	0.325
CD4^{+}	0.864	0.283	0.882	0.046	19.902	11.786	$14.638^{0.0913}$	3.574
CD4^{+} CD25^{+}	0.002	0.002	0.005	0.004	0.263	0.280	0.430	0.356
CD8^{+}	0.591	0.166	0.459	0.189	16.055	10.256	8.010**	1.423
CD8^{+} CD25^{+}	0.003	0.003	0.004	0.004	0.028	0.025	0.018	0.014
NK Cells	1.253	0.430	0.556	0.223	7.219	4.402	$2.016^{0.0971}$	0.159

Liver								
Eosinophils	1.157	0.161	1.189	0.973	1.990	0.571	1.195	0.960
Macrophages	3.760	1.556	3.363	0.776	3.207	1.685	3.429	1.967
Monocytes Ly6Clo	6.171	0.888	7.319	2.816	6.739	0.770	4.565	0.581
Monocytes Ly6Chi	5.086	1.093	2.467	0.839	4.944	1.386	2.569	0.615
Neutrophils	3.738	2.861	0.835	0.679	16.105	7.960	15.513	5.436
$CD4^+$	3.522	2.035	5.336	3.860	15.064	8.346	4.210****	1.281
$CD4^+$ $CD25^+$	0.011	0.016	0.016	0.027	0.039	0.037	0.052	0.064
$CD8^+$	1.000	0.764	1.114	0.749	7.102	4.766	$2.260^{0.0941}$	0.888
$CD8^+$ $CD25^+$	0.015	0.013	0.039	0.037	0.060	0.045	0.004	0.008
NK Cells	3.657	2.095	2.095	1.293	3.404	1.773	1.671	1.378
Lung								
Eosinophils	0.462	0.630	0.248	0.250	2.160	1.610	0.7108	0.6591
Macrophages	4.390	2.775	2.206	0.909	7.911	5.096	7.7789	6.0497
Monocytes Ly6Clo	3.821	1.422	3.123	0.884	13.337	6.045	$7.057^{0.0692}$	1.8071
Monocytes Ly6Chi	4.782	0.548	1.458	1.059	7.045	1.296	5.5846	4.0008
Neutrophils	1.175	0.400	0.513	0.195	16.706	2.841	17.393	13.034
$CD4^+$	0.634	0.516	1.023	1.279	5.495	3.504	4.777	4.4043
$CD4^+$ $CD25^+$	0.003	0.004	0.002	0.001	0.022	0.021	0.0216	0.0243
$CD8^+$	0.605	0.514	0.679	0.698	3.785	1.756	3.8606	4.2835
$CD8^+$ $CD25^+$	0.011	0.007	0.004	0.003	0.063	0.033	0.1058	0.1528
NK Cells	4.334	1.960	3.459	2.032	4.374	1.672	4.5266	0.791

5.4. Exogenous Gal-9 induces myeloid cell migration *in vivo*

In previous chapters an upregulation of Gal-9 in inflammatory environments and Gal-9-induced monocyte activation and cytokine release from macrophages was observed. Therefore, the effect of exogenous Gal-9 on leukocyte migration in zymosan induced peritonitis in C57BL6 mice was assessed. Therefore mice were treated *i.p*. with zymosan in the presence or absence of Gal-9. The peritoneal lavages were collected 2, 4 or 16 h post injection and monocyte and PMN counts were quantified as well as the levels of CXCL1, CCL2, TNFα and IL-6.

Neutrophil infiltration into the peritoneum peaked at 4 h post injection in both treatment groups (Figure 36A). However, no differences in neutrophil numbers were detected at either time point. Monocytes counts peaked in both treatment groups at 16 h (Figure 36B). While there were no differences detected in monocyte numbers after 4 h, there

were significantly more monocytes present in the peritoneal lavages 16 h in mice treated with zymosan and Gal-9 compared to zymosan alone.

Since cytokines are released early on in the immune response, the levels of CXCL1, CCL2, TNFα and IL-6 in the peritoneal lavages were measured at 2 and 4 h post injection. The analysis revealed peak levels of CXCL1 (Figure 36C) and TNFα (Figure 36E) 2 h post injection while the levels of CCL2 (Figure 36D) and IL-6 (Figure 36F) do not change significantly between the two time points. However, there was a significant difference between zymosan and zymosan and Gal-9 treated mice after 2 h in the level of all chemokines and cytokines: mice which received also Gal-9 had increased levels of all four proteins. These differences were not observed at the 4 h time point.

In summary these data indicate that exogenous Gal-9 has a pro-inflammatory role *in vivo* by increasing chemo- and cytokine release and monocyte migration intraperitoneally.

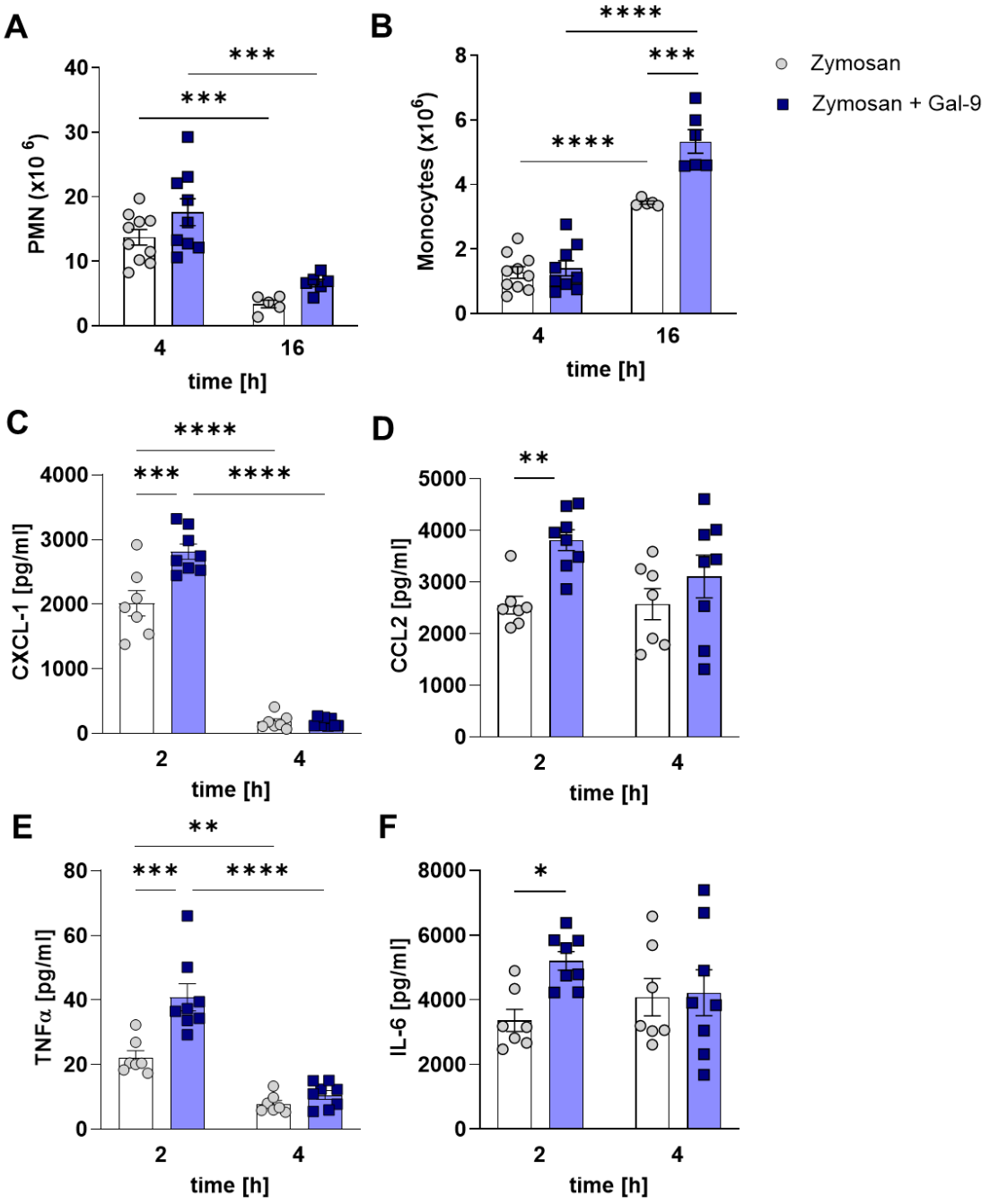

Figure 36: Monocyte and Neutrophil counts as well as cytokine levels isolated from peritonea of C57BL6 mice after injection with zymosan with or without Gal-9. Peritoneal lavages of C57BL6 mice injected with zymosan in the presence and absence of Gal-9 were analysed 2, 4 or 16 h post injection. Neutrophil (A) and monocyte (B) counts were quantified using flow cytometry. Levels of CXCL1 (C), CCL2 (D), TNFα (E) and IL-6 (F) were analysed using Luminex technology. N= 5-10. Statistical significant differences were calculated using Two Way ANOVA with Tukey's post test.*= p<0.05; **= p<0.01; ***= p<0.005; ****= p<0.001.

5.5. Discussion

In this chapter, the role of Gal-9 in monocyte trafficking was assessed. Previous studies have demonstrated a pro-inflammatory function for Gal-9[100,238,256,301,357] and various studies have investigated the role of Gal-9, first described as an eosinophil chemoattractant[300], in leukocyte trafficking more specifically[207,255,309,321]. For example, soluble Gal-9 has been reported to increase the adhesion of B-cells, T-Cells, neutrophils, eosinophils and monocytes to endothelial cells under static[255] and physiological flow conditions[321] *in vitro.* Additionally, Imaizumi *et al.* showed that endothelial Gal-9 increased the adhesion of human eosinophilic leukemia 1 cells[214,288]. However, there is still a lack of understanding of the precise mechanisms involved.

Here, the current understanding of Gal-9 in the context of monocyte recruitment, which is critical in driving atherosclerotic plaque progression[186], was expanded. Using a flow-based adhesion assay, it was shown that Gal-9 captures PBMCs as well as monocytes. Interestingly, while monocyte capture seemed to be highest at 20 µg/ml Gal-9, the adhesion and activation of monocytes was concentration independent. Whether the reduced number of adherent monocytes at higher concentrations of Gal-9 is due to reduced availability of binding sites because of more tightly packed Gal-9 molecules on the channel surface, requires further investigation.

Remarkably, no rolling was observed, which is traditionally considered to be the first step in the leukocyte migration cascade[6]. Rolling is mediated by the transient interactions of selectins with glycans on glycoproteins such as PSGL-1. The interactions between immobilised Gal-9 and its binding partner(s) on PBMCs and monocytes are evidently strong enough to withstand the applied physiological wall

shear stress, suggesting that Gal-9 is interacting with a different protein than selectins on the monocyte surface.

Furthermore, a fraction of the adherent PBMC and the majority of monocytes were also activated and adhered firmly, evident by spreading, indicated by the change from phase bright to phase dark. Using anti-CD18 blocking antibodies, we were able to block monocyte adhesion, indicating a interaction between Gal-9 an ß2 integrins. This confirms our findings in Chapter 4 which suggest an interaction between Gal-9 and ß2 integrins. As a subunit of LFA-1 and Mac-1, CD18 is known to be involved in monocyte adhesion and spreading through interaction with adhesion molecules such as VCAM-1 on the endothelium[24]. Various studies have also demonstrated that some galectins can interact directly with integrin subunits[327,328,330,358,359]. For example, Gal-1 was shown to interact with the ß1 integrin subunit on smooth muscle cells, which impacted their adhesion[359]. Gal-3 mediates adhesion of HUVECs by interacting with aV and ß1 integrins[331] while its interaction with ß1 also induces apoptosis in T-cells[360] and adhesion of Madin-Darby canine kidney cells to extracellular matrix substrates[358]. Furthermore, ß3 integrins are known to interact with Gal-3 to regulate endometrial cell proliferation and adhesion[330]. Another galectin of the tandem-repeat family, Gal-8 was also interacts with integrins. Gal-8 binds to ß1 integrins which inhibits cell adhesion of a human carcinoma cell line[328] and induces spreading in Jurkat T cells[327]. Interestingly, Gal-8 has also been identified as a binding partner of the ß2 integrin LFA-1 which inhibits the interaction of PBMC with immobilised ICAM-1 under static conditions[329]. These studies further support the hypothesis of an interaction between Gal-9 and ß2 integrins, particularly since it was shown in a previous study that Gal-9 mediated capture of primary human neutrophils is also ß2 integrin dependent[315]. Whether the

observed reduction of adherent cells to Gal-9 after their treatment with anti-CD18-antibodies is due to the blocking of a direct interaction between Gal-9 and CD18 remains to be determined. Nevertheless, these findings suggest a novel, selectin-independent capture mechanism of monocytes mediated through a glycan-dependent interaction between Gal-9 and ß2 integrins.

The current dogma indicates monocyte activation is predominantly mediated through chemokines, expressed by activated endothelial cells and chemokine receptors on monocytes[6]. These interactions activate intracellular G-protein coupled receptor mediated pathways and lead to integrin activation, which allows monocytes to adhere firmly to activated endothelium[6,361]. Whether this novel activation mechanism mediated by Gal-9 observed here is also driven through G-protein coupled receptor pathways and which binding partners of Gal-9 mediate activation requires further investigations. Interestingly, another galectin, Gal-3, has been found to form heterodimers with chemokine CXCL12 which inhibits the migration of leukocytes[248]. Further studies are required to understand if similar interactions are occurring between chemokines and Gal-9 and whether they contribute to monocyte capture, adhesion and spreading.

Gal-9 is only one of two proteins capable of inducing capture, adhesion and spreading of leukocytes[362]. Recombinant immobilised fractalkine, a ligand for CX_3CR1, has also been shown to promote immediate capture and cause adhesion and spreading of leukocytes. However, the CX_3CR1 mediated capture occurs a integrin-independent manner under physiological wall shear stress[362].

While the capture and spreading of PBMC by immobilised Gal-9 is independent of age, Gal-9 enhanced the capture, adhesion and spreading of PBMCs from PAD patients.

Additionally, the majority of adherent and spread PBMCs are monocytes. This study documents for the first time a disease dependent differences in capture and adhesion to Gal-9 However, other studies have highlighted increased adhesion of monocytes to VCAM-1 and activated endothelium in other inflammatory conditions such as RA[363] and hypertriglyceridemia[337]. Both studies concluded that the increased adhesion to IL-1ß stimulated endothelium and VCAM-1 respectively was due to heightened activation of monocytes. Increased basal activation of monocytes in PAD patients, indicated by decreased CD62L levels were shown in Chapter 4, which confirms findings from previous studies in HA and individuals with hypertriglyceridemia[307,337]. Interestingly, no increased levels of the active conformation of CD18 in monocytes of PAD patients were detected (Chapter 4) which could have also explained the increased adhesion of PBMCs to immobilised Gal-9, based on the interaction of Gal-9 with ß2 integrins. However, in this study total CD18 levels were not assessed, but several other studies have reported the upregulation of total ß2 integrin[337] in monocytes of PAD patients and increased CD11b/CD18 in patients with unstable angina[347], as well as CD11c, Mac-1 and LFA-1 in patients with myocardial infarction[45,348]. These findings suggest that Gal-9 may not require the active confirmation of CD18 for its binding and that the increased number of adherent PBMCs in PAD patients is due to increased levels of total CD18 as well as increased activation of monocytes in PAD patients.

Gal-9 is a glycan binding protein, known to bind O-glycans[364] as well as linear N-glycans[311] on glycosylated proteins such as TIM-3[333], CD44[309] and CD45[311]. The treatment of Gal-9 coated channels with 25 mM of lactose reduced capture by 90 %, indicating a glycan-dependent capture mechanism, confirming results from Chapter 4 and other studies demonstrating glycan-dependent binding of Gal-9[296,365]. Additionally,

inflammatory diseases can alter the glycan profile of cells[349,350]. Further research is required to define all specific Gal-9 binding partners on monocytes and their glycosylation profiles. Whether PAD dependent changes in the glycan profile of PBMCs also contributes to enhanced capture by Gal-9 also remains unknown.

As shown in Chapter 3, Gal-9 is expressed in endothelial cells in inflammatory environments and various *in vivo* studies have highlighted a role for Gal-9 in inflammation[319,366] and is required for monocyte adhesion to endothelium, highlighting a role as a physiological capture and adhesion molecule during inflammation. Here these findings were expanded by showing that there were no differences in migration of leukocyte populations in various tissues of WT and Gal-9$^{-/-}$ mice under basal, non-inflammatory conditions 1 h after cell labelling. However, extending the time period between cell labelling and tissue analysis might reveal differences. On the other hand a previous study has shown that monocyte and PMN recruitment during acute inflammation is reduced in Gal-9 deficient mice[315]. Here it was shown that exogenous Gal-9 increases monocyte migration into the peritoneum during acute inflammation. The *in vivo* data confirms *in vitro* data from Chapter 4 of increased cytokine release after Gal-9 treatment. Other studies have also reported a pro-inflammatory role of Gal-9 on myeloid cells *in vivo*: a pro-inflammatory function for Gal-9 was reported in a pre-clinical model of pristane-induced lupus with Gal-9 deficient mice exhibiting less severe nephritis and arthritis[238] and the injection of Gal-9 into mouse knees increased infiltration with F4/80^{+} cells[301]. These findings further indicate a role of Gal-9 in leukocyte recruitment during inflammation but not under basal conditions. However, other *in vivo* studies have demonstrated an anti-inflammatory role of exogenous Gal-9 in various disease models, for example, administration of Gal-9 induced apoptosis of

Th1-cells and in turn improved SLE- associated arthritis and proteinuria[303] as well as diabetes in NOD mice[298]. These studies highlight the complexity in the mode of action of endogenous and exogenous Gal-9 in different inflammatory models and further studies are required to understand the mechanisms involved in Gal-9 modulated inflammation. Furthermore, more studies are needed to understand the mechanisms involved in Gal-9 mediated cyto- and chemokine release and whether the increased monocyte migration is due to increased cytokine release *in vivo* or due to an upregulation of Gal-9 on the endothelium in the peritoneal vasculature.

In summary, this chapter has shown that Gal-9 can function as a direct capture and adhesion molecule of PBMC and monocytes, particularly during inflammation *in vitro* and *in vivo*, and that PBMC are captured in an age-independent but peripheral arterial disease-dependent manner *in vitro*. It has previously been suggested that suppressing monocyte recruitment to plaques is more beneficial to plaque regression than macrophage egress from plaques[186], therefore targeting Gal-9 to prevent monocyte recruitment could prove to be an attractive therapeutic strategy.

CHAPTER 6:

GAL-9 CONTRIBUTES TO ATHEROSCLEROTIC PLAQUE PROGRESSION

6. Chapter 6: Gal-9 contributes to atherosclerotic plaque progression

6.1. Rational

During atherosclerotic plaque formation, monocytes migrate into the intima layer of the vessel wall. They differentiate into macrophages or phagocytose lipid deposits and turn into foam cells[144,367]. These cell types release pro-inflammatory mediators which further drive the progression of plaque formation[96,368]. On the other hand, migration of monocytes differentiating into pro-resolving macrophages is crucial for regression of atherosclerosis[184].

Many proteins involved in the monocyte migration cascade have been well characterised[6,113] and Gal-9 is required for monocyte migration as well as being involved in creating a pro-inflammatory milieu, as shown in Chapters 5 and 4, respectively. While Gal-9 has also been shown to modulate other inflammatory diseases, its role in atherosclerosis is not yet understood. A recent review by Yu *et al*. suggests that it has an atheroprotective role[282]. However this hypothesis is based on studies using a blocking antibody against TIM-3, a binding partner of Gal-9 and by blocking TIM-3, atherosclerosis was improved in mice.

Here we use the ApoE$^{-/-}$ mouse model of diet induced atherosclerosis to investigate the role of Gal-9 in atherogenesis. ApoE$^{-/-}$ mice were crossed with Gal-9$^{-/-}$ mice to generate ApoE$^{-/-}$ Gal-9$^{-/-}$ mice which were placed on a high fat diet (HFD) for 12 weeks to analyse plaque development and morphology. RNA sequencing data was used to investigate *Lgals9* levels in leukocyte populations from atherosclerosis progression and regression.

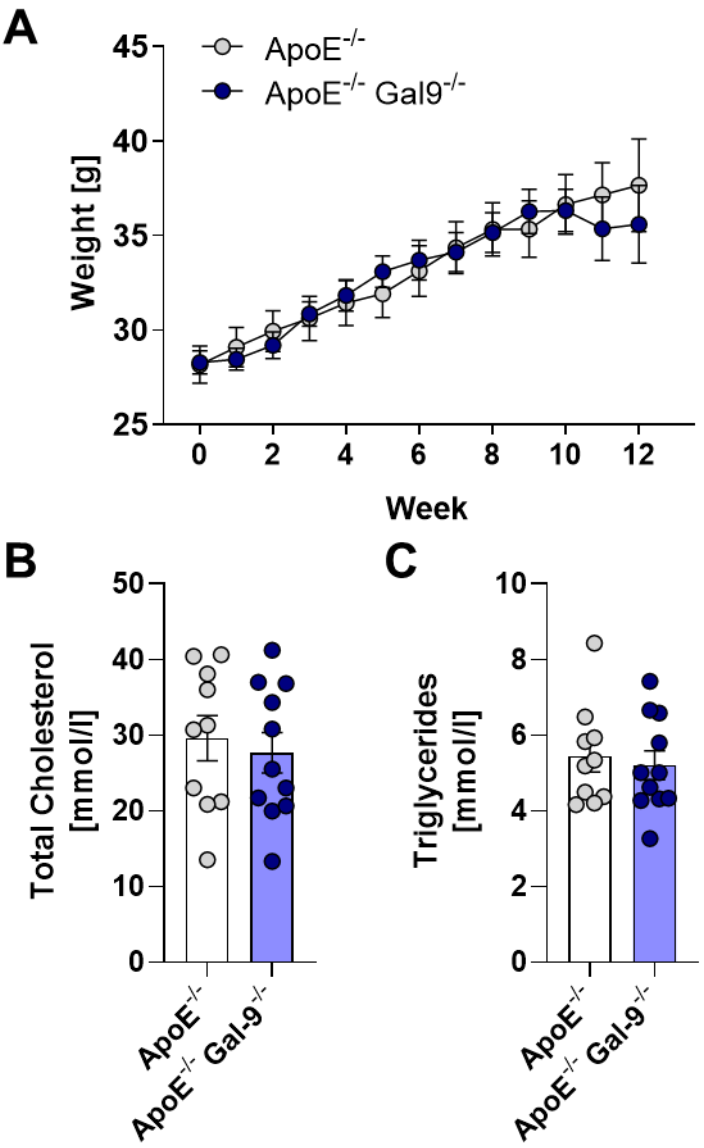

Figure 37: Weight gain and Total Cholesterol and Triglyceride levels in ApoE$^{-/-}$ and ApoE$^{-/-}$Gal-9$^{-/-}$ mice on a 12 week long high fat diet. ApoE$^{-/-}$ and ApoE$^{-/-}$Gal-9$^{-/-}$ mice were placed on a high fat diet for 12 weeks. The weight of the mice was monitored weekly (A). After 12 weeks, the mice were sacrificed and blood was collected for serum total cholesterol (B) and triglyceride (C) levels were measured. N=10-11. Statistical significant differences were calculated using Student's t-test.

6.2. Plaque progression is Gal-9 dependent

6.2.1. High fat diet induced weight gain and increase in lipid serum levels are independent of Gal-9

The weights of all mice were measured weekly from the start of the HFD. The average starting weight of both mice strains were between 26 and 29 g per mouse. Over the period of 12 weeks, both strains gained 8-10 g per mouse to a final weight between 35 and 37 g per mouse (Figure 37A). No significant differences in weight between the strains at any of the time points were detected, indicating that Gal-9 has no effect on diet-induced weight gain.

Increased lipid levels, particularly cholesterol and triglyceride levels, contribute to atherosclerosis. ApoE$^{-/-}$ mice on HFD are known to have elevated cholesterol and triglyceride levels[198]. To determine whether Gal-9 deficiency affects cholesterol and triglyceride levels, serum samples of both mouse strains were collected when the mice were sacrificed. Biochemical analysis of these serum samples revealed no significant differences in cholesterol or triglyceride levels between the mouse strains (Figure 37 B and C). Both, ApoE$^{-/-}$ and ApoE$^{-/-}$Gal-9$^{-/-}$ mice had an average of about 30 mmol/l of total cholesterol (Figure 37B) and about 5 mmol/l triglycerides (Figure 37C) in the collected serum.

These data indicate that Gal-9 has no impact on weight gain and lipid levels in mice.

6.2.2. *En face* staining of plaques reveals role of Gal-9 in plaque formation

In order to determine the role of Gal-9 in plaque progression, ApoE$^{-/-}$ and ApoE$^{-/-}$Gal-9$^{-/-}$ mice were sacrificed after 12 weeks of HFD. The aorta was harvested and stained *en face* with Oil Red O, a dye staining lipids and neutral triglycerides. The plaque

burden was defined as the total plaque (Oil Red O^+) area as percentage of the total surface area of the aorta (Figure 38A).

The *en face* staining of plaques revealed that there was a significantly reduced plaque burden in the aortas of $ApoE^{-/-}Gal\text{-}9^{-/-}$ mice compared to $ApoE^{-/-}$ mice (Figure 38B). When separate sections of the aortas were analysed for plaque burden, the data showed that there were no significant differences between $ApoE^{-/-}$ and $ApoE^{-/-}Gal\text{-}9^{-/-}$ mice in the aortic arches and thoracic aortas. However, significantly lower plaque burden were detected in the abdominal aortas of $ApoE^{-/-}Gal\text{-}9^{-/-}$ mice compared to $ApoE^{-/-}$ mice.

Additionally, the number of plaques were determined by counting the individual plaques determined using thresholding parameters on ImageJ (Fig. 38A). $ApoE^{-/-}Gal\text{-}9^{-/-}$ mice had significantly less plaques in the whole aorta compared to $ApoE^{-/-}$ mice (Figure 38C). No significant differences were detected in the individual parts of the aortas. However, the number of plaques in $ApoE^{-/-}Gal\text{-}9^{-/-}$ mice in all three parts of the aorta trended towards a decreased number.

These data indicate that Gal-9 enhances atheroprogression *in vivo* without affecting weight gain or circulating lipid levels.

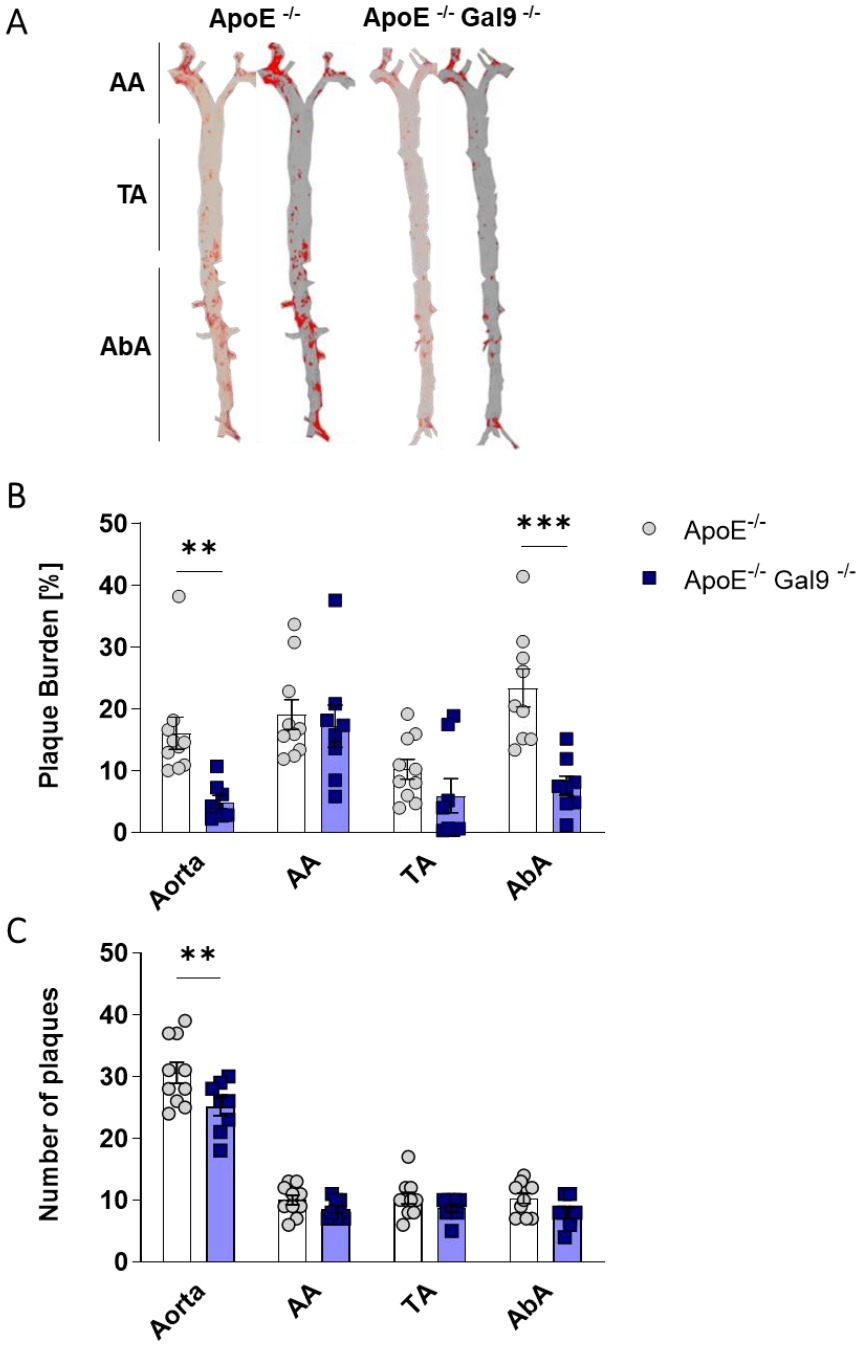

Figure 38: Plaque burden and number of plaques in whole aortas of in ApoE$^{-/-}$ and ApoE$^{-/-}$Gal-9$^{-/-}$ mice on a 12 week long high fat diet. in ApoE$^{-/-}$ and ApoE$^{-/-}$Gal-9$^{-/-}$ mice were placed on a high fat diet for 12 weeks. After 12 weeks, the mice were sacrificed and the aortas were stained with Oil Red O (A). After imaging, the plaque burden was determined by thresholding (A) and represented as percentage of the area of the aorta (B) while the number of aortic plaques were counted. Aortic Arch (AA),

thoratic aorta (TA) and abdominal aorta (AbA) sections were also analysed. N=8-10. Statistical significant differences were calculated using t test.**= p<0.01; ***= p<0.005.

6.2.3. Plaque morphology is Gal-9 dependent

To further investigate the role of Gal-9 in atheroprogression *in vivo*, aortic root sections were analysed for plaque size and composition (Figure 39A). Oil Red O staining was used to quantify the lipid content of the aortic root plaque cross sections. Van Gieson staining, a differential dye stains collagen in pink and other cellular components in yellow was used for the quantification of collagen. Collagen deposition is an indication of plaque progression and regression and can therefore be used to indicate the state of plaques[192]. The macrophage content of plaques was determined by immunofluorescent staining of CD68, a macrophage marker, since macrophage content within the plaque can be used as measure of plaque progression. Macrophage levels are high during atheroprogression and decrease during regression[183-186].

By determining the total plaque area as well as the average size of plaques in the aortic root cross section, it was shown that both measures of plaque size were significantly reduced in ApoE$^{-/-}$Gal-9$^{-/-}$ mice compared to ApoE$^{-/-}$ mice (Figure 39B and C).

By characterising the collagen content as percentage of the total plaque area, the analysis shows significantly less collagen in ApoE$^{-/-}$Gal-9$^{-/-}$ mice compared to ApoE$^{-/-}$ mice (Figure 39D). In ApoE$^{-/-}$ mice, about 38 % of the total area was collagen, while only around 13 % in plaques of ApoE$^{-/-}$Gal-9$^{-/-}$mice was collagen.

Macrophages levels within plaques can also indicate the stage of atherosclerosis. Macrophage content was determined as the percentage of CD68^{+} area of total plaque area. Analysis of the macrophage content of aortic root plaques revealed a significantly

lower proportion of macrophages in plaques of ApoE$^{-/-}$Gal-9$^{-/-}$ mice, approximately 22 %, compared to 55 % in ApoE$^{-/-}$ mice (Figure 39E).

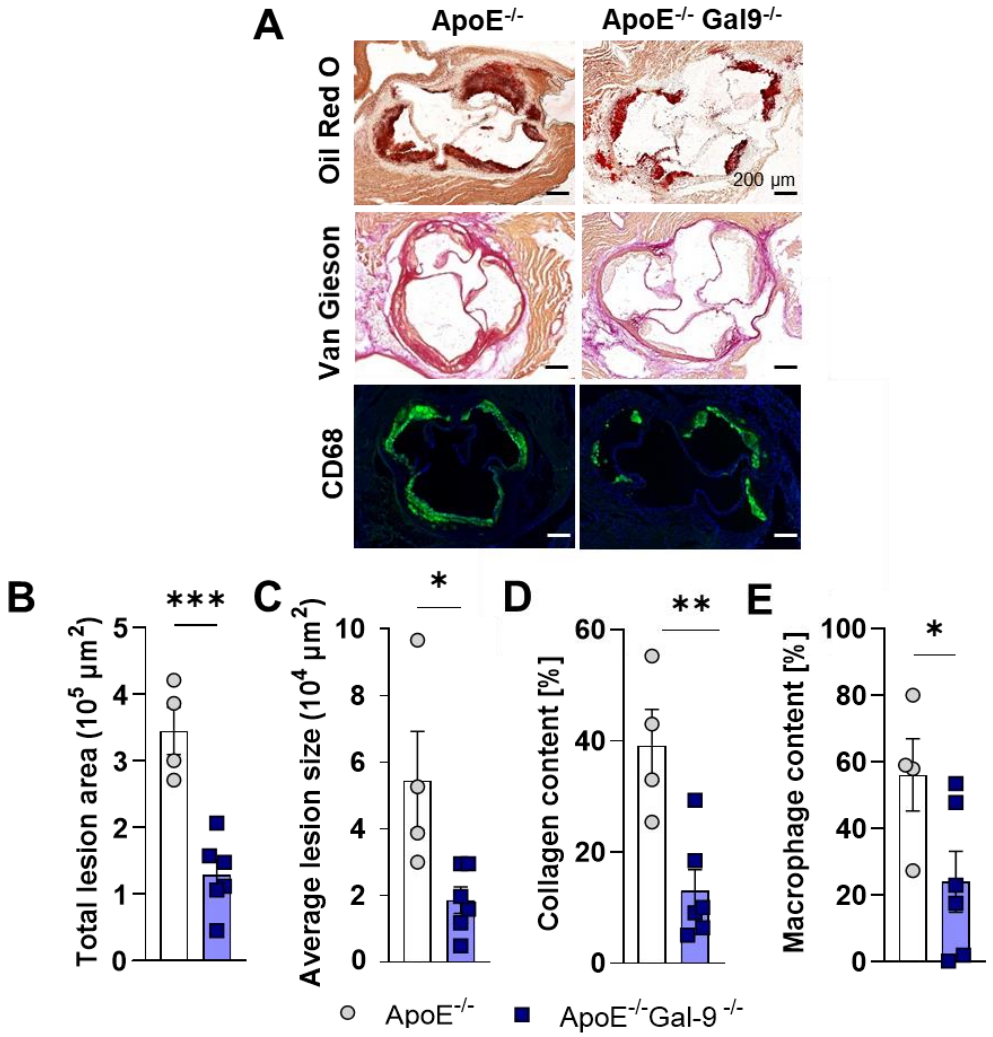

Figure 39: Plaque area, plaque size, collagen content and macrophage content in aortic root plaques of ApoE$^{-/-}$ and ApoE$^{-/-}$Gal-9$^{-/-}$ mice on a 12 week long high fat diet. ApoE$^{-/-}$ and ApoE$^{-/-}$Gal-9$^{-/-}$ mice were placed on a high fat diet for 12 weeks. After 12 weeks, the mice were sacrificed and the aortas were stained with Oil Red O, Van Gieson as well as immunohistochemically with CD68 antibodies (A). The total plaque area in the aortic root (B) as well as the average size of each plaque (C) in the sections of the aortic root were determined by using Oil Red O staining. Collagen was stained using Van Gieson and expressed as percentage of total plaque area (D). Macrophage content was quantified by presenting the CD68+ area as percentage of

total plaque area (E). N=4-6. Statistical significant differences were calculated using Student's t-test.*= p<0.05; **= p<0.01; ***= p<0.005.

In summary, these data show that Gal-9 contributes to increases in plaque burden, collagen content and macrophage content, indicating a role in atherosclerotic plaque progression.

6.3. RNA sequencing reveals decreased expression of *Lgals9* in plaque macrophage populations during atherosclerotic regression

Based on previous findings of an immune-specific regulation of monocyte migration and the pro-inflammatory role in atherosclerosis by Gal-9, Gal-9 levels in leukocytes during plaque regression were examined. By collaborating with researchers from the New York University Cardiovascular Research Center RNA sequencing data from $CD45^{+}$ cells isolated from aortas of $Ldlr^{-/-}$ mice with diet induced atherosclerotic progression and regression were analysed. Bioinformatic analysis was performed to cluster leukocyte subsets based on gene expression (Figure 40A). The relative *Lgals9* levels in these clusters during progression were blotted (Figure 40A) and reveal *Lgals9* expression in most leukocyte subsets, particularly the macrophage clusters, which confirms findings from the *in vitro* studies in Chapter 3. Interestingly, when relative *Lgals9* expression in these macrophage clusters during progression were compared to the levels in regressing plaques, a significant decreases in *Lgals9* levels in almost all macrophage subsets in regressing plaques were found (Figure 40B). The only macrophage cluster which *Lgals9* levels did not change significantly was the activated macrophage cluster.

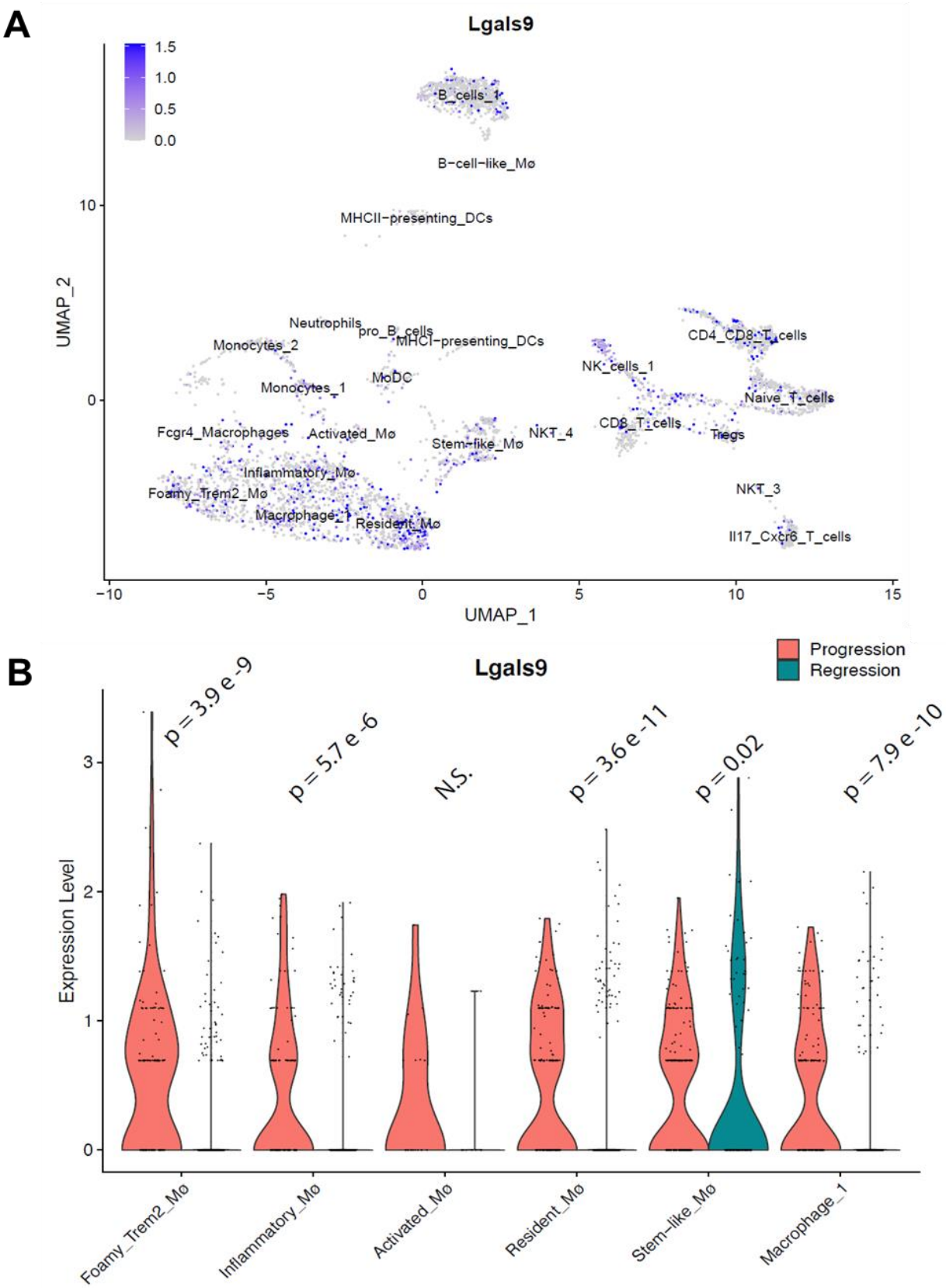
A
Lgals9
1.5
1.0
0.5
0.0
B_cells_1
B−cell−like_Mø
MHCII−presenting_DCs
Neutrophils
pro_B_cells
MHCI−presenting_DCs
Monocytes_2
MoDC
Monocytes_1
Fcgr4_Macrophages
Activated_Mø
Stem−like_Mø
NKT_4
Inflammatory_Mø
Foamy_Trem2_Mø
Macrophage_1
Resident_Mø
CD4_CD8_T_cells
NK_cells_1
Naive_T_cells
CD8_T_cells
Tregs
NKT_3
Il17_Cxcr6_T_cells
UMAP_2
UMAP_1
B
Lgals9
Progression
Regression
p = 3.9 e -9
p = 5.7 e -6
N.S.
p = 3.6 e -11
p = 0.02
p = 7.9 e -10
Expression Level
Foamy_Trem2_Mø
Inflammatory_Mø
Activated_Mø
Resident_Mø
Stem−like_Mø
Macrophage_1

Figure 40: *Lgals9* levels in CD45^{+} cells isolated from progressing and regressing plaques of Ldlr$^{-/-}$ mice. Bioinformatic analysis of *Lgals9* levels was provided by collaborators E. Brown and E.A. Fisher from New York University Cardiovascular Research Centre. Ldlr$^{-/-}$ mice were fed a high fat diet for 20 weeks to induce generation of progressing atherosclerotic plaques. Regression was induced by reducing the diet by 50 % for 3 weeks. The mice were sacrificed and the CD45+ cells of the aorta were isolated before RNA was isolated and analysed using RNA Sequencing. Leukocyte populations were clustered based on RNA expression profiles and their relative *Lgals9* expression blotted (A). The relative expression of *Lgals9* in macrophages clusters in progressing and regressing plaques was blotted and compared using a Student's t-test (B).

These findings further confirm a inflammation- specific expression of Gal-9 and indicate a pro-inflammatory role of Gal-9 in atherosclerosis. However, further studies are required whether Gal-9 protein levels also decrease in regressing plaques and whether targeting Gal-9 therapeutically can induce atherosclerotic plaque regression.

6.4. Discussion

Gal-9 has been demonstrated to play a role in a range of inflammatory diseases. In this chapter, the ApoE$^{-/-}$ mouse model of diet-induced atherosclerosis was applied, which revealed for the first time, a pro-atherogenic role of Gal-9.

Interestingly, a previous study in Gal-9$^{-/-}$ mice has shown that these mice gain less weight on a high fat high sucrose diet compared to C57BL6 wild type mice after at least 20 weeks, but not yet after 12 weeks on diet[369]. Our findings also show that weight gain is not affected after 12 weeks of HFD. However, whether ApoE$^{-/-}$ Gal-9$^{-/-}$ also have a reduced weight gain over a period exceeding 12 weeks of HFD compared to ApoE$^{-/-}$ mice, as observed in Gal-9$^{-/-}$ mice, needs to be established and considered when conducting further diet-induced atherosclerosis and obesity studies exceeding 12 weeks of weight gain.

Increased cholesterol and not just weight gain is a main contributor of plaque formation and increased triglyceride levels are a biomarker of atherogenic lipoproteins[149]. Both have been extensively reported in atherosclerosis mouse models as a result of HFD[171,183,196]. As expected, serum levels of cholesterol and triglycerides were increased after 12 weeks of high fat diet. The weight gain-study in Gal-9$^{-/-}$ and C57BL6 wild type mice did not report differences in cholesterol or triglyceride serum levels[369] which confirm these findings which suggest that Gal-9 plays no role in lipid metabolism.

Even though we did not observe differences in weight, cholesterol and triglyceride levels between the two mouse strains, Gal-9 ablation in mice results in a significant inhibition of diet-induced atherogenesis. The plaque burden was significantly decreased in ApoE$^{-/-}$ Gal-9$^{-/-}$ indicating that Gal-9 has an effect on atherosclerosis through other mechanisms such as inflammation, particularly since earlier in this study the inflammation specific role of Gal-9 was highlighted. Interestingly, different parts of the aorta were affected differently. An early study in ApoE$^{-/-}$ mice has reported that plaques in the aortic arches are the first ones to appear, plaques in the abdominal aortic region appear much later[370]. The reduced plaque burden in the abdominal aorta and the reduced number of plaques in the aorta of ApoE$^{-/-}$ Gal-9$^{-/-}$ mice therefore suggests a delayed atheroprogression in ApoE$^{-/-}$ Gal-9$^{-/-}$ compared to ApoE$^{-/-}$ mice on HFD, which suggests a role of Gal-9 in the inflammatory response of atherosclerosis.

In this study, reduced collagen and macrophage content within the plaques were reported. While a decrease in plaque size and macrophage content can be measures of plaque regression, regression is also marked by an increase in collagen content within plaques[183]. This is not the case in ApoE$^{-/-}$ Gal-9$^{-/-}$ when compared to ApoE$^{-/-}$ mice. The decreased collagen content in combination with reduced macrophage content further indicate that plaque progression is delayed in the absence of Gal-9.

The recruitment of monocytes into the intima is crucial for the progression of atherosclerosis and Gal-9 modulates migration of leukocytes in inflammatory settings. In context with results from Chapter 5 and previous publications, which showed that monocyte migration is dependent on endothelial Gal-9 and that endogenous[315] and that exogenous Gal-9 induce monocyte migration in acute peritonitis, it is hypothesised that the absence of Gal-9 reduces the amount of circulating monocytes migrating into

the vessel wall leading to a decrease in accumulation of pro-inflammatory macrophages and in turn decreased inflammation. Expression patterns of Gal-9 in plaques, particularly the endothelial cells and *in vivo* atherosclerosis studies with endothelial specific knock out of Gal-9 should be applied to investigate this further.

While this study is the first to report a pro-inflammatory role for Gal-9 in atherosclerosis, another member of the galectin family, Gal-3, has also been shown to contribute to atherosclerosis. Lee *et al*. demonstrated an increase of Gal-3 protein expression in progressing plaques which also co-localised with macrophages and decreased in regressing plaques induced by atorvastatin treatment[257]. However, the study compared C57BL6 WT mice on chow diet to ApoE$^{-/-}$ mice on high cholesterol diet. Nevertheless, these findings complement the findings in this study of reduced *Lgals9* levels in macrophages of regressing plaques. Other studies further investigated the role of Gal-3 in atherosclerosis further and reported a reduction in lesions of ApoE$^{-/-}$ Gal-3$^{-/-}$ double deficient mice[270,271] and decreased perivascular inflammatory infiltrates[270]. Various publications have demonstrated additional, immunomodulatory functions of Gal-9, independent of its role in leukocyte migration. For example, intracellular Gal-9 regulates gene expression of inflammatory cytokines such as IL-1a and -1ß via direct interaction with NF-IL6 in THP-1 cells, a monocyte cell line[297]. Therefore, the role of Gal-9 inside plaques needs further investigation, particularly since an increased cyto- and chemokine release by macrophages was reported in Chapter 4. Whether the presence of Gal-9 prevents atherosclerotic regression by contributing to a pro-inflammatory milieu also needs further research.

These data clearly show the pro-inflammatory role of Gal-9 in atherosclerosis. This confirms findings from studies using other models of inflammatory diseases. Gal-9

deficient mice had improved nephritis and arthritis in a pre-clinical model of pristane-induced lupus[238], while the direct injection of Gal-9 into knees of mice resulted in increased knee swelling as well as increased F4/80^{+} macrophage infiltration[301]. However, other studies using exogenous Gal-9 have shown that it improved various clinical symptoms such as arthritis in MRL/lpr mice, a murine model of SLE[303] and Arikawa *et al*., showed that subcutaneous injections of Gal-9 to mice with collagen induced arthritis improved their clinical scores significantly[281]. Collectively, these studies highlight the complexity in the mode of action of endogenous and exogenous Gal-9 in different inflammatory settings.

In summary, Gal-9 modulates atherosclerosis by modulating monocyte migration into the atherosclerotic plaque which in leads to decreased inflammation and therefore decreased plaque progression. This proposes Gal-9 as a therapeutic target in the prevention of atherosclerotic plaque progression.

CHAPTER 7:

CONCLUDING REMARKS

AND

FUTURE DIRECTIONS

7. Chapter 7: Concluding remarks and future directions

7.1. Concluding remarks

This study shows that Gal-9 is expressed by monocytes, macrophages and endothelial cells. Gal-9 is upregulated during inflammatory conditions which confirmed findings from previous studies[214,288-290,306]. Furthermore, it was shown that macrophages and endothelial cells release Gal-9 in these conditions which suggests that they are a source of increased circulating Gal-9 levels detected in plasma of PAD patients but also in patients with other inflammatory diseases[239,293]. Further studies are required to get a better understanding of the mechanisms that regulate Gal-9 expression and its release, especially since previous studies have highlighted the role of intracellular Gal-9 in various leukocyte subsets: for example it induces the expression of IL-12 and IL-23 in monocytes[215].

Here, it was also demonstrated that Gal-9 modulates inflammation through two distinct mechanisms. Firstly, soluble Gal-9 can modulated monocyte responses by inducing CD62L shedding and pro-inflammatory cytokine release in macrophages and secondly, immobilised and endothelially expressed Gal-9 acts in monocyte capture and adhesion.

These findings propose Gal-9 as novel therapeutic target in the prevention of inflammation and induction of inflammatory resolution. Particularly, since novel, inflammation-targeting drugs have provided promising results in atherosclerosis[152], RA, psoriasis and inflammatory bowel diseases[371]. However, further experiments are required to identify the binding partner of Gal-9 on monocytes and macrophages, whether increased circulating Gal-9 levels during inflammatory diseases are able to

induce monocyte activation and whether Gal-9 protein expression is increased in progressing atherosclerotic plaques which could contribute to the pro-inflammatory environment within plaques.

The second mechanism through which Gal-9 modulates inflammation is through facilitating monocyte migration, specifically during inflammation. These findings further highlight the potential of Gal-9 as therapeutic target by interfering with leukocyte trafficking which drives the immune response, particularly since a number of studies have already highlighted the potential of targeting leukocyte trafficking as therapeutic strategy for inflammatory diseases[372]. Further studies are required in determining the Gal-9 expression of which cell type is responsible for the Gal-9 induced modulation of leukocyte migration; whether it is Gal-9 expressed by endothelial cells as adhesion molecules, Gal-9 released into circulation which induces activation of circulating leukocytes or local, soluble Gal-9 acting as chemoattractant, as has been described for eosinophils[300], or whether it is a combination of all three.

More specifically, Gal-9 acts in the progression of atherosclerotic plaques *in vivo*. Promoting a pro-inflammatory environment and increasing monocyte migration are two major factors which contribute to atherosclerosis, and this study has shown that Gal-9 facilitates both. These findings fit in with other studies which have demonstrated a pro-inflammatory role of Gal-9 in inflammatory diseases[298,301,315,373]. Further studies are required to define the role of Gal-9 within plaques in more detail and whether it also plays a role in atherosclerotic plaque regression.

In conclusion, the results of this study suggest that Gal-9 is an inflammation-specific promoter of atherosclerotic plaque progression, acting in two ways: i) as soluble

protein, activating monocyte through its increased presence in circulation during inflammation and inducing pro-inflammatory cytokine release in macrophages; and ii) as surface protein expressed by endothelial cells, facilitating monocyte recruitment as a direct capture molecule in a glycan- and ß2 integrin dependent manner. These findings suggest that Gal-9 is an interesting, novel therapeutic target in the prevention of atherosclerotic plaque progression. Further studies are required to understand the pathways which regulate Gal-9 mediated inflammation, particularly during plaque progression and if decreasing Gal-9 levels could facilitate atherosclerotic regression by reducing inflammation and monocyte influx.

7.2. Future directions

Whilst the work outlined in this thesis has described a role of Gal-9 in monocyte driven atherosclerotic progression, it also raises additional questions which require further investigation.

Gal-9 expression

Multiple aspects of Gal-9 expression in endothelial cells, monocytes and macrophages have been outlined in this thesis. However, the precise regulation and pathways leading to Gal-9 protein expression remain unknown. Therefore, it is important to Investigate the pathways which determine Gal-9 expression in endothelial cells, monocytes and macrophages. Using RNA sequencing data of endothelial cells, monocytes and macrophages treated with substances known to upregulate Gal-9 expression might provide a better understanding of the pathways involved and using inhibitors, siRNAs and knock out cell lines to block parts of the found pathway might be helpful to confirm these findings *in vitro*.

This study provided evidence that Gal-9 is released by endothelial cells and it has been previously shown that it is increased in serum and plasma of patients with inflammatory diseases. Furthermore it was demonstrated that exogenous, soluble Gal-9 plays a role in the regulation of inflammatory responses. However, there is still a great lack of understanding in how Gal-9 is released by cells. Using broad spectrum inhibitors of known proteases to screen if Gal-9 release can be blocked could provide a better understanding in the mechanisms involved in the release of Gal-9. Depending on these findings potential targets can be narrowed down and more specific inhibitors or knock down models could be used. Furthermore, extracellular vesicles (EVs) have previously been shown to contain galectins. If they contain Gal-9 should be determined by isolating EVs from cell culture medium and determining Gal-9 contents via for example Western blot. If Gal-9 is present in EVs, a better characterisation of these vesicles using nanoparticle tracking analysis and electron microscopy might be useful to better understand their role.

Furthermore, shear stress is known to modulate gene expression in endothelial cells[374]. Whether Gal-9 expression can also be regulated through shear stress remains unknown. However, since it is well known that atherosclerotic plaque formation occurs predominantly in areas of disturbed laminar flow, shear stress regulated expression of Gal-9 should be investigated. To assess this, Gal-9 expression in endothelial cells exposed to different shear stress profiles in vitro should be analysed. These findings could be furthered by in vivo studies in mice using cuffs implanted around the carotid arteries and subsequent analysis of Gal-9 expression in the areas exposed to different flow conditions due to the cuff.

Role of Intracellular vs. extracellular/exogenous Gal-9

While findings in this study clearly demonstrated an interaction of Gal-9 with monocytes and macrophages, the Gal-9 ligand(s) on these cells remains unknown. Performing co-immunoprecipitation using antibodies targeting Gal-9 and subsequent mass spectrometric analysis of samples will determine these ligands. These can be confirmed using, for example, blocking antibodies. Furthermore, whether the interactions are glycan-dependent can be analysed by including lactose in the assays. This study provided evidence that Gal-9 induces the release of pro-inflammatory cytokines in macrophages. RNA sequencing can be employed for pathways analysis of macrophages treated with Gal-9. These findings could then be confirmed *in vitro* using inhibitors against parts of pathway.

Furthermore, Gal-9 is known to bind specific glycans and it is known that glycosylation of cells can be altered in diseases. Whether aging or peripheral arterial disease also alter the glycosylation of monocytes is unknown but could provide better understanding of how increased capture of PBMCs of PAD patients by Gal-9 under flow is obserbved. Therefore, glycomic analysis using glycan isolation and subsequent mass spectrometric analysis of monocytes of HY, HA and PAD should be performed to determine the glycosylation patterns of these cells.

Role of Gal-9 in monocyte migration

This study has demonstrated for the first time that Gal-9 acts as capture and adhesion molecule for monocytes under physiological flow. This data was supported by zymosan induced peritonitis models in Gal-$9^{-/-}$ mice which showed reduced leukocyte recruitment into the peritoneal cavity compared to WT mice. However, whether endothelial Gal-9 alone acts in monocyte recruitment, as indicated in findings in this

thesis or whether monocytic Gal-9 also plays a role needs further investigation. Therefore, generation of endothelial specific and monocyte specific Gal-9 knock out mice would be a helpful tool in uncovering the role of Gal-9 in the respective cell type during monocyte recruitment.

Furthermore, this study only provides information of monocyte capture by Gal-9. However, whether Gal-9 affects monocyte subsets differently remains to be determined. Since it is known that monocyte subsets have different roles during inflammation, better understanding of their Gal-9 mediated capture and adhesion might provide a potential therapeutic target. To investigate this, human monocyte subsets from whole blood using CD14 and CD16 coated microbeads could be isolated and perfused over recombinant Gal-9 or endothelial cells treated with Gal-9 siRNA.

While Gal-9 mediated capture was reported in this study *in vitro*, further studies are required to understand its role *in vivo*. Determine whether endothelial Gal-9 can capture monocytes in the absence of selectins. For example, whether Gal-9 can act alone as capture molecule without the support of selectins could be investigated by knocking down Gal-9 and E-selectin in endothelial cells for flow adhesion assays. Findings from these experiments could be confirmed *in vivo* by generating Gal-9$^{-/-}$ and E-selectin$^{-/-}$ or L-selectin$^{-/-}$ double knock out mice and performing *in vivo* imaging experiments of leukocyte trafficking.

Leukocyte migration is also dependent on the respective tissue, due to different shear stress and endothelial cells for example. Whether there are tissue specific differences in Gal-9-modulated monocyte migration remains unknown. To investigate these further, endothelial cells from different tissues, for example human aortic endothelial

cells or human liver-derived endothelial cells could be used in vitro to determine their Gal-9 expression levels and to use them in flow adhesion assays. Furthermore, *in vivo* imaging of leukocyte migration in different tissues of Gal-9$^{-/-}$ and WT mice could be used.

Gal-9 in atherosclerosis

The results of this study have highlighted that Gal-9 contributes to atherosclerotic plaque formation by contributing to monocyte migration and a pro-inflammatory phenotype in macrophages. However, whether Gal-9 also plays a role in lipid uptake by macrophages and foam cell formation, a crucial step in atherosclerotic plaque formation, remains unknown. The generation of Gal-9 deficient macrophages from bone marrow cells of Gal-9$^{-/-}$ mice and treatment of these cells with oxLDL to quantify lipid uptake and foam cell formation could provide important information on the role of Gal-9 in this mechanism. Since the roles of intracellular and exogenous Gal-9 can differ, treatment of BMDM of WT mice with oxLDL in the presence of Gal-9 would be important to distinguish the role of intracellular and exogenous Gal-9 in this process. Characterise Gal-9 protein expression within plaques.

RNA sequencing data in this study has shown that Gal-9 is expressed in leukocytes, particularly macrophages, in plaques. Whether the same expression patterns occur on a protein level should be determined performing immunohistochemical analysis of Gal-9 in aortic root sections. Flow cytometric analysis of Gal-9 expression of cell types such as leukocyte subsets, endothelial cells and smooth muscle cells from atherosclerotic aortas of mice could provide information on Gal-9 expression in plaques.

While the mechanisms involved in atherosclerotic plaque progression are well understood, mechanisms inducing or contributing to atherosclerotic plaque regression remain poorly understood. Data from RNA sequencing in this study has shown that Gal-9 mRNA levels are decreased in macrophages of regressing plaques. Further studies should be performed to investigate the role of Gal-9 in atherosclerotic plaque regression and whether Gal-9 removal is required for regression. Using atherosclerotic plaque regression models such as caloric restriction of high fat diet in Gal-$9^{-/-}$ mice and subsequent analysis of plaques of these mice could provide valuable information of the role of Gal-9 in atherosclerotic plaque regression.

8. References

1 Leick, M., Azcutia, V., Newton, G. & Luscinskas, F. W. Leukocyte recruitment in inflammation: basic concepts and new mechanistic insights based on new models and microscopic imaging technologies. *Cell Tissue Res* **355**, 647-656, doi:10.1007/s00441-014-1809-9 (2014).

2 Nourshargh, S. & Alon, R. Leukocyte migration into inflamed tissues. *Immunity* **41**, 694-707, doi:10.1016/j.immuni.2014.10.008 (2014).

3 Medzhitov, R. Origin and physiological roles of inflammation. *Nature* **454**, 428-435, doi:10.1038/nature07201 (2008).

4 Roh, J. S. & Sohn, D. H. Damage-Associated Molecular Patterns in Inflammatory Diseases. *Immune Netw* **18**, e27, doi:10.4110/in.2018.18.e27 (2018).

5 Zhang, X. & Mosser, D. M. Macrophage activation by endogenous danger signals. *J Pathol* **214**, 161-178, doi:10.1002/path.2284 (2008).

6 Ley, K., Laudanna, C., Cybulsky, M. I. & Nourshargh, S. Getting to the site of inflammation: the leukocyte adhesion cascade updated. *Nat Rev Immunol* **7**, 678-689, doi:10.1038/nri2156 (2007).

7 Barany, P. Inflammation, serum C-reactive protein, and erythropoietin resistance. *Nephrol Dial Transplant* **16**, 224-227, doi:10.1093/ndt/16.2.224 (2001).

8 Fadok, V. A. *et al.* Macrophages that have ingested apoptotic cells in vitro inhibit proinflammatory cytokine production through autocrine/paracrine mechanisms involving TGF-beta, PGE2, and PAF. *J Clin Invest* **101**, 890-898, doi:10.1172/JCI1112 (1998).

9 Ma, W. T., Gao, F., Gu, K. & Chen, D. K. The Role of Monocytes and Macrophages in Autoimmune Diseases: A Comprehensive Review. *Front Immunol* **10**, 1140, doi:10.3389/fimmu.2019.01140 (2019).

10 Ortega-Gomez, A., Perretti, M. & Soehnlein, O. Resolution of inflammation: an integrated view. *EMBO Mol Med* **5**, 661-674, doi:10.1002/emmm.201202382 (2013).

11 Sugimoto, M. A., Sousa, L. P., Pinho, V., Perretti, M. & Teixeira, M. M. Resolution of Inflammation: What Controls Its Onset? *Frontiers in immunology* **7**, 160, doi:10.3389/fimmu.2016.00160 (2016).

12 Hopkin, S. J., Lewis, J. W., Krautter, F., Chimen, M. & McGettrick, H. M. Triggering the Resolution of Immune Mediated Inflammatory Diseases: Can Targeting Leukocyte Migration Be the Answer? *Front Pharmacol* **10**, 184, doi:10.3389/fphar.2019.00184 (2019).

13 Serhan, C. N. Resolution phase of inflammation: novel endogenous anti-inflammatory and proresolving lipid mediators and pathways. *Annu Rev Immunol* **25**, 101-137, doi:10.1146/annurev.immunol.25.022106.141647 (2007).

14 Serhan, C. N. & Savill, J. Resolution of inflammation: the beginning programs the end. *Nat Immunol* **6**, 1191-1197, doi:10.1038/ni1276 (2005).

15 Law, S. C., Benham, H., Reid, H. H., Rossjohn, J. & Thomas, R. Identification of self-antigen-specific T cells reflecting loss of tolerance in autoimmune disease underpins preventative immunotherapeutic strategies in rheumatoid arthritis. *Rheum Dis Clin North Am* **40**, 735-752, doi:10.1016/j.rdc.2014.07.015 (2014).

16 Baillière, J. B. Recherches anatomiques et physiologiques sur la structure intime des animaux et des végetaux, et sur leur motilité. 1-233 (1824).

17 Wagner, R. *Erläuterungstafeln zur Phyisologie und Entwicklungsgeschichte* (L. Voss, 1839).

18 Gedeit, R. G. Tumor necrosis factor-induced E-selectin expression on vascular endothelial cells. *Crit Care Med* **24**, 1543-1546, doi:10.1097/00003246-199609000-00019 (1996).

19 Wong, D. & Dorovini-Zis, K. Regualtion by cytokines and lipopolysaccharide of E-selectin expression by human brain microvessel endothelial cells in primary culture. *J Neuropathol Exp Neurol* **55**, 225-235, doi:10.1097/00005072-199602000-00011 (1996).

20 Watson, C. *et al.* IL-6 acts on endothelial cells to preferentially increase their adherence for lymphocytes. *Clin Exp Immunol* **105**, 112-119, doi:10.1046/j.1365-2249.1996.d01-717.x (1996).
21 McEver, R. P., Beckstead, J. H., Moore, K. L., Marshall-Carlson, L. & Bainton, D. F. GMP-140, a platelet alpha-granule membrane protein, is also synthesized by vascular endothelial cells and is localized in Weibel-Palade bodies. *J Clin Invest* **84**, 92-99, doi:10.1172/JCI114175 (1989).
22 Hsu-Lin, S., Berman, C. L., Furie, B. C., August, D. & Furie, B. A platelet membrane protein expressed during platelet activation and secretion. Studies using a monoclonal antibody specific for thrombin-activated platelets. *J Biol Chem* **259**, 9121-9126 (1984).
23 Griffin, J. D. *et al.* Granulocyte-macrophage colony-stimulating factor and other cytokines regulate surface expression of the leukocyte adhesion molecule-1 on human neutrophils, monocytes, and their precursors. *J Immunol* **145**, 576-584 (1990).
24 Luscinskas, F. W. *et al.* Monocyte rolling, arrest and spreading on IL-4-activated vascular endothelium under flow is mediated via sequential action of L-selectin, beta 1-integrins, and beta 2-integrins. *J Cell Biol* **125**, 1417-1427, doi:10.1083/jcb.125.6.1417 (1994).
25 Hidalgo, A., Peired, A. J., Wild, M., Vestweber, D. & Frenette, P. S. Complete identification of E-selectin ligands on neutrophils reveals distinct functions of PSGL-1, ESL-1, and CD44. *Immunity* **26**, 477-489, doi:10.1016/j.immuni.2007.03.011 (2007).
26 Kanabar, V. *et al.* Base-modified UDP-sugars reduce cell surface levels of P-selectin glycoprotein 1 (PSGL-1) on IL-1beta-stimulated human monocytes. *Glycobiology* **26**, 1059-1071, doi:10.1093/glycob/cww053 (2016).
27 Krishnamurthy, V. R. *et al.* Glycopeptide analogues of PSGL-1 inhibit P-selectin in vitro and in vivo. *Nat Commun* **6**, 6387, doi:10.1038/ncomms7387 (2015).
28 Buffone, A., Jr. *et al.* Silencing alpha1,3-fucosyltransferases in human leukocytes reveals a role for FUT9 enzyme during E-selectin-mediated cell adhesion. *J Biol Chem* **288**, 1620-1633, doi:10.1074/jbc.M112.400929 (2013).
29 Chen, J., Haller, C. A. & Chaikof, E. L. Immune checkpoint regulator: a new assignment proposed for the classic adhesion molecule P-selectin glycoprotein ligand-1. *Transl Cancer Res* **5**, S668-S671, doi:10.21037/tcr.2016.10.05 (2016).
30 Hobbs, S. J. & Nolz, J. C. Regulation of T Cell Trafficking by Enzymatic Synthesis of O-Glycans. *Front Immunol* **8**, 600, doi:10.3389/fimmu.2017.00600 (2017).
31 Lim, Y. C. *et al.* IL-12, STAT4-dependent up-regulation of CD4(+) T cell core 2 beta-1,6-n-acetylglucosaminyltransferase, an enzyme essential for biosynthesis of P-selectin ligands. *J Immunol* **167**, 4476-4484, doi:10.4049/jimmunol.167.8.4476 (2001).
32 An, G. *et al.* P-selectin glycoprotein ligand-1 is highly expressed on Ly-6Chi monocytes and a major determinant for Ly-6Chi monocyte recruitment to sites of atherosclerosis in mice. *Circulation* **117**, 3227-3237, doi:10.1161/CIRCULATIONAHA.108.771048 (2008).
33 McEver, R. P., Moore, K. L. & Cummings, R. D. Leukocyte trafficking mediated by selectin-carbohydrate interactions. *J Biol Chem* **270**, 11025-11028, doi:10.1074/jbc.270.19.11025 (1995).
34 McEver, R. P. & Cummings, R. D. Role of PSGL-1 binding to selectins in leukocyte recruitment. *J Clin Invest* **100**, S97-103 (1997).
35 Spertini, O. *et al.* Leukocyte adhesion molecule-1 (LAM-1, L-selectin) interacts with an inducible endothelial cell ligand to support leukocyte adhesion. *J Immunol* **147**, 2565-2573 (1991).
36 Abbal, C. *et al.* Lipid raft adhesion receptors and Syk regulate selectin-dependent rolling under flow conditions. *Blood* **108**, 3352-3359, doi:10.1182/blood-2006-04-013912 (2006).

37 DeGrendele, H. C., Estess, P., Picker, L. J. & Siegelman, M. H. CD44 and its ligand hyaluronate mediate rolling under physiologic flow: a novel lymphocyte-endothelial cell primary adhesion pathway. *J Exp Med* **183**, 1119-1130, doi:10.1084/jem.183.3.1119 (1996).
38 Xu, H. *et al.* Involvement of CD44 in leukocyte trafficking at the blood-retinal barrier. *J Leukoc Biol* **72**, 1133-1141 (2002).
39 Middleton, J. *et al.* Transcytosis and surface presentation of IL-8 by venular endothelial cells. *Cell* **91**, 385-395, doi:10.1016/s0092-8674(00)80422-5 (1997).
40 Proudfoot, A. E. *et al.* Glycosaminoglycan binding and oligomerization are essential for the in vivo activity of certain chemokines. *Proc Natl Acad Sci U S A* **100**, 1885-1890, doi:10.1073/pnas.0334864100 (2003).
41 Tsang, Y. T. *et al.* Synergy between L-selectin signaling and chemotactic activation during neutrophil adhesion and transmigration. *J Immunol* **159**, 4566-4577 (1997).
42 Stadtmann, A. *et al.* The PSGL-1-L-selectin signaling complex regulates neutrophil adhesion under flow. *J Exp Med* **210**, 2171-2180, doi:10.1084/jem.20130664 (2013).
43 Diamond, M. S. & Springer, T. A. A subpopulation of Mac-1 (CD11b/CD18) molecules mediates neutrophil adhesion to ICAM-1 and fibrinogen. *J Cell Biol* **120**, 545-556, doi:10.1083/jcb.120.2.545 (1993).
44 Diamond, M. S., Staunton, D. E., Marlin, S. D. & Springer, T. A. Binding of the integrin Mac-1 (CD11b/CD18) to the third immunoglobulin-like domain of ICAM-1 (CD54) and its regulation by glycosylation. *Cell* **65**, 961-971, doi:10.1016/0092-8674(91)90548-d (1991).
45 Meisel, S. R. *et al.* Increased expression of neutrophil and monocyte adhesion molecules LFA-1 and Mac-1 and their ligand ICAM-1 and VLA-4 throughout the acute phase of myocardial infarction: possible implications for leukocyte aggregation and microvascular plugging. *J Am Coll Cardiol* **31**, 120-125, doi:10.1016/s0735-1097(97)00424-5 (1998).
46 Gerszten, R. E. *et al.* MCP-1 and IL-8 trigger firm adhesion of monocytes to vascular endothelium under flow conditions. *Nature* **398**, 718-723, doi:10.1038/19546 (1999).
47 Luscinskas, F. W. *et al.* C-C and C-X-C chemokines trigger firm adhesion of monocytes to vascular endothelium under flow conditions. *Ann N Y Acad Sci* **902**, 288-293, doi:10.1111/j.1749-6632.2000.tb06324.x (2000).
48 Weber, M. *et al.* Interstitial dendritic cell guidance by haptotactic chemokine gradients. *Science* **339**, 328-332, doi:10.1126/science.1228456 (2013).
49 Middleton, J., Patterson, A. M., Gardner, L., Schmutz, C. & Ashton, B. A. Leukocyte extravasation: chemokine transport and presentation by the endothelium. *Blood* **100**, 3853-3860, doi:10.1182/blood.V100.12.3853 (2002).
50 Joseph, P. R., Mosier, P. D., Desai, U. R. & Rajarathnam, K. Solution NMR characterization of chemokine CXCL8/IL-8 monomer and dimer binding to glycosaminoglycans: structural plasticity mediates differential binding interactions. *Biochem J* **472**, 121-133, doi:10.1042/BJ20150059 (2015).
51 Goldblatt, J. *et al.* A Requirement for Neutrophil Glycosaminoglycans in Chemokine:Receptor Interactions Is Revealed by the Streptococcal Protease SpyCEP. *J Immunol* **202**, 3246-3255, doi:10.4049/jimmunol.1801688 (2019).
52 Bao, X. *et al.* Endothelial heparan sulfate controls chemokine presentation in recruitment of lymphocytes and dendritic cells to lymph nodes. *Immunity* **33**, 817-829, doi:10.1016/j.immuni.2010.10.018 (2010).
53 Gangavarapu, P. *et al.* The monomer-dimer equilibrium and glycosaminoglycan interactions of chemokine CXCL8 regulate tissue-specific neutrophil recruitment. *J Leukoc Biol* **91**, 259-265, doi:10.1189/jlb.0511239 (2012).
54 Rajarathnam, K., Sepuru, K. M., Joseph, P. R. B., Sawant, K. V. & Brown, A. J. Glycosaminoglycan Interactions Fine-Tune Chemokine-Mediated Neutrophil Trafficking:

Structural Insights and Molecular Mechanisms. *J Histochem Cytochem* **66**, 229-239, doi:10.1369/0022155417739864 (2018).
55 Schenkel, A. R., Mamdouh, Z. & Muller, W. A. Locomotion of monocytes on endothelium is a critical step during extravasation. *Nat Immunol* **5**, 393-400, doi:10.1038/ni1051 (2004).
56 Carman, C. V. *et al.* Transcellular diapedesis is initiated by invasive podosomes. *Immunity* **26**, 784-797, doi:10.1016/j.immuni.2007.04.015 (2007).
57 Giannotta, M., Trani, M. & Dejana, E. VE-cadherin and endothelial adherens junctions: active guardians of vascular integrity. *Dev Cell* **26**, 441-454, doi:10.1016/j.devcel.2013.08.020 (2013).
58 Vestweber, D. Relevance of endothelial junctions in leukocyte extravasation and vascular permeability. *Ann N Y Acad Sci* **1257**, 184-192, doi:10.1111/j.1749-6632.2012.06558.x (2012).
59 Broermann, A. *et al.* Dissociation of VE-PTP from VE-cadherin is required for leukocyte extravasation and for VEGF-induced vascular permeability in vivo. *J Exp Med* **208**, 2393-2401, doi:10.1084/jem.20110525 (2011).
60 Santoso, S. *et al.* The junctional adhesion molecule 3 (JAM-3) on human platelets is a counterreceptor for the leukocyte integrin Mac-1. *J Exp Med* **196**, 679-691, doi:10.1084/jem.20020267 (2002).
61 Ostermann, G., Weber, K. S., Zernecke, A., Schroder, A. & Weber, C. JAM-1 is a ligand of the beta(2) integrin LFA-1 involved in transendothelial migration of leukocytes. *Nat Immunol* **3**, 151-158, doi:10.1038/ni755 (2002).
62 Ferrero, E., Ferrero, M. E., Pardi, R. & Zocchi, M. R. The platelet endothelial cell adhesion molecule-1 (PECAM1) contributes to endothelial barrier function. *FEBS Lett* **374**, 323-326, doi:10.1016/0014-5793(95)01110-z (1995).
63 Privratsky, J. R. *et al.* Relative contribution of PECAM-1 adhesion and signaling to the maintenance of vascular integrity. *J Cell Sci* **124**, 1477-1485, doi:10.1242/jcs.082271 (2011).
64 Osawa, M., Masuda, M., Kusano, K. & Fujiwara, K. Evidence for a role of platelet endothelial cell adhesion molecule-1 in endothelial cell mechanosignal transduction: is it a mechanoresponsive molecule? *J Cell Biol* **158**, 773-785, doi:10.1083/jcb.200205049 (2002).
65 Tzima, E. *et al.* A mechanosensory complex that mediates the endothelial cell response to fluid shear stress. *Nature* **437**, 426-431, doi:10.1038/nature03952 (2005).
66 Muller, W. A., Weigl, S. A., Deng, X. & Phillips, D. M. PECAM-1 is required for transendothelial migration of leukocytes. *J Exp Med* **178**, 449-460, doi:10.1084/jem.178.2.449 (1993).
67 Nourshargh, S., Krombach, F. & Dejana, E. The role of JAM-A and PECAM-1 in modulating leukocyte infiltration in inflamed and ischemic tissues. *J Leukoc Biol* **80**, 714-718, doi:10.1189/jlb.1105645 (2006).
68 Kapellos, T. S. *et al.* Human Monocyte Subsets and Phenotypes in Major Chronic Inflammatory Diseases. *Front Immunol* **10**, 2035, doi:10.3389/fimmu.2019.02035 (2019).
69 Cros, J. *et al.* Human CD14dim monocytes patrol and sense nucleic acids and viruses via TLR7 and TLR8 receptors. *Immunity* **33**, 375-386, doi:10.1016/j.immuni.2010.08.012 (2010).
70 Chimen, M. *et al.* Monocyte Subsets Coregulate Inflammatory Responses by Integrated Signaling through TNF and IL-6 at the Endothelial Cell Interface. *J Immunol* **198**, 2834-2843, doi:10.4049/jimmunol.1601281 (2017).
71 Ley, K., Miller, Y. I. & Hedrick, C. C. Monocyte and macrophage dynamics during atherogenesis. *Arterioscler Thromb Vasc Biol* **31**, 1506-1516, doi:10.1161/ATVBAHA.110.221127 (2011).
72 Shi, C. & Pamer, E. G. Monocyte recruitment during infection and inflammation. *Nat Rev Immunol* **11**, 762-774, doi:10.1038/nri3070 (2011).
73 Ziegler-Heitbrock, L. The CD14+ CD16+ blood monocytes: Their role in infection and inflammation. *Journal of leukocyte biology* **81**, 584–592, doi:10.1189/jlb.0806510 (2007).

74 Belge, K. U. *et al.* The proinflammatory CD14+CD16+DR++ monocytes are a major source of TNF. *J Immunol* **168**, 3536-3542, doi:10.4049/jimmunol.168.7.3536 (2002).
75 Wong, K. L. *et al.* Gene expression profiling reveals the defining features of the classical, intermediate, and nonclassical human monocyte subsets. *Blood* **118**, e16-31, doi:10.1182/blood-2010-12-326355 (2011).
76 Geissmann, F., Jung, S. & Littman, D. R. Blood monocytes consist of two principal subsets with distinct migratory properties. *Immunity* **19**, 71-82, doi:10.1016/s1074-7613(03)00174-2 (2003).
77 Auffray, C., Sieweke, M. H. & Geissmann, F. Blood monocytes: development, heterogeneity, and relationship with dendritic cells. *Annu Rev Immunol* **27**, 669-692, doi:10.1146/annurev.immunol.021908.132557 (2009).
78 Yona, S. *et al.* Fate mapping reveals origins and dynamics of monocytes and tissue macrophages under homeostasis. *Immunity* **38**, 79-91, doi:10.1016/j.immuni.2012.12.001 (2013).
79 Patel, A. A. *et al.* The fate and lifespan of human monocyte subsets in steady state and systemic inflammation. *J Exp Med* **214**, 1913-1923, doi:10.1084/jem.20170355 (2017).
80 Rossol, M., Kraus, S., Pierer, M., Baerwald, C. & Wagner, U. The CD14(bright) CD16+ monocyte subset is expanded in rheumatoid arthritis and promotes expansion of the Th17 cell population. *Arthritis Rheum* **64**, 671-677, doi:10.1002/art.33418 (2012).
81 Tapp, L. D., Shantsila, E., Wrigley, B. J., Pamukcu, B. & Lip, G. Y. The CD14++CD16+ monocyte subset and monocyte-platelet interactions in patients with ST-elevation myocardial infarction. *J Thromb Haemost* **10**, 1231-1241, doi:10.1111/j.1538-7836.2011.04603.x (2012).
82 Poehlmann, H., Schefold, J. C., Zuckermann-Becker, H., Volk, H. D. & Meisel, C. Phenotype changes and impaired function of dendritic cell subsets in patients with sepsis: a prospective observational analysis. *Crit Care* **13**, R119, doi:10.1186/cc7969 (2009).
83 Urra, X. *et al.* Monocyte subtypes predict clinical course and prognosis in human stroke. *J Cereb Blood Flow Metab* **29**, 994-1002, doi:10.1038/jcbfm.2009.25 (2009).
84 Kaito, M. *et al.* Relevance of distinct monocyte subsets to clinical course of ischemic stroke patients. *PLoS One* **8**, e69409, doi:10.1371/journal.pone.0069409 (2013).
85 Baeten, D. *et al.* Human cartilage gp-39+,CD16+ monocytes in peripheral blood and synovium: correlation with joint destruction in rheumatoid arthritis. *Arthritis Rheum* **43**, 1233-1243, doi:10.1002/1529-0131(200006)43:6<1233::AID-ANR6>3.0.CO;2-9 (2000).
86 Zouggari, Y. *et al.* B lymphocytes trigger monocyte mobilization and impair heart function after acute myocardial infarction. *Nat Med* **19**, 1273-1280, doi:10.1038/nm.3284 (2013).
87 Tsou, C. L. *et al.* Critical roles for CCR2 and MCP-3 in monocyte mobilization from bone marrow and recruitment to inflammatory sites. *J Clin Invest* **117**, 902-909, doi:10.1172/JCI29919 (2007).
88 Carlin, L. M. *et al.* Nr4a1-dependent Ly6C(low) monocytes monitor endothelial cells and orchestrate their disposal. *Cell* **153**, 362-375, doi:10.1016/j.cell.2013.03.010 (2013).
89 Menezes, S. *et al.* The Heterogeneity of Ly6C(hi) Monocytes Controls Their Differentiation into iNOS(+) Macrophages or Monocyte-Derived Dendritic Cells. *Immunity* **45**, 1205-1218, doi:10.1016/j.immuni.2016.12.001 (2016).
90 Boyette, L. B. *et al.* Phenotype, function, and differentiation potential of human monocyte subsets. *PLoS One* **12**, e0176460, doi:10.1371/journal.pone.0176460 (2017).
91 Fingerle, G. *et al.* The novel subset of CD14+/CD16+ blood monocytes is expanded in sepsis patients. *Blood* **82**, 3170-3176 (1993).
92 Nockher, W. A. & Scherberich, J. E. Expanded CD14+ CD16+ monocyte subpopulation in patients with acute and chronic infections undergoing hemodialysis. *Infect Immun* **66**, 2782-2790, doi:10.1128/IAI.66.6.2782-2790.1998 (1998).

93 Ancuta, P. *et al.* Fractalkine preferentially mediates arrest and migration of CD16+ monocytes. *J Exp Med* **197**, 1701-1707, doi:10.1084/jem.20022156 (2003).
94 Auffray, C. *et al.* Monitoring of blood vessels and tissues by a population of monocytes with patrolling behavior. *Science* **317**, 666-670, doi:10.1126/science.1142883 (2007).
95 Olingy, C. E. *et al.* Non-classical monocytes are biased progenitors of wound healing macrophages during soft tissue injury. *Sci Rep* **7**, 447, doi:10.1038/s41598-017-00477-1 (2017).
96 Bae, Y. S. *et al.* Macrophages generate reactive oxygen species in response to minimally oxidized low-density lipoprotein: toll-like receptor 4- and spleen tyrosine kinase-dependent activation of NADPH oxidase 2. *Circ Res* **104**, 210-218, 221p following 218, doi:10.1161/CIRCRESAHA.108.181040 (2009).
97 Moore, K. J. & Tabas, I. Macrophages in the pathogenesis of atherosclerosis. *Cell* **145**, 341-355, doi:10.1016/j.cell.2011.04.005 (2011).
98 Mosser, D. M., Hamidzadeh, K. & Goncalves, R. Macrophages and the maintenance of homeostasis. *Cell Mol Immunol* **18**, 579-587, doi:10.1038/s41423-020-00541-3 (2021).
99 Murray, P. J. *et al.* Macrophage activation and polarization: nomenclature and experimental guidelines. *Immunity* **41**, 14-20, doi:10.1016/j.immuni.2014.06.008 (2014).
100 Krautter, F. *et al.* Characterisation of endogenous Galectin-1 and -9 expression in monocyte and macrophage subsets under resting and inflammatory conditions. *Biomed Pharmacother* **130**, 110595, doi:10.1016/j.biopha.2020.110595 (2020).
101 Li, H. *et al.* Tim-3/galectin-9 signaling pathway mediates T-cell dysfunction and predicts poor prognosis in patients with hepatitis B virus-associated hepatocellular carcinoma. *Hepatology (Baltimore, Md.)* **56**, 1342–1351, doi:10.1002/hep.25777 (2012).
102 Raggi, F. *et al.* Regulation of Human Macrophage M1-M2 Polarization Balance by Hypoxia and the Triggering Receptor Expressed on Myeloid Cells-1. *Front Immunol* **8**, 1097, doi:10.3389/fimmu.2017.01097 (2017).
103 Martinez, F. O. & Gordon, S. The M1 and M2 paradigm of macrophage activation: time for reassessment. *F1000Prime Rep* **6**, 13, doi:10.12703/P6-13 (2014).
104 Sica, A. & Mantovani, A. Macrophage plasticity and polarization: in vivo veritas. *J Clin Invest* **122**, 787-795, doi:10.1172/JCI59643 (2012).
105 Sharma, M. *et al.* Regulatory T Cells License Macrophage Pro-Resolving Functions During Atherosclerosis Regression. *Circ Res* **127**, 335-353, doi:10.1161/CIRCRESAHA.119.316461 (2020).
106 Kawanishi, N., Yano, H., Yokogawa, Y. & Suzuki, K. Exercise training inhibits inflammation in adipose tissue via both suppression of macrophage infiltration and acceleration of phenotypic switching from M1 to M2 macrophages in high-fat-diet-induced obese mice. *Exerc Immunol Rev* **16**, 105-118 (2010).
107 Mylonas, K. J., Nair, M. G., Prieto-Lafuente, L., Paape, D. & Allen, J. E. Alternatively activated macrophages elicited by helminth infection can be reprogrammed to enable microbial killing. *J Immunol* **182**, 3084-3094, doi:10.4049/jimmunol.0803463 (2009).
108 Stout, R. D. *et al.* Macrophages sequentially change their functional phenotype in response to changes in microenvironmental influences. *J Immunol* **175**, 342-349, doi:10.4049/jimmunol.175.1.342 (2005).
109 Guilliams, M. & van de Laar, L. A Hitchhiker's Guide to Myeloid Cell Subsets: Practical Implementation of a Novel Mononuclear Phagocyte Classification System. *Front Immunol* **6**, 406, doi:10.3389/fimmu.2015.00406 (2015).
110 Mosser, D. M. & Edwards, J. P. Exploring the full spectrum of macrophage activation. *Nat Rev Immunol* **8**, 958-969, doi:10.1038/nri2448 (2008).
111 Takeda, Y. *et al.* Macrophage skewing by Phd2 haplodeficiency prevents ischaemia by inducing arteriogenesis. *Nature* **479**, 122-126, doi:10.1038/nature10507 (2011).

112 Hashimoto, D. *et al.* Tissue-resident macrophages self-maintain locally throughout adult life with minimal contribution from circulating monocytes. *Immunity* **38**, 792-804, doi:10.1016/j.immuni.2013.04.004 (2013).
113 Gerhardt, T. & Ley, K. Monocyte trafficking across the vessel wall. *Cardiovascular Research* **107**, 321-330, doi:10.1093/cvr/cvv147 %J Cardiovascular Research (2015).
114 Dai, X. M. *et al.* Targeted disruption of the mouse colony-stimulating factor 1 receptor gene results in osteopetrosis, mononuclear phagocyte deficiency, increased primitive progenitor cell frequencies, and reproductive defects. *Blood* **99**, 111-120, doi:10.1182/blood.v99.1.111 (2002).
115 Pridans, C. *et al.* Pleiotropic Impacts of Macrophage and Microglial Deficiency on Development in Rats with Targeted Mutation of the Csf1r Locus. *J Immunol* **201**, 2683-2699, doi:10.4049/jimmunol.1701783 (2018).
116 Wang, Y. *et al.* IL-34 is a tissue-restricted ligand of CSF1R required for the development of Langerhans cells and microglia. *Nat Immunol* **13**, 753-760, doi:10.1038/ni.2360 (2012).
117 Stanley, E. *et al.* Granulocyte/macrophage colony-stimulating factor-deficient mice show no major perturbation of hematopoiesis but develop a characteristic pulmonary pathology. *Proc Natl Acad Sci U S A* **91**, 5592-5596, doi:10.1073/pnas.91.12.5592 (1994).
118 Nicola, N. A. *et al.* Functional inactivation in mice of the gene for the interleukin-3 (IL-3)-specific receptor beta-chain: implications for IL-3 function and the mechanism of receptor transmodulation in hematopoietic cells. *Blood* **87**, 2665-2674 (1996).
119 Niida, S. *et al.* Vascular endothelial growth factor can substitute for macrophage colony-stimulating factor in the support of osteoclastic bone resorption. *J Exp Med* **190**, 293-298, doi:10.1084/jem.190.2.293 (1999).
120 Murphy, C. A. *et al.* Divergent pro- and antiinflammatory roles for IL-23 and IL-12 in joint autoimmune inflammation. *J Exp Med* **198**, 1951-1957, doi:10.1084/jem.20030896 (2003).
121 Kamada, N. *et al.* Unique CD14 intestinal macrophages contribute to the pathogenesis of Crohn disease via IL-23/IFN-gamma axis. *J Clin Invest* **118**, 2269-2280, doi:10.1172/JCI34610 (2008).
122 Sindrilaru, A. *et al.* An unrestrained proinflammatory M1 macrophage population induced by iron impairs wound healing in humans and mice. *J Clin Invest* **121**, 985-997, doi:10.1172/JCI44490 (2011).
123 Parisi, L. *et al.* Macrophage Polarization in Chronic Inflammatory Diseases: Killers or Builders? *J Immunol Res* **2018**, 8917804, doi:10.1155/2018/8917804 (2018).
124 Fujisaka, S. *et al.* Regulatory mechanisms for adipose tissue M1 and M2 macrophages in diet-induced obese mice. *Diabetes* **58**, 2574-2582, doi:10.2337/db08-1475 (2009).
125 Sutterwala, F. S., Noel, G. J., Salgame, P. & Mosser, D. M. Reversal of proinflammatory responses by ligating the macrophage Fcgamma receptor type I. *J Exp Med* **188**, 217-222, doi:10.1084/jem.188.1.217 (1998).
126 Pesce, J. T. *et al.* Arginase-1-expressing macrophages suppress Th2 cytokine-driven inflammation and fibrosis. *PLoS Pathog* **5**, e1000371, doi:10.1371/journal.ppat.1000371 (2009).
127 Herbert, D. R. *et al.* Arginase I suppresses IL-12/IL-23p40-driven intestinal inflammation during acute schistosomiasis. *J Immunol* **184**, 6438-6446, doi:10.4049/jimmunol.0902009 (2010).
128 Moore, K. W., de Waal Malefyt, R., Coffman, R. L. & O'Garra, A. Interleukin-10 and the interleukin-10 receptor. *Annu Rev Immunol* **19**, 683-765, doi:10.1146/annurev.immunol.19.1.683 (2001).
129 London, A. *et al.* Neuroprotection and progenitor cell renewal in the injured adult murine retina requires healing monocyte-derived macrophages. *J Exp Med* **208**, 23-39, doi:10.1084/jem.20101202 (2011).

130 Murray, P. J. & Wynn, T. A. Protective and pathogenic functions of macrophage subsets. *Nat Rev Immunol* **11**, 723-737, doi:10.1038/nri3073 (2011).
131 Roberts, A. B. *et al.* Transforming growth factor type beta: rapid induction of fibrosis and angiogenesis in vivo and stimulation of collagen formation in vitro. *Proc Natl Acad Sci U S A* **83**, 4167-4171, doi:10.1073/pnas.83.12.4167 (1986).
132 Shimokado, K. *et al.* A significant part of macrophage-derived growth factor consists of at least two forms of PDGF. *Cell* **43**, 277-286, doi:10.1016/0092-8674(85)90033-9 (1985).
133 Huang, W. C., Sala-Newby, G. B., Susana, A., Johnson, J. L. & Newby, A. C. Classical macrophage activation up-regulates several matrix metalloproteinases through mitogen activated protein kinases and nuclear factor-kappaB. *PLoS One* **7**, e42507, doi:10.1371/journal.pone.0042507 (2012).
134 Yoshida, H. *et al.* The murine mutation osteopetrosis is in the coding region of the macrophage colony stimulating factor gene. *Nature* **345**, 442-444, doi:10.1038/345442a0 (1990).
135 Van Wesenbeeck, L. *et al.* The osteopetrotic mutation toothless (tl) is a loss-of-function frameshift mutation in the rat Csf1 gene: Evidence of a crucial role for CSF-1 in osteoclastogenesis and endochondral ossification. *Proc Natl Acad Sci U S A* **99**, 14303-14308, doi:10.1073/pnas.202332999 (2002).
136 Stefater, J. A., 3rd, Ren, S., Lang, R. A. & Duffield, J. S. Metchnikoff's policemen: macrophages in development, homeostasis and regeneration. *Trends Mol Med* **17**, 743-752, doi:10.1016/j.molmed.2011.07.009 (2011).
137 Boulter, L. *et al.* Macrophage-derived Wnt opposes Notch signaling to specify hepatic progenitor cell fate in chronic liver disease. *Nat Med* **18**, 572-579, doi:10.1038/nm.2667 (2012).
138 Kawane, K. *et al.* Requirement of DNase II for definitive erythropoiesis in the mouse fetal liver. *Science* **292**, 1546-1549, doi:10.1126/science.292.5521.1546 (2001).
139 Stefater, J. A., 3rd *et al.* Regulation of angiogenesis by a non-canonical Wnt-Flt1 pathway in myeloid cells. *Nature* **474**, 511-515, doi:10.1038/nature10085 (2011).
140 Rao, S. *et al.* Obligatory participation of macrophages in an angiopoietin 2-mediated cell death switch. *Development* **134**, 4449-4458, doi:10.1242/dev.012187 (2007).
141 Tammela, T. *et al.* VEGFR-3 controls tip to stalk conversion at vessel fusion sites by reinforcing Notch signalling. *Nat Cell Biol* **13**, 1202-1213, doi:10.1038/ncb2331 (2011).
142 Ross, R. Atherosclerosis--an inflammatory disease. *N Engl J Med* **340**, 115-126, doi:10.1056/NEJM199901143400207 (1999).
143 Singh, R. B., Mengi, S. A., Xu, Y. J., Arneja, A. S. & Dhalla, N. S. Pathogenesis of atherosclerosis: A multifactorial process. *Exp Clin Cardiol* **7**, 40-53 (2002).
144 Soehnlein, O. & Libby, P. Targeting inflammation in atherosclerosis - from experimental insights to the clinic. *Nat Rev Drug Discov* **20**, 589-610, doi:10.1038/s41573-021-00198-1 (2021).
145 McGill, H. C., Jr., McMahan, C. A. & Gidding, S. S. Preventing heart disease in the 21st century: implications of the Pathobiological Determinants of Atherosclerosis in Youth (PDAY) study. *Circulation* **117**, 1216-1227, doi:10.1161/CIRCULATIONAHA.107.717033 (2008).
146 Gao, Z. *et al.* Galectin-3 Is a Potential Mediator for Atherosclerosis. *J Immunol Res* **2020**, 5284728, doi:10.1155/2020/5284728 (2020).
147 Roth, G. A. *et al.* Global Burden of Cardiovascular Diseases and Risk Factors, 1990-2019: Update From the GBD 2019 Study. *J Am Coll Cardiol* **76**, 2982-3021, doi:10.1016/j.jacc.2020.11.010 (2020).
148 Gomez Sandoval, Y. H., Braganza, M. V. & Daskalopoulou, S. S. Statin discontinuation in high-risk patients: a systematic review of the evidence. *Curr Pharm Des* **17**, 3669-3689, doi:10.2174/138161211798220891 (2011).

149 Talayero, B. G. & Sacks, F. M. The role of triglycerides in atherosclerosis. *Curr Cardiol Rep* **13**, 544-552, doi:10.1007/s11886-011-0220-3 (2011).
150 Ridker, P. M. *et al.* Antiinflammatory Therapy with Canakinumab for Atherosclerotic Disease. *N Engl J Med* **377**, 1119-1131, doi:10.1056/NEJMoa1707914 (2017).
151 Nidorf, S. M., Eikelboom, J. W., Budgeon, C. A. & Thompson, P. L. Low-dose colchicine for secondary prevention of cardiovascular disease. *J Am Coll Cardiol* **61**, 404-410, doi:10.1016/j.jacc.2012.10.027 (2013).
152 Opstal, T. S. J. *et al.* Colchicine Attenuates Inflammation Beyond the Inflammasome in Chronic Coronary Artery Disease: A LoDoCo2 Proteomic Substudy. *Circulation* **142**, 1996-1998, doi:10.1161/CIRCULATIONAHA.120.050560 (2020).
153 Ridker, P. M. *et al.* Low-Dose Methotrexate for the Prevention of Atherosclerotic Events. *N Engl J Med* **380**, 752-762, doi:10.1056/NEJMoa1809798 (2019).
154 Gijsen, F., van der Giessen, A., van der Steen, A. & Wentzel, J. Shear stress and advanced atherosclerosis in human coronary arteries. *J Biomech* **46**, 240-247, doi:10.1016/j.jbiomech.2012.11.006 (2013).
155 Kopprasch, S., Pietzsch, J., Westendorf, T., Kruse, H. J. & Grassler, J. The pivotal role of scavenger receptor CD36 and phagocyte-derived oxidants in oxidized low density lipoprotein-induced adhesion to endothelial cells. *Int J Biochem Cell Biol* **36**, 460-471, doi:10.1016/j.biocel.2003.08.001 (2004).
156 Chen, M., Masaki, T. & Sawamura, T. LOX-1, the receptor for oxidized low-density lipoprotein identified from endothelial cells: implications in endothelial dysfunction and atherosclerosis. *Pharmacol Ther* **95**, 89-100, doi:10.1016/s0163-7258(02)00236-x (2002).
157 Cominacini, L. *et al.* Antioxidants inhibit the expression of intercellular cell adhesion molecule-1 and vascular cell adhesion molecule-1 induced by oxidized LDL on human umbilical vein endothelial cells. *Free Radic Biol Med* **22**, 117-127, doi:10.1016/s0891-5849(96)00271-7 (1997).
158 Li, D. *et al.* Statins modulate oxidized low-density lipoprotein-mediated adhesion molecule expression in human coronary artery endothelial cells: role of LOX-1. *J Pharmacol Exp Ther* **302**, 601-605, doi:10.1124/jpet.102.034959 (2002).
159 Stewart, C. R. *et al.* CD36 ligands promote sterile inflammation through assembly of a Toll-like receptor 4 and 6 heterodimer. *Nat Immunol* **11**, 155-161, doi:10.1038/ni.1836 (2010).
160 Yvan-Charvet, L. *et al.* Increased inflammatory gene expression in ABC transporter-deficient macrophages: free cholesterol accumulation, increased signaling via toll-like receptors, and neutrophil infiltration of atherosclerotic lesions. *Circulation* **118**, 1837-1847, doi:10.1161/CIRCULATIONAHA.108.793869 (2008).
161 Basatemur, G. L., Jorgensen, H. F., Clarke, M. C. H., Bennett, M. R. & Mallat, Z. Vascular smooth muscle cells in atherosclerosis. *Nat Rev Cardiol* **16**, 727-744, doi:10.1038/s41569-019-0227-9 (2019).
162 Ross, R. *et al.* Localization of PDGF-B protein in macrophages in all phases of atherogenesis. *Science* **248**, 1009-1012, doi:10.1126/science.2343305 (1990).
163 Andreeva, E. R., Pugach, I. M. & Orekhov, A. N. Collagen-synthesizing cells in initial and advanced atherosclerotic lesions of human aorta. *Atherosclerosis* **130**, 133-142, doi:10.1016/s0021-9150(96)06056-x (1997).
164 Vengrenyuk, Y. *et al.* Cholesterol loading reprograms the microRNA-143/145-myocardin axis to convert aortic smooth muscle cells to a dysfunctional macrophage-like phenotype. *Arterioscler Thromb Vasc Biol* **35**, 535-546, doi:10.1161/ATVBAHA.114.304029 (2015).
165 Clarke, M. C. *et al.* Apoptosis of vascular smooth muscle cells induces features of plaque vulnerability in atherosclerosis. *Nat Med* **12**, 1075-1080, doi:10.1038/nm1459 (2006).

166 Kong, Y. Z. *et al.* Evidence for vascular macrophage migration inhibitory factor in destabilization of human atherosclerotic plaques. *Cardiovasc Res* **65**, 272-282, doi:10.1016/j.cardiores.2004.09.020 (2005).
167 Sukhova, G. K. *et al.* Evidence for increased collagenolysis by interstitial collagenases-1 and -3 in vulnerable human atheromatous plaques. *Circulation* **99**, 2503-2509, doi:10.1161/01.cir.99.19.2503 (1999).
168 Yu, H. *et al.* FOXO3a (Forkhead Transcription Factor O Subfamily Member 3a) Links Vascular Smooth Muscle Cell Apoptosis, Matrix Breakdown, Atherosclerosis, and Vascular Remodeling Through a Novel Pathway Involving MMP13 (Matrix Metalloproteinase 13). *Arterioscler Thromb Vasc Biol* **38**, 555-565, doi:10.1161/ATVBAHA.117.310502 (2018).
169 Vengrenyuk, Y. *et al.* A hypothesis for vulnerable plaque rupture due to stress-induced debonding around cellular microcalcifications in thin fibrous caps. *Proc Natl Acad Sci U S A* **103**, 14678-14683, doi:10.1073/pnas.0606310103 (2006).
170 Hutcheson, J. D. *et al.* Genesis and growth of extracellular-vesicle-derived microcalcification in atherosclerotic plaques. *Nat Mater* **15**, 335-343, doi:10.1038/nmat4519 (2016).
171 Soehnlein, O. *et al.* Distinct functions of chemokine receptor axes in the atherogenic mobilization and recruitment of classical monocytes. *EMBO Mol Med* **5**, 471-481, doi:10.1002/emmm.201201717 (2013).
172 Tacke, F. *et al.* Monocyte subsets differentially employ CCR2, CCR5, and CX3CR1 to accumulate within atherosclerotic plaques. *J Clin Invest* **117**, 185-194, doi:10.1172/JCI28549 (2007).
173 Boring, L., Gosling, J., Cleary, M. & Charo, I. F. Decreased lesion formation in CCR2-/- mice reveals a role for chemokines in the initiation of atherosclerosis. *Nature* **394**, 894-897, doi:10.1038/29788 (1998).
174 Applebaum-Bowden, D. *et al.* Down-regulation of the low-density lipoprotein receptor by dietary cholesterol. *Am J Clin Nutr* **39**, 360-367, doi:10.1093/ajcn/39.3.360 (1984).
175 Kzhyshkowska, J., Neyen, C. & Gordon, S. Role of macrophage scavenger receptors in atherosclerosis. *Immunobiology* **217**, 492-502, doi:10.1016/j.imbio.2012.02.015 (2012).
176 Maxfield, F. R. & Tabas, I. Role of cholesterol and lipid organization in disease. *Nature* **438**, 612-621, doi:10.1038/nature04399 (2005).
177 Zhu, X. *et al.* Macrophage ABCA1 reduces MyD88-dependent Toll-like receptor trafficking to lipid rafts by reduction of lipid raft cholesterol. *J Lipid Res* **51**, 3196-3206, doi:10.1194/jlr.M006486 (2010).
178 Feng, B. *et al.* The endoplasmic reticulum is the site of cholesterol-induced cytotoxicity in macrophages. *Nat Cell Biol* **5**, 781-792, doi:10.1038/ncb1035 (2003).
179 Tabas, I. Consequences and therapeutic implications of macrophage apoptosis in atherosclerosis: the importance of lesion stage and phagocytic efficiency. *Arterioscler Thromb Vasc Biol* **25**, 2255-2264, doi:10.1161/01.ATV.0000184783.04864.9f (2005).
180 Duewell, P. *et al.* NLRP3 inflammasomes are required for atherogenesis and activated by cholesterol crystals. *Nature* **464**, 1357-1361, doi:10.1038/nature08938 (2010).
181 Freigang, S. *et al.* Nrf2 is essential for cholesterol crystal-induced inflammasome activation and exacerbation of atherosclerosis. *Eur J Immunol* **41**, 2040-2051, doi:10.1002/eji.201041316 (2011).
182 Gage, J., Hasu, M., Thabet, M. & Whitman, S. C. Caspase-1 deficiency decreases atherosclerosis in apolipoprotein E-null mice. *Can J Cardiol* **28**, 222-229, doi:10.1016/j.cjca.2011.10.013 (2012).
183 Weinstock, A. *et al.* Wnt signaling enhances macrophage responses to IL-4 and promotes resolution of atherosclerosis. *Elife* **10**, doi:10.7554/eLife.67932 (2021).
184 Rahman, K. *et al.* Inflammatory Ly6Chi monocytes and their conversion to M2 macrophages drive atherosclerosis regression. *J Clin Invest* **127**, 2904-2915, doi:10.1172/JCI75005 (2017).

185 Llodra, J. *et al.* Emigration of monocyte-derived cells from atherosclerotic lesions characterizes regressive, but not progressive, plaques. *Proc Natl Acad Sci U S A* **101**, 11779-11784, doi:10.1073/pnas.0403259101 (2004).
186 Potteaux, S. *et al.* Suppressed monocyte recruitment drives macrophage removal from atherosclerotic plaques of Apoe-/- mice during disease regression. *J Clin Invest* **121**, 2025-2036, doi:10.1172/JCI43802 (2011).
187 van Gils, J. M. *et al.* The neuroimmune guidance cue netrin-1 promotes atherosclerosis by inhibiting the emigration of macrophages from plaques. *Nat Immunol* **13**, 136-143, doi:10.1038/ni.2205 (2012).
188 Trogan, E. *et al.* Laser capture microdissection analysis of gene expression in macrophages from atherosclerotic lesions of apolipoprotein E-deficient mice. *Proc Natl Acad Sci U S A* **99**, 2234-2239, doi:10.1073/pnas.042683999 (2002).
189 Feig, J. E. *et al.* Reversal of hyperlipidemia with a genetic switch favorably affects the content and inflammatory state of macrophages in atherosclerotic plaques. *Circulation* **123**, 989-998, doi:10.1161/CIRCULATIONAHA.110.984146 (2011).
190 Rong, J. X. *et al.* Elevating high-density lipoprotein cholesterol in apolipoprotein E-deficient mice remodels advanced atherosclerotic lesions by decreasing macrophage and increasing smooth muscle cell content. *Circulation* **104**, 2447-2452, doi:10.1161/hc4501.098952 (2001).
191 Trogan, E. *et al.* Gene expression changes in foam cells and the role of chemokine receptor CCR7 during atherosclerosis regression in ApoE-deficient mice. *Proc Natl Acad Sci U S A* **103**, 3781-3786, doi:10.1073/pnas.0511043103 (2006).
192 Fisher, E. A. Regression of Atherosclerosis: The Journey From the Liver to the Plaque and Back. *Arterioscler Thromb Vasc Biol* **36**, 226-235, doi:10.1161/ATVBAHA.115.301926 (2016).
193 Cardilo-Reis, L. *et al.* Interleukin-13 protects from atherosclerosis and modulates plaque composition by skewing the macrophage phenotype. *EMBO Mol Med* **4**, 1072-1086, doi:10.1002/emmm.201201374 (2012).
194 Feig, J. E. *et al.* Regression of atherosclerosis is characterized by broad changes in the plaque macrophage transcriptome. *PLoS One* **7**, e39790, doi:10.1371/journal.pone.0039790 (2012).
195 Paigen, B., Morrow, A., Holmes, P. A., Mitchell, D. & Williams, R. A. Quantitative assessment of atherosclerotic lesions in mice. *Atherosclerosis* **68**, 231-240, doi:10.1016/0021-9150(87)90202-4 (1987).
196 Zhang, S. H., Reddick, R. L., Piedrahita, J. A. & Maeda, N. Spontaneous hypercholesterolemia and arterial lesions in mice lacking apolipoprotein E. *Science* **258**, 468-471, doi:10.1126/science.1411543 (1992).
197 Piedrahita, J. A., Zhang, S. H., Hagaman, J. R., Oliver, P. M. & Maeda, N. Generation of mice carrying a mutant apolipoprotein E gene inactivated by gene targeting in embryonic stem cells. *Proc Natl Acad Sci U S A* **89**, 4471-4475, doi:10.1073/pnas.89.10.4471 (1992).
198 Plump, A. S. *et al.* Severe hypercholesterolemia and atherosclerosis in apolipoprotein E-deficient mice created by homologous recombination in ES cells. *Cell* **71**, 343-353, doi:10.1016/0092-8674(92)90362-g (1992).
199 Ishibashi, S. *et al.* Hypercholesterolemia in low density lipoprotein receptor knockout mice and its reversal by adenovirus-mediated gene delivery. *J Clin Invest* **92**, 883-893, doi:10.1172/JCI116663 (1993).
200 Bjorklund, M. M. *et al.* Induction of atherosclerosis in mice and hamsters without germline genetic engineering. *Circ Res* **114**, 1684-1689, doi:10.1161/CIRCRESAHA.114.302937 (2014).
201 Reis, E. D. *et al.* Dramatic remodeling of advanced atherosclerotic plaques of the apolipoprotein E-deficient mouse in a novel transplantation model. *J Vasc Surg* **34**, 541-547, doi:10.1067/mva.2001.115963 (2001).

202 Crooke, R. M. *et al.* An apolipoprotein B antisense oligonucleotide lowers LDL cholesterol in hyperlipidemic mice without causing hepatic steatosis. *J Lipid Res* **46**, 872-884, doi:10.1194/jlr.M400492-JLR200 (2005).
203 Wagner-Hulsmann, C. *et al.* A galectin links the aggregation factor to cells in the sponge (Geodia cydonium) system. *Glycobiology* **6**, 785-793, doi:10.1093/glycob/6.8.785-d (1996).
204 Cummings, R. D., Liu, F.-T. & Vasta, G. R. (Cold Spring Harbor (NY), 2015).
205 Houzelstein, D. *et al.* Phylogenetic analysis of the vertebrate galectin family. *Mol Biol Evol* **21**, 1177-1187, doi:10.1093/molbev/msh082 (2004).
206 Laaf, D., Bojarova, P., Elling, L. & Kren, V. Galectin-Carbohydrate Interactions in Biomedicine and Biotechnology. *Trends Biotechnol* **37**, 402-415, doi:10.1016/j.tibtech.2018.10.001 (2019).
207 Zhang, F. *et al.* Different roles of galectin-9 isoforms in modulating E-selectin expression and adhesion function in LoVo colon carcinoma cells. *Mol Biol Rep* **36**, 823-830, doi:10.1007/s11033-008-9251-2 (2009).
208 Varki, A. *et al.* (Cold Spring Harbor (NY), 2015).
209 Kupper, C. E. *et al.* Fluorescent SNAP-tag galectin fusion proteins as novel tools in glycobiology. *Curr Pharm Des* **19**, 5457-5467, doi:10.2174/1381612811319300017 (2013).
210 Carlsson, S. *et al.* Affinity of galectin-8 and its carbohydrate recognition domains for ligands in solution and at the cell surface. *Glycobiology* **17**, 663-676, doi:10.1093/glycob/cwm026 (2007).
211 Liu, F.-T., Yang, R.-Y. & Hsu, D. K. Galectins in acute and chronic inflammation. *Annals of the New York Academy of Sciences* **1253**, 80–91, doi:10.1111/j.1749-6632.2011.06386.x (2012).
212 Johannes, L., Jacob, R. & Leffler, H. Galectins at a glance. *J Cell Sci* **131**, doi:10.1242/jcs.208884 (2018).
213 Alam, S. *et al.* Galectin-9 protein expression in endothelial cells is positively regulated by histone deacetylase 3. *J Biol Chem* **286**, 44211-44217, doi:10.1074/jbc.M111.242289 (2011).
214 Imaizumi, T. *et al.* Interferon-gamma stimulates the expression of galectin-9 in cultured human endothelial cells. *Journal of leukocyte biology* **72**, 486–491 (2002).
215 Ma, C. J. *et al.* Cis association of galectin-9 with Tim-3 differentially regulates IL-12/IL-23 expressions in monocytes via TLR signaling. *PloS one* **8**, e72488, doi:10.1371/journal.pone.0072488 (2013).
216 Niki, T. *et al.* Plasma Galectin-9 Concentrations in Normal and Diseased Condition. *Cell Physiol Biochem* **50**, 1856-1868, doi:10.1159/000494866 (2018).
217 Seki, M. *et al.* Beneficial effect of galectin 9 on rheumatoid arthritis by induction of apoptosis of synovial fibroblasts. *Arthritis and rheumatism* **56**, 3968–3976, doi:10.1002/art.23076 (2007).
218 Zhu, R. *et al.* Serum Galectin-9 Levels Are Associated with Coronary Artery Disease in Chinese Individuals. *Mediators Inflamm* **2015**, 457167, doi:10.1155/2015/457167 (2015).
219 Boer, R. A. d., Yu, L. & van Veldhuisen, D. J. Galectin-3 in cardiac remodeling and heart failure. *Current heart failure reports* **7**, 1–8, doi:10.1007/s11897-010-0004-x (2010).
220 Lee, Y. J. *et al.* Serum galectin-3 and galectin-3 binding protein levels in Behçet's disease and their association with disease activity. *Clinical and experimental rheumatology* **25**, S41-45 (2007).
221 Popa, S. J., Stewart, S. E. & Moreau, K. Unconventional secretion of annexins and galectins. *Semin Cell Dev Biol* **83**, 42-50, doi:10.1016/j.semcdb.2018.02.022 (2018).
222 Harazono, Y. *et al.* Galectin-3 leads to attenuation of apoptosis through Bax heterodimerization in human thyroid carcinoma cells. *Oncotarget* **5**, 9992–10001, doi:10.18632/oncotarget.2486 (2014).
223 Delacour, D., Koch, A. & Jacob, R. The role of galectins in protein trafficking. *Traffic* **10**, 1405-1413, doi:10.1111/j.1600-0854.2009.00960.x (2009).

224 Cooper, D. N. & Barondes, S. H. Evidence for export of a muscle lectin from cytosol to extracellular matrix and for a novel secretory mechanism. *The Journal of cell biology* **110**, 1681–1691 (1990).
225 Harrison, F. L. & Wilson, T. J. The 14 kDa beta-galactoside binding lectin in myoblast and myotube cultures: Localization by confocal microscopy. *Journal of cell science* **101 (Pt 3)**, 635–646 (1992).
226 Keryer-Bibens, C. *et al.* Exosomes released by EBV-infected nasopharyngeal carcinoma cells convey the viral latent membrane protein 1 and the immunomodulatory protein galectin 9. *BMC cancer* **6**, 283, doi:10.1186/1471-2407-6-283 (2006).
227 Lukyanov, P., Furtak, V. & Ochieng, J. Galectin-3 interacts with membrane lipids and penetrates the lipid bilayer. *Biochemical and biophysical research communications* **338**, 1031–1036, doi:10.1016/j.bbrc.2005.10.033 (2005).
228 Schäfer, T. *et al.* Unconventional secretion of fibroblast growth factor 2 is mediated by direct translocation across the plasma membrane of mammalian cells. *The Journal of biological chemistry* **279**, 6244–6251, doi:10.1074/jbc.M310500200 (2004).
229 Villeneuve, C. *et al.* Mitochondrial proteomic approach reveals galectin-7 as a novel BCL-2 binding protein in human cells. *Molecular biology of the cell* **22**, 999–1013, doi:10.1091/mbc.E10-06-0534 (2011).
230 Dagher, S. F., Wang, J. L. & Patterson, R. J. Identification of galectin-3 as a factor in pre-mRNA splicing. *Proceedings of the National Academy of Sciences of the United States of America* **92**, 1213–1217 (1995).
231 Vyakarnam, A., Dagher, S. F., Wang, J. L. & Patterson, R. J. Evidence for a role for galectin-1 in pre-mRNA splicing. *Molecular and cellular biology* **17**, 4730–4737 (1997).
232 Coppin, L. *et al.* Galectin-3 is a non-classic RNA binding protein that stabilizes the mucin MUC4 mRNA in the cytoplasm of cancer cells. *Scientific reports* **7**, 43927, doi:10.1038/srep43927 (2017).
233 Dai, S.-Y. *et al.* Galectin-9 induces maturation of human monocyte-derived dendritic cells. *Journal of immunology (Baltimore, Md. : 1950)* **175**, 2974–2981 (2005).
234 Pace, K. E., Lee, C., Stewart, P. L. & Baum, L. G. Restricted receptor segregation into membrane microdomains occurs on human T cells during apoptosis induced by galectin-1. *Journal of immunology (Baltimore, Md. : 1950)* **163**, 3801–3811 (1999).
235 He, J. & Baum, L. G. Galectin interactions with extracellular matrix and effects on cellular function. *Methods in enzymology* **417**, 247–256, doi:10.1016/s0076-6879(06)17017-2 (2006).
236 Fujii, A., Shearer, T. R. & Azuma, M. Galectin-3 enhances extracellular matrix associations and wound healing in monkey corneal epithelium. *Experimental eye research* **137**, 71–78, doi:10.1016/j.exer.2015.06.010 (2015).
237 Kleshchenko, Y. Y. *et al.* Human galectin-3 promotes Trypanosoma cruzi adhesion to human coronary artery smooth muscle cells. *Infection and immunity* **72**, 6717–6721, doi:10.1128/iai.72.11.6717-6721.2004 (2004).
238 Zeggar, S. *et al.* Role of Lgals9 Deficiency in Attenuating Nephritis and Arthritis in BALB/c Mice in a Pristane-Induced Lupus Model. *Arthritis Rheumatol* **70**, 1089-1101, doi:10.1002/art.40467 (2018).
239 He, X. W. *et al.* Serum levels of galectin-1, galectin-3, and galectin-9 are associated with large artery atherosclerotic stroke. *Sci Rep* **7**, 40994, doi:10.1038/srep40994 (2017).
240 Chihara, M., Kurita, M., Yoshihara, Y., Asahina, A. & Yanaba, K. Clinical Significance of Serum Galectin-9 and Soluble CD155 Levels in Patients with Systemic Sclerosis. *J Immunol Res* **2018**, 9473243, doi:10.1155/2018/9473243 (2018).
241 Matsuoka, N. *et al.* Galectin-9 as a biomarker for disease activity in systemic lupus erythematosus. *PLoS One* **15**, e0227069, doi:10.1371/journal.pone.0227069 (2020).

242 La, M. *et al.* A novel biological activity for galectin-1: Inhibition of leukocyte-endothelial cell interactions in experimental inflammation. *The American journal of pathology* **163**, 1505–1515 (2003).
243 Cooper, D., Norling, L. V. & Perretti, M. Novel insights into the inhibitory effects of Galectin-1 on neutrophil recruitment under flow. *Journal of leukocyte biology* **83**, 1459–1466, doi:10.1189/jlb.1207831 (2008).
244 Alves, C. M. *et al.* Galectin-3 is essential for reactive oxygen species production by peritoneal neutrophils from mice infected with a virulent strain of Toxoplasma gondii. *Parasitology* **140**, 210-219, doi:10.1017/S0031182012001473 (2013).
245 Gittens, B. R., Bodkin, J. V., Nourshargh, S., Perretti, M. & Cooper, D. Galectin-3: A Positive Regulator of Leukocyte Recruitment in the Inflamed Microcirculation. *J Immunol* **198**, 4458-4469, doi:10.4049/jimmunol.1600709 (2017).
246 Suryawanshi, A., Cao, Z., Thitiprasert, T., Zaidi, T. S. & Panjwani, N. Galectin-1-mediated suppression of Pseudomonas aeruginosa-induced corneal immunopathology. *J Immunol* **190**, 6397-6409, doi:10.4049/jimmunol.1203501 (2013).
247 Robinson, B. S. *et al.* The Sweet-Side of Leukocytes: Galectins as Master Regulators of Neutrophil Function. *Front Immunol* **10**, 1762, doi:10.3389/fimmu.2019.01762 (2019).
248 Eckardt, V. *et al.* Chemokines and galectins form heterodimers to modulate inflammation. *EMBO Rep* **21**, e47852, doi:10.15252/embr.201947852 (2020).
249 Zernecke, A. *et al.* Protective role of CXC receptor 4/CXC ligand 12 unveils the importance of neutrophils in atherosclerosis. *Circ Res* **102**, 209-217, doi:10.1161/CIRCRESAHA.107.160697 (2008).
250 Liehn, E. A. *et al.* Double-edged role of the CXCL12/CXCR4 axis in experimental myocardial infarction. *J Am Coll Cardiol* **58**, 2415-2423, doi:10.1016/j.jacc.2011.08.033 (2011).
251 De Filippo, K. & Rankin, S. M. CXCR4, the master regulator of neutrophil trafficking in homeostasis and disease. *Eur J Clin Invest* **48 Suppl 2**, e12949, doi:10.1111/eci.12949 (2018).
252 Dong, R. *et al.* Galectin-3 as a novel biomarker for disease diagnosis and a target for therapy (Review). *Int J Mol Med* **41**, 599-614, doi:10.3892/ijmm.2017.3311 (2018).
253 Di Gregoli, K. *et al.* Galectin-3 Identifies a Subset of Macrophages With a Potential Beneficial Role in Atherosclerosis. *Arterioscler Thromb Vasc Biol*, ATVBAHA120314252, doi:10.1161/ATVBAHA.120.314252 (2020).
254 Norling, L. V., Sampaio, A. L., Cooper, D. & Perretti, M. Inhibitory control of endothelial galectin-1 on in vitro and in vivo lymphocyte trafficking. *FASEB J* **22**, 682-690, doi:10.1096/fj.07-9268com (2008).
255 Yamamoto, H. *et al.* Induction of cell adhesion by galectin-8 and its target molecules in Jurkat T-cells. *Journal of biochemistry* **143**, 311–324, doi:10.1093/jb/mvm223 (2008).
256 Iqbal, A. J. *et al.* Endogenous galectin-1 and acute inflammation: emerging notion of a galectin-9 pro-resolving effect. *Am J Pathol* **178**, 1201-1209, doi:10.1016/j.ajpath.2010.11.073 (2011).
257 Lee, Y. J. *et al.* Spatial and temporal expression, and statin responsiveness of galectin-1 and galectin-3 in murine atherosclerosis. *Korean Circ J* **43**, 223-230, doi:10.4070/kcj.2013.43.4.223 (2013).
258 Tsai, M. S. *et al.* Galectin-1 Restricts Vascular Smooth Muscle Cell Motility Via Modulating Adhesion Force and Focal Adhesion Dynamics. *Sci Rep* **8**, 11497, doi:10.1038/s41598-018-29843-3 (2018).
259 Casanegra, A. I. *et al.* Differences in galectin-3, a biomarker of fibrosis, between participants with peripheral artery disease and participants with normal ankle-brachial index. *Vasc Med* **21**, 437-444, doi:10.1177/1358863X16644059 (2016).
260 Fort-Gallifa, I. *et al.* Galectin-3 in Peripheral Artery Disease. Relationships with Markers of Oxidative Stress and Inflammation. *Int J Mol Sci* **18**, doi:10.3390/ijms18050973 (2017).

261 Jirak, P. *et al.* Analysis of novel cardiovascular biomarkers in patients with peripheral artery disease. *Minerva Med* **109**, 443-450, doi:10.23736/S0026-4806.18.05628-8 (2018).
262 Oyenuga, A., Folsom, A. R., Fashanu, O., Aguilar, D. & Ballantyne, C. M. Plasma Galectin-3 and Sonographic Measures of Carotid Atherosclerosis in the Atherosclerosis Risk in Communities Study. *Angiology* **70**, 47-55, doi:10.1177/0003319718780772 (2019).
263 Anyfanti, P. *et al.* Association of galectin-3 with markers of myocardial function, atherosclerosis, and vascular fibrosis in patients with rheumatoid arthritis. *Clin Cardiol* **42**, 62-68, doi:10.1002/clc.23105 (2019).
264 Pusuroglu, H. *et al.* Galectin-3 is associated with coronary plaque burden and obstructive sleep apnoea syndrome severity. *Kardiol Pol* **75**, 351-359, doi:10.5603/KP.a2016.0185 (2017).
265 Ozturk, D. *et al.* Association between serum galectin-3 levels and coronary atherosclerosis and plaque burden/structure in patients with type 2 diabetes mellitus. *Coron Artery Dis* **26**, 396-401, doi:10.1097/MCA.0000000000000252 (2015).
266 Aksan, G. *et al.* Is galectin-3 a biomarker, a player-or both-in the presence of coronary atherosclerosis? *J Investig Med* **64**, 764-770, doi:10.1136/jim-2015-000041 (2016).
267 Madrigal-Matute, J. *et al.* Galectin-3, a biomarker linking oxidative stress and inflammation with the clinical outcomes of patients with atherothrombosis. *J Am Heart Assoc* **3**, doi:10.1161/JAHA.114.000785 (2014).
268 Gleissner, C. A. *et al.* Galectin-3 binding protein plasma levels are associated with long-term mortality in coronary artery disease independent of plaque morphology. *Atherosclerosis* **251**, 94-100, doi:10.1016/j.atherosclerosis.2016.06.002 (2016).
269 Langley, S. R. *et al.* Extracellular matrix proteomics identifies molecular signature of symptomatic carotid plaques. *J Clin Invest* **127**, 1546-1560, doi:10.1172/JCI86924 (2017).
270 Nachtigal, M., Ghaffar, A. & Mayer, E. P. Galectin-3 gene inactivation reduces atherosclerotic lesions and adventitial inflammation in ApoE-deficient mice. *Am J Pathol* **172**, 247-255, doi:10.2353/ajpath.2008.070348 (2008).
271 MacKinnon, A. C. *et al.* Inhibition of galectin-3 reduces atherosclerosis in apolipoprotein E-deficient mice. *Glycobiology* **23**, 654-663, doi:10.1093/glycob/cwt006 (2013).
272 Chen, X. *et al.* Galectin-3 exacerbates ox-LDL-mediated endothelial injury by inducing inflammation via integrin beta1-RhoA-JNK signaling activation. *J Cell Physiol* **234**, 10990-11000, doi:10.1002/jcp.27910 (2019).
273 Ou, H. C. *et al.* Galectin-3 aggravates ox-LDL-induced endothelial dysfunction through LOX-1 mediated signaling pathway. *Environ Toxicol* **34**, 825-835, doi:10.1002/tox.22750 (2019).
274 Sano, H. *et al.* Human galectin-3 is a novel chemoattractant for monocytes and macrophages. *J Immunol* **165**, 2156-2164, doi:10.4049/jimmunol.165.4.2156 (2000).
275 Tian, L. *et al.* Galectin-3-induced oxidized low-density lipoprotein promotes the phenotypic transformation of vascular smooth muscle cells. *Mol Med Rep* **12**, 4995-5002, doi:10.3892/mmr.2015.4075 (2015).
276 Tian, L. *et al.* Galectin3 induces the phenotype transformation of human vascular smooth muscle cells via the canonical Wnt signaling. *Mol Med Rep* **15**, 3840-3846, doi:10.3892/mmr.2017.6429 (2017).
277 Menini, S. *et al.* The galectin-3/RAGE dyad modulates vascular osteogenesis in atherosclerosis. *Cardiovasc Res* **100**, 472-480, doi:10.1093/cvr/cvt206 (2013).
278 Sun, Z. *et al.* RAGE/galectin-3 yields intraplaque calcification transformation via sortilin. *Acta Diabetol* **56**, 457-472, doi:10.1007/s00592-018-1273-1 (2019).
279 Lu, Y. *et al.* Modified citrus pectin inhibits galectin-3 function to reduce atherosclerotic lesions in apoE-deficient mice. *Mol Med Rep* **16**, 647-653, doi:10.3892/mmr.2017.6646 (2017).
280 Kadoglou, N. P. *et al.* Galectin-3, Carotid Plaque Vulnerability, and Potential Effects of Statin Therapy. *Eur J Vasc Endovasc Surg* **49**, 4-9, doi:10.1016/j.ejvs.2014.10.009 (2015).

281 Arikawa, T. *et al.* Galectin-9 ameliorates immune complex-induced arthritis by regulating Fc gamma R expression on macrophages. *Clin Immunol* **133**, 382-392, doi:10.1016/j.clim.2009.09.004 (2009).
282 Yu, J. *et al.* Galectin-9: A Suppressor of Atherosclerosis? *Front Immunol* **11**, 604265, doi:10.3389/fimmu.2020.604265 (2020).
283 Heusschen, R., Schulkens, I. A., van Beijnum, J., Griffioen, A. W. & Thijssen, V. L. Endothelial LGALS9 splice variant expression in endothelial cell biology and angiogenesis. *Biochim Biophys Acta* **1842**, 284-292, doi:10.1016/j.bbadis.2013.12.003 (2014).
284 Shimizu, Y. *et al.* Expression and localization of galectin-9 in the human uterodome. *Endocr J* **55**, 879-887, doi:10.1507/endocrj.k08e-111 (2008).
285 Spitzenberger, F., Graessler, J. & Schroeder, H. E. Molecular and functional characterization of galectin 9 mRNA isoforms in porcine and human cells and tissues. *Biochimie* **83**, 851-862, doi:10.1016/s0300-9084(01)01335-9 (2001).
286 Igawa, K., Satoh, T., Hirashima, M. & Yokozeki, H. Regulatory mechanisms of galectin-9 and eotaxin-3 synthesis in epidermal keratinocytes: possible involvement of galectin-9 in dermal eosinophilia of Th1-polarized skin inflammation. *Allergy* **61**, 1385-1391, doi:10.1111/j.1398-9995.2006.01130.x (2006).
287 Tanikawa, R. *et al.* Interaction of galectin-9 with lipid rafts induces osteoblast proliferation through the c-Src/ERK signaling pathway. *J Bone Miner Res* **23**, 278-286, doi:10.1359/jbmr.071008 (2008).
288 Imaizumi, T. *et al.* 15-deoxy-delta(12,14)-prostaglandin J2 inhibits IFN-gamma-induced galectin-9 expression in cultured human umbilical vein endothelial cells. *Int Arch Allergy Immunol* **131**, 57-61, doi:10.1159/000070436 (2003).
289 Imaizumi, T. *et al.* Double-stranded RNA induces galectin-9 in vascular endothelial cells: involvement of TLR3, PI3K, and IRF3 pathway. *Glycobiology* **17**, 12C-15C, doi:10.1093/glycob/cwm045 (2007).
290 Ishikawa, A. *et al.* Double-stranded RNA enhances the expression of galectin-9 in vascular endothelial cells. *Immunol Cell Biol* **82**, 410-414, doi:10.1111/j.0818-9641.2004.01248.x (2004).
291 Matsuoka, N. *et al.* Galectin-9 in autoimmune hepatitis: Correlation between serum levels of galectin-9 and M2BPGi in patients with autoimmune hepatitis. *Medicine (Baltimore)* **98**, e16924, doi:10.1097/MD.0000000000016924 (2019).
292 Sun, J. *et al.* Galectin-9 expression correlates with therapeutic effect in rheumatoid arthritis. *Sci Rep* **11**, 5562, doi:10.1038/s41598-021-85152-2 (2021).
293 Moar, P. & Tandon, R. Galectin-9 as a biomarker of disease severity. *Cell Immunol* **361**, 104287, doi:10.1016/j.cellimm.2021.104287 (2021).
294 Bi, S., Earl, L. A., Jacobs, L. & Baum, L. G. Structural features of galectin-9 and galectin-1 that determine distinct T cell death pathways. *The Journal of biological chemistry* **283**, 12248–12258, doi:10.1074/jbc.M800523200 (2008).
295 He, J. & Baum, L. G. Presentation of galectin-1 by extracellular matrix triggers T cell death. *The Journal of biological chemistry* **279**, 4705–4712, doi:10.1074/jbc.M311183200 (2004).
296 Bi, S., Hong, P. W., Lee, B. & Baum, L. G. Galectin-9 binding to cell surface protein disulfide isomerase regulates the redox environment to enhance T-cell migration and HIV entry. *Proceedings of the National Academy of Sciences of the United States of America* **108**, 10650–10655, doi:10.1073/pnas.1017954108 (2011).
297 Matsuura, A. *et al.* Intracellular galectin-9 activates inflammatory cytokines in monocytes. *Genes to cells : devoted to molecular & cellular mechanisms* **14**, 511–521, doi:10.1111/j.1365-2443.2009.01287.x. (2009).
298 Kanzaki, M. *et al.* Galectin-9 and T cell immunoglobulin mucin-3 pathway is a therapeutic target for type 1 diabetes. *Endocrinology* **153**, 612-620, doi:10.1210/en.2011-1579 (2012).

299 Zhang, C. X. *et al.* Galectin-9 promotes a suppressive microenvironment in human cancer by enhancing STING degradation. *Oncogenesis* **9**, 65, doi:10.1038/s41389-020-00248-0 (2020).
300 Matsumoto, R. *et al.* Human ecalectin, a variant of human galectin-9, is a novel eosinophil chemoattractant produced by T lymphocytes. *J Biol Chem* **273**, 16976-16984, doi:10.1074/jbc.273.27.16976 (1998).
301 O'Brien, M. J. *et al.* A unique role for galectin-9 in angiogenesis and inflammatory arthritis. *Arthritis Res Ther* **20**, 31, doi:10.1186/s13075-018-1519-x (2018).
302 Nonaka, Y. *et al.* Self-association of the galectin-9 C-terminal domain via the opposite surface of the sugar-binding site. *Journal of biochemistry* **153**, 463–471, doi:10.1093/jb/mvt009 (2013).
303 Moritoki, M. *et al.* Galectin-9 ameliorates clinical severity of MRL/lpr lupus-prone mice by inducing plasma cell apoptosis independently of Tim-3. *PLoS One* **8**, e60807, doi:10.1371/journal.pone.0060807 (2013).
304 Sato, M. *et al.* Functional analysis of the carbohydrate recognition domains and a linker peptide of galectin-9 as to eosinophil chemoattractant activity. *Glycobiology* **12**, 191-197, doi:10.1093/glycob/12.3.191 (2002).
305 Munir, H., Rainger, G. E., Nash, G. B. & McGettrick, H. Analyzing the effects of stromal cells on the recruitment of leukocytes from flow. *J Vis Exp*, e52480, doi:10.3791/52480 (2015).
306 Zhang, W., Zhang, Y., He, Y., Wang, X. & Fang, Q. Lipopolysaccharide mediates time-dependent macrophage M1/M2 polarization through the Tim-3/Galectin-9 signalling pathway. *Exp Cell Res* **376**, 124-132, doi:10.1016/j.yexcr.2019.02.007 (2019).
307 Hearps, A. C. *et al.* Aging is associated with chronic innate immune activation and dysregulation of monocyte phenotype and function. *Aging Cell* **11**, 867-875, doi:10.1111/j.1474-9726.2012.00851.x (2012).
308 Sadeghi, H. M., Schnelle, J. F., Thoma, J. K., Nishanian, P. & Fahey, J. L. Phenotypic and functional characteristics of circulating monocytes of elderly persons. *Exp Gerontol* **34**, 959-970, doi:10.1016/s0531-5565(99)00065-0 (1999).
309 Katoh, S. *et al.* Galectin-9 inhibits CD44-hyaluronan interaction and suppresses a murine model of allergic asthma. *Am J Respir Crit Care Med* **176**, 27-35, doi:10.1164/rccm.200608-1243OC (2007).
310 Bailly, C., Thuru, X. & Quesnel, B. Modulation of the Gal-9/TIM-3 Immune Checkpoint with alpha-Lactose. Does Anomery of Lactose Matter? *Cancers (Basel)* **13**, doi:10.3390/cancers13246365 (2021).
311 Giovannone, N. *et al.* Galectin-9 suppresses B cell receptor signaling and is regulated by I-branching of N-glycans. *Nature communications* **9**, 3287, doi:10.1038/s41467-018-05770-9 (2018).
312 Gosselin, D. *et al.* Environment drives selection and function of enhancers controlling tissue-specific macrophage identities. *Cell* **159**, 1327-1340, doi:10.1016/j.cell.2014.11.023 (2014).
313 Lavin, Y. *et al.* Tissue-resident macrophage enhancer landscapes are shaped by the local microenvironment. *Cell* **159**, 1312-1326, doi:10.1016/j.cell.2014.11.018 (2014).
314 Bonnardel, J. *et al.* Stellate Cells, Hepatocytes, and Endothelial Cells Imprint the Kupffer Cell Identity on Monocytes Colonizing the Liver Macrophage Niche. *Immunity* **51**, 638-654 e639, doi:10.1016/j.immuni.2019.08.017 (2019).
315 Iqbal, A. J. *et al.* Galectin-9 mediates neutrophil capture and adhesion in a CD44 and beta2 integrin-dependent manner. *FASEB J* **36**, e22065, doi:10.1096/fj.202100832R (2022).
316 Nishio, A. *et al.* CD14(+) monocyte-derived galectin-9 induces natural killer cell cytotoxicity in chronic hepatitis C. *Hepatology* **65**, 18-31, doi:10.1002/hep.28847 (2017).
317 Chabot, S. *et al.* Regulation of galectin-9 expression and release in Jurkat T cell line cells. *Glycobiology* **12**, 111-118, doi:10.1093/glycob/12.2.111 (2002).

318 Hsu, D. K., Yang, R. Y., Saegusa, J. & Liu, F. T. Analysis of the intracellular role of galectins in cell growth and apoptosis. *Methods Mol Biol* **1207**, 451-463, doi:10.1007/978-1-4939-1396-1_29 (2015).
319 Steichen, A. L. *et al.* Alarmin function of galectin-9 in murine respiratory tularemia. *PLoS One* **10**, e0123573, doi:10.1371/journal.pone.0123573 (2015).
320 Sidorkiewicz, I. *et al.* Plasma levels of M-CSF and VEGF in laboratory diagnostics and differentiation of selected histological types of cervical cancers. *BMC Cancer* **19**, 398, doi:10.1186/s12885-019-5558-8 (2019).
321 Chakraborty, A. *et al.* Galectin-9 bridges human B cells to vascular endothelium while programming regulatory pathways. *J Autoimmun* **117**, 102575, doi:10.1016/j.jaut.2020.102575 (2021).
322 Benagiano, M. *et al.* T helper type 1 lymphocytes drive inflammation in human atherosclerotic lesions. *Proc Natl Acad Sci U S A* **100**, 6658-6663, doi:10.1073/pnas.1135726100 (2003).
323 Botti, C. *et al.* Circulating cytokines present in the serum of peripheral arterial disease patients induce endothelial dysfunction. *J Biol Regul Homeost Agents* **26**, 67-79 (2012).
324 Schlitt, A. *et al.* CD14+CD16+ monocytes in coronary artery disease and their relationship to serum TNF-alpha levels. *Thromb Haemost* **92**, 419-424, doi:10.1160/TH04-02-0095 (2004).
325 Symons, A., Cooper, D. N. & Barclay, A. N. Characterization of the interaction between galectin-1 and lymphocyte glycoproteins CD45 and Thy-1. *Glycobiology* **10**, 559-563, doi:10.1093/glycob/10.6.559 (2000).
326 Wu, C. *et al.* Galectin-9-CD44 interaction enhances stability and function of adaptive regulatory T cells. *Immunity* **41**, 270–282, doi:10.1016/j.immuni.2014.06.011 (2014).
327 Carcamo, C. *et al.* Galectin-8 binds specific beta1 integrins and induces polarized spreading highlighted by asymmetric lamellipodia in Jurkat T cells. *Exp Cell Res* **312**, 374-386, doi:10.1016/j.yexcr.2005.10.025 (2006).
328 Hadari, Y. R. *et al.* Galectin-8 binding to integrins inhibits cell adhesion and induces apoptosis. *J Cell Sci* **113 (Pt 13)**, 2385-2397 (2000).
329 Vicuna, L. *et al.* Galectin-8 binds to LFA-1, blocks its interaction with ICAM-1 and is counteracted by anti-Gal-8 autoantibodies isolated from lupus patients. *Biol Res* **46**, 275-280, doi:10.4067/S0716-97602013000300008 (2013).
330 Lei, C. X., Zhang, W., Zhou, J. P. & Liu, Y. K. Interactions between galectin-3 and integrinbeta3 in regulating endometrial cell proliferation and adhesion. *Hum Reprod* **24**, 2879-2889, doi:10.1093/humrep/dep250 (2009).
331 Sedlar, A. *et al.* Interaction between Galectin-3 and Integrins Mediates Cell-Matrix Adhesion in Endothelial Cells and Mesenchymal Stem Cells. *Int J Mol Sci* **22**, doi:10.3390/ijms22105144 (2021).
332 Hyduk, S. J. *et al.* Phospholipase C, calcium, and calmodulin are critical for alpha4beta1 integrin affinity up-regulation and monocyte arrest triggered by chemoattractants. *Blood* **109**, 176-184, doi:10.1182/blood-2006-01-029199 (2007).
333 Elahi, S., Niki, T., Hirashima, M. & Horton, H. Galectin-9 binding to Tim-3 renders activated human CD4+ T cells less susceptible to HIV-1 infection. *Blood* **119**, 4192–4204, doi:10.1182/blood-2011-11-389585 (2012).
334 Kwiecien, I. *et al.* Blood Monocyte Subsets with Activation Markers in Relation with Macrophages in Non-Small Cell Lung Cancer. *Cancers (Basel)* **12**, doi:10.3390/cancers12092513 (2020).
335 Stockfelt, M. *et al.* Increased CD11b and Decreased CD62L in Blood and Airway Neutrophils from Long-Term Smokers with and without COPD. *J Innate Immun* **12**, 480-489, doi:10.1159/000509715 (2020).

336 Bravo, F. *et al.* Prospective Validation of CD-62L (L-Selectin) as Marker of Durable Response to Infliximab Treatment in Patients With Inflammatory Bowel Disease: A 5-Year Clinical Follow-up. *Clin Transl Gastroenterol* **12**, e00298, doi:10.14309/ctg.0000000000000298 (2021).
337 Gower, R. M. *et al.* CD11c/CD18 expression is upregulated on blood monocytes during hypertriglyceridemia and enhances adhesion to vascular cell adhesion molecule-1. *Arterioscler Thromb Vasc Biol* **31**, 160-166, doi:10.1161/ATVBAHA.110.215434 (2011).
338 Tang, J. *et al.* Adam17-dependent shedding limits early neutrophil influx but does not alter early monocyte recruitment to inflammatory sites. *Blood* **118**, 786-794, doi:10.1182/blood-2010-11-321406 (2011).
339 Tsubota, Y., Frey, J. M., Tai, P. W., Welikson, R. E. & Raines, E. W. Monocyte ADAM17 promotes diapedesis during transendothelial migration: identification of steps and substrates targeted by metalloproteinases. *J Immunol* **190**, 4236-4244, doi:10.4049/jimmunol.1300046 (2013).
340 Rzeniewicz, K. *et al.* L-selectin shedding is activated specifically within transmigrating pseudopods of monocytes to regulate cell polarity in vitro. *Proc Natl Acad Sci U S A* **112**, E1461-1470, doi:10.1073/pnas.1417100112 (2015).
341 Ivetic, A., Hoskins Green, H. L. & Hart, S. J. L-selectin: A Major Regulator of Leukocyte Adhesion, Migration and Signaling. *Front Immunol* **10**, 1068, doi:10.3389/fimmu.2019.01068 (2019).
342 Stewart, M. & Hogg, N. Regulation of leukocyte integrin function: affinity vs. avidity. *J Cell Biochem* **61**, 554-561, doi:10.1002/(sici)1097-4644(19960616)61:4<554::aid-jcb8>3.0.co;2-n (1996).
343 Humphries, M. J. Integrin structure. *Biochem Soc Trans* **28**, 311-339 (2000).
344 Li, J. *et al.* Conformational equilibria and intrinsic affinities define integrin activation. *EMBO J* **36**, 629-645, doi:10.15252/embj.201695803 (2017).
345 Luo, B. H., Carman, C. V. & Springer, T. A. Structural basis of integrin regulation and signaling. *Annu Rev Immunol* **25**, 619-647, doi:10.1146/annurev.immunol.25.022106.141618 (2007).
346 Sun, Z., Costell, M. & Fassler, R. Integrin activation by talin, kindlin and mechanical forces. *Nat Cell Biol* **21**, 25-31, doi:10.1038/s41556-018-0234-9 (2019).
347 Mazzone, A. *et al.* Increased expression of neutrophil and monocyte adhesion molecules in unstable coronary artery disease. *Circulation* **88**, 358-363, doi:10.1161/01.cir.88.2.358 (1993).
348 Foster, G. A. *et al.* On-chip phenotypic analysis of inflammatory monocytes in atherogenesis and myocardial infarction. *Proc Natl Acad Sci U S A* **110**, 13944-13949, doi:10.1073/pnas.1300651110 (2013).
349 Axford, J. S. *et al.* Changes in normal glycosylation mechanisms in autoimmune rheumatic disease. *J Clin Invest* **89**, 1021-1031, doi:10.1172/JCI115643 (1992).
350 Reily, C., Stewart, T. J., Renfrow, M. B. & Novak, J. Glycosylation in health and disease. *Nat Rev Nephrol* **15**, 346-366, doi:10.1038/s41581-019-0129-4 (2019).
351 Seidler, S., Zimmermann, H. W., Bartneck, M., Trautwein, C. & Tacke, F. Age-dependent alterations of monocyte subsets and monocyte-related chemokine pathways in healthy adults. *BMC immunology* **11**, 30, doi:10.1186/1471-2172-11-30 (2010).
352 Brevetti, G. *et al.* Endothelial dysfunction in peripheral arterial disease is related to increase in plasma markers of inflammation and severity of peripheral circulatory impairment but not to classic risk factors and atherosclerotic burden. *Journal of vascular surgery* **38**, 374-379, doi:10.1016/s0741-5214(03)00124-1 (2003).
353 Cooper, D., Iqbal, A. J., Gittens, B. R., Cervone, C. & Perretti, M. The effect of galectins on leukocyte trafficking in inflammation: Sweet or sour? *Annals of the New York Academy of Sciences* **1253**, 181–192, doi:10.1111/j.1749-6632.2011.06291.x (2012).

354 Woollard, K. J. & Geissmann, F. Monocytes in atherosclerosis: Subsets and functions. *Nature reviews. Cardiology* **7**, 77–86, doi:10.1038/nrcardio.2009.228 (2010).
355 Meurer, R. D., Forrest, M. J. & MacIntyre, D. E. The effects of IB4, a monoclonal antibody to the CD18 leukocyte integrin on phorbol myristate acetate (PMA)-induced polymorphonuclear leukocyte (PMN) accumulation and endothelial injury in rabbit lungs. *Inflammation* **23**, 51-62, doi:10.1023/a:1020239600981 (1999).
356 Kanse, S. M., Matz, R. L., Preissner, K. T. & Peter, K. Promotion of leukocyte adhesion by a novel interaction between vitronectin and the beta2 integrin Mac-1 (alphaMbeta2, CD11b/CD18). *Arterioscler Thromb Vasc Biol* **24**, 2251-2256, doi:10.1161/01.ATV.0000146529.68729.8b (2004).
357 Pearson, M. J. *et al.* Endogenous Galectin-9 Suppresses Apoptosis in Human Rheumatoid Arthritis Synovial Fibroblasts. *Sci Rep* **8**, 12887, doi:10.1038/s41598-018-31173-3 (2018).
358 Friedrichs, J., Manninen, A., Muller, D. J. & Helenius, J. Galectin-3 regulates integrin alpha2beta1-mediated adhesion to collagen-I and -IV. *J Biol Chem* **283**, 32264-32272, doi:10.1074/jbc.M803634200 (2008).
359 Moiseeva, E. P., Williams, B., Goodall, A. H. & Samani, N. J. Galectin-1 interacts with beta-1 subunit of integrin. *Biochem Biophys Res Commun* **310**, 1010-1016, doi:10.1016/j.bbrc.2003.09.112 (2003).
360 Fukumori, T. *et al.* CD29 and CD7 mediate galectin-3-induced type II T-cell apoptosis. *Cancer Res* **63**, 8302-8311 (2003).
361 Imhof, B. A. & Aurrand-Lions, M. Adhesion mechanisms regulating the migration of monocytes. *Nat Rev Immunol* **4**, 432-444, doi:10.1038/nri1375 (2004).
362 Fong, A. M. *et al.* Fractalkine and CX3CR1 mediate a novel mechanism of leukocyte capture, firm adhesion, and activation under physiologic flow. *J Exp Med* **188**, 1413-1419, doi:10.1084/jem.188.8.1413 (1998).
363 Liote, F., Boval-Boizard, B., Weill, D., Kuntz, D. & Wautier, J. L. Blood monocyte activation in rheumatoid arthritis: increased monocyte adhesiveness, integrin expression, and cytokine release. *Clin Exp Immunol* **106**, 13-19, doi:10.1046/j.1365-2249.1996.d01-820.x (1996).
364 Schaefer, K. *et al.* Galectin-9 binds to O-glycans on protein disulfide isomerase. *Glycobiology* **27**, 878–887, doi:10.1093/glycob/cwx065 (2017).
365 Liu, J., Huang, S., Su, X. Z., Song, J. & Lu, F. Blockage of Galectin-receptor Interactions by alpha-lactose Exacerbates Plasmodium berghei-induced Pulmonary Immunopathology. *Sci Rep* **6**, 32024, doi:10.1038/srep32024 (2016).
366 Golden-Mason, L. *et al.* Galectin-9 functionally impairs natural killer cells in humans and mice. *J Virol* **87**, 4835-4845, doi:10.1128/JVI.01085-12 (2013).
367 Libby, P. The changing landscape of atherosclerosis. *Nature* **592**, 524-533, doi:10.1038/s41586-021-03392-8 (2021).
368 Bentzon, J. F., Otsuka, F., Virmani, R. & Falk, E. Mechanisms of plaque formation and rupture. *Circ Res* **114**, 1852-1866, doi:10.1161/CIRCRESAHA.114.302721 (2014).
369 Nunoue, T. *et al.* Lgals9 deficiency ameliorates obesity by modulating redox state of PRDX2. *Sci Rep* **11**, 5991, doi:10.1038/s41598-021-85080-1 (2021).
370 Nakashima, Y., Plump, A. S., Raines, E. W., Breslow, J. L. & Ross, R. ApoE-deficient mice develop lesions of all phases of atherosclerosis throughout the arterial tree. *Arterioscler Thromb* **14**, 133-140, doi:10.1161/01.atv.14.1.133 (1994).
371 Solari, R., Pease, J. E. & Begg, M. "Chemokine receptors as therapeutic targets: Why aren't there more drugs?". *Eur J Pharmacol* **746**, 363-367, doi:10.1016/j.ejphar.2014.06.060 (2015).
372 Krautter, F. & Iqbal, A. J. Glycans and Glycan-Binding Proteins as Regulators and Potential Targets in Leukocyte Recruitment. *Front Cell Dev Biol* **9**, 624082, doi:10.3389/fcell.2021.624082 (2021).

373 Wiersma, V. R. *et al.* Galectin-9 Is a Possible Promoter of Immunopathology in Rheumatoid Arthritis by Activation of Peptidyl Arginine Deiminase 4 (PAD-4) in Granulocytes. *Int J Mol Sci* **20**, doi:10.3390/ijms20164046 (2019).
374 Braddock, M. *et al.* Fluid Shear Stress Modulation of Gene Expression in Endothelial Cells. *News Physiol Sci* **13**, 241-246, doi:10.1152/physiologyonline.1998.13.5.241 (1998).

9. **Appendix – Published papers**